

Studies on the role of WEE1 in the plant cell cycle

A thesis submitted for the degree of Doctor of Philosophy

by

Golnaz Rafiei

**School of Biosciences
Cardiff University**

April 2012

Contents

Chapter 1: General Introduction

1.1 The plant cell cycle and its regulation.....	2
1.1.1 Cyclin Dependent Kinases (CDKs).....	4
1.1.2 Cyclins.....	6
1.1.3 CDK regulation.....	8
1.1.4 G1/S transition.....	10
1.1.5 G2/M transition.....	11
1.1.5 .1Phosphoregulation of CDKs.....	11
1.1.5.1.1 WEE1 kinase.....	11
1.1.5.1.2 Cdc25 phosphatase.....	12
1.1.5.2 14-3-3 proteins.....	13
1.1.5.3 GSTF9 and redox regulation of the cell cycle.....	14
1.1.6 Mitosis.....	16
1.1.6.1 Cytokinesis.....	17
1.2 Cell cycle checkpoints.....	18
1.3 Interaction of WEE1 with other proteins.....	20
2. Experimental Aims.....	26

Chapter 2: General Materials and Methods

2.1 Plant materials.....	28
2.2 Media and antibiotics	29
2.3PCR.....	39
2.4 Agarose gel electrophoresis.....	30

2.5 DNA extraction from leaf discs.....	31
2.6 RNA Extraction.....	31
2.7 DNase treatment and cDNA synthesis.....	32
2.8 Protein extraction from plant tissue.....	33
2.9 Bradford assay.....	33
2.10 SDS-PAGE.....	34
2.11 Western blotting.....	34
2.12 Sterilization of Arabidopsis seeds.....	36
2.13 Fixing the roots.....	36
2.14 Staining the roots.....	36
2.15 Measuring primary root length, number of lateral roots, length of meristem and cell size of epidermal meristem cells.....	37
2.16 Growth of Arabidopsis plants in soil.....	37
2.17 Sterilization of tobacco seeds and growth in sterile conditions.....	38
2.18 Crossing Arabidopsis plants.....	38
2.19 Mitotic index measurements	39
2.20 Statistical analysis.....	39

Chapter 3: The interaction of wee1-1 and gsf9

3.1 Introduction.....	40
3.2 Aims	43
3.3 Materials and Methods.....	45
3.3.1 Arabidopsis lines.....	45
3.3.2 Growth of Arabidopsis lines on agar.....	45

3.3.3 Microdensitometry.....	46
3.4 Results	48
3.4.1 Genotyping and expression analysis of the <i>gstf9</i> insertion allele.....	48
3.4.2 Cross between <i>gstf9</i> and <i>wee1-1</i>	49
3.4.3 Response of Arabidopsis <i>wee1-1</i> and <i>gstf9</i> mutant lines to hydroxyurea (HU) treatment.....	52
3.4.3.1 Primary root length and rate of lateral root production.....	52
3.4.3.2 Meristem length.....	60
3.4.3.3 Number of epidermal cells along the meristem.....	62
3.4.3.4 Epidermal cell length.....	64
3.4.4.2 Elongation Zone.....	68
3.4.3.4 Percentage of cells in each component phase of the cell cycle in the RAM of WT, <i>wee1-1</i> and <i>gstf9</i> ± HU treatment.....	72
3.4.4 Response of Arabidopsis insertional mutant lines <i>wee1-1</i> and <i>gstf9</i> to zeocin treatment.....	75
3.4.4.1 Primary root length and rate of lateral root production.....	83
3.4.4.2 Meristem length.....	83
3.4.4.3 Number of epidermal cells along the meristem.....	86
3.4.4.4 Epidermal cell length	86
3.4.4.5 Percentage of cells in each component phase of the cell cycle in RAM of WT, <i>wee1-1</i> and <i>gstf9</i> ± zeocin treatment.....	89
3.5 Discussion	91
3.5.1 Primary root elongation of both <i>wee1-1</i> and <i>gstf9</i> mutants is hypersensitive to HU and zeocin compared to WT.....	91

3.5.2 Lateral root production in the presence of HU or zeocin was enhanced in <i>wee1-1</i> but not <i>gstf9</i> compared to WT	93
3.5.3 Root apical meristem length in the presence of HU or zeocin was reduced in <i>wee1-1</i>	94
3.5.4 HU or zeocin affects cell size and number in the epidermal layer of the RAM in both <i>wee1-1</i> and <i>gstf9</i> compared to WT.....	95
3.5.5 HU or zeocin affects the percentage of cells in each component phase of the cell cycle in the RAM in both <i>wee1-1</i> and <i>gstf9</i> compared to WT.....	96
Chapter 4: Studying the interaction between Arabidopsis GF14 Š and Arath;WEE1	
4.1 Introduction.....	98
4.2 Materials and methods.....	101
4.2.1 Plant material.....	101
4.2.2 Phenotypic analysis of an GF14 overexpressing line.....	101
4.2.3 Cross between an GF14 overexpressing line and <i>wee1-1</i> mutant.....	101
4.3 Results.....	103
4.3.1 Optimising the oestradiol treatment for induction of the GF14 in the GF14 OEX line.....	103
4.3.2 Genotyping progeny from the cross between an GF14 OEX and <i>wee1-1</i> ..	105

4.3.3 Phenotype of progeny from the cross between an GF14 OEX and <i>wee1-1</i>..	106
4.4 Discussion.....	111
Chapter5: Investigating the effects of expressing <i>Nicta;WEE1</i> in <i>Arabidopsis thaliana</i> and <i>Arath;WEE1</i> in <i>Nicotiana tabacum</i>	
5.1 Introduction.....	113
5.2 Materials and Methods	115
5.2.1 Expression of <i>Nicta;WEE1</i> in <i>Arabidopsis</i>	115
5.2.2 Expression of <i>Arath; WEE1</i> in tobacco plants	116
5.3 Results.....	117
5.3.1 Selection of T1 transgenic tobacco lines transformed with <i>Arath;WEE1</i>.....	117
5.3.2 WEE1 protein levels in the tobacco lines expressing <i>Arath;WEE1</i>.....	118
5.3.3 Root phenotype in tobacco seedlings expressing <i>Arath; WEE1</i> grown on Petri dishes	119
5.3.3.1 Effect of treatment with HU on primary root growth and production of lateral roots.....	119
5.3.3.2 Effect of treatment with HU on meristem length.....	123
5.3.3.3 Effect of treatment with HU on meristem length.....	125
5.3.3.4 Effect of treatment with HU on epidermal cell length along a file of the root apical meristem.....	127

5.3.3.5 Effects of treatment with zeocin on primary root growth and production of lateral roots	128
5.3.3.6 Effects of treatment with zeocin on root meristem length	132
5.3.3.7 Effects of treatment with zeocin on number of cells along a file of the epidermal region in the rest meristem	134
5.3.3.8 Effects of treatment with zeocin on the length of cells along a file of the epidermal region in the root meristem	135
5.3.4 Arabidopsis seedlings expressing <i>Nicta;WEE1</i>	137
5.3.4.1 Effect of <i>Nicta;WEE1</i> expression on primary root length and on the production of lateral roots and primordia.....	138
5.3.4.2 Effect of <i>Nicta;WEE1</i> expression on cell number in a file of epidermal cells of the RAM.....	140
5.3.4.3 Effect of <i>Nicta;WEE1</i> expression on cell length in a file of epidermal cells of the RAM.....	141
5.3.4.4 Effect of <i>Nicta;WEE1</i> expression on root meristem length.....	142
5.3.4.5 Effect of <i>Nicta;WEE1</i> expression on the proportion of cells at different stages in the cell cycle.....	143
5.4 Discussion.....	145

Chapter6: General Discussion

6.1 Interaction of <i>Arath;WEE1</i> with <i>GSTF9</i>	152
6.2 Interaction of <i>Arath;WEE1</i> with <i>GF14Š</i>.....	156
6.3 Regulation of <i>Arath;WEE1</i> and <i>Nicta;WEE1</i>	158

6.4 Further work.....	161
6.4.1 Interaction of <i>Arath;WEE1</i> with other cellular proteins: GSTF9 and GF14S.....	161
6.4.2 Regulation of <i>Arath;WEE1</i> and <i>Nicta;WEE1</i>	163
7. References.....	165

Acknowledgements

I would like to thank my supervisors, Dr Hilary Rogers and Dr Dennis Francis for their advice and support throughout the different stages of this project.

I would like to thank Dr Stuart Davies as my advisor during my studies.

I am grateful to Mr Mike O'Reilly for his help and technical support.

I would also like to thank lab members Adel, Anna, Lara, Riccardo, Wafa, Julie, Natasha, Jennifer from whom I benefited from their comments.

I would like to especially thank my best friends Porya Khosrowfar, and Dr Georgia Eglezou for their encouragement and emotional support during my PhD.

I am deeply indebted to my parents who supported me both financially and emotionally.

List of Abbreviations

ATP	adenosine triphosphate
<i>Arath; WEE1</i>	<i>Arabidopsis thaliana WEE1</i>
bp	base pair
°C	degrees centigrade
cdc	cell division cycle
cDNA	complementary deoxyribonucleic acid
CDK	cyclin dependent kinase
Cyc	cyclin
C-terminus	carboxy-terminus
DEX or dex	dexamethasone
DNA	deoxyribonucleic acid
Dnase	deoxyribonuclease
dNTP	deoxy nucleotide triphosphate
ETOH	Ethanol
G1	gap 1
G2	gap 2
GF14 ω OEX	14-3-3 over expression
h	Hour
HU	hydroxyurea
Hyg	hygromycin
M-phase	mitosis
M	molar
MeOH	methanol
MI	mitotic index
M & S	Murashige and Skoog medium
min	minute
mRNA	messenger ribonucleic acid
N-terminus	amino-terminus
OE	oestradiol

ORF	open reading frame
PAGE	polyacrylamide gel electrophoresis
PCR	polymerase chain reaction
Rb	retinoblastoma protein
RNA	ribonucleic acid
RT-PCR	reverse transcriptase polymerase chain reaction
S	DNA synthesis phase
<i>S. cerevisiae</i>	<i>Saccharomyces cerevisiae</i>
SDS	sodium dodecyl sulphate
SDW	sterile distilled H ₂ O
SE	standard error
<i>S. pombe</i>	<i>Schizosaccharomyces pombe</i>
TBY-2	tobacco bright yellow var. 2 cell line
WEE1OEX	over-expression of WEE1
WT	wild type

Abstract

WEE 1 is a key eukaryotic cell cycle regulator. In plants it has a clear role at the DNA damage/DNA replication checkpoints. I aimed to discover the functional significance of interactions between WEE1 and other cellular proteins in *Arabidopsis thaliana* and *Nicotiana tabacum*. First I examined effects of ectopic expression of Arabidopsis *WEE1* (*Arath;WEE1*) in transgenic tobacco and tobacco *WEE1* (*Nicta;WEE1*) in transgenic Arabidopsis. Western blotting using a plant WEE1 antibody showed that expression of *Nicta;WEE1* in Arabidopsis caused increases in total WEE1 protein. The response of primary root length, numbers of lateral roots and primordia, and meristem length to zeocin (a DNA damaging agent) and hydroxyurea, (which perturbs DNA replication), resembled the *wee1-1* insertional mutant rather than *Arath;WEE1* over-expression. Expression of *Arath;WEE1* in tobacco resulted in reduced WEE1 protein but also induced similar phenotypic changes as *Nicta;WEE1* expression in Arabidopsis under zeocin and HU stress. I concluded that interactions with cellular proteins in the alien species resulted in down-regulation of WEE1 activity.

In a yeast 2-hybrid screen *Arath;WEE1* interacted with the glutathione-S-transferase protein, *GSTF9*. To test the functionality of this interaction I analysed the root and cell cycle phase phenotypes of single mutants: *wee1-1* and *gstf9* and I generated the double mutant *wee1-1;gstf9*. I demonstrated that both *Arath;WEE1* and *GSTF9* have roles in the DNA replication and damage checkpoints, but largely act in different genetic pathways.

Arath;WEE1 also interacts with GF14 ω , a 14-3-3 protein in a yeast 2-hybrid assay. In other eukaryotes this stabilizes WEE1. I confirmed that over-expression of GFF14 ω in transgenic Arabidopsis (GFF14 ω OEX) results in a very similar root phenotype to over-expression of *Arath;WEE1* as predicted from a stabilization of WEE1. However the GFF14 ω OEX phenotype

was not abolished in a *wel-1* genetic background. indicating that Arath;WEE1 is not required for the action of *GF14 ω* .

1. General Introduction

In this thesis, I present work on the role of the cell cycle gene, *WEE1*, its interface with other genes in the cell cycle, and its effect on plant growth, and development. I focused on the role of this gene in response to treatments that induced chromosomal DNA damage and perturbation of nuclear DNA replication. I used two model systems, *Arabidopsis thaliana* and *Nicotiana tabacum*.

Arabidopsis thaliana is a dicot species that over the past 25 years has become an important model system in plant biology. It has various traits that make it ideal as a model system. For example, it has a very small nuclear genome (0.6 pg C value 125 Mb with 5 chromosomes per haploid set) (www.DNACvalue.kew.org, www.arabidopsis.org). Generally, *Arabidopsis* genes have few introns and that has made DNA sequencing relatively straight forward. Not surprisingly, it was the first higher plant genome to be fully sequenced (*A. thaliana* Genome Initiative, 2000). *Arabidopsis* is an ephemeral weed capable of extremely fast growth enabling it to rapidly exploit open ecosystems. Indeed, it can set seed within 5-6 weeks of germination. A vast array of developmental and physiological mutants are also available that have been used to break new ground in the understanding of plant growth and development. In addition, there is also a vast collection of T-DNA insertional mutants freely available so that it is possible to access knockout lines deficient in a gene(s) of interest (<http://signal.salk.edu/cgi-bin/dnaexpress>). It is a member of the Brassicaceae and related to crop species within this family.

Nicotiana tabacum (tobacco) has also been widely used both as a whole plant and to generate cell cultures. Tobacco is easily transformed and in fact was the first plant species to be transformed (James, 1996), and the TBV-2 cell culture derived from the cultivar

Bright Yellow is easy to maintain, and is particularly useful for cell cycle studies due to the ease with which its cell division can be synchronised (Kumagai *et al.*, 2006).

In the following sections, I review the plant cell cycle and genes/proteins that are important in its regulation particularly in relation to *WEE1*, and the *Arabidopsis* protein GSTF9. The latter was initially identified as being relevant to the cell cycle because it interacts at the protein level with *Arabidopsis* WEE1 (Cardiff lab, unpublished data).

1.1 The plant cell cycle and its regulation

Cell division is a central component of plant growth and development and has been an important topic for cell biologists for more than one hundred years (reviewed by Kuijit, 2006). The plant cell cycle consists of G1 (post mitotic interphase), S-phase (DNA synthesis phase), G2 (premitotic interphase) and mitosis/cytokinesis. Two major transition points are recognized in the cell cycle regulating entry into S phase and into M phase (reviewed by Francis, 2006).

In S-phase DNA is replicated by a semi conservative mechanism during which a single arm chromosome changes to a chromosome with double arms (Fig 1.1). DNA is replicated semi-conservatively at multiple initiation sites along the chromosome. Each one is known as a replicon. An origin of replication and two termini defines each replicon; semi conservative replication proceeds outwards from the origin to the termini. The DNA is unwound at an origin of replication. DNA primase primes the 3' OH group of exposed single stranded DNA with a short molecule of RNA (Lewin, 1998). By this mechanism, replication is in both directions from the starting point. This creates two-replication forks, moving in opposite directions (Griffiths *et al.*, 1999).

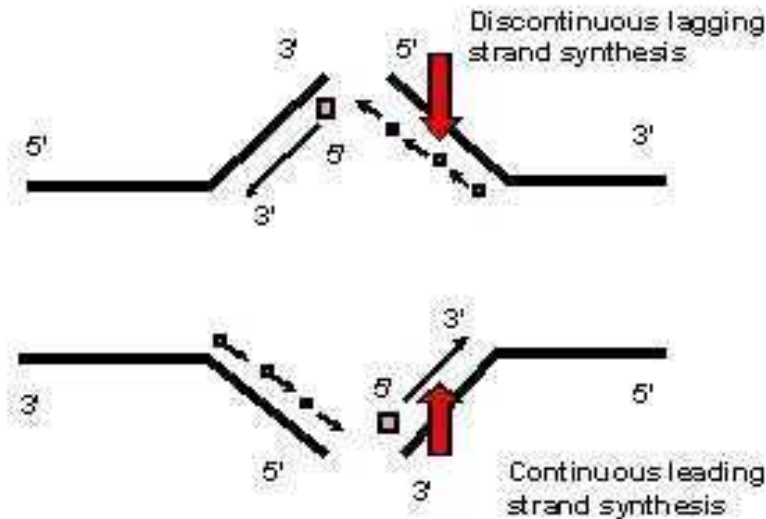


Figure 1.1 DNA replication from an origin: (a) Continuous strand synthesis: In the asymmetric structure of the replication fork the 3' to 5' strand is known as the leading strand, DNA polymerase synthesises the daughter strand from 5' to 3' continuously (b) Discontinuous strand synthesis: The 5' to 3' is known as the lagging strand which is synthesized in opposite direction to the overall direction of DNA chain growth. The replication of lagging strand occurs with delay in comparison with the leading strand, these fragments which are synthesised discontinuously are named Okazaki fragments. Note that the middle of the structure shows a clear gap between strands creating 5' and 3' binding sites, but is normally followed by rejoining in less than a second .

DNA polymerase () binds to the 3'-OH of the RNA primer molecule. It then catalyzes the addition of new nucleotide monophosphates into the new strand of DNA and the cleavage and release of pyrophosphate molecules into the nucleoplasm. Because DNA polymerase () can only work in the 5' to 3' direction, DNA replication is bidirectional from the common origin. Once continuous leading strand DNA replication has begun, discontinuous 5' to 3' replication in the lagging strand occurs as a series of short sections known as Okazaki fragments (Fig.1.1). Eventually, these fragments are joined together by DNA ligase (see Alberts *et al.*, 1985).

Plants show considerable plasticity in the way they replicate their nuclear DNA. During G2 phase the cell grows to an optimum size prior to its entry into mitosis. A number of genes are expressed that regulate cell size some of which will be mentioned later in this chapter.

The basic features of cell cycle control are remarkably conserved in all eukaryotes (Huntley and Murray, 1999), but in higher eukaryotes the cell cycle is regulated by different variants of the essential drivers, cyclin-dependent kinases (Eckardt, 2001).

1.1.1 Cyclin Dependent Kinases (CDKs)

In all eukaryotes the plant cell cycle is regulated by a super-family of serine/threonine protein kinases known as cyclin-dependent kinases (CDKs) and cyclins which cooperate with CDKs (Becker *et al.*, 2003) (Fig. 1.2). Cyclins are the activating subunits of CDKs and are essential for both kinase activity and substrate specificity (Elledge, 1996; Nigg, 1995). The T-loop is the part of the CDK which restricts access to the active site of the CDK. In *Schizosaccharomyces pombe*, in a non-catalytic domain there is a sequence within the T-loop comprising the following amino acids- PSTAIRE; the T-loop is responsible for binding with a cyclin partner. This PSTAIRE sequence is conserved in animal CDKs and in CDKA;1 in Arabidopsis. Note that a hallmark feature of PSTAIRE-containing CDKs is their property to rescue temperature sensitive *cdc2-/cdc28* mutants of fission and budding yeast (*Saccharomyces cerevisiae*), respectively (BursSENS *et al.*, 1998). In plants, a range of additional CDKs have also been identified and grouped: B, C, D, E, F and G. In these CDKs the PSTAIRE domain has been altered during evolution (Joubes *et al.*, 2000). Thus, in plants CDKA types are prototypical CDKs, which share the conserved PSTAIRE, found in *cdc2/CDC28* in fission/budding yeast (Huntley and Murray, 1999), which is normally active from the beginning of S-phase, until the end of

the G2/M transition. CDKA; 1 which is homologous to *Schizosaccharomyces pombe* SpCdc2 homologue, and animal CDK1 and 2, is encoded by a single gene in Arabidopsis, and its kinase activity peak is at G1/S and G2/M (Mironov *et al.*, 1999; Iwakawa *et al.*, 2006; Nowack *et al.*, 2006). However other plant CDKs including a *CDKB* is represented by a multigene family that cannot complement the temperature sensitive *cdc25⁻* mutant of *S. pombe* (Boudolf *et al.*, 2004). The B-types are unique to plants, and as yet not found in any other organism (Mironov *et al.*, 1999; Joubès *et al.*, 2000; Inzé and DeVeylde; 2006; Boruc *et al.*, 2010), and they only function at the G2/M transition (Huntley and Murray, 1999).

C-type CDKs in tomato failed to interact with cyclins A, B and D (Joubes *et al.*; 2001). D-type CDKs have two functions, they participate in phosphoregulation of the activity of RNA polymerase II, and also in phosphorylation of other CDKs during the cell cycle (Harper and Elledge, 1998). An E-type CDK was observed in Arabidopsis (Vandepoele, 2002); its activity may be restricted to reproductive growth and in specifying stamens and carpels, and also in termination of stem cell division in floral meristems. Its function in reproductive systems is similar to CDK8 in mammals (Wang and Chen, 2004). CDKG has homology with the human cytokinesis- associated p58 galactosyltransferase protein (Menges *et al.*, 2005).

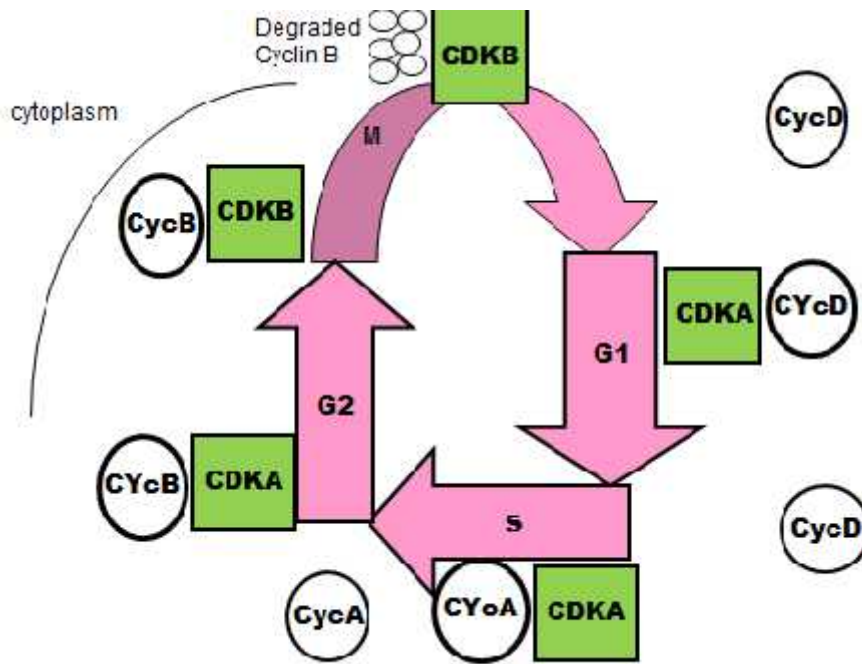


Figure 1.2 Cell cycle regulatory proteins at different stages of the plant cell cycle, and the interaction between different CDK and cyclins during G1, S, G2, and M phase. During G1 CDKA binds to CycD, at G1/S CycD is released and CDKA binds to CycA. During G1 phase cyclin D conjugates with CDKA. CycA is replaced by CycD during S-phase. In G2 to M-phase and within G2, the CycA is substituted by CycB. CycB conjugates to both CDKA and CDKB. CycB is degraded by the Anaphase Promoting Complex (APC) at metaphase.

1.1.2 Cyclins

Cyclins are proteins that bind to, and activate CDKs; they have large conserved sequences within the cyclin box, and these sequences are responsible for substrate selection, subcellular localization and stability of the CDK–cyclin complexes in relation to binding with the T-loop of CDKs (Genschik *et al.*, 1998; Wang *et al.*, 2004). Sixty genes were proved to regulate seven classes of cyclins: A, B, C, D, H, P and (T) (Francis, 2007).

Expressions of A- and B-type cyclins are at their highest at the S-G2-M and G2/M transitions (Ito *et al.*, 1998, 2001; Ito, 2000). A conserved N-terminal sequence called the destruction box (D-box) exists in both A and B cyclins. The D-box serves as a binding site

which ubiquitin residues bind to prior to proteolytic destruction of the cyclin (Renaudin *et al.*, 1996; Vandepoele *et al.*, 2002; Wang *et al.*, 2004).

A-type cyclins are subdivided into three different subclasses: CYCA1, CYCA2, CYCA3 (Chaubet, 2000). A-type cyclins are involved in S-phase progression and are expressed before B-Type cyclins in the plant cell cycle, before S-phase (Fuerst *et al.*, 1996; Setiady *et al.*, 1995; Lew *et al.*, 1991). The expressions of two A3-type cyclins are up-regulated at the G1/S transition (Reichheld *et al.*, 1996).

B-type cyclins are expressed specifically in late G2, at the G2/M transition, and in early M-phase of the cell cycle (Ito, 2000). B-type cyclins are subdivided into three subclasses in Arabidopsis, CycB1, CycB2, and CycB3 (Vandepole *et al.*, 2002). CycB1, CycB2 are found in other eukaryotes whereas the third subclass is specific to Arabidopsis (Renaudin *et al.*, 1996).

Cyclin levels are regulated through transcription or specific protein degradation (Lees and Harlow, 1993). During the transition from metaphase to anaphase, cyclin A-types and B-types are degraded; this degradatory pathway involves priming of the cyclin with ubiquitin residues which makes the cyclin unstable. This unstable complex is then degraded in the 26S proteasome (Genschik *et al.*, 2007) (Fig. 1.2).

Ten D-type cyclins have been classified in Arabidopsis (Vandepoele *et al.*, 2002). D-type cyclins can be controlled both transcriptionally and post-transcriptionally. For example, sucrose, cytokinin, and brassinosteroids can control the expression of *CycD* (Riou-Khamilichi *et al.*, 2002; Hu *et al.*, 2000). In suspension cultures of Arabidopsis, cytokinin can induce *CycD3* expression and sucrose can induce *CycD2* and *CycD4* expression (Riou-Khamilichi *et al.*, 2000). Most encoded Cyclin Ds contain a combination of amino acids rich in proline, glutamate, serine and threonine (PEST), amino acids that are responsible for targeting ubiquitin/proteasome-mediated proteolysis by the so-called

SCF complex; these cyclins have an N-terminal LxCx(D/E) retinoblastoma-binding motif (Renaudin *et al.*, 1996; Vandepoele *et al.*, 2002; Planchais *et al.*, 2004; Yanagawa and Kimura, 2005 ; Sorrell *et al.*, 1999). G1- specific D-type cyclins regulate the progression from G1 to S-phase (Soni *et al.*, 1995; Vandepoele *et al.*, 2002; Menges *et al.*, 2005; Boruc *et al.*, 2010). The genes which encode these types of cyclins are expressed at a constant level during the cell cycle (Sorrell *et al.*, 1999).

H-type cyclin is known as a partner of a cyclin activating kinase (CAK) which catalyses the phosphorylation of a tyrosine residue of a CDK (Tyr-160/167) enabling, for example, CycD–CDKA binding (Yamaguchi *et al.*, 2000; Shimotohno *et al.*, 2004).

Transcriptional regulators, cytoskeleton, nuclear matrix, nuclear membrane proteins, and chromatin-associated proteins can all be substrates of CDK–cyclin complexes (Norbury and Nurse, 1992; Koch and Nasmyth, 1994; Joubès *et al.*, 2000).

1.1.3 CDK regulation

Cyclins are not the only proteins which control CDK activity. Cyclin-dependent Activating Kinases (CAKs) can positively regulate CDKs by phosphorylating a threonine residue (T 160/167) within the CDK loop. This phosphorylation event occurs at the same time as cyclin binding to the CDK and in its absence this binding will not take place. The binding of a CDK with its partner cyclin is catalysed by the CAK kinase and at the same time the cyclin binds to the CDK. Two classes of CAK have been identified: D-type CDKs (homologous to vertebrate CAKs) and F-type CDKs (plant specific CAKs) (Umeda *et al.*, 2005).

Environmental and developmental signals cause the inhibition of CDK/CYC complexes by Cyclin-dependent Kinase Inhibitors (CKIs) (LaBaer *et al.*, 1997; Cheng *et al.*, 1999). Two major classes of CKI proteins have been identified in mammalian cells which are Kip/Cip and INK4 (Sherr and Roberts, 1999). Kip related proteins have been identified in Arabidopsis but with only limited sequence homology compared with mammalian cells. The first plant CKIs were detected in yeast two hybrid screens (Wang *et al.*, 1997; Verkest *et al.*, 2005). They were initially discovered by this approach in plants in the lab. of L. Fowke in the 1990s and were named Interactors with CDKs (ICKs, Wang *et al.*, 1999). Because of their limited homology with animal CKIs, they were renamed by L. DeVeylder as KRP (Kip-related) proteins of which there are seven in the Arabidopsis genome (Ormenese *et al.*, 2004). KRPs/ICKs can negatively regulate CDK activity by binding to both the CDK and cyclin subunit (Wang *et al.*, 1999). This will cause cycle arrest or delay cell cycle progression in response to intracellular or extracellular signals (Verkest *et al.*, 2005). Arabidopsis; ICK1/KRP1 and Arabidopsis;ICK2/KRP2 are unstable proteins (Zhou *et al.*, 2003b; Verkest *et al.*, 2005). In plants ICK/KRP members were isolated either by the yeast two-hybrid approach from Arabidopsis (Wang *et al.*, 1997; Lui *et al.*, 2000; Zhou *et al.*, 2002), tobacco (Jasinski *et al.*, 2002a, 2003) and alfalfa (Pettko-Szandtner *et al.*, 2006), or by data mining from Arabidopsis (De Veylder *et al.*, 2001), maize (Coelho *et al.*, 2005), rice (Barroco *et al.*, 2006) and tomato (Bisbis *et al.*, 2006). Homologous proteins to INK4 have not been identified in Arabidopsis. Over-expression of ICK/KRP genes inhibits cell cycle progression at both G1/S and G2/M transitions, causing smaller plant size, serrated leaves, reduced cell number and enlarged cells (Wang *et al.*, 2000; De Veylder *et al.*, 2001; Zhou *et al.*, 2002; Jasinski *et al.*, 2002a, 2003; Barroco *et al.*, 2006; Kang *et al.*, 2007; Bemis and Torii, 2007), while weak overexpression of *ICK1* (*KRP1*) or *ICK2* (*KRP2*) caused inhibition of mitosis (Verkest *et al.*, 2005; Weigl *et al.*, 2005). Recombinant ICK1 protein in *Tradescantia virginiana*

stamen cells increased transition time to metaphase so that mitosis is slowed down (Cleary *et al.*, 2002).

1.1.4 G1/S transition

The conserved mechanism of G1/S transition in mammals and plants is partly dependent on the retinoblastoma protein (Rb), and the progression to S-phase is controlled by the activity of E2F transcription factors (He *et al.*, 2004). E2F is bound to the Rb protein and this represses the transcription of E2F-dependent genes. Six E2Fs have been identified in Arabidopsis: E2Fa, E2Fb, E2Fc, E2Fd/DEL2, E2Fe/DEL1 and E2Ff/DEL3 (Inzé, 2005). In Arabidopsis, there are also dimer proteins (DP(s)) that bind (dimerise) with E2Fa, E2Fb, E2Fc and DPs and only have one DNA-binding domain to interact with the canonical E2F motif, whereas E2Fd/DEL2, E2Fe/DEL1 and E2Ff/DEL3 proteins contain two DNA-binding domains allowing them to bind to the E2F site (Mariconti *et al.*, 2002; Vandeopoele *et al.*, 2002). In G1/G0, CDKA/cyclinD phosphorylate Rb and this causes the release of E2Fs which then bind to the promoters of genes that drive the cell into S-phase; as a result, E2F responsive genes are activated.

Homologues of the Rb protein have been identified in maize, *Zea mays* (*Z. mays*, Zm), tobacco, *Nicotiana tabacum* (*N. tabacum*, Nt), and in Arabidopsis (Grafí *et al.*, 1996; Nakagami *et al.*, 1999; Kong *et al.*, 2000). In Arabidopsis the Rb protein can be phosphorylated by the CDKA/CYCD complex, which thereby releases E2F (De Veylder *et al.*, 2002). In the green alga *Chlamydomonas reinhardtii* (*C. reinhardtii*), mutation in the Rb protein genes did not result in a shortened G1-phase or premature entry into S-phase as a result, normal differentiation in cells was observed, while in mammalian cells loss of Rb proteins results in a shortened G1, suggesting that the *Chlamydomonas* Rb pathway is not

an S-phase switch, but a size sensor restraining cell cycle progression (Umen and Goodenough, 2001).

1.1.5 G2/M transition

In most eukaryotes, phosphoregulation of CDKs controls the G2/M transition. In mammals, the CDK-cyclin complex forms during the S and G2 phases and it is inactivated by inhibitory phosphoregulation of two adjacent amino acid residues, Thr 14 and Tyr 15, towards the NH₂-terminus of the protein (Mueller *et al.*, 1995). Phosphoregulation is partly controlled by a family of protein kinases, WEE1, MIK1, and MYT1 (Lundgren *et al.*, 1991; Mueller *et al.*, 1995; Porceddu *et al.*, 2001).

1.1.5.1 Phosphoregulation of CDKs:

1.1.5 .1 .1 WEE1 kinase

WEE1 kinases are proteins which phosphorylate CDKs at Tyr15. Typically, WEE1s have a C-terminal catalytic domain and an N-terminal regulatory domain. In fission yeast, Wee1 causes a delay in mitosis by phosphorylation of the CDK at tyrosine 15. Wee1 level rises during S and G2 phase, and decreases during M phase (McGowan *et al.*, 1995; Watanabe *et al.*, 1995). Loss of Wee1 function resulted in premature entry into mitosis at a smaller mitotic cell size. Hence, WEE1 is a negative regulator of cell size at cell division.

The first WEE1 in plants was cloned in maize (Sun *et al.*, 1999), and in Arabidopsis (Sorrel *et al.* 2002). *Arath*; *WEE1* was identified by sequence homology (Sorrel *et al.*, 2002) and shares a high homology with *Zeama*; *WEE1* that has been shown to inhibit the CDK complex in plants (Sun *et al.*, 1999). Over-expression of Arabidopsis and maize WEE1 in *Schizosaccharomyces pombe* inhibited cell division and caused an increase in cell size (Sun *et al.*, 1999; Sorrell *et al.*, 2002). However, when *Arath*; *WEE1*

was expressed in tobacco BY-2 culture cells, it induced a small mitotic cell size in comparison with the wild type (Siciliano, 2006).

In animal cells, WEE1 is found in the nucleus most of the time, and after mitosis begins, it is transferred to the cytoplasm (Baldin and Ducommun, 1995). In animal cells, 14-3-3 proteins together with Chk1 are positive regulators of Wee1, and during mitosis the interaction between 14-3-3 and Wee1 proteins is reduced leading to a decrease in Wee1 kinase activity (Lee *et al.*, 2001). In *wee1* mutants (*Xwee1*) lacking the ability to bind 14-3-3 proteins, WEE1 becomes less active in CDK phosphorylation and is therefore not efficient in regulating G2/M (Wang *et al.*, 2000). In *S. pombe*, mitotic inhibitory kinase (Mik1) has a similar role to Wee1 in the cell cycle (Lundgren *et al.*, 1991), although Mik1 is not present in Arabidopsis.

Phosphoregulation of the ATP-binding domain of the kinase protein regulates the activity of the CDK-cyclin complex. In fission yeast, the activity of CDK-cyclin is induced by the dephosphorylation of Tyr15 whereas this occurs on both Tyr15 and Thr14 in higher eukaryotes (Russell and Nurse, 1986; Dunphy, 1994; Watanabe *et al.*, 1995). This activation of the CDK-Cyclin complex is catalysed by a unique class of enzymes, the CDC25 phosphatases.

1.1.5.1.2 Cdc25 phosphatase

In animals and yeasts, CDC25 is a positive regulator of CDKs at the G2/M transition. An increase in WEE1 activity causes delay in entering mitosis at an enlarged cell size whilst an increase in CDC25 activity can cause premature entry to mitosis at a reduced cell size (Russell and Nurse, 1987). A putative homologue of animal and yeast *CDC25* was discovered in plants (Landrieu *et al.*, 2004; Sorrell *et al.*, 2005). Arabidopsis *CDC25* protein shares homology with the catalytic domains of CDC25A, CDC25B, and CDC25C in

humans, and CDC25 in yeast, however it lacks a regulatory domain. The *Arath*; CDC25 also has arsenate reductase activity under arsenate stress conditions (Bleecker *et al.*, 2006) but acts as a phosphatase in the presence of a phosphorylated substrate *in vitro* (Landrieu *et al.*, 2004). The role of *CDC25* in plants is controversial because *Arabidopsis* T-DNA insertional lines for *Arath*;CDC25 grow and develop normally (Dissmeyer *et al.*, 2009). However, *cdc25* knockout lines were hypersensitive to hydroxyurea treatment, a drug that induces the DNA replication checkpoint (Spadafora *et al.*, 2011). Hence, *CDC25* may be a necessary component of the DNA replication checkpoint in plants.

1.1.5.2 14-3-3 proteins

14-3-3 refers to the elution and migration pattern of these proteins following DEAE-cellulose chromatography and starch-gel electrophoresis. The 14-3-3 proteins eluted in the 14th fraction of bovine brain extract/homogenate and were found on positions 3.3 during subsequent electrophoresis (Moore and Perez, 1967).

The role of 14-3-3 proteins in cell cycle regulation was first recognized in *S. pombe* (Ford *et al.*, 1994). These proteins can regulate the cell cycle by modulating protein localization (Zeng and Piwnica-Worms, 1999); for example they can control intracellular distribution of Cdc25 (Lopez Girona *et al.*, 1999). Nuclear accumulation of Cdc25 was observed in *S. pombe* when the 14-3-3 protein, Rad24, was knocked out causing the activation of the CDK/cyclin complex (Zeng and Piwnica-Worms, 1999). In *H. sapiens*, a 14-3-3 protein stabilizes WEE1, and a *wee1* mutant lacking the ability to bind 14-3-3 proteins is less efficient in inducing a G2 cell cycle delay (Wang *et al.*, 2000). 14-3-3 proteins protect phosphorylated sites on Wee1 and Cdc25 under checkpoint conditions thereby preventing further phosphorylation by polo-like kinases (Forbes *et al.*, 1998; Kumagai and Dunphy, 1999; Lee *et al.*, 2001).

1.1.5.3 GSTF9 and redox regulation of the cell cycle

GSTF9 (glutathione S-transferase transmembrane (GST) family) belongs to a family of multifunctional, dimeric enzymes that catalyse the nucleophilic attack of the tripeptide, glutathione, on lipophilic compounds which have electrophilic centres (Wagner *et al.*, 2002). In plants the GST gene family is derived from an ancestral class of all eukaryote GSTs the theta class, also present in vertebrates and insects. Based on amino acid sequence, six classes of plant GSTs are now recognized (Dixon *et al.*, 2002), composed of 54 members in *Arabidopsis* (Dixon *et al.*, 2009). GSTs in plants are divided into six classes based on amino acid sequence: phi (GSTF), tau (GSTU), zeta (GSTZ), theta (GSTT), lambda (L), and dehydroascorbate reductases (DHAR) (Dixon *et al.*, 2002; Moons, 2005; Dixon *et al.*, 2009). Two of these classes are found in mammals: the theta class and zeta classes, while the remaining larger classes of tau, phi (GSTF), lambda, and dehydroascorbate reductase (DHAR) are specific to plants (Droog, 1997; Dixon *et al.*, 1998a; Edwards *et al.*, 2000). These enzymes are found in the cytosol of the cell although there is some evidence for the expression of some GSTs in the nucleus and peroxisomes (Dixon *et al.*, 2009).

Z class GSTs are involved in tyrosine metabolism, and the DHAR class is involved in ascorbic acid recycling (Dixon *et al.*, 2009). One of the most important activities of the phi class of GSTs is glutathione peroxidase which causes reduction of organic hydroperoxides to their respective alcohols (Dixon *et al.*, 2010).

A function has also been ascribed to individual GSTs e.g. in responses to stress and plant growth regulators (Moons, 2005), flavonoid metabolism (Kitamura *et al.*, 2004) and as hydroperoxide-reducing glutathione peroxidases (Dixon *et al.*, 2009). In addition, GSTs are also considered as transporter proteins for secondary metabolites (Alfenito *et al.*, 1998; Muller *et al.*, 2000; Dixon *et al.*, 2002; Kilihi *et al.*, 2004; Dixon *et al.*, 2010). Li *et al.* (2007)

also showed GSTs catalyse cis-trans isomerisation in the carotenoid synthesis pathway. They can also function as storage proteins for reactive oxylipins, phenolics, and flavonoids, (Dixon *et al.*, 2010).

Expression of *GSTs* is induced in response to some stresses such as general cellular injury and oxidative stress (Dixon *et al.*, 2002). The roles of plant GSTs are not only confined to function in stresses but also to plant growth and development (Gong *et al.*, 2005; Moons, 2005). However, the exact function *in vivo* for the majority of GSTs is unknown (Dixon *et al.*, 2010).

GSTs are not able to catalyse conventional conjugation reactions, so cells require GSHs as a cofactor GSTs bind to hydrophobic ligands which react with the thiol group of GSH which is active in transferase function. (Dixon *et al.*, 2010). All GSTs are therefore dependent on glutathione (GSH) which has a role in endogenous metabolism including detoxification and buffering redox reactions in response to oxidative stress, flavonoid binding, and regulation of apoptosis. Abiotic stresses in plants cause production of GSH (Dixon *et al.*, 2002, Klein *et al.*, 2006). GSH is imported to the vacuole by ATP-binding cassette (ABC) transporter proteins when plants are exposed to abiotic stresses (Rea, 2007).

The first step of GSH synthesis in *Arabidopsis* takes place exclusively in the chloroplasts (Meister, 1995). In other plant species the situation is less clear (Wachter *et al.*, 2005). Glutathione at millimolar concentrations is present in many cellular compartments (Foyer *et al.*, 2005), and in both animal and plant cells, glutathione is a key regulator of cell proliferation (Harris *et al.*, 1969). Microinjection studies showed that GSH in early G1 is in the nucleus. At the end of prophase/beginning of metaphase there is a change in cytosolic GSH availability. A change in cytosolic redox enables GSH synthesis in the cytoplasm leading to a rapid increase in the total GSH pool of the cell. When the nuclear envelope dissolves in prophase, it allows equilibration between the cytosol and nuclear GSH pools.

When the nuclear envelope re-forms during telophase the cellular GSH pool is re-distributed between the daughter cells (Briviba *et al.*, 1993, Pedro *et al.*, 2010). Various residues in the histone tails are subject to posttranslational modification, and the GSH pool could have effects on DNA or histone methylation or maybe other histone modifications such as those catalysed by histone acetyltransferases (Jenuwin *et al.*, 2001).

Redox signalling is an important regulator of the cell cycle (Atzori *et al.*, 1990; Hirt, 2000). In early G1-phase, an oxidation event is a critical regulatory step in the progression to S-phase (Menon *et al.*, 2003). Moreover, in the G1-phase, GSH levels are low and progress of cells from the G1- to the S-phase needs an increase in total GSH (Kerk *et al.*, 1995). Thus the current model of cell-cycle regulation incorporates an intrinsic redox cycle, which means transient oxidations regulate key proteins and cell-cycle progression or cause an arrest in the proliferation cycle (Menon *et al.*, 2007). This redox-balance provides a powerful mechanism for strategic development of antioxidant defence mechanisms during the cell cycle in animals and plants (Vivancos *et al.*, 2010).

Although expression of several GST genes has been shown to be cell cycle regulated (Takahashi and Nagata, 1992; Menges *et al.*, 2002), the role of GST proteins in the cell cycle is as yet unclear.

1.1.6 Mitosis

Plant cell division has five phases: Prophase, prometaphase, metaphase, anaphase and Telophase and is followed by cytokinesis. In prophase, the chromosomes begin to contract maximally so that they can be seen as double-armed structures held together by cohesin (Kuijt, 2006). Towards the end of prophase, the nuclear envelope breaks down, and mitotic spindles are synthesized, however, they are unable to bind to the chromosomes. Instead, the spindles attach to a specialized protein structure, the

kinetochore. The latter then binds to the centromere (Nigg, 2001). Chromosomes move to the metaphase plate that is the equatorial plane. At this stage chromosomes gather in the central part of the cell and they are held under tension by the mitotic microtubules. At anaphase, chromatids separate. Each set of sister chromatids, which are separating from each other, are once again named as a set of chromosomes. Anaphase can be divided into different parts: Anaphase A: the stage in which microtubules are shortening by the action of microtubules-dependent motors (Kuijt, 2006). Anaphase B: the separation of chromosomes is regulated by separase that is held inactive for most of the cell cycle by securin (Bilou *et al.*, 2002). Separase catalyses the breakdown of cohesin. Here the Anaphase Promotion Complex (APC) also has an important role in degradation of securin that releases separase and also regulates the ubiquitination of B-type cyclins (Hall *et al.*, 2004). This causes their proteolytic destruction in the 26S proteasome (Morris *et al.*, 1976; Passmore *et al.*, 2003). In the eukaryotic APC/C there are at least 13 conserved subunits (Nasmyth, 2005). Most targets of the APC/C are short N-terminal motifs which are called D or KEN boxes (Burton, 2001; Harper, 2002; Passmore, 2003). Cdc20p and Cdh1p are two conserved targeting/adaptor factors which are responsible for linking the APC/C to specific substrates (Pringle *et al.*, 1991; Schott *et al.*, 1998; Thornton *et al.*, 2003).

At telophase, chromosomes move to the pole of cell, and a nuclear envelope reforms around the clustered daughter chromosomes. After this stage chromatin decondensation begins (Kuijt, 2007).

1.1.6.1 Cytokinesis

Plant cytokinesis is the stage in which the construction of a new cell wall is occurring; this wall can form at the centre of the cell or towards one end of the mother cell. In cytokinesis, a

bunch of microtubules which is called the phragmoplast remains at the division plane, the phragmoplast is stabilizing under the expanding cell plate through HINKEL, which is a kinesin-related protein (Strompen *et al.*, 2002). Cytokinesis protein (NACK1) via MAP kinase helps to regulate depolymerization of MTs beneath the cell plate (Nishihama *et al.*, 2002). NACK1 protein accumulates at anaphase and telophase when NPK1 is activated (nucleus and phragmoplast NACK1-like localized protein kinase) (Ishikawa *et al.*, 2002). Degradation of a B-type cyclin is an important factor which affects the timing of cytokinesis (Weingartner *et al.*, 2004). B-type cyclin degradation is dependent on a specific sequence element in its N-terminal region, which is known as the destruction box (D-box) (Glutzer *et al.*, 1991). During anaphase non-degradable cyclin B1 may associate with a B-type CDK (Lee *et al.*, 2003) and in BY-2 cells was shown to disrupt anaphase and telophase (Weingartner *et al.*, 2004). The formation of a phragmoplast was disrupted and separated nuclei were observed because of the deactivation of a cytokinetic kinesin-related protein related to cyclin B1; under these conditions separated nuclei fuse (Weingartner *et al.*, 2004).

1.2 Cell cycle checkpoints

Cell cycle checkpoints arrest the cell cycle during DNA damage or perturbation to nuclear DNA replication (Reviewed by Francis *et al.*, 2003). In higher eukaryotes *ATM* /*ATR* are the cell cycle checkpoint sensors while in *S. pombe* *RAD3* is the sole sensor (Elledge, 1996; Weinert, 1998, Abraham *et al.*, 2000). *ATM* and *ATR* both have been identified in plants (Culligan *et al.*, 2004). In animals, *ATM*/*ATR* are up-stream of *WEE1* and *CDC25* (Elledge, 1996; Martinho *et al.*, 1998; Weinert, 1998; Abraham *et al.*, 2000), and checkpoint protein kinases (*CHK1/2*) are phosphorylated by either *ATM* or *ATR* (Rhind and Russell, 1998). *CHK1/2* does not exist in the Arabidopsis genome (Garcia *et al.*, 2000); hence, it is assumed that higher plants have a different signalling pathway compared with yeast and animals.

As mentioned earlier, in yeasts and animals, the SWE1/WEE1 tyrosine kinases, negatively regulate CDC28/Cdc2. In fission yeast, Wee1 kinase phosphorylate Cdc2 at its tyrosin15 residue. In animals the homologous WEE1 and the unique MYT1, phosphorylate both T14 and Y15 of the CDK. The latter CDK loses its kinase activity and the cell is unable to enter mitosis. Only in favourable conditions does a phosphatase, CDC25, catalyse the dephosphorylation of T14/Y15 on the CDK. The latter regains its activity providing the CDC2 protein is binding with a partner cyclin. Under these conditions, the cell enters mitosis. (Tang *et al.*, 1993✦; Lundgren *et al.*, 1991✦; Millar *et al.*, 1991). In higher animals, MYT1, an additional kinase, also phosphorylates Cdc2 on threonine 14 (T14), although in a different study phosphorylation of this residue was not involved in checkpoint control (Fletcher *et al.*, 2002). Through the activities of Wee1 and Mik1 in response to DNA damage, phosphorylation of Y15 of fission yeast Cdc2 is maintained (Kharbanda *et al.*, 1994; O'Connell *et al.*, 1997; Rhind *et al.*, 1997). In animals, Chk1 via phosphorylation may cause cell cycle arrest in response to DNA damage by stabilising the activity of Wee1 and Mik1 proteins (O'Connell *et al.*, 1997; Baber-Furnari *et al.*, 2000) and inhibiting Cdc25 phosphatase (Peng *et al.*, 1997; Sanchez *et al.*, 1997). The phosphorylated WEE1 kinase and Cdc25 phosphatase are protected from dephosphorylation by 14-3-3 proteins (see above). In *Xenopus laevis*, 14-3-3 proteins together with Chk1 function as positive regulators of Wee1 (Lee *et al.*, 2001). In plants neither Chk1 nor Chk2 exist. Therefore in plants, in to response to DNA damage, WEE1 kinase may be responding to an as yet unidentified CHK1-type protein capable of responding to plant ATM/ATR and in turn capable of regulating WEE1 (reviewed in De Veylder *et al.*, 2007; Francis 2007). In *H. sapiens*, 14-3-3 acts as a positive regulator and stabilizer for Wee1 during the cell cycle by binding to the C-terminal catalytic region of Wee1 (Wang *et al.*, 2000; Rothblum-Oviatt *et al.*, 2001). As mentioned above, the role of CDC25 in the plant cell cycle is unclear but over-expression of *Arath;CDC25* did

accelerate the elongation rate of primary roots of *Arabidopsis*. Whilst T-DNA knockouts of this gene were hypersensitive to HU the over-expressing lines were relatively insensitive to HU. However, the over-expressing lines were as sensitive to a zeocin treatment, or salinity stress as were the *cdc25* KO lines. Hence, *CDC25* may have a role restricted to the DNA replication checkpoint in plants (Spadafora *et al.*, 2011).

However, when *Arabidopsis* is exposed to hydroxyurea, an agent that stalls DNA replication, this induces the DNA replication checkpoint. Zeocin is an agent that mimics DNA damage caused by radiation, and at both checkpoints *WEE1* is highly expressed at the RNA and protein levels (De Schutter *et al.*, 2007). Moreover, treatment of *Arath;wee1* knockouts with zeocin and HU caused a hypersensitive response (De Schutter *et al.*, 2007). This suggest that *Arath;WEE1* has a major role in preventing cells from dividing until the DNA is repaired or until replication is normalised (Boudolf *et al.*, 2006).

1.3 Interaction of WEE1 with other proteins

In budding yeast, an intricate signalling network of kinases including *Gin4*, *Hsl1*, *Cla4* and *Elm1* is required for regulation of *SWE1* which affects cell growth and cell division at G2/M (Altman and Kellogg, 1997; Barral *et al.*, 1999; Carroll *et al.*, 1998; Edgington *et al.*, 1999; Kellogg and Murray, 1995; Longtine *et al.*, 2000; Ma *et al.*, 1996; Shulewitz *et al.*, 1999; Sreenivasan and Kellogg, 1999; Tjandra *et al.*, 1998). Inactivation of this signalling network causes cells to undergo continuous polar growth which causes abnormally large cells during a prolonged G2/M delay, producing highly elongated cells that are abnormally large. Several kinases have been identified in fission yeast and budding yeast for regulation of *Wee1* (Young and Fantes, 1987). The fission yeast kinases

Cdr1/Nim1 and Cdr2 were identified to promote entry into mitosis by inhibiting Wee1 activity (Coleman *et al.*, 1993; Kanoh and Russell, 1998; Parker *et al.*, 1993; Wu and Russell, 1993). Moreover, the yeast two-hybrid system indicated the interaction of Nim1 with Wee1 (Wu, 1997).

A variety of different methodologies have been employed to find interactors between WEE1 and other proteins in animals and yeasts (thebiogrid.org/113303/summary/homo-sapiens/wee1.html, Table 1.1). In humans this has led to the identification of nine unique interactors with WEE1 (Table 1.1).

Table 1.1: Proteins interacting with WEE1 in humans.

(data from thebiogrid.org/113303/summary/homo-sapiens/wee1.html and references therein)

Method	Protein name	function
Affinity capture Western	FBXW11	F-box protein
Affinity capture Western/Far Western	PIN1	Peptidyl-prolyl cis-trans isomerase NIMA-interacting 1, Essential PPIase that regulates mitosis presumably by interacting with NIMA
Affinity capture Western/2-hybrid	YWHAB	14-3-3 protein
Affinity capture Western	UBC	Polyubiquitin-C
Affinity capture Western	SKP2	F-box protein S-phase kinase-associated protein 2
Affinity capture Western	BTRC	F-box protein
Affinity capture Western	CRK	Proto-oncogene
Reconstituted complex	CDCA3	cell division cycle-associated protein 3
Affinity capture-MS	SFN	14-3-3 protein

Three of these are F-box proteins and one is involved in ubiquitination, a process related to proteasome mediated degradation. This fits with the requirement for WEE1 removal at mitosis (McGowan and Russell, 1995). Two other proteins belong to the 14-3-3 family, known to interact with WEE1 and modulate its activity (see section 1.1.5.3). The remaining proteins are related to cell cycle control and hence again interaction with

WEE1 is consistent with the role of WEE1 in cell cycle regulation in human cells. In addition, in human cells, CDC2 can phosphorylate WEE1 (Watanabe *et al.*, 2003).

In plant cells, the role of WEE1 is far less well-defined (as has been discussed above). Some published data on protein-protein interactions with WEE1 is available (Fig 1.3; Table 1.2).

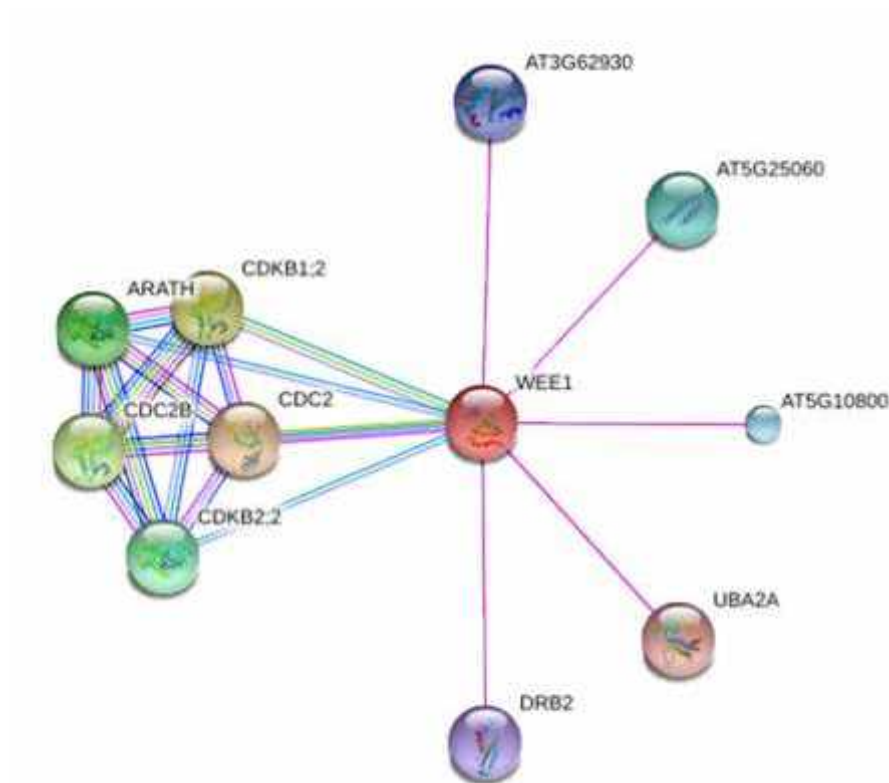


Figure 1.3 Interaction of Arath;WEE1 protein with other proteins in the cell cycle (Adapted from <http://string-db.org>) (Purple lines are based on experimental evidence and details of these proteins are listed in Table 1.2)

Table 1.2 Experimental evidence for protein interactors with *Arath*;WEE1(data from <http://string-db.org>)

Gene name/code	function
CDC2	cyclin-dependent protein kinase
AT5G25060	RNA recognition motif (RRM)-containing protein
AT5G10800	RNA recognition motif (RRM)-containing protein
AT3G62930	glutaredoxin family protein
DRB2	DRB2 (DSRNA-BINDING PROTEIN 2); double-stranded RNA binding
UBA2A	UBP1 interacting protein 2a (UBA2a); encodes a nuclear protein that binds to RNA

In addition, the 2-hybrid technique was used to show that *Arabidopsis* WEE1 interacted with the Non-Epsilon group of 14-3-3 proteins (Lentz Grønlund *et al.*, 2009). In a wider 2-hybrid screen undertaken in the Cardiff lab WEE1 was shown to interact with a much broader range of over 60 different proteins (Table 1.3). Some of these interactions have been verified by bimolecular fluorescence (BiFC) using the split YFP system (Walter, *et al.*, 2004) (Table 1.3), and part of my work focussed on the interaction between GSTF9 and WEE1.

Table 1.3: proteins identified by a 2-hybrid screen (Lentz Grønlund, 2007). Those in bold were further studied using BiFC and the interaction with Arath; WEE1 confirmed.

Transcription factors/ DNAor RNA binding proteins, histone modifications	
At2g18160	bZIPTranscription factor GBF5:
At4g00150	Transcription factor (?) SCL6:GRAS protein, <i>ham</i> family,
At2g33610	SWIRM domain containing protein (chromatin interactions)
AT5G13780	histone modification? GCN5 related N-terminal acetyltransferase, ,
At4g14465	DNA binding protein possible function in positioning of chromatin fibers
AT5G49400	putative role in splicing zinc knuckle (CCHC-type) family protein,
PGRs and Signal transduction	
At1g48480	Receptor kinase gene RLK1
AT1G08980	IAA biosynthesis
At3g07350	Unknown protein,
AT3G22440	hydroxyproline-rich glycoprotein
AT1G64570	Unknown function,
AT5G35570	auxin perception and transduction
Stress responses/ detoxification/ pathogen responses	
At2g41300	Strictosidine synthase:alkaloid biosynthesis
At3g56240	Copper chaperone ATX1:
At2g30860 At2g30870	GST AtGSTF9: Phi class GST cell cycle regulated GST AtGSTF10 phi class GST dehydration induced
At1g04960	Unknown, up-regulated by ozone
At2g40800	Unknown: down regulated by H ₂ O ₂
At1g06040	Zinc finger, salt tolerance protein
At2g37040	PAL1(1)
At4g11650	Osmotin OSM34: role in caesium detoxification
AT1G14730	Cyt B561 protein, transcript salt and osmotic stress induced
AT2G38730	putatively involved in protein folding/stress response
AT1G18970	Germin-like protein, transcripts up-regulated by genotoxic stress
<u>AT4G15610</u>	integral membrane family protein, up regulated by bacterial pathogens
AT4G23680	pathogenesis response
AT5G60640	Possible role in protein folding,

Table 1.3 continued Cell division/cell size/ cell wall and cell growth

At1g05850	Chitinase AtCTL1:Lignin deposition affecting cell shape
At3g09840	Cdc48A: Cell cycle gene, spindle pole body separation,
At3g10220	Tubulin folding co-factor B
At5g62350	Pectin methyl esterase inhibitor family
At4g24780	Pectate lyase family protein
At3g61430	Aquaporin PIP1A: role in cell expansion?
At3g11070	OMP85: mitochondrial membrane biogenesis protein
At3g16640	Loosely bound cell wall protein, tumour family protein
Ribosomes/ protein synthesis	
At4g01560	Brix domain protein:Ribosomal biogenesis
At2g43970	La domain protein:RNA binding proteins associated with polyribosomes
At1g07830	Ribosomal protein
At1g54270	translation initiation factor
At1g56070	E2F
Ubiquitin mediated degradation	
At5g57900	SKP1/SCF interacts with SKP1/ASK1 subunit of SCF ubiquitin ligase
At5g23540	26S proteasome regulatory subunit (1)
At4g39600	F-box family protein
At1g06630	F-box family protein up-regulated in seeds(1)
At1g67340	F-box family protein
other	
AT1G28580	Lipase down regulated by bacterial pathogen elicitor
AT1G29900	carbamoylphosphate synthetase, N metabolism,
AT2G05440	Glycine rich protein: structural role? Protein interactor?
AT2G10950	BSD domain containing protein: could be a transcription factor??
<u>AT2G44100</u>	rab-specific GDP dissociation inhibitor,
AT3G02090	mitochondrial processing peptidase
At3g02470	S-adenosylmethionine decarboxylase - polyamine biosynthesis.
At3g03773	Unknown protein, no info on function or responses
AT3G55410	Mitochondrial protein, oxidoreductase activity,
AT3G55440	cytosolic triose phosphate isomerase (glycolysis) (1)
AT4G27870	integral membrane family protein, unknown function
AT4G31350	Predicted protein of unknown function, no expression info available (1)
AT5G03940	Chloroplast Signal Recognition Particle Subunit,
AT4G22920	Chloroplast protein unknown function.
AT5G43330	cytosolic malate dehydrogenase, <u>tricarboxylic acid cycle intermediate metabolism</u> (1)

1.4 Experimental Aims

The main focus of my work has been to further investigate the regulation of WEE1 function in plants. As discussed above, in animal and yeast cells a complex network of regulatory proteins has been unravelled that controls WEE1 function. In plants very little is known about the regulation of WEE1 activity. Two-hybrid screens have revealed numerous interacting proteins (Lentz, 2007, <http://string-db.org>), however the function of these interactions is unknown.

I became interested in the extent to which the two proteins, *Arath*;WEE1 and GSTF9, might interact in the cell cycle in whole plants both in normal and genotoxic environments. I investigated the extent of this interaction by studying phenotypic responses of T-DNA insertional mutants for *Arath*;WEE1 and *GSTF9* following exposure to hydroxyurea (HU) and zeocin, treatments that induce the DNA replication and DNA damage checkpoints, respectively. By making the double mutant, *wee1-1 gstf9*, and analysing its root phenotype following HU and zeocin treatments, I was also able to test the extent to which the interaction of *Arath*;WEE1 and *GSTF9* on rooting phenotype was additive under either normal or checkpoint conditions.

Previous work in Cardiff had shown that in yeast two-hybrid assays, *Arath*;WEE1 interacted with 14-3-3 protein GF14 ω (Lentz *et al.*, 2009). Moreover, mutation of the WEE1 protein at residue 485 (S485A) abolished binding between WEE1 and 14-3-3 ω both *in vivo* and *in vitro* (Lentz *et al.*, 2009). I investigated this aspect of cell cycle control further by examining phenotypic responses of a line created by crossing a T-DNA insertional line for *WEE1*, *wee1-1*, with a GF14 ω over-expressing line. My hypothesis was that over-expression of GF14 ω would result in a similar phenotype to over-expression of

Arath;WEE1 due to a stabilising effect on the WEE1 protein. Furthermore I also hypothesised that this effect would be abolished in the absence of a functional WEE1 protein as is the case in the *wee1-1* insertion mutants.

Finally, I followed up an unusual observation made in the Cardiff lab. Siciliano (2006) found that expression of the Arabidopsis *WEE1* in tobacco BY-2 cells induced a small as opposed to a predicted large cell size phenotype, and a premature as opposed to a delayed entry into mitosis. I tested the hypothesis that Arabidopsis *WEE1* in a tobacco genetic background might have resulted in these perturbed the cell cycles. To do this I examined the phenotype of transgenic lines in which Arabidopsis *WEE1* was expressed in tobacco and the converse, tobacco *WEE1* in Arabidopsis. In this way, I further tested whether the tobacco *WEE1* would have the same effect in the Arabidopsis genetic background.

2. General Materials and Methods

2.1 Plant materials

Plants used in this work are listed in Table 2.1.

Table 2.1 Transgenic and mutant lines used in this work

Name	Description/use	Origin and reference	Plant species
<i>Arath;WEE1^{oe}</i>	<i>Constitutive Arath;WEE1^{oe}</i>	Cardiff lab collection; Bohner <i>et al</i> (1999)	<i>Arabidopsis</i> Origin Cardiff lab
NT-Arath;Wee1	<i>Arath;WEE1</i> ORF fused to the C- terminal portion of YFP driven by 35S promoter. Used to express <i>Arath;WEE1</i> in tobacco plants	Walter <i>et al.</i> (2004); Lentz Grønlund <i>et al.</i> (2009)	Tobacco Origin Cardiff lab
At Nt;WEE1	<i>Nicta;WEE1</i> ORF driven by an inducible promoter. Used to express <i>Nicta;WEE1</i> in <i>Arabidopsis</i> plants	Cardiff Lab (unpublished)	<i>Arabidopsis</i> Origin Cardiff lab
<i>wee1-1</i> (GABI_270E05)	T-DNA insertion 7 th intron	Alonso <i>et al.</i> (2003); De Schutter <i>et al.</i> (2007)	<i>Arabidopsis</i> Origin NASC, UK
<i>gstf9</i>	T-DNA insertion 2 nd intron	Dixon <i>et al.</i> , (2002)	<i>Arabidopsis</i> Origin NASC, UK

2.2 Media and Antibiotics

Table 2.2 Media used in this work are listed in Table 2.2.

Organism	Medium	Recipe
<i>Arabidopsis</i>	MS medium	4.708 g ^l ⁻¹ MS basic salts (Duchefa), 30g ^l ⁻¹ Sucrose, 10g ^l ⁻¹ bacto agar
<i>Tobacco</i>		

2.3 PCR

A master mix with a volume of 24 μ l for each sample was prepared including 2.5 μ l of 10x PCR buffer (100 mM Tris-HCl pH 8.8, 200 mM KCl, 15 mM MgCl₂), 0.5 μ l of 10mM dNTPs, 1 μ l of each required primer (10 μ M), 0.125 μ l of Taq polymerase which is purified in house within the Cardiff Laboratory and 18.9 μ l of autoclaved SDW .

The master mix was pipetted (24 μ l) into a sterile labelled Eppendorf tube. For PCR 1 μ l of genomic DNA was used as template to make a 25 μ l reaction. The standard PCR programme was as follows: 1 cycle for initial denaturation for 3 min at 95°C; 40 cycles of denaturation for 1 min at 95 °C; annealing for 1 min at 55 °C; extension for 1 min 72 °C; 1 cycle of final extension for 5 min at 72°C. Primers used in this project are listed in Table 2.3.

Table 2.3 PCR primers used for this work. All primers used were purchased from SIGMA-GENOSYS, UK.

Primer name	Sequence	bp
1 AtWEE1 fw	AGCTTGTCAGCTTTGCCT	18
2 AtWEE1 rv	TCAACCTCGAATCCTATCA	19
3 PUV2	TTCCATGCTAATGTATTCAGAC	22
4 PUV4	ATGGTGGTGACGGGTGAC	18
5 35STRS	ACGCTGAAGCTAGTCGACTC	20
6 14-3-3 RV	ACTCGGATCCTCACTGCTGTTCCCTCGG	27
7 P4b	GAAATCATTCAAATTCTACCTGGTC	25
8 p6	ATATTGACCATCATACTCATTGC	23
9 T-DNA	CGCGTTCAAAGTCGCCTAAG	21
10 GST9F	GTGCTAAAGGTGTACGGAC	19
11 GST9R	TGACCTGTACTTCTCAGCTAC	20

2.4 Agarose gel electrophoresis

For 1% gels, 0.5 g of agarose (Bioline) was added to 50 ml of 1x TAE buffer (50 x : 242 gl^{-1} Tris, 100 ml l^{-1} 0.5M NaEDTA pH 8.0, 57.1 ml l^{-1} glacial acetic acid). Then the solution was mixed and microwaved on top power for approximately 1-2 min checking every 10-20 seconds until all the agarose had dissolved. After cooling down to approximately 50°C, 5 μl of ethidium bromide (10 mg ml^{-1}) was added. The gel was poured in a tray and when

set, the tape was removed and the gel tray was placed in the running tank and covered completely by 1 x TAE buffer. The gel was loaded with sample mixed with 1/10 volume of loading buffer (50 mM Tris-HCl pH.7.6, 60% glycerol, bromophenol blue). 10 μ l (250-500 ng).Marker (10 μ l) of 1 kb DNA ladder (Invitrogen) was loaded in to the first well, before loading 10 μ l of each sample into the remaining wells and run in 1x TAE buffer at approximately 100 V. Afterwards, the DNA was detected by the UV light using a Genius Bio imaging System (SYNGENE LTD).

2.5 DNA extraction from leaf discs

DNA was extracted from leaf discs essentially as described by Edwards *et al.* (1991). Leaf tissue (10-50 mg) was ground with a sterile Eppendorf grinder for approximately 2 min in a sterile Eppendorf tube. Sterile extraction buffer (200 μ l of 0.5 % SDS, 250 mM NaCl, 100 mM Tris-HCl pH 8.0, 25 mM EDTA) was added to the Eppendorf tube and left for 5 min; afterwards, the extract was centrifuged at top speed in an Eppendorf MiniSpin centrifuge for 5 mins. The supernatant was removed and 150 μ l of it added to 150 μ l of isopropanol, mixed and placed on ice. The mixture was centrifuged for 10 min. The supernatant was carefully removed. The pellets were air dried at 60 °C for 5-10 min. Pellets were resuspended in 100 μ l of TE (10mM Tris-HCl pH 8.0, 0.1 mM EDTA) and samples were stored at 20 °C. The extract (1 μ l) was used in 25 μ l PCR reactions.

2.6 RNA Extraction

Leaf RNA was extracted by grinding 200 mg of tissue in liquid N₂ in a mortar and pestle that had been pre-cooled at -20°C. Tri Reagent (SIGMA) (2 ml) were added to the ground tissue. Then the liquid was divided into two 1.5 ml Eppendorf tubes, the tubes were

vortexed for 5s, left at room temperature for 5 min, and then they were centrifuged in a BECKMAN Coulter Allegra 21R centrifuge with a F2402H rotor for 15 min at 12000 rpm, at a temperature of 4°C. The supernatant was transferred to fresh sterile Eppendorf tubes and chloroform (0.2 ml) was added. Following vortexing for 15 seconds the tubes were then incubated at room temperature for 5 min. The samples were then centrifuged for 15 min at 12000 rpm, 4 °C as above and the supernatant transferred to a fresh Eppendorf tube. Isopropanol was added (500 µl), and following mixing, incubated for 10 min at room temperature. The samples were centrifuged again as above, the supernatant was removed and the pellet washed in 1 ml of 75% ethanol and vortexed for 5s. The pellets were then air dried for 30 min. The pellets were re-suspended in 50 µl of SDW and the contents of the two tubes combined. The extracted RNA was stored at -80 °C but prior to freezing 10 µl was checked by agarose gel electrophoresis. To ensure removal of contaminating RNAses, the tank, gel tray and comb for the gel electrophoresis were treated for 1 h with 0.1M NaOH and then washed copiously with SDW.

2.7 DNase treatment and cDNA synthesis

DNase treatment was carried out by mixing 5 µg of RNA with 1x RQ1 DNase buffer (400 mM Tris-HCl pH 8, 100 mM MgSO₄, 10 mM CaCl₂) 1 U RQ1 DNase (PROMEGA), and SDW was added to reach the final volume of 20 µl, Then the tubes were incubated at 37°C for 30 min. After 30 min 2 µl of RQ1 DNase stop solution (20 mM EGTA pH 8.0) was added, and the samples incubated at 65°C for 10 min.

RNA was used for cDNA synthesis. DNase treated RNA (1 µg) was mixed with 500 ng of Oligo(dt)15 primer (PROMEGA), and made up to a final volume of 20 µl. The samples were incubated at 70°C for 10 min in a PTC-100 Thermocycler and then cooled on ice for 10 min.

Then 6 μ L 5x M-MLV RT buffer (250 mM Tris-HCl pH 8.3, 375 mM KCl, 15 mM MgCl₂, 50 mM DTT), 2 μ l 0.1 M DTT and 1 μ l 10 mM dNTP mix were added and the reaction was incubated at 42°C for 2 min. M-MLV Reverse Transcriptase RNase H Minus (200 U) (PROMEGA), were added and the samples were incubated for 50 min at 42°C. The samples were heated at 70°C for 15 min. The synthesized cDNA was checked by PCR and stored at -20°C.

2.8 Protein extraction from plant tissue

Protein extraction was carried out from leaf material that was ground to a powder in liquid N₂ in a mortar and pestle pre-cooled at -20°C. The powder (1-2 ml) was transferred to a 14 ml tube on ice and the following were added: 986 μ l lysis buffer (50 mM Tris-HCl pH. 7.5, 75 mM NaCl, 15 mM EGTA, 15 mM MgCl₂, 60 mM β -glycerophosphate), 42 μ l 25x PI (one complete protease inhibitors (Roche) dissolved in 2 ml SDW and filter sterilized), 21 μ l 50x PPI (50 mM NaF, 10 mM Na₃VO₄, 100 mM Na₄P₂O₇) and 1 μ l 1M DTT. A Soniprep 150 sonicator (MSE) was used to homogenize the samples with four bursts of 30 s. The samples were placed on ice for 30s between each sonication. The samples were then transferred to pre-chilled Eppendorf tubes and centrifuged in a Beckman Coulter AllegraTM 21R centrifuge with a F2402H rotor for 30 min at 14000 rpm, 4°C. The supernatant was stored at -80°C in 100 μ l aliquots.

2.9 Bradford assay

A Bradford Assay was carried out to measure the concentration of protein extracts (Bradford, 1976) making sure that Bradford Reagent (Sigma) was mixed gently in the bottle and brought to room temperature before use. BSA protein standards with the range of 0.1 – 1.4 mgml⁻¹

were prepared in an appropriate lysis buffer. The protein standards (5 μ l) were added to a multi-well plate in separate wells alongside 5 μ l of each sample. Bradford Reagent (250 μ l) was mixed with the sample in each well for 30 s, and reactions were incubated at room temperature for 5 min. The absorbance of the proteins was measured at 570 nm, and it was then plotted against the protein concentration of each standard. From the standard curve the protein concentration of the unknown sample was determined.

2.10 SDS-PAGE

The SDS-PAGE separation gel was made by mixing the following: 3.3 ml of 40% acrylamide/*bis*-acrylamide (MELFORD LABORATORIES), 4.4 ml of 2.5x separation buffer (1.875 M Tris-HCl, pH 7.5, 0.25% SDS), 3.3 ml of SDW, 100 μ l of 10% ammonium persulfate (APS), 10 μ l of N,N,N',N'-tetramethyl-ethylenediamine (TEMED) (SIGMA) and divided between two sets of glass plates. The stacking gel was made by mixing the following: 0.56 ml 40% acrylamide/*bis*-acrylamide (37.5:1), 0.66 ml 5x stacking buffer (0.3 M Tris-HCl, pH 6.7, 0.5% SDS), 2 ml SDW, 30 μ l 10% APS, 5 μ l TEMED and was cast on top of the separation gel. Samples were prepared by adding an appropriate amount of 5x loading buffer (250 mM Tris-HCl pH. 6.8, 10% SDS, 30% glycerol, 0.5 M DTT, 0.02% bromophenol blue) and were boiled for 5 min before loading onto the gel. The gel was then run in 1x Laemmli buffer (10x: 10 g l^{-1} SDS, 30.3 g l^{-1} Tris base, 144.1 g l^{-1} glycine) at 100 – 200 V. and proteins were detected by staining with Coomassie Brilliant Blue (2.5 g Coomassie Brilliant Blue staining R-250 (Sigma), 450 ml EtOH, 100 ml acetic acid, 450 ml SDW). PageRuler™ pre-stained protein markers (FERMENTAS) were used as a marker for the SDS-PAGE.

2.11 Western blotting

A Hybond-P PVDF membrane (AMERSHAM PHARMACIA BIOTECH) was pre-wetted in 100% MetOH for 30 s then rinsed in SDW for 5 min. Then the membrane, sponges, filter paper and SDS gel were all soaked in blotting buffer (20% MetOH, 0.01% SDS, 14 gl^{-1} glycine, 3 gl^{-1} Tris base) for 15 min. The sponge, filter paper, SDS gel, PVDF membrane, filter paper and sponge were assembled into the cassette of a Mini-Trans Blot[®] Western Blotting system (Bio-rad), and placed in the gel tank which was filled with blotting buffer. To effect the transfer, 0.35 mA were applied for 1 h. After 1 h the cassette was removed and the PVDF membrane soaked in 25 ml blocking solution (20 mM Tris-HCl pH 7.5, 150 mM NaCl, 0.05% Tween-20, 5% dry milk powder) for 1 h on a shaking platform. The primary antibody (NtWEE1 (1:1000) (Sigma; Lentz Grønlund *et al.*, 2009) in the blocking buffer was added to the membrane and incubated on the shaking platform for 1 h. The membrane was then washed three times with wash buffer (20 mM Tris-HCl pH 7.5, 150 mM NaCl, 0.05% Tween-20, 1% Triton[®] X-100), once for 15 min and twice for 5 min. The membrane was then incubated with the blocking buffer including the secondary antibody (-rabbit IgG (1:2500) (Sigma)) in a 25 ml volume and on the shaking platform for 1 h. Then the membrane was rinsed with wash buffer three times: once for 15 min and twice for 5 min. The membrane was carefully placed on cling film and 0.125 ml cm^{-2} of ECL solution (Amersham Pharmacia Biotech) (Western blotting detection reagents in a ratio of reagent1: reagent2, 50:50) were pipetted onto the membrane. The detection reagent was then removed and the membrane was wrapped in cling film and exposed to Hyperfilm[™] ECL (AMERSHAM BIOSCIENCE) in an X-ray cassette (GRI MOLECULAR BIOLOGY) from 20 s to overnight. The film was developed using a Curix 60 developer (AGFA).

2.12 Sterilization of *Arabidopsis* seeds

Wild type and transgenic *Arabidopsis* seeds were surface-sterilized by adding 1 ml of bleach solution (1:10 dilution of hypochlorite) to each tube of seeds. The tubes were inverted and then seeds allowed to settle for 5 min. The bleach solution was removed and 1 ml of ethanol mix (21 ml of ethanol, 3 ml of hypochlorite and 6 ml of SDW) was added to each Eppendorf tube for 5 min. The ethanol mix was removed and 1 ml of SDW was added to each Eppendorf for 5 min. Then the seeds were washed three times in 1 ml of SDW. The seeds were sown on Petri dishes containing solid MS medium (see Section 2.2) using a pipette. To induce germination, the seeds were stratified by placing the plates at 4°C for 24-48 h. After that plates were transferred to a SANYO growth cabinet at 22 °C with 16 h light and 8 h dark per day. For phenotypic analyses seeds were sown in a line of about 5 seeds at one end of the Petri dish and Petri dishes were placed in a vertical system such that roots grew along the surface of the solid medium.

2.13 Fixing the roots

After 10 days growth in the incubator, 8 ml fixative solution (3:1 (v/v) absolute ethanol: glacial acetic acid) was added to each plate before wrapping in cling-film and storing at 4°C for 24 h.

2.14 Staining the roots

Seedlings were washed for 5 min by adding 8 ml of H₂O directly to the agar plate. After that the water was removed, 8 ml of 5 M HCl was added and the plates incubated for

exactly 25 min at 25 °C, and subsequently washed twice with 8 ml ice-cold SDW for 5 min. After the wash, 8ml of Feulgen stain (BDH CHEMICALS Ltd) was poured onto the plate and the seedlings were incubated for 2 h at room temperature.

2.15 Measuring primary root length, number of lateral roots, length of meristem and cell size of epidermal meristem cells

Primary root length was recorded as the distance between the junction of the base of the primary root/hypocotyl to the root tip. Arabidopsis seedlings were Feulgen-stained as above (BDH CHEMICALS Ltd). To avoid damaging lateral roots, seedlings were not removed from the agar. Roots were analyzed by light microscopy using an Olympus BH2 microscope equipped with a x10 objective. Firstly, the number of lateral roots and lateral root primordia were scored. Then, root apical meristem length was estimated as the distance between the apex of the meristem to the basipetal border between intensely staining-to- lightly stained tissue. Finally, using the x40 objective, the number of epidermal cells were counted along the contour of the RAM. This enabled a calculation of epidermal cell length in the meristem as length of meristem divided by the number of epidermal cells that spanned that meristem. The SPSS 15 statistics program was used to analyze the data.

2.16 Growth of *Arabidopsis* plants in soil

Arabidopsis seeds were sown in pots containing moist compost, left for 24 h at 4°C to ensure uniform germination and then placed in a SANYO-GALLENKAMP growth chamber at 21°C, 16 h light (300-400 $\mu\text{mol m}^{-2} \text{s}^{-1}$) and 8 h dark (standard condition). Plants for seed collection were grown in the same pot until formation of siliques. Before

the siliques became yellow when they were still green, leaf material was collected for DNA, RNA or protein extraction.

2.17 Sterilization of tobacco seeds and growth in sterile conditions

Tobacco seeds were sterilized by adding 1 ml of 1:10 dilute bleach solution to each Falcon tube of seeds. The tubes were inverted and then left for 5 min. The bleach was removed and 1 ml of ethanol mix (ethanol: hypochlorite: distilled water in a ratio of 7:1:2) was added to each Eppendorf for 5 min. Three drops of Tween-20 were added to the ethanol mix prior to use. The ethanol mix was removed and 1 ml of SDW was added to each Eppendorf and left to stand for 5 min. Then the seeds were washed three times in 1 ml of SDW. After the third wash, water was not removed from the Eppendorf and seeds were settled for 2 h, then the seeds were poured onto a sterile filter paper, and by using sterile forceps 5 seeds were placed on appropriately labelled MS plates. Each plate was wrapped in cling film and placed at 4°C for 24 h. Plates were transferred vertically into an incubator exposed to 16 h of light at 20 °C and seeds were left to germinate. After four weeks the phenotype of these seedlings was analysed.

2.18 Crossing Arabidopsis plants

For crossing Arabidopsis lines, seeds were surface-sterilised and sown as described in Section 2.14 then grown horizontally in a SANYO growth cabinet in conditions of 22 °C with 16 h light and 8 h dark per day. When the seedlings had 4-6 leaves they were transferred carefully using forceps into pots and watered. A transparent cover (cloche) was put over the pots for a few days, and then the cloche was removed and they were watered as normal. When the plants had a fully formed rosette, but before they started to flower, a

small portion of a leaf was taken and DNA was extracted to confirm the genotype. Flowers not yet open but with a mature stigma were selected under the dissecting microscope and used as targets for the crossing. Flowers were selected for crossing as the male parent which were just open with yellow anthers, and then under the dissecting microscope with fine forceps immature flowers (small and green), the sepal, petal and opened flowers were removed from the plant. The anthers of plant used as the male parent were brushed on the stigmas of plants used as the female parent in which anthesis had not yet occurred. All anthers were removed from the female parent flower prior to crossing. Crossed flowers were marked, and were left to set seed. When the siliques became yellow, seeds were collected and following seed germination, seedlings were checked by PCR.

2.19 Mitotic index measurements

The mitotic index, the sum of prophase, metaphase, anaphase and telophase mitotic figures as a percentage of all cells, was measured for a minimum of 100 cells per slide in a random transect. Cells and mitotic figures were visualized using a fluorescence microscope (OLYMPUS BH2, UV, $\lambda=420\text{nm}$).

2.20 Statistical analysis

The data were analyzed using SPSS (version 14[®]), Significant interactions were detected using t-test and chi square tests.

3. The interaction of *wee1-1* and *gstf9*

3.1 Introduction

wee1-1 is a T-DNA insertion line carrying an insertion in the *Arath;WEE1* (AT1G02970) gene and originates from the SALK collection of T-DNA insertion lines (Alonso *et al.*, 2003). This insertion allele carries the T-DNA insertion in the seventh intron and has been characterised by De Schutter *et al.* (2007) (see also Fig. 3.1). The *wee1-1* line has two major phenotypes: 1) it is hypersensitive to hydroxyurea (HU) compared to WT; 2) it produces more lateral roots than WT (Lentz Grønlund, 2007).

Arath;WEE1 was used as a probe in a 2-hybrid screen to identify a number of interacting proteins including *GSTF9*. The interaction was confirmed by BiFC and found to occur in the nucleus (Lentz Grønlund, 2007, Cardiff Laboratory unpublished data).

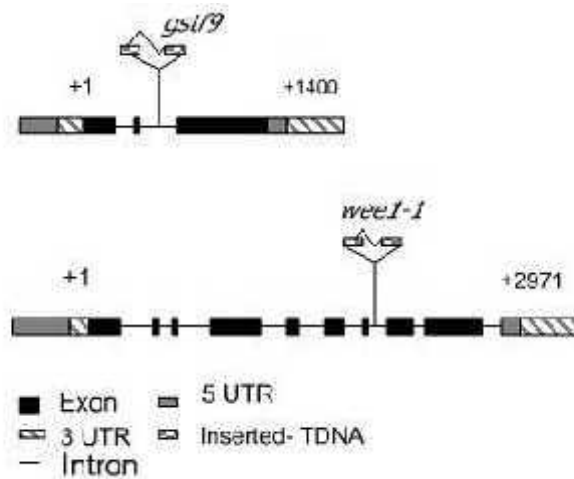


Figure 3.1 Schematic Diagram of the gene map of *GSTF9* and *Arath;WEE1* genes (to scale) with USS/promoter (grey), exons in black, intron (thin black line), and 3' and 5' UTRs with the position of the T-DNA insertion.

Arabidopsis GSTF9 (AT2G30860) encodes a glutathione S-transferase (GST), important enzymes of glutathione metabolism (Dixon *et al.*, 2002). *GSTF9* is from the phi class of GSTs, and is a member of a pair of GST genes *GSTF9* and *GSTF10* which share a high level of homology and form a tandem array on chromosome 2 (Dixon and Edwards, 2010). *GSTF9* is expressed at high levels in most tissues (Wagner *et al.*, 2002) with high expression in leaves, and the shoot apical meristem (TAIR; <http://arabidopsis.org/index.jsp>). Together *GSTF6*, *7*, *9* and *10* contribute 65% of the transcript pool in seedlings and 50% in roots and leaves (Sappl *et al.*, 2008). A T-DNA insertion line for *GSTF9* (SALK_001519) was found not to have a clear phenotype (Sappl *et al.*, 2008) and RNAi of four phi class GSTs including *GSTF9* (*GSTF6,7,9* and *10*) also did not elicit any striking phenotypic traits (Sappl *et al.*, 2008). However in another report (Dixon and Edwards, 2010) RNAi knockdown lines of *GSTF9* and *GSTF10* were found to have more compact rosettes, increased levels of anthocyanins and an increased sensitivity to salt and chemical stresses.

All GST classes have a conserved gene structure. The phi class of GSTs have two introns (Wanger *et al.*, 2002) (Fig. 3.1). In the current work the insertion mutant studied was derived from the JIC Suppressor Mutator collection and was reported to have an insertion in the second intron which would be 64 amino acids into the open reading frame. GSTF9 is from the phi class of GSTs, and the phi class of GSTs have two introns (Wanger *et al.*, 2002).

In my study, hydroxyurea (HU) and zeocin were used to induce the DNA replication and DNA damage checkpoints respectively. HU inhibits the enzyme ribonucleotide reductase, arresting cells during S-phase (Eklund *et al.*, 2001). Zeocin is a member of the bleomycin/ phleomycin family of antibiotics isolated from *Streptomyces*. Zeocin is a water soluble, copper-chelated glycopeptide; this copper-chelated form is inactive (Calmels *et al.*, 1991; Drocourt *et al.*, 1990; Gatignol *et al.*, 1987; Mulsant *et al.*, 1988; Perez *et al.*, 1989). When the antibiotic enters the cell, the copper cation is reduced from Cu^{2+} to Cu^{1+} and then removed by sulfhydryl compounds in the cell. Upon removal of the copper, zeocin is activated and will bind to DNA and cleave it (Berdy, 1980). Zeocin induces chromosomal DNA breaks in *Arabidopsis* (Trastoy *et al.*, 2005).

Very little is known about DNA surveillance systems in plants. However, recently, in *Arabidopsis*, by using knock-out mutants in genes encoding the ATM and ATR kinases (see Introduction Section 1.2), it was demonstrated that the DNA replication checkpoint is routed through ATR while the DNA damage checkpoint is through ATM (Garcia *et al.*, 2003; Culligan *et al.*, 2004). The *atr* mutant is insensitive to replication blocking agents like HU but it is hypersensitive to DNA damaging agents, such as gamma irradiation (Garcia *et al.*, 2003). In contrast, The *atm* mutant is hypersensitive to gamma irradiation and relatively insensitive to HU (Culligan *et al.*, 2004). De Schutter *et al.* (2007) showed that transcript levels of *Arath;WEE1* increase upon HU or zeocin treatment in an ATM/ATR dependent

manner. This makes *Arath;WEE1* a down-stream target gene of the ATM/ATR signalling cascade.

3.2 Aims

Part of my thesis is aimed at a better understanding of cell cycle checkpoints (see Section 3.1). Given the interaction between *Arath;WEE1* and *GSTF9* proteins, the hypothesis is that the interaction of the two proteins may be functional in the DNA replication and damage checkpoints (Fig 3.2). To test this hypothesis, the response of *wee1-1* and *gstf9* insertion lines to HU and zeocin was examined. Hence, the aims of the work reported in this chapter were to examine:

- Root phenotypes of the *wee1-1* and *gstf9* mutants in response to HU and zeocin compared to wild type. As previous studies showed repression in root growth of *wee1-1* plants treated with HU, I examined whether this was so following a zeocin treatment. If *GSTF9* is also implicated in the DNA replication/DNA damage checkpoint, I would also expect a similar repression in primary root length and total number of lateral roots and primordia in *gstf9* plants following HU and zeocin treatment.
- The effect of HU and zeocin on the component phases of the cell cycle in *wee1-1* and *gstf9* mutants. The hypothesis was that increasing concentrations of HU resulted in increases in the percentage of cells in G1, and, consequently, a decrease in the percentage in S-phase cells, the presumed role of *WEE1* in the cell cycle provides the expectation that *wee1-1* plants have a higher cell number and shorter cell length.

- I also made a cross between *wee1-1* and *gstf9* to generate the double recessive mutant. This could then be used to establish whether the phenotypic effects of the two mutations were additive. If the interaction of the proteins is important in modulating the function of one or both of them (Fig. 3.2) one would not expect an additive effect. If however the protein-protein interaction is not in fact functional and the phenotypes of the mutants are independent of each other then the expectation is that the effects would be additive in a double mutant.

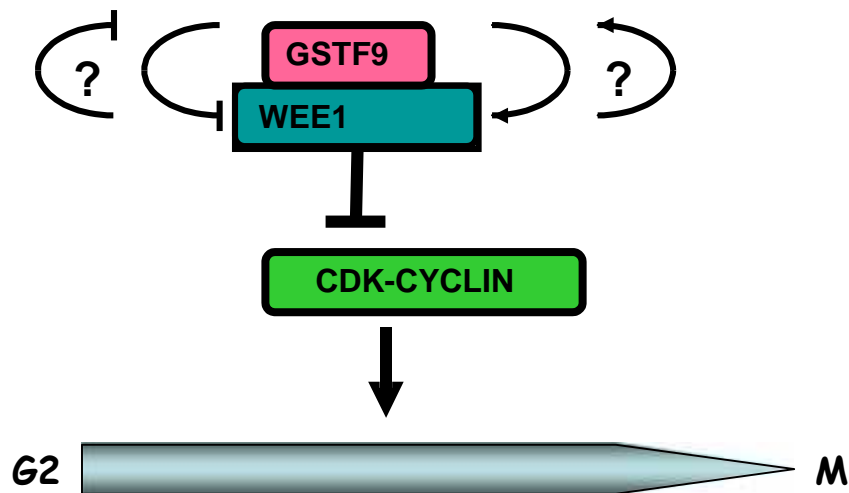


Figure 3.2 Can the interaction between GSTF9 and WEE1 be important for modulating the activity of either enzyme?

3.3 Materials and Methods

3.3.1 Arabidopsis lines

A homozygous line for the *gstf9* T-DNA insertion mutant, which carries the T-DNA insertion in the second intron (Fig. 3.1), was donated to our lab by Prof. Rob Edwards (Durham University). The *wee1-1* line was obtained from the GABI-KAT T-DNA insertion collection (GABI_270E05) from NASC, and a homozygous line had been previously derived in the Cardiff Lab. WT and mutant (*wee1-1* and *gstf9*) Arabidopsis *thaliana* cv. Columbia lines were maintained by selfing of plants grown at 20°C with 18h light, 6 h dark.

3.3.2 Growth of Arabidopsis lines on agar

Media contained different concentrations of HU: 0, 1 or 2 mM. To prevent HU from degradation, it was added to MS medium after autoclaving. Stocks containing different concentrations of HU as above were prepared and added to the medium using sterile pipettes. Surface sterilization of the seeds is described in the General Materials and Methods Chapter, Section 2.3.

Also another medium which contained different concentrations of zeocin 0, 5, 10, 20, and 50 μ M was prepared. Zeocin was added to the MS medium after autoclaving.

Seeds were sown in a line of about five seeds at one end of 90 mm diameter Petri dishes which were placed vertically (Fig. 3.3) so that roots grew vertically down along the surface of the solid medium.

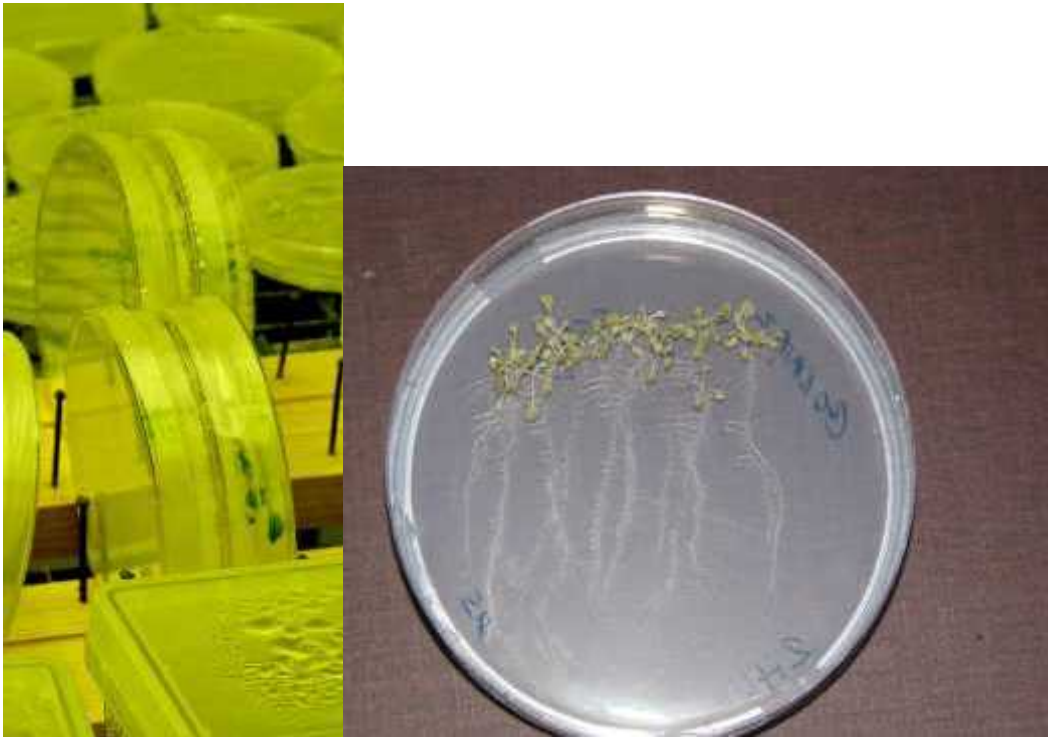


Figure 3.3 Plants growing vertically for measuring phenotypic traits (diameter of Petri dishes = 90 mm)

Roots were stained and fixed (see General Materials and Methods Chapter, Sections 2.15 and 2.16), and root phenotypic analysis was performed on 10 day old wild type and mutant seedlings by light microscopy using an Olympus BH2 microscope equipped with a 40X objective.

3.3.3 Microdensitometry

Roots were fixed and stained by the Feulgen reaction (see General Materials and Methods Section 2.14). Using a fine-point needle, the intensely staining part of the root tip (meristem) was dissected into a small droplet of 45% (v/v) acetic acid on a microscope slide. A coverslip was applied and tapped gently to create a monolayer of stained cells. Slides were then placed on frozen CO₂, until the coverslip frosted over. The coverslip was then flicked off with a single edge razor blade. The slides were then stacked into glass holders and passed through the following reagents each for 10 min:

45% acetic acid, SO₂ water (twice), and then an alcohol dehydration series (from 10% at 20% increments through to 100% ethanol). The latter rinse was repeated and finally, the slides were rinsed in xylene (twice) before a fresh coverslip was reapplied to the squash preparation using DPX-mountant. Slides were left to dry in darkness for a minimum of 24 h. Each slide was then analysed using a Vickers (UK) M85A integrating scanning microdensitometer at spot size 1, a wavelength of 570 nm with a band width of 80 nm. Each nucleus in the preparation was positioned centrally under bright-field illumination and then scanned in darkness (scanning time = 10 seconds). Absorbance values were then recorded following each scan. For each slide, the relative nuclear DNA amounts of Feulgen-stained nuclei were scored normalised to C values against densities of internal mitotic standards: prophase = 4C, and half-telophase = 2C (where 1C is the amount of nuclear DNA in an unreplicated haploid nucleus of a gamete). Several slides per genotype were analysed in this way with the cumulative number of nuclei being approximately 100 to 150 nuclei per genotype. Because each slide was normalised with internal standards, the densities of interphase nuclei, for several slides per genotype, could be plotted on a unified 2C 4C X-axis and presented as percentage frequencies per genotype. In addition, the mitotic index was measured for each preparation per genotype (see general General Materials and Methods Chapter Section 2.21).

The percentage frequency of cells in G1, S-phase and G2 were then calculated according to the following range of DNA C values: 1.6-2.2C = G1, 2.2-3.6 C = S-phase, 3.6-4.4C = G2, >4C = polyploid. These ranges are *normal* microdensitometric distributions for proliferative cells of meristems in each of these phases (Francis D. unpublished data). The mitotic index (% frequency of cells in mitosis) was also scored for each preparation and added to the total percentage obtained by microdensitometry. For example, a mitotic index of 4% on a given slide would be added to the 100% of interphase nuclei and the above-mentioned percentages in G1, S, and G2 corrected by dividing each value by 104.

Thus, the proportion of cells in each stage of interphase was corrected according to the true frequency of cells in each phase of the cell cycle. The percentage frequency histograms were then analysed statistically using contingency chi square.

3.4 Results

3.4.1 Genotyping and expression analysis of the *gstf9* insertion allele

Firstly the position of the DNA insertion in the *gstf9* mutant was checked by PCR. PCR products of the expected size were obtained (sequence details of the primers are in the General Materials and Methods Chapter, Table 2.3) thus confirming the position of the T-DNA insertion (Fig 3.4a and b). Seedlings were confirmed to be homozygous for the insertion.

Then the *gstf9* insertion mutant was checked by RT-PCR (Fig. 3.4c) which showed that although there was no transcription using primers for the WT *GSTF9* gene, there is some transcript produced even in the homozygous *gstf9* mutant revealed using primers from within the T-DNA insertion and the 3' end of the gene.

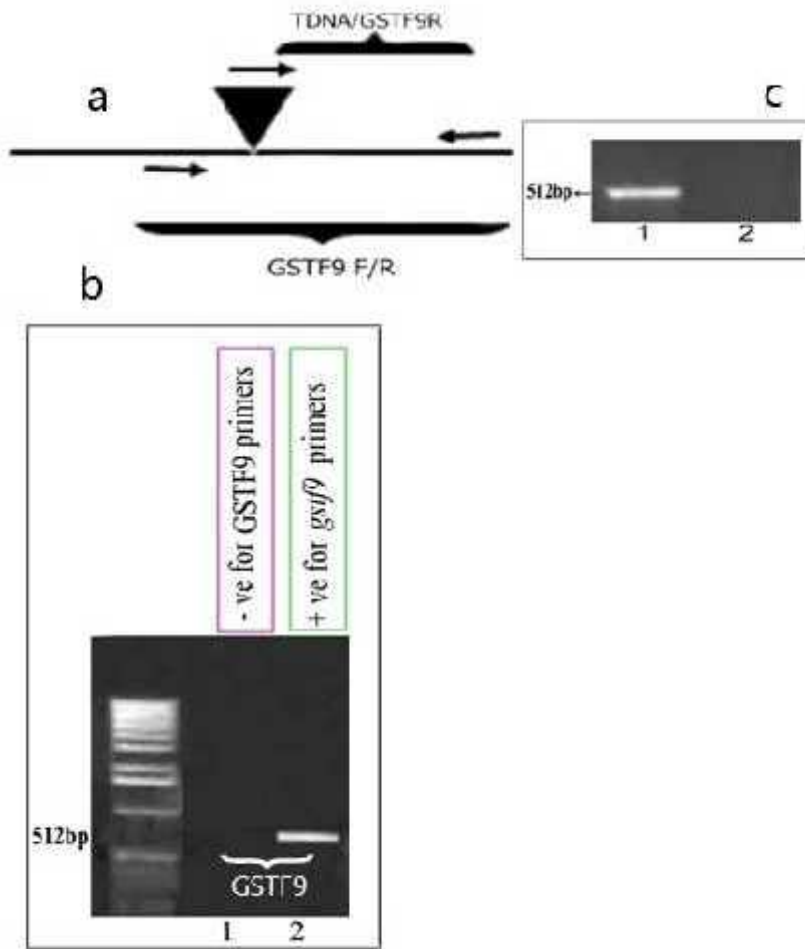


Figure 3.4 Genotyping of T-DNA lines (a) Schematic diagram of primer design for the *gstf9* gene: TDNA/GSTF9R positive for mutant, negative for WT, and GSTF9F/GSTF9R positive for WT and negative for *gstf9* (b) PCR confirming the position of the T-DNA insertion in the *gstf9* mutant and homozygosity of the *gstf9* line using primers described in (a) (c) RT-PCR indicating transcription was positive with TDNA/GSTF9R (1), while this expression was negative with WT primers (GSTF9F/GSTF9R)(2) in the *gstf9* mutant line

3.4.2 Cross between *gstf9* and *wee1-1* mutants

To investigate whether there is a genetic interaction between GSTF9 and *Arath*;WEE1, a cross was made between the *gstf9* and the *wee1-1* lines. The F1 generation was allowed to self-fertilise and set seed, and one line which was homozygous for both mutant alleles, was selected by PCR (Fig 3.5).

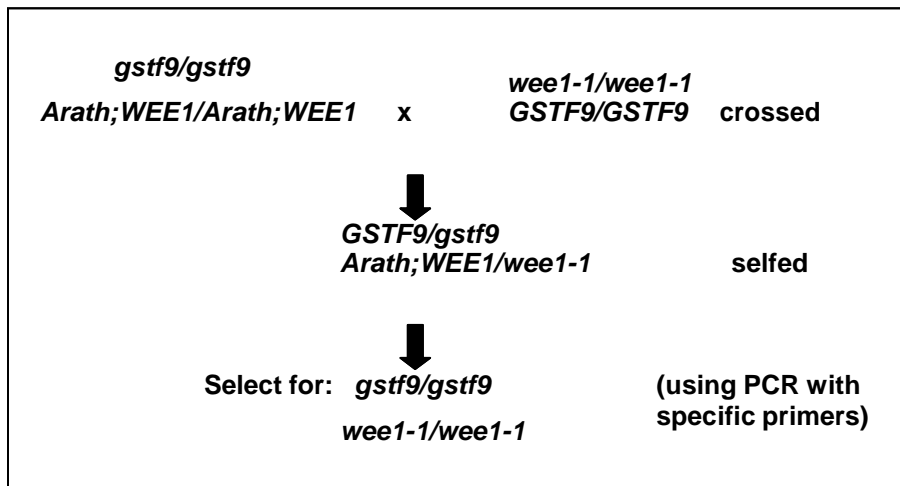


Figure 3.5 Flow chart for the cross between *wee1-1* and *gstf9* to obtain double mutants. The *gstf9* insertion mutant was crossed with the *wee1-1* insertion line to obtain heterozygotes for both genes. These were then selfed to select for homozygotes for the insertion mutants of both genes.

The homozygous double mutant line was selected by PCR analysis and was positive for *gstf9* and *wee1-1* primers, but negative for the wild type *GSTF9* and *Arath;WEE1* primers (Fig 3.6). This line was used for all further experiments and was denoted *dm*.

a



b

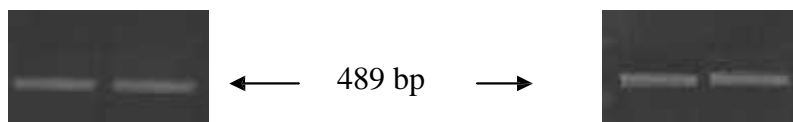


Figure 3.6 PCR analysis of the line selected from the cross between *wee1-1* and *gstf9 (dm)* to verify that it was indeed (a) positive for *wee1-1* primers (P4b/P6) and negative for the WT *Arath;WEE1* primers: P60 and P61 (b) negative for the *GSTF9* primers GSTF9F/GSTF9R and positive for the *gstf9* primers TDNA/GSTF9R. (c,d) all reactions were positive with 18S primers (PUV2 and PUV4).

3.4.3 Response of *Arabidopsis wee1-1* and *gstf9* mutant lines to hydroxyurea (HU) treatment

It was already established that the insertion mutant *wee1-1* line is hypersensitive to HU (De Schutter *et al.*, 2007). Given the discovery of the 2-hybrid interaction between Arath;WEE1 and GSTF9 I wanted to test how the *gstf9* insertion mutant responds to HU. If *gstf9* is also hypersensitive to HU this would support the hypothesis that GSTF9 is involved in the DNA replication checkpoint and that its interaction with Arath;WEE1 may therefore be of functional significance.

I also analysed the phenotype of the double mutant *wee1-1 gstf9* to assess whether the phenotypes were additive. If both genes were operating on the same pathway, the effect of mutating both genes should be similar to mutating just one of them. However, if the two genes were operating on different pathways, the effect of mutating both of them would be additive. The lack of an additive phenotype would thus support the hypothesis that the two genes are acting in the same pathway. Furthermore I also extended the work of De Schutter *et al.* (2007) with *wee1-1* to provide a more detailed analysis of root growth at the macroscopic and cellular levels.

3.4.3.1 Primary root length and rate of lateral root production

In the controls, primary root length of 10 day old seedlings was significantly longer in *wee1-1*, *gstf9* and *dm* when each was compared with WT ($P < 0.05$). The magnitude of increase compared with WT was: *wee1-1*, 1.25-fold, *gstf9*, 1.12-fold, *dm*, 1.46 consistent with an additive effect of these genes on primary root elongation (Fig. 3.7, Table 3.1).

The *wee1-1* and *gstf9* genotypes were extremely hypersensitive to 1 mM HU with a highly significant decrease in primary root length compared with the control grown without HU ($P < 0.001$) (Table 3.1). The magnitude of decrease in primary root length for each genotype \pm 1mM HU was: WT, 1.26, *wee1-1*, 6.80, *gstf9*, 3.80, *dm*, 10.54, thereby providing evidence of an additive effect of these genes on primary root length when seedlings were stressed with 1 mM HU.

Effects of different treatments of *wee1-1*: *wee1-1* +1mM HU and *wee1-1* +2 mM HU on primary root growth were all significant compared to the same treatment of HU in WT ($P < 0.01$). This concentration-dependent effect was also evident for, *gstf9* and the double mutant compared to WT ($P < 0.01$) (Fig 3.7, Table 3.1).

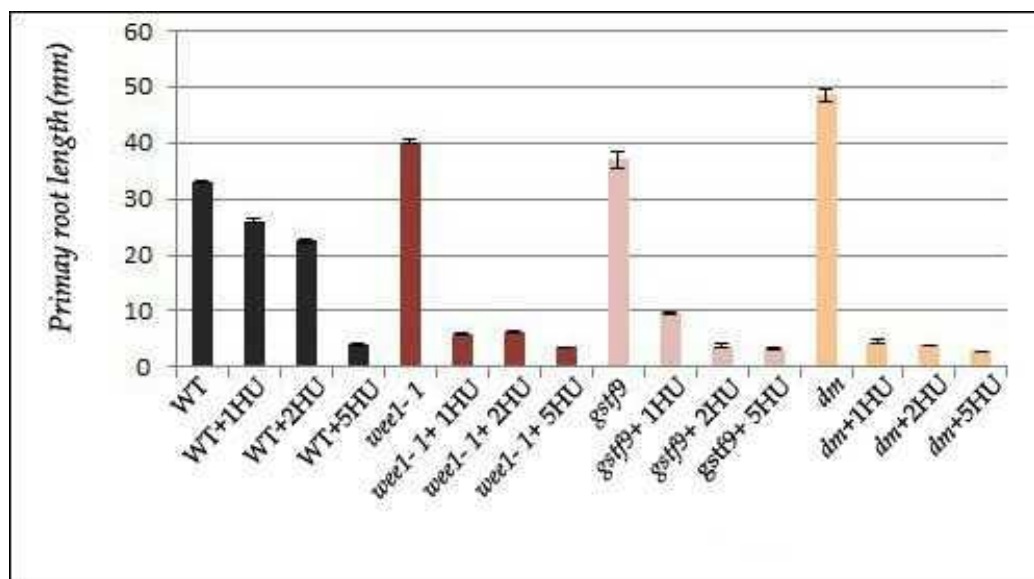


Figure 3.7 Primary root length of 10 day old Arabidopsis *wee1-1*, *gstf9* and *dm* mutant lines compared to wild type (WT) grown on MS agar plates treated with 1, 2 and 5 mM hydroxyurea (HU). (Mean \pm SE, n = 20)

Table 3.1 Student's t-test within a genotype in 10 days old primary root length or total number of lateral roots and primordia +1, 2 or 5 mM HU compared with -HU .

	Level of significant difference + 1mM HU	
	primary root length	No. of laterals + lrp
WT	*	*
<i>wee1-1</i>	***	***
<i>gstf9</i>	***	***
<i>dm</i>	***	***

	Level of significant difference + 2 mM HU	
	primary root length	No. of laterals + lrp
WT	***	**
<i>wee1-1</i>	***	***
<i>gstf9</i>	***	***
<i>dm</i>	***	***

	Level of significant difference + 5 mM HU	
	primary root length	No. of laterals + lrp
WT	***	***
<i>wee1-1</i>	***	***
<i>gstf9</i>	***	***
<i>dm</i>	***	***

Key. *** < 0.001, ** = 0.02-0.001 P, * = 0.02-0.05 P, NS >0.05

In addition to measuring root length at 10 days (Fig. 3.7) in another experiment, I recorded root length daily for 6 days \pm HU treatment (Fig 3.8). These kinetic data were then analysed by linear regressions that enabled measurement of rates of primary root elongation per day for all genotypes \pm HU (Table 3.2).

Root elongation rate differed between the wild type and each of the mutant lines in the presence or absence of HU (Fig 3.8). For example, -HU, the rate for *wee1-1* was 1.2-fold faster than WT whilst *gstf9*'s was marginally slower (1.09-fold) and the *dm*'s was the fastest (1.40-fold). The rates of elongation are consistent in showing that the absence of functional WEE1 enables faster rates of elongation compared with WT. *GSTF9* appears to have no impact on rates of primary root elongation, and this is also reflected in the rate

for the *dm*, which has a rate of elongation much closer to that of *wee1-1* than *gstf9*. Hence functional *WEE1* but not *GSTF9*, is a contributor in regulating primary root elongation in normal conditions.

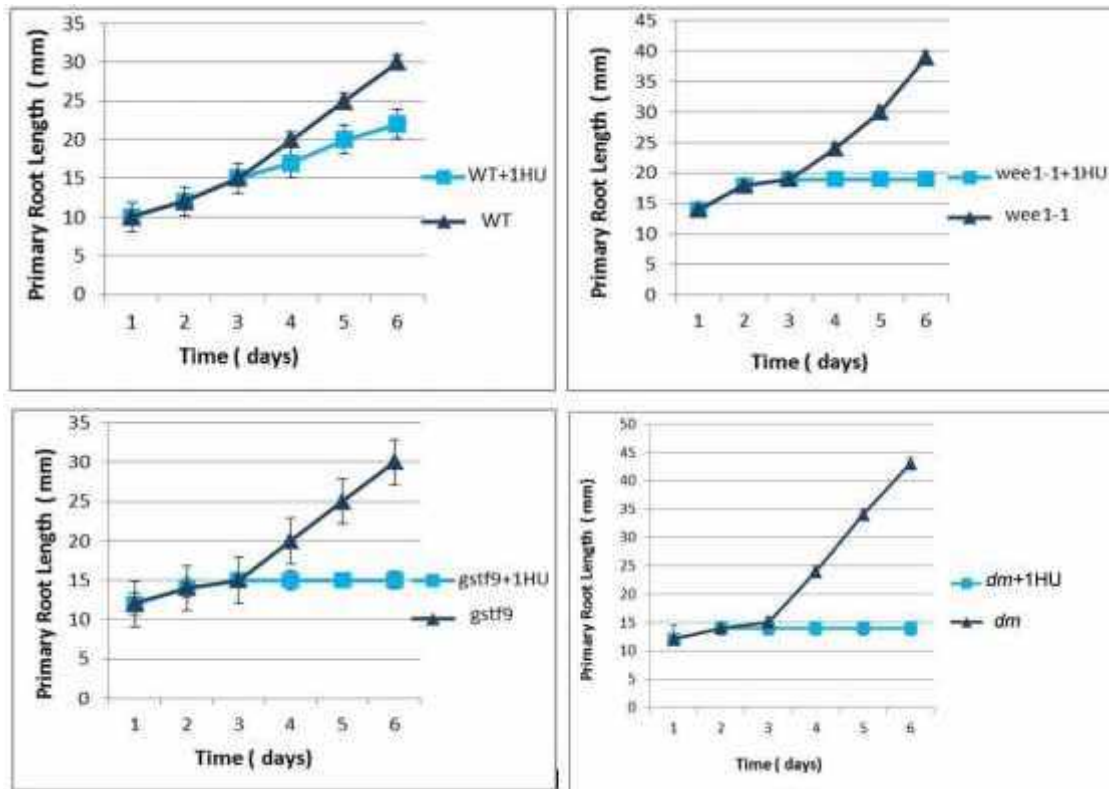


Figure 3.8 The relationship between mean \pm S.E. primary root length (mm) and time (days) \pm 1 mM hydroxyurea (HU) in the genotypes: WT, *wee1-1*, *gstf9* and *wee1-1 gstf9* (*dm*) (n=4).

Table 3.2. regression equation for each of the plots in Fig. 3.8, together with the level of significance of the regression followed by the rate (mm per day). Key *** P<0.001; NS=non significant (n=7).

Genotype	Regression equation	P value	Rate (mm per day)
WT	$y=4.57x+2.29$	***	4.57
WT+HU	$y=3.25x+2.29$	***	3.25
<i>wee1-1</i>	$y=5.54x+3.96$	***	5.54
<i>wee1-1</i> +HU	$y=1.86x+6.71$	NS	--
<i>gstf9</i>	$y=4.36x+3.50$	***	4.36
<i>gstf9</i> +HU	$y=1.86x+6.71$	NS	--
<i>dm</i>	$y=6.406x+1.27$	***	6.41
<i>dm</i> +HU	$Y=0.286x+0.89$	NS	---

In the presence of HU, the rate for WT decreased by %29. Although a regression could be calculated for the mutants +HU, in each case the regression was not significant. Indeed, in Fig. 3.8 it can be observed that whilst the primary root data were virtually identical for 3 days \pm HU, thereafter there was no further increase in primary root length in the mutant genotype +HU. The data are consistent in showing that in the presence of HU each mutant was able to elongate at virtually the same rate \pm HU for 3 d but thereafter, elongation was terminated. Hence, the suggestion is that cells in the RAM of the mutants escaped from the DNA replication checkpoint for 3 days but this was followed by an arrest of elongation perhaps because of an accumulation of perturbed S-phases in successive cell cycles. However, WT+1HU was able to elongate over the entire experiment albeit at a slower rate than WT because presumably, perturbation of DNA replication was overcome but the time taken to overcome the perturbation at successive cell cycles resulted in an eventual slow down of primary root elongation.

The number of lateral roots and primordia (L+LRP) was greater in all three mutant genotypes compared to WT in the absence of HU (Fig. 3.9). With 1mM HU there was a

dramatic reduction in L+LRPs in the mutants compared to WT, indicating a hypersensitivity to the HU stress. As HU levels increased, WT L+LRPs decreased further, whereas in the mutants the decrease was less marked (Table 3.3).

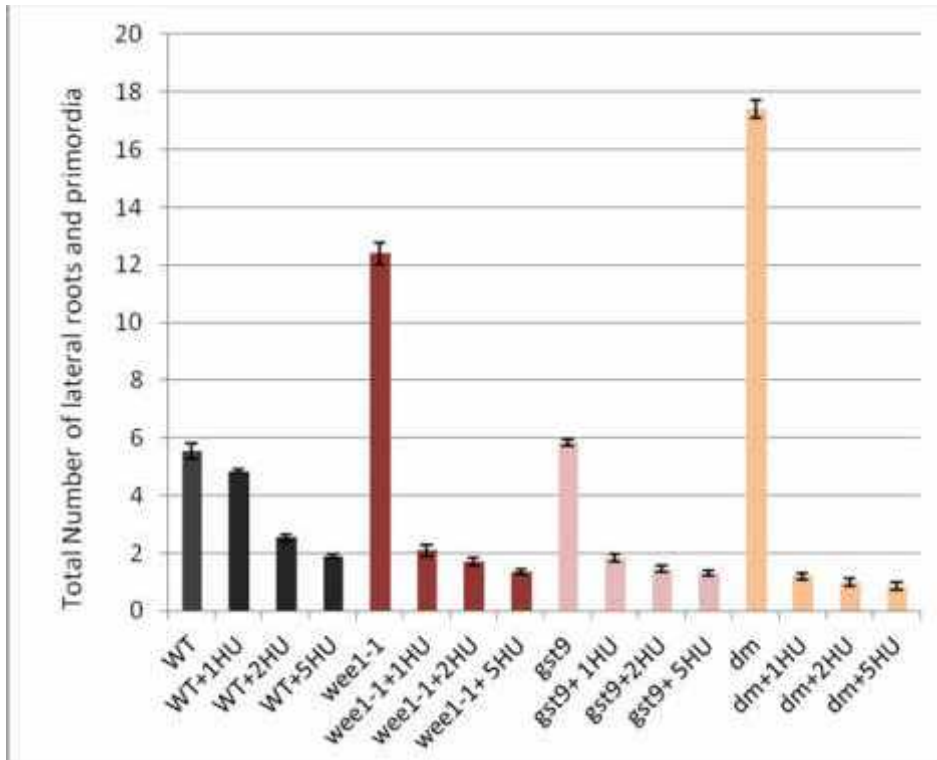


Figure 3.9 Total number of lateral roots and primordia (\pm SE) of 10 day old Arabidopsis seedlings in the Arabidopsis genotypes: WT, *wee1-1*, *gstf9* and *wee1-1 gstf9 (dm)* grown on MS agar plates supplemented with 1, 2 or 5 mM hydroxyurea (HU) (n=20)

Table 3.3 Student's t-test within genotype for number of lateral roots and primordia \pm 1,2 or 5mM HU compared with -HU

	WT	<i>wee1-1</i>	<i>gstf9</i>	<i>dm</i>
	Total number of lateral roots and primordia			
1 mM HU	*	***	***	***
2 mM HU	***	***	***	***
5 mM HU	***	***	***	***

Key. *** < 0.001, ** = 0.02-0.001 P, * = 0.02-0.05 P, NS >0.05

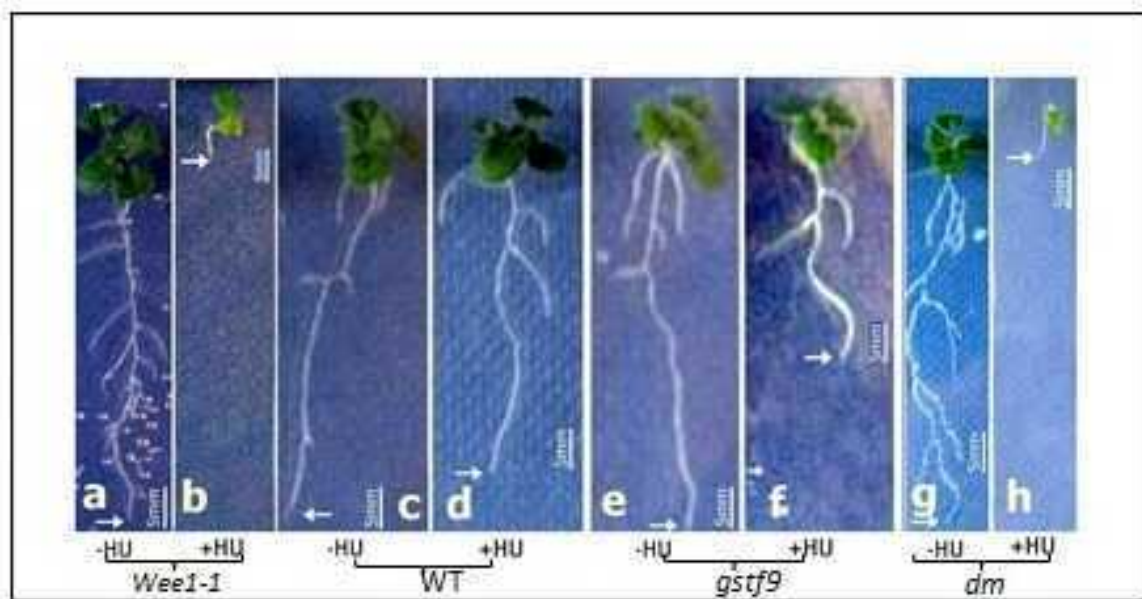
Table 3.4 Student's t-test results for number of lateral roots and primordia in 2mM HU compared with the 1mM HU treatment within each genotype.

	2 mM HU
	Total number of lateral roots and primordia
WT	**
<i>wee1-1</i>	*
<i>gstf9</i>	*
<i>dm</i>	NS

Since root growth and numbers of laterals are linked, lateral root production was calculated as a function of primary root length (Fig 3.10). In other words what is important is the frequency of lateral root formation per mm of primary root tissue per genotype per treatment (Fig.3.10, Table 3.3, Table 3.5). This is calculated as x-coordinate divided by y coordinate for each point plotted in Fig. 3.10. For example, the mean rate of lateral root production per mm of primary in WT is 0.17 per mm of primary root, compared with 0.19 in the 1 mM HU treatment. In the same way, in the HU treatment, the mutant phenotypes exhibit similar rates of increase in lateral root formation relative to -HU. However, if the rate for each mutant genotype +HU is compared with WT +HU, a 1.89- and 2.21-fold increase in the rate of lateral root production is evident for *wee1-1* and the double mutant, respectively but there is no change in the rate for *gstf9* compared with WT.

Hence, in the presence of HU, *wee1-1*, lacking a copy of *WEE1* makes more laterals than *gstf9* which has a copy of *WEE1* but the double mutant shows a similar rate (and response) to *wee1-1*. These data suggest that the lateral root phenotypes \pm HU are governed by *WEE1* without any interaction with *GSTF9*.

A



B

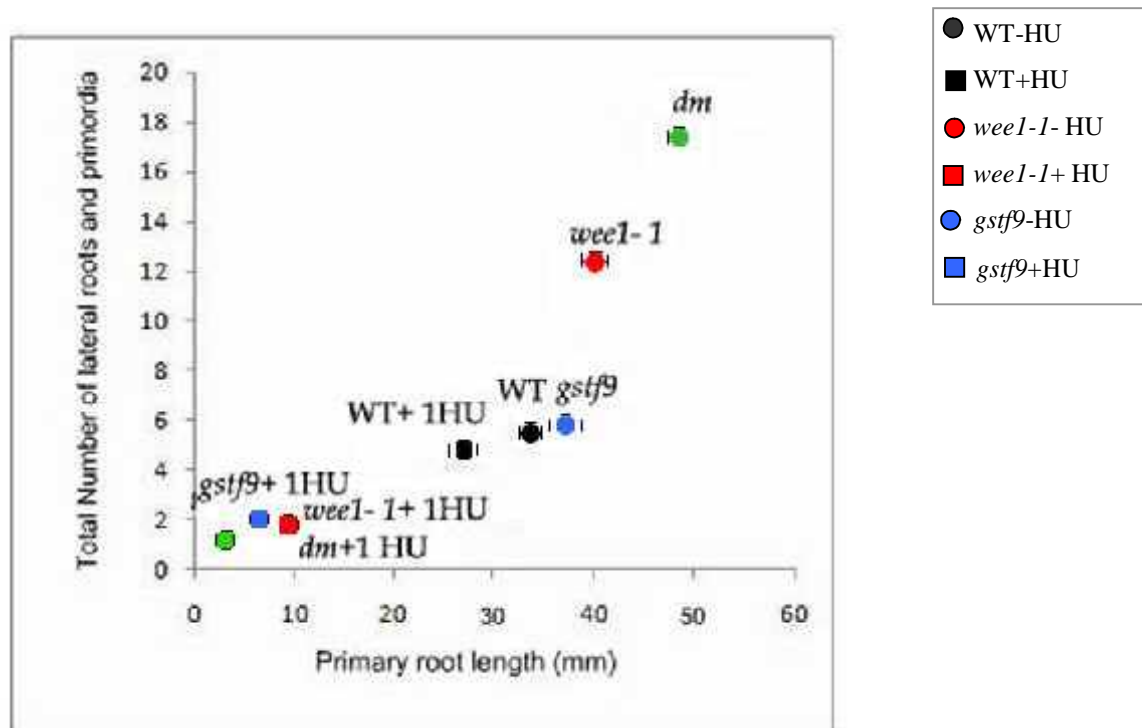


Figure 3.10 Root phenotype analysis of 10 day old Arabidopsis *wee1-1*, and *gstf9* mutant lines compared to wild type (WT) grown on MS agar plates treated with 1mM hydroxyurea (HU). (A) (a) *wee1-1* (b) *wee1-1* +1mM HU (c) WT (d) WT+1mM HU (e) *gstf9* (f) *gstf9*+1mM HU (g) *wee1-1 gstf9 (dm)* (h) *wee1-1 gstf9 (dm)*+1mM HU (B) The relationship between primary root length and total number of lateral roots and primordia in seedlings of the same genotypes listed above. Means \pm SE are plotted with error bars for both x and y coordinates. Where error bars are absent the variation about the mean was less than the diameter of the symbol. (n =20)

Table 3.5 Rate of lateral root production mm primary root⁻¹ in the different genotypes of 10 day old Arabidopsis seedlings obtained by dividing the x by the y coordinates for each point plotted in Fig. 3.9.

	Rate of lateral root production mm primary root ⁻¹			
	-HU	1mM	2mM	5mM
WT	0.17	0.19	0.11	0.47
<i>wee1-1</i>	0.31	0.36	0.27	0.38
<i>gstf9</i>	0.16	0.19	0.37	0.39
<i>dm</i>	0.36	0.42	0.26	0.30

3.4.3.2 Meristem length

To investigate whether the effects on primary root elongation were related to changes in meristematic activity, the meristem length was examined in all genotypes in response to different concentrations of HU. Compared with WT-HU, meristem length tended to be longer for each mutant genotype but not to a significant extent ($P > 0.05$) (Table 3.5).

In general, there was a negative concentration-dependent relationship between meristem length and HU concentration for all genotypes (Fig. 3.11). This fits with the general concentration-dependent inhibition of primary root length for all genotypes.

In WT, the decrease in meristem length in the 1 mM HU and 2 mM HU treatment was not significant compared with the control ($P > 0.05$) but it was so at 5 mM ($P = 0.001^{***}$). For the mutant genotypes, increasing concentrations of HU resulted in a gradual decrease in meristem length but the reductions between concentrations were significant ($P < 0.01^{**}$).

The data suggest that *wee1-1* and *wee1-1 gstf9 (dm)* exhibited a very similar pattern of reduction in meristem length in response to increasing HU concentration but with the greatest reduction occurring for *wee1-1* in response to 1 mM HU (< 0.01). In contrast, the

pattern of reduction in meristem length in *gstf9* in response to increasing concentrations of HU was almost linear. Overall, the pattern of reduction in meristem length to increasing HU concentrations was very similar in *wee1-1* and the *dm*, whilst in this respect WT and *gstf9* were most similar to each other. Hence, in the absence of a functional WEE1 in *wee1-1*, meristem shortening in response to 1 mM HU (1.3-fold) was hypersensitive. This means that in the absence of *WEE1* or in the double mutant, the RAM is unable to maintain a normal size when the roots are stressed with 1mM HU. However, the functional absence of *GSTF9* either in *gstf9* or in the *dm* appears to make no substantial difference to the pattern of shortening of meristem length in response to 1mM HU. Concentrations of HU >1mM, result in significant reductions in meristem length in all genotypes suggesting that they begin to impose a toxic effect on the roots and this was clearly evident in the reductions in primary root length at increasing HU concentrations.

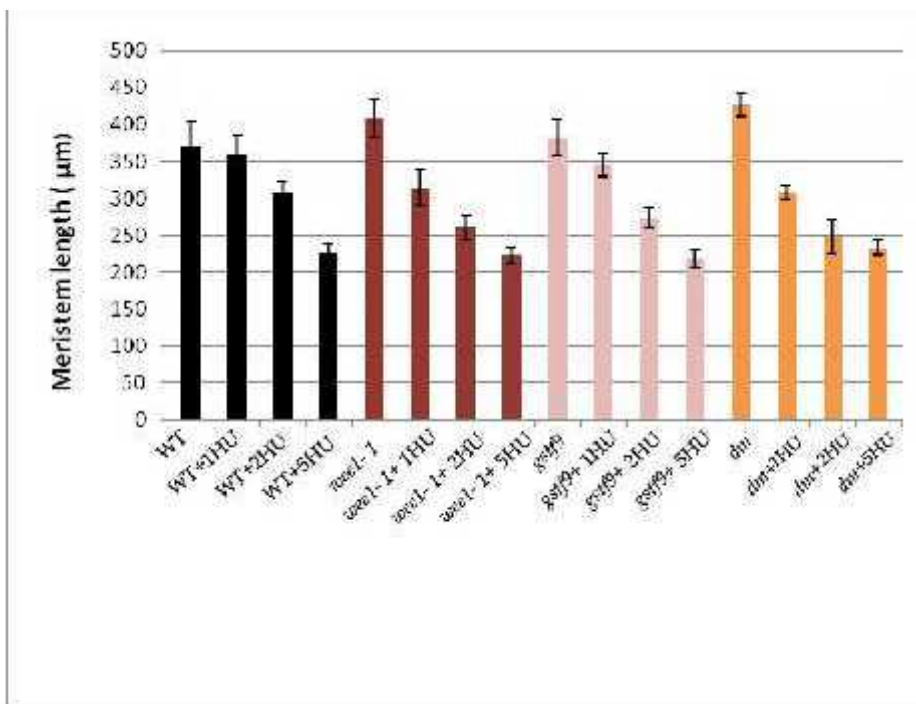


Fig 3.11 Mean (\pm SE.) length of the primary root apical meristem in 10 day old seedlings of various genotypes of Arabidopsis grown in daily cycles of 16 h light and 8 h dark at 21 °C \pm either 1, 2 or 5 mM hydroxyurea (HU) n=20

Table 3.6 Mean meristem length (\pm SE) in 10 day old seedlings of various genotypes of *Arabidopsis* \pm hydroxyurea (HU). Probability values are based on meristem length \pm HU within a genotype. (n = 20)

	<u>Root apical meristem length</u>		P value \pm HU
	-HU	+ 1mM HU	
WT	370.10 (\pm 34.38)	359.55(\pm 26.09)	0.808 NS
<i>wee1-1</i>	408.15(\pm 25.85)	314.35 (\pm 23.64)	0.006**
<i>gstf9</i>	382.85 (\pm 24.54)	345.65 (\pm 15.6)	0.231 NS
<i>dm</i>	426.52 (\pm 15.98)	308.23 (\pm 9.65)	<0.001***

3.4.3.3 Number of epidermal cells along the meristem

The data in Fig. 3.12 are consistent in revealing a differential response of WT compared with all three mutant genotypes because whilst increasing HU concentration had a negative effect on epidermal cell number in the RAM in WT, cell number remained remarkably constant in each of the mutant lines regardless of HU concentration.

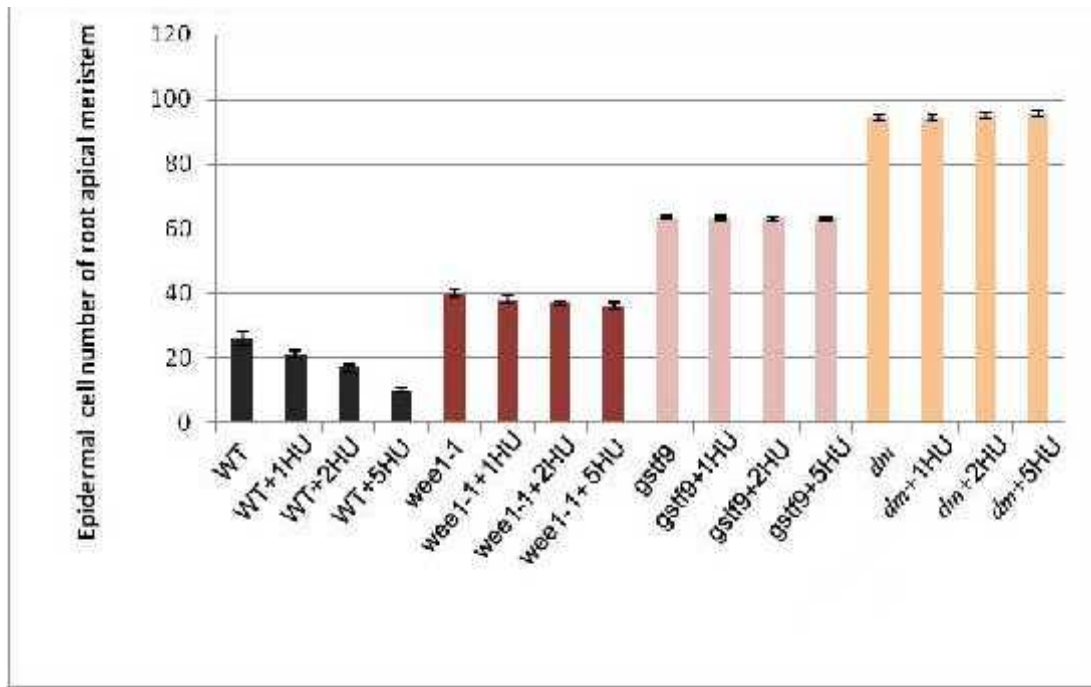


Figure 3.12 The relationship between mean (\pm S.E.) number of cells in epidermis of the RAM in different genotypes: wild type (WT), *wee1-1*, *gstf9* and *wee1-1 gstf9* with 1 or 5 mM hydroxyurea treatment in 10 day old Arabidopsis plants grown in 16 h light and 8 h dark at 21°C. n =20

Table 3.7 Student t-tests within genotype for number of cells in RAM \pm 1, 2 and 5 mM HU compared with -HU for each genotype (see Fig. 3. 13)

	Level of significant difference + 1 mM HU	Level of significant difference + 2 mM HU	Level of significant difference + 5 mM HU
	Number of cells in RAM	Number of cells in RAM	Number of cells in RAM
WT	NS	**	***
<i>wee1-1</i>	NS	**	**
<i>gstf9</i>	NS	NS	NS
<i>dm</i>	NS	***	***

Key. *** < 0.001, ** = 0.02-0.001 P, * = 0.02-0.05 P, NS >0.05

Epidermal cell number was significantly greater in the RAM of each mutant genotype compared with WT in all HU concentrations ($P < 0.001$). Indeed epidermal cell number in the RAM was clearly buffered within each mutant genotype. In rank order and minus HU the magnitude of increase was: *wee1-1*, 1.53-fold, *gstf9* 2.42-fold and the *dm*, 3.61-fold. To be a strictly additive effect the magnitude of increase would be the sum of each single mutant (3.96-fold). Hence the magnitude of increase is very near additive.

No significant differences could be detected between epidermal cell number in the RAM \pm 1 mM HU for any genotype. Note from above, that 1 mM HU resulted in decreases in the size of the RAM in all genotypes although only significantly so for *wee1-1* and the *dm*. Mean cell number began to decrease significantly in WT as increased concentrations of HU were applied (Table 3.7). Given that cell number in the mutants does not alter \pm HU this suggests that a major effect of HU was to reduce cell size in all genotypes. This was tested and described below in section 3.4.3.4.

3.4.3.4 Epidermal cell length

Epidermal cell length in the 0mM HU treatment was significantly shorter in all genotypes compared with WT . This effect was accentuated at increasing concentrations of HU (Fig. 3.13 and 3.14). Thus, at 0 mM HU, epidermal cell length was 1.41-fold different in *wee1-1* 2.32-fold different in *gstf9* and 3.12-fold different in the *dm* compared with WT. These data suggest an additive effect of *WEE1* and *GSTF9* on epidermal cell length within the RAM.

The hypothesis that HU at all concentrations induced a decrease in cell size in all genotypes was proven for *wee1-1*, *gstf9* and the *dm* but not for WT. In the latter, there was a significant increase in cell length in at 1, 2 and 5 mM HU treatments compared with 0 mM HU. Thus under these conditions, there were larger but fewer cells in the meristem, explaining why meristem size remained unaltered in WT \pm HU (Fig. 3.11).

For the mutant genotypes treated with 1 mM HU, the reverse was true for *wee1-1* and the *dm*, but there was no change in epidermal cell size in *gstf9* \pm 1mM HU (Table 3.8).

For WT, the increase in cell size would be consistent with the induction of the DNA replication checkpoint and an enforced delay in the transition from G2 to M but continued

cell growth whilst DNA replication is being normalised. Unpublished data from the Cardiff lab. for synchronised BY-2 cells showed such a delay in entry to mitosis under HU conditions. The absence of a functional *WEE1* in *wee1-1* resulted in a significantly smaller epidermal cell size which would be consistent with cells escaping the DNA replication checkpoint and dividing prematurely at a reduced cell size. However, the absence of a functional *GSTF9* had a null effect on epidermal cell size in the 1 mM HU, although there was a downward trend from 1, to 2 through to 5 mM HU whilst in the *dm*, a significantly reduced cell size was detected once more in the 1 mM HU compared with 0 mM. Hence, for cell size regulation under 1 mM HU stress, there does not seem to be an interaction between *GSTF9* and *WEE1*.

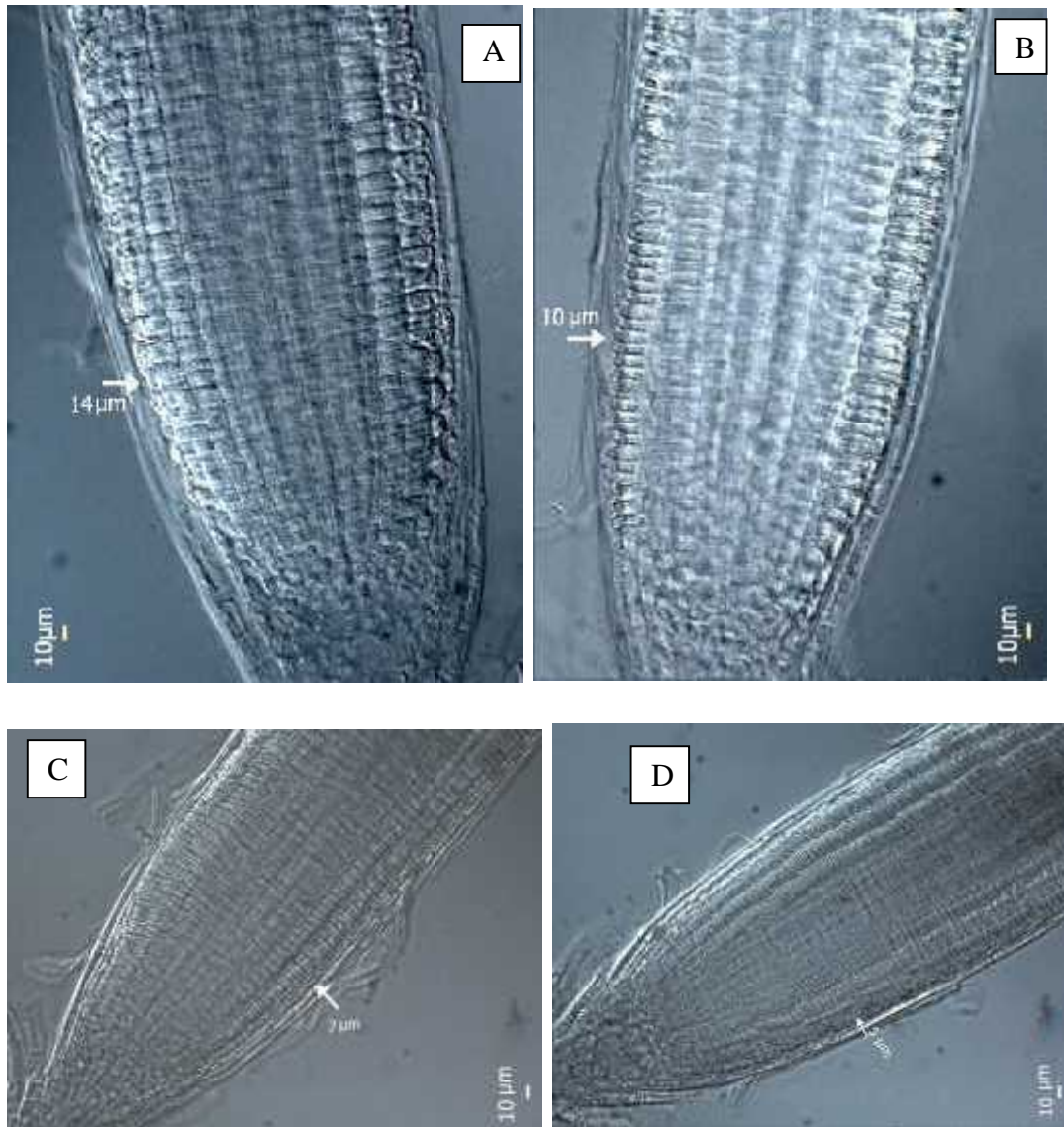


Fig 3.13 Whole mounts of root tips of (A) wild type meristem (B) *wee1-1* meristem (C) *gstf9* meristem (D) *dm*. Scale bar = 10 μm. Arrows indicate length of representative cells in the image.

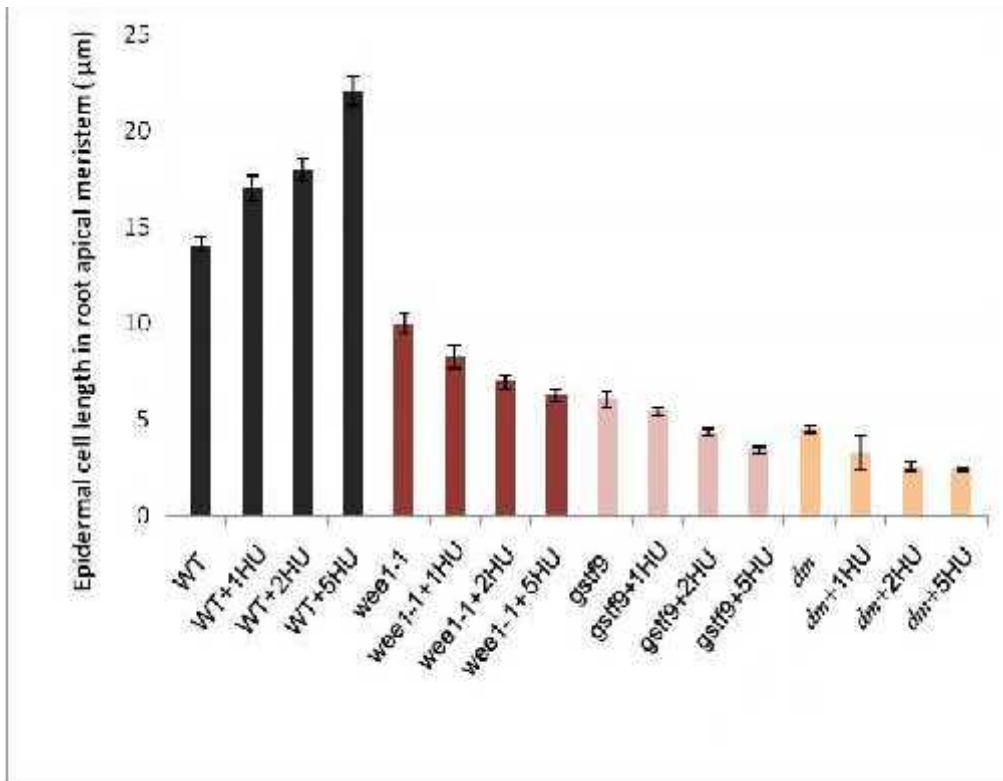


Fig 3.14 The relationship between mean (\pm S.E n=20.) cell length in the epidermis of the RAM in different genotypes: wild type (WT) , *wee1-1*, *gstf9* and *dm* with HU treatment in 10 day old Arabidopsis plants grown in 16 h light and 8 h dark at 21°C.

Table 3.8 Student t-test within a genotype for cell length \pm 1, 2 and 5 mM HU (see Fig. 3.14). Key: NS = not significant ($P > 0.05$) * $P = 0.05-0.02$; ** $P = 0.02-0.001$; *** $P < 0.001$). n=20

	Level of significant difference \pm 1 mM HU	Level of significant difference \pm 2 mM HU	Level of significant difference \pm 5 mM HU
	Cell length in RAM	Cell length in RAM	Cell length in RAM
WT	***	***	***
<i>wee1-1</i>	*	***	***
<i>gstf9</i>	NS	***	***
<i>dm</i>	***	***	***

Key. *** < 0.001 , ** = 0.02-0.001 P, * = 0.02-0.05 P, NS > 0.05

3.4.4.2 Elongation Zone

Root elongation is the product of cell division in the root apical meristem and the subsequent displacement of cells from the meristem which then elongate markedly. Cells at the basipetal margin of the meristem divide and their descendants begin to elongate and are eventually displaced to a position at which they no longer do so prior to differentiation. However, it is well known that the contribution of each component parameter to primary root elongation rate can vary with respect to species and environmental conditions (Fiorani *et al*, 2002). It was therefore of interest to compare cell division, cell number and cell length in the meristem, and the extent of the elongation zone in all three genotypes studied. Here, I have added measurements of the elongation zone to the various RAM parameters in relation to primary root elongation rates for all three genotypes reported above.

The distance of each successive transverse epidermal cell wall to the margin of the meristem (as judged by the transition point in this lineage) was measured along the root until the measurements began to plateau. This measurement was carried out in three replicate primary roots from 10 day old seedlings. For WT, these data are displayed in Fig. 3.15a and Table 3.9. Vertical lines are drawn at the point at which the data plateau resulting in a mean elongation zone of $2933 \pm 57.7 \mu\text{m}$ for WT. Similarly the mean elongation zone in *wee1-1* (Fig. 3.15b, Table 3.9), *gst9* and the *dm* (Fig. 3.16a, b, Table 3.9) is 2833 ± 66.7 , 2500 ± 153 , and $3000 \pm 10 \mu\text{m}$, respectively. T-tests on elongation zone data showed there is no significant difference between the size of the elongation zone in *wee1-1* or the *dm* compared with WT. This suggests that the absence of functional *WEE1* has no major impact on the elongation zone of primary roots of these genotypes. It would appear that the elongation zone is significantly smaller in *gstf9* compared with WT but possible greater replication would be necessary to confirm this in future work.

Note that for all three genotypes, there is considerable fluctuation in the cell length measurements in the elongation zone. This is the result of asymmetric cell divisions and, in many cases, unequal divisions that lead to root hair production. This type of fluctuation has been demonstrated in the elongation zone of primary roots of other species (Luxova, 1981).

Cell length in the elongation zone showed more fluctuation in *wee1-1* compared with WT, but the distance from the beginning of the elongation zone and their higher point was not different. This was the same in *gstf9* and the *dm*.

There were no significant differences between the elongation zone for each mutant genotype compared with WT (control) (Table 3.10). Hence the zone of elongation remains remarkably constant for all genotypes and it is highly likely that neither *WEE1* nor *GSTF9* contribute to the cell elongation mechanism operating in primary roots under normal conditions.

Table 3.9 Mean (\pm SE) of the elongation zone for each genotype

WT	<i>wee1-1</i>	<i>gstf9</i>	<i>dm</i>
2500 \pm 153	2867 \pm 57	2500 \pm 150	2967 \pm 33

Table 3.10 Levels of significant differences between the elongation zone length for each genotype compared to WT (see Fig. 3.16, Fig. 3.17)

	Elongation zone
<i>wee1-1</i>	NS
<i>gstf9</i>	NS
<i>dm</i>	NS

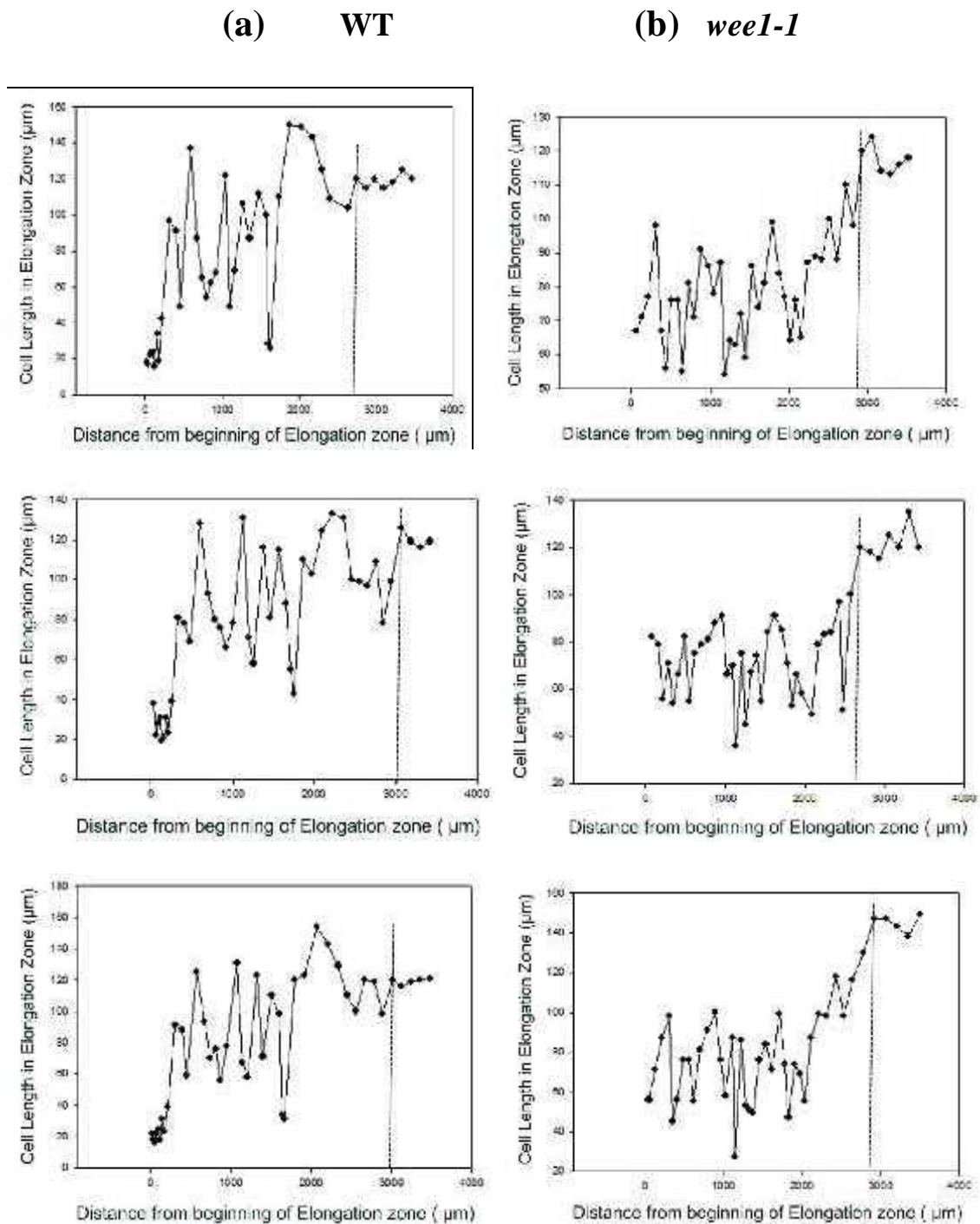


Fig 3.15 The distance (μm) between the margin of the RAM and successive transverse cell walls of successive cells along an epidermal lineage in two individual primary roots of (a) WT (b) *wee1-1*. Vertical dashed lines indicate the point at which the data begin to plateau and hence represent the basipetal limit of the elongation zone for each root.

(a) *gstf9*

(b) *dm*

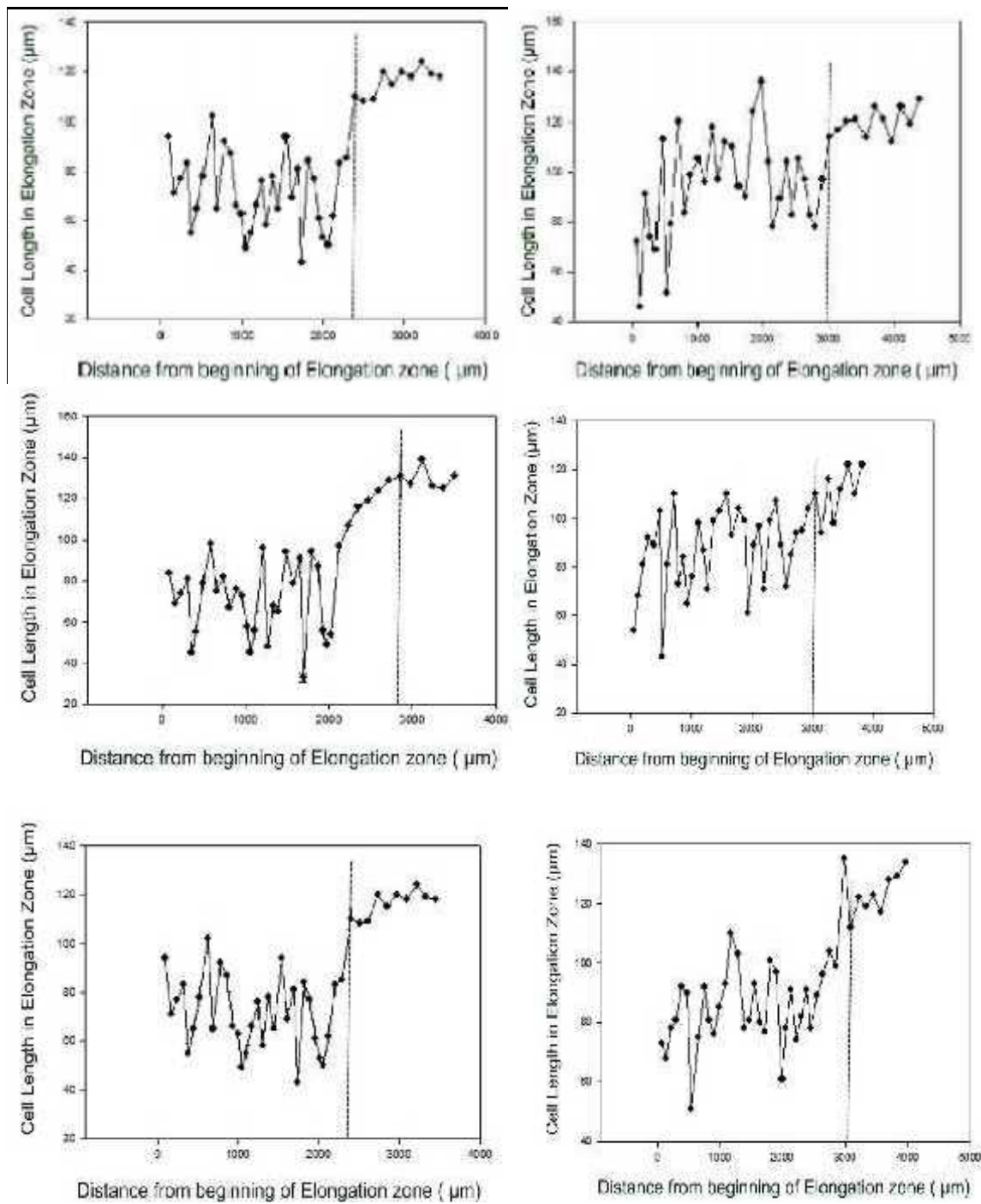


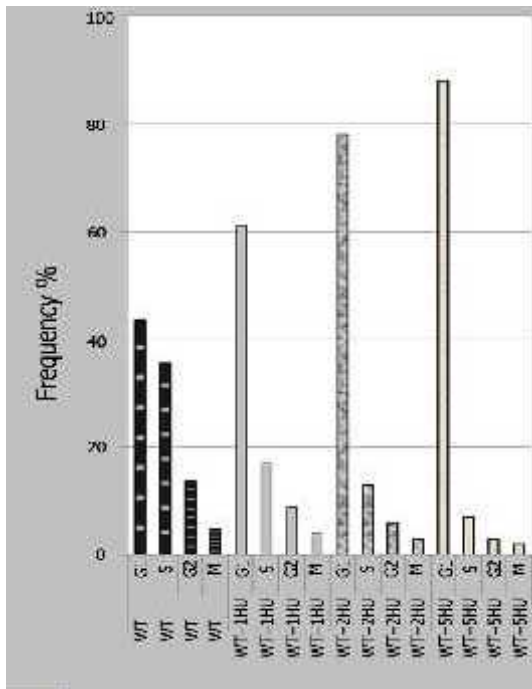
Fig 3.16 The distance (μm) between the proximal margin of the RAM and successive transverse cell walls of successive cells along an epidermal lineage in three individual primary roots of (a) *gstf9* and (b) *wee1-1 gstf9 (dm)*. Vertical dashed lines indicate the point at which the data begin to plateau and hence represent the basipetal limit of the elongation zone for each root.

3.4.3.4 Percentage of cells in each component phase of the cell cycle in the RAM of WT, *wee1-1* and *gstf9* ± HU treatment

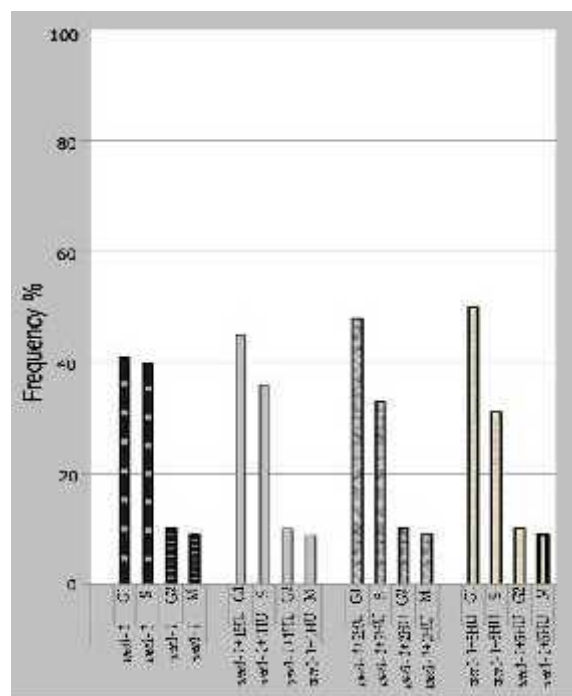
Given the various phenotypic changes that occur in response to HU, there was the suggestion that the mutant lines are able to escape the DNA replication and DNA damage checkpoints. For example, in *wee1-1*, although primary root growth was repressed in the 1 mM HU treatment, this mutant line exhibited a faster rate of lateral root production than wild type. Cell division is necessary for lateral root production which would suggest an escape by the mutants from the DNA replication checkpoint. To test this hypothesis I measured the proportion of cells in different phases of the cell cycle using microdensitometry. This analysis also enabled me to measure the extent to which HU might be inducing endoreduplication in each of the genotypes.

In the RAM of WT seedlings, most cells were detected in G1 and then in descending order: S-phase, G2 and M-phase. The effect of increasing concentrations of HU was to cause a progressive increase in the percentage of cells in G1, and a progressive decrease in S-phase whilst percentages in G2 and M remained relatively constant in the 1 and 2 mM HU treatments but decreased more so in the 5 mM treatment. There was no evidence of polyploid nuclei in these treatments (Fig. 3.17A). The data are consistent in showing a concentration-dependent accumulation of cells in G1 phase. In WT, The progressive increase in the accumulation of cells in G1 as a result of HU treatment is consistent with the induction of the DNA replication checkpoint.

A



B



C

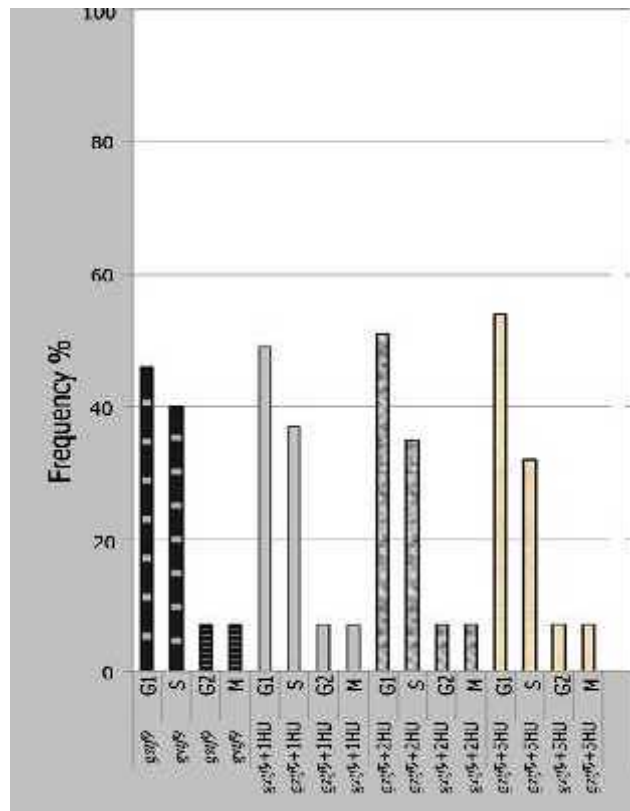


Figure 3.17 The percentage frequency of cells in G1, S-phase, G2 and M-phase in squash preparations from RAMs of 10 day old seedlings of (A)WT, (B) *wee1-1* and (C) *gstf9* treated with 1, 2 or 5 mM HU (n = 20).

Table 3.11 Percentage of cells in M-phase of wild type (WT), *wee1-1*, *gstf9* and the *dm* with HU treatment

Mitotic Index	0 mM HU	1 mM HU	2mM HU	5 mM HU
WT (%)	4	3	2	2
<i>wee1-1</i> (%)	9	9	9	9
<i>gstf9</i> (%)	7	7	7	7
<i>dm</i> (%)	12	12	12	12

In comparison with the WT±HU data, the pattern of alteration in the percentage of cells in each phase appears to be more buffered in the *wee1-1* mutant genotype. For example, there was no significant difference in the pattern of cells in G1, S, G2 and M-phase ± 1mM HU ($t = 0.197$, NS, df3), and the % in S, G2 and M remained remarkably unaltered as the concentration of HU was increased in the 2 and 5 mM treatments. In general, the same holds true in *gstf9*. However, time did not permit for microdensitometry in the *dm*.

The only progressive change was a slight increase in the percentage of cells in G1 at the higher HU concentrations. However, again, there is no evidence to show that HU induced any polyploidy in these RAMs.

3.4.4 Response of Arabidopsis insertional mutant lines *wee1-1* and *gstf9* to zeocin treatment

3.4.4.1 Primary root length and rate of lateral root production

When root length is compared between genotypes in the 0 mM zeocin treatment, the rank order (longest to shortest) is: *dm*, *wee1-1*, WT, *gstf9*. Hence it is the absence of a functional *Arath;WEE1* that leads to longer roots whilst *GSTF9* appears to have no effect on root length in 10 day old seedlings under normal conditions (Fig. 3.18) These data collected are very similar to those in the HU treatments (see Section 3.4.3.1).

WT responds to increasing concentrations of zeocin by a near proportional decrease in root length. In contrast, in the mutant genotypes, the 5 μ M treatment induces a hypersensitive response. However > 5 μ M there is a virtually proportional reduction in primary root length in the mutants. On closer inspection, the extent of reduction in root length, from 0 to the 5 μ m zeocin treatment is more similar between the *wee1-1* (8-fold) and the *dm* (9.6-fold) compared with *gstf9* (2.9-fold) and WT (1.3-fold). This suggests a strong involvement of *WEE1* upon the induction of the DNA damage checkpoint. However, *gstf9* must have a wild type copy of *Arath;WEE1* and yet there is a hypersensitive response in this mutant compared with WT but one which is not as great as that in *wee1-1* and the *dm*. Thus *GSTF9* is also exerting an albeit weaker effect on the DNA damage checkpoint. However, the phenotype of the *dm* which shows a partially additive effect suggests that the *GSTF9* effect on the DNA damage checkpoint is independent of *Arath;WEE1*.

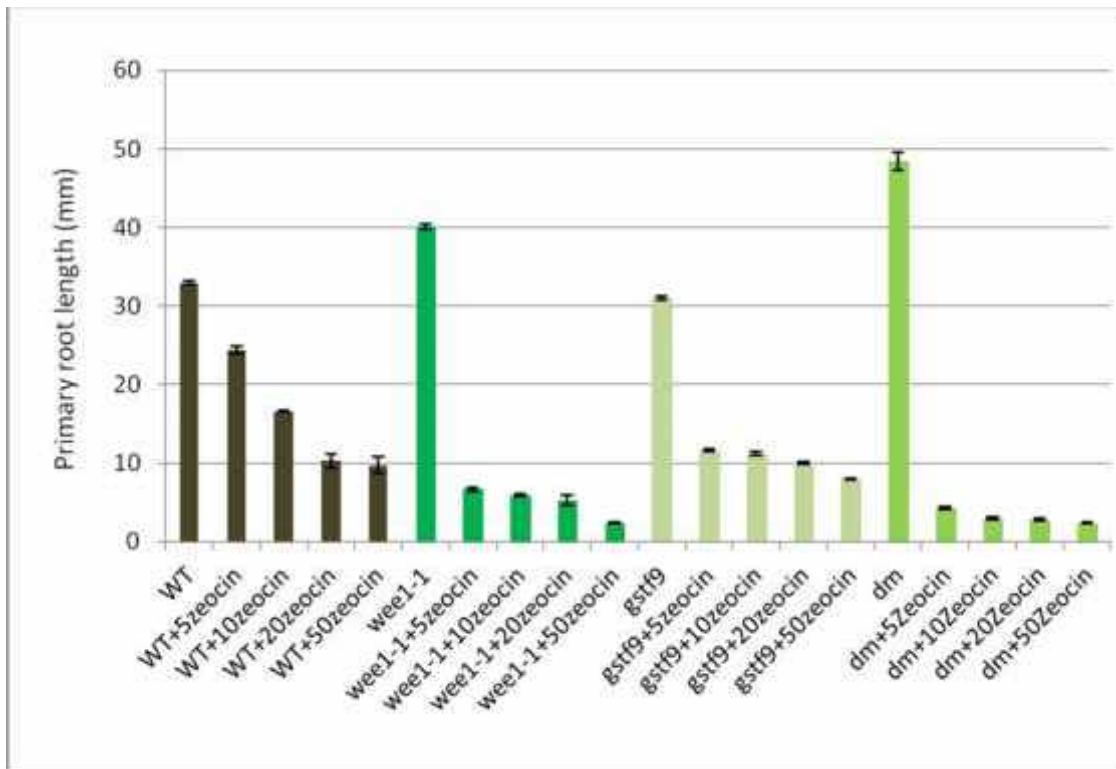


Figure 3.18 Primary root length of 10 day old Arabidopsis seedlings in the genotypes: WT, *wee1-1*, *gstf9* and *wee1-1 gstf9 (dm)* grown on MS agar plates supplemented with 5, 10, 20 or 50 μ M zeocin. (mean \pm SE, n = 20)

Table 3.12 Student's t-test results for primary root length within a genotype in 5, 10, 20 or 50 μM zeocin compared with the 0 μM zeocin treatment within a genotype. For example, in WT, primary root length in 0 μM zeocin was not significantly different from WT grown on 5 μM zeocin.

	Level of significant difference \pm 5 μM zeocin
	primary root length
WT	*
<i>wee1-1</i>	***
<i>gstf9</i>	***
<i>dm</i>	***

	Level of significant difference \pm 10 μM zeocin
	primary root length
WT	***
<i>wee1-1</i>	***
<i>gstf9</i>	***
<i>dm</i>	***

	Level of significant difference \pm 20 μM zeocin
	primary root length
WT	***
<i>wee1-1</i>	***
<i>gstf9</i>	***
<i>dm</i>	***

	Level of significant difference \pm 50 μM zeocin
	primary root length
WT	***
<i>wee1-1</i>	***
<i>gstf9</i>	***
<i>dm</i>	***

Key. *** < 0.001, ** = 0.02-0.001 P, * = 0.02-0.05 P, NS >0.05

In a separate experiment, the rates of elongation of the primary roots were analysed over 6 days \pm zeocin treatment (Fig. 3.19) by linear regression analysis (Table 3.13). As for the HU, treatment with zeocin also almost abolished root elongation in the mutants, but the timing differed between the mutant lines: the dramatic reduction in growth rate occurred on d 3 on *wee1-1*, d 4 in *gstf9* but d 2 in the *dm* indicating an additive effect of the two mutations.

In the absence of zeocin, over the linear portion of the growth in each genotype, (d3 to d6), the fastest rate of elongation was in the WT (Table 3.13) and yet *wee1-1* and *dm*

showed the longest primary root in the 10-day samples (Fig. 3.18). This anomaly could be due to the difference in age of the seedlings and indicates that this analysis needs to be repeated.

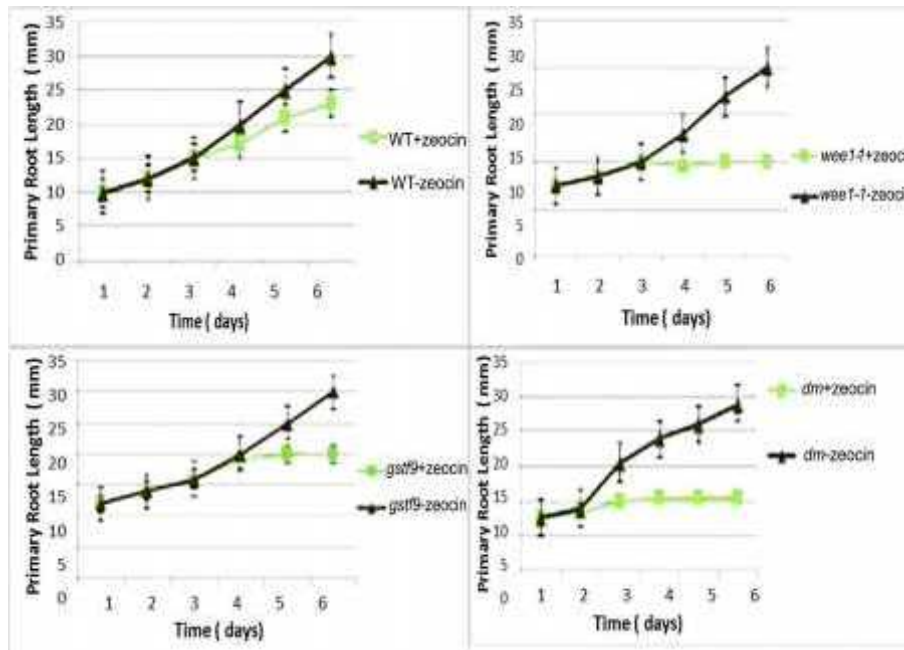


Figure 3.19 The relationship between mean \pm S.E. primary root length (mm) and time (days) \pm 5 μ M zeocin in the genotypes: WT, *wee1-1*, *gstf9* and *wee1-1 gstf9* (*dm*) (n=4).

Table 3.13 Regression equation for each of the plots in Fig. 3.19, together with the level of significance of the regression followed by the rate (mm per day). Key *** P<0.001; NS=non significant (n=7)

Genotype	Regression equation	P value	Rate (mm per day)
WT	$y=2.85x+4.9$	***	2.9
WT+ zeocin	$y=3.1x+1.6$	***	3.1
<i>wee1-1</i>	$y=1.7x+2.75$	***	1.7
<i>wee1-1</i> + zeocin	$y=2.36x+3.45$	NS	2.3
<i>gstf9</i>	$y=2.6x+2.1$	***	2.6
<i>gstf9</i> + zeocin	$y=1.28x+4.8$	NS	1.28
<i>dm</i>	$y=7.51x+0.71$	***	7.5
<i>dm</i> + zeocin	$Y=0.78x+0.45$	NS	0.78

Like HU, zeocin also induced a reduction in lateral roots +lateral root primordia (L+LRP) in all genotypes (Fig. 3.20, Table 3.14). Again the mutants were hypersensitive to the zeocin stress. As with the HU treatment, in the WT increasing levels of chemical induced a progressive reduction in L+LRPs with a striking drop from 10 to 20 μ M zeocin. However in the mutant lines there was a less significant (*wee1-1*) or not significant (*gstf9* and *dm*) difference in L+LRPs between these two concentrations (Table 3.15).

Again as for the HU treatment the rates of lateral root production per mm of primary root were calculated (Fig 3.21, Table 3.16). In the absence of zeocin, the rate of lateral root production was almost 2-fold higher in the *wee1-1* mutant and the *dm*, whereas lateral root production in the *gstf9* mutant was similar to WT. Treatment with 5 μ M zeocin resulted in an almost 2-fold increase in lateral root production in *wee1-1* whereas it had little effect on either *gstf9* or the *dm*. In this case, in contrast with the HU treatments, the

effect of zeocin on *dm* was more similar to the WT and the *gstf9* mutant than with the *wee1-1*, suggesting that in this case *gstf9* was acting epistatically over *wee1-1*.

Table 3.14 Student's t-test results for total number of lateral roots and primordia within a genotype in 5, 10 or 20, 50 μ M zeocin compared with the 0 zeocin treatment within a genotype. For example, in WT, primary root length in 0 zeocin was not significantly different from WT grown on 5 μ M zeocin

	Level of significant difference \pm 5 μM zeocin
	Total number of lateral roots and primordia
WT	NS
<i>wee1-1</i>	***
<i>gstf9</i>	***
<i>dm</i>	***

	Level of significant difference \pm 10 μM zeocin
	Total number of lateral roots and primordia
WT	***
<i>wee1-1</i>	***
<i>gstf9</i>	***
<i>dm</i>	***

	Level of significant difference \pm 20 μM zeocin
	Total number of lateral roots and primordia
WT	***
<i>wee1-1</i>	***
<i>gstf9</i>	***
<i>dm</i>	***

	Level of significant difference \pm 50 μM zeocin
	Total number of lateral roots and primordia
WT	***
<i>wee1-1</i>	***
<i>gstf9</i>	***
<i>dm</i>	***

Key. *** < 0.001, ** = 0.02-0.001 P, * = 0.02-0.05 P, NS >0.05

Table 3.15 Student's t-test results for total number of lateral roots and primordia within a genotype in 10 compared with the 20 μ M zeocin treatment within each genotype.

	<i>wee1-1</i>	<i>gstf9</i>	<i>dm</i>
	Total number of lateral roots and primordia	Total number of lateral roots and primordia	Total number of lateral roots and primordia
20 μ M zeocin	*	NS	NS

Key. *** < 0.001, ** = 0.02-0.001 P, * = 0.02-0.05 P, NS >0.05

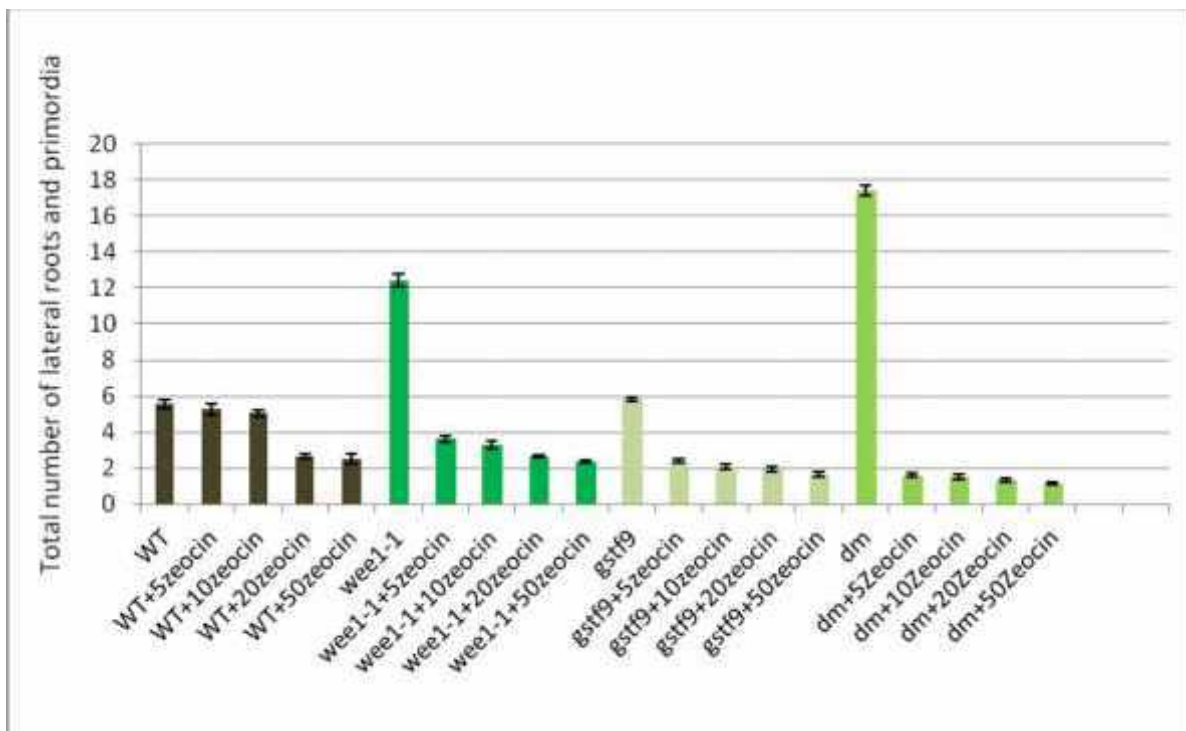


Figure 3.20 Total number of lateral roots and primordia (\pm SE) of 10 day old Arabidopsis seedlings in the genotypes: WT, *wee1-1*, *gstf9* and *wee1-1 gstf9 (dm)* grown on MS agar plates supplemented with 5, 10, 20 or 50 μ M zeocin (n=20)

Table 3.16 Rate of lateral root production $\text{mm primary root}^{-1}$ in the different genotypes of 10 day old Arabidopsis seedlings obtained by dividing the x by the y coordinates for each point plotted in Fig. 3.22.

	Rate of lateral root production $\text{mm primary root}^{-1}$				
	-HU	5 μM zeocin	10 μM zeocin	20 μM zeocin	50 μM zeocin
WT	0.17	0.21	0.3	0.26	0.2
<i>wee1-1</i>	0.31	0.58	0.56	0.51	1
<i>gstf9</i>	0.19	0.20	0.19	0.19	0.2
<i>dm</i>	0.36	0.37	0.5	0.5	0.48

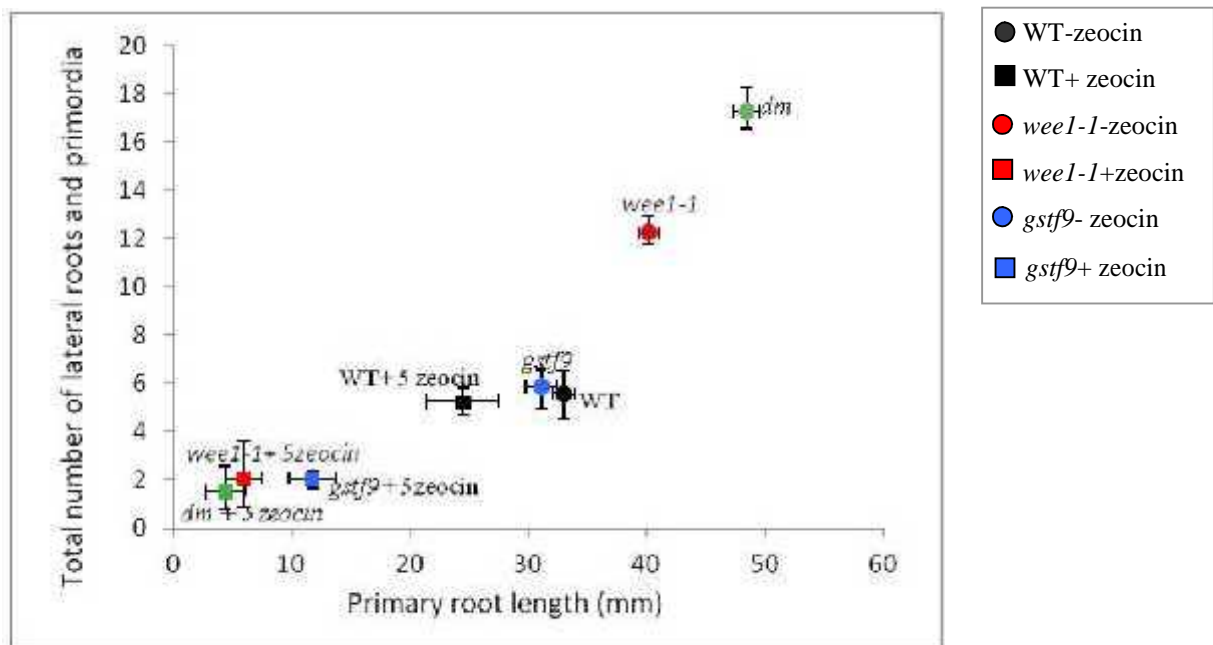


Fig 3.21 The relationship between primary root length and total number of lateral roots and primordia in 10 day old seedlings of WT, *wee1-1*, *gstf9* and the *dm*. Means \pm SE are plotted with error bars for both x and y coordinates. Where error bars are absent the variation about the mean was less than the diameter of the symbol. (n =20)

3.4.4.2 Meristem length

The meristem length was examined in all genotypes in response to different concentrations of zeocin. In agreement with the experiment relating to HU treatments, in untreated seedlings, mean meristem length was again slightly higher than in the WT in 5 μ M zeocin, but again differences were not statistically significant (Table 3.17). From my results it is obvious there was a negative concentration-dependent relationship between meristem length and zeocin concentration for all genotypes (Fig. 3.23). This is in agreement with the inhibition of primary root length by increasing the amount of zeocin in all genotypes. The pattern of reduction in meristem length was remarkably similar to that elicited with HU.

In WT, the decrease in meristem length in the 5 μ M zeocin treatment was less significant compared with the control ($P = 0.04$) but it was more significant with increasing zeocin concentrations ($P = 0.001^{***}$). For the mutant genotypes, increasing concentrations of zeocin resulted in a gradual decrease in meristem length but the reductions between concentrations were significant ($P = 0.02^*$).

wee1-1 and *wee1-1 gstf9 (dm)* exhibited a very similar pattern of reduction in meristem length in response to increasing zeocin concentration but with the greatest reduction occurring for the *dm* in response to 5 μ M zeocin ($P = 0.001^{***}$). A more or less linear pattern of reduction in meristem length in *gstf9* in response to increasing concentrations of zeocin was observed.

Hence, the induction of the DNA damage checkpoint resulted in progressively shortened RAMs in a similar way to the reductions observed in RAM length in the HU experiments (see Fig. 3.22 compared to Fig. 3.11) Furthermore the absence of a functional

Arabidopsis; *WEE1* appears to have a greater effect on the response to DNA damage than the lack of a functional *GSTF9*, as was also the case for the HU treatment which induces the DNA replication checkpoint. Note that in *wee1-1* and the *dm* meristems, there was a hypersensitive responses (Fig 3.22), in the 0 to 5 μ M zeocin step up. This is consistent of a functional role for *WEE1* but not *GSTF9* in regulating meristem length.

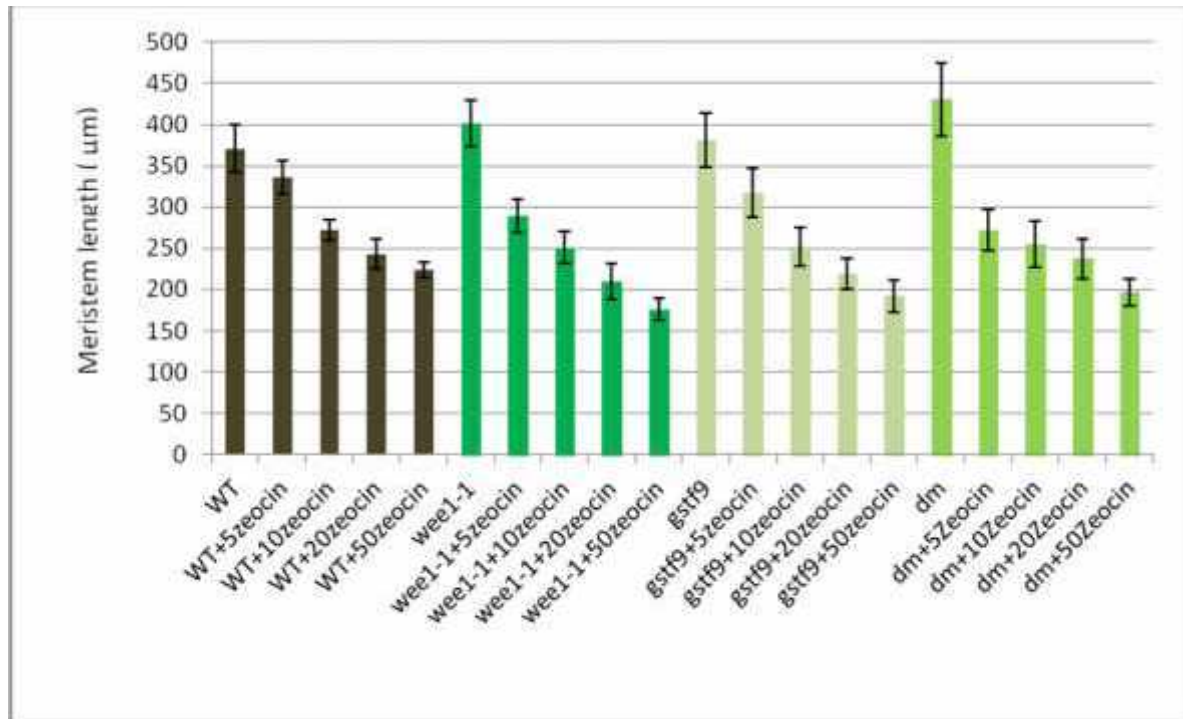


Figure 3.22 Mean (\pm SE) length of the primary root apical meristem in 10 day old seedlings of various genotypes of *Arabidopsis*: wild type plants (WT), *wee1-1*, *gstf9*, and the *dm* with treatments with four different concentrations of zeocin (5, 10, 20 and 50 μ M) n =20

Table 3.17 Student's t-test results for total number meristem length within a genotype in 5, 10 or 20, 50 μ M zeocin compared with the 0 zeocin treatment .

	Level of significant difference \pm 5 μM zeocin
	Meristem length
WT	NS
<i>wee1-1</i>	**
<i>gstf9</i>	NS
<i>dm</i>	***

	Level of significant difference \pm 10 μM zeocin
	Meristem length
WT	**
<i>wee1-1</i>	***
<i>gstf9</i>	***
<i>dm</i>	***

	Level of significant difference \pm 20 μM zeocin
	Meristem length
WT	***
<i>wee1-1</i>	***
<i>gstf9</i>	***
<i>dm</i>	***

	Level of significant difference \pm 50 μM zeocin
	Meristem length
WT	***
<i>wee1-1</i>	***
<i>gstf9</i>	***
<i>dm</i>	***

Key. *** < 0.001, ** = 0.02-0.001 P, * = 0.02-0.05 P, NS >0.05

3.4.4.3 Number of epidermal cells along the meristem

In WT, in response to progressive increases in zeocin concentration, there was a progressive decrease in the number of epidermal cells within the RAM. Fig 3.23 is very similar to the cell number response of WT in the HU treatments (compared to Fig. 3.12). However, as with the HU treatments, the mutant genotypes responded differently to zeocin. Indeed, there was a remarkable buffering of epidermal cell number in response to increasing zeocin concentrations for all three mutant genotypes exactly as there was in response to HU (Figs 3.23 and 3.12). There was a subtle difference between the mutant genotypes: while, 5 μM zeocin elicited a significant response in *wee1-1* this was not the case in *gstf9* or the *dm*. (Table 3.18). Again as seen with the HU treatment, cell number in the RAM was higher for both *wee1-1* and *gstf9* compared to WT.

3.4.4.4 Epidermal cell length

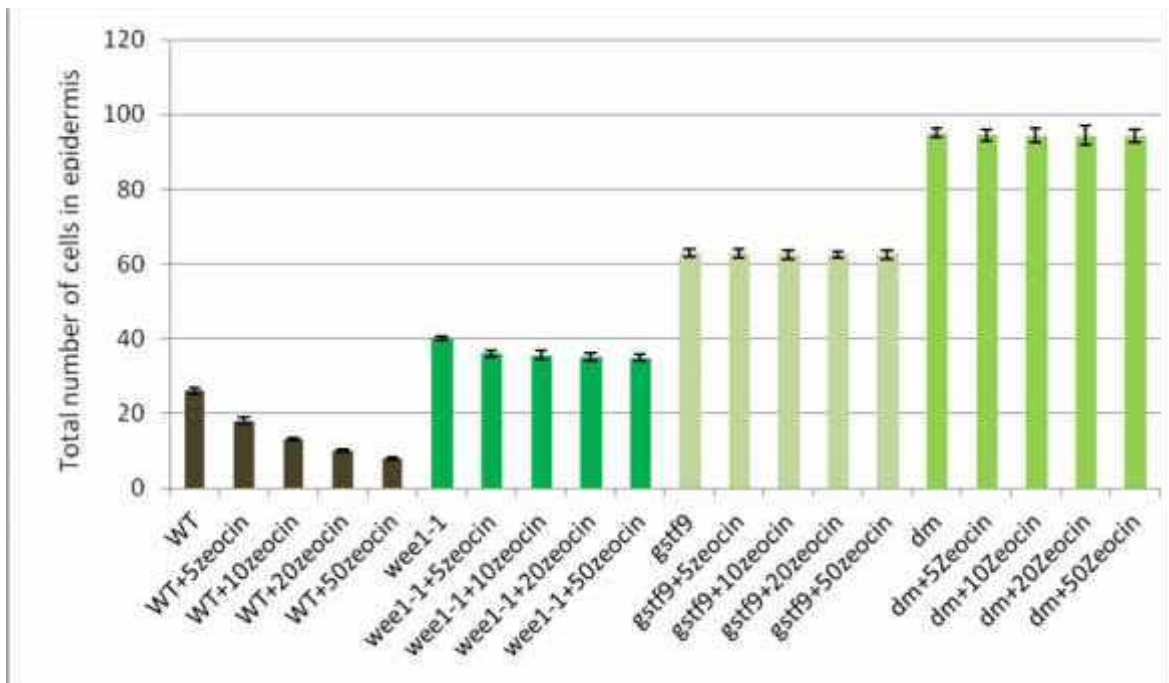


Figure 3.23 Mean numbers of cells in an epidermal file of cells from the RAM (\pm SE) in 10 day old seedlings of various genotypes of Arabidopsis: (WT), *wee1-1*, *gstf9*, and the *dm*, \pm four different concentrations of zeocin (5, 10, 20 and 50 μM grown in 16 h light and 8 h dark at 21°C). (n = 20)

Table 3.18 Levels of significant differences between the number of epidermal cells in the RAM in 5, 10 or 20, 50 μ M zeocin compared with the 0 zeocin treatment within a genotype.

	Level of significant difference \pm 5 μ M zeocin	Level of significant difference \pm 10 μ M zeocin	Level of significant difference \pm 20 μ M zeocin	Level of significant difference \pm 50 μ M zeocin
	Number of cells in RAM	Number of cells in RAM	Number of cells in RAM	Number of cells in RAM
WT	*	**	***	***
<i>wee1-1</i>	*	NS	NS	NS
<i>gstf9</i>	NS	NS	NS	NS
<i>dm</i>	NS	NS	NS	NS

Key. *** < 0.001, ** = 0.02-0.001 P, * = 0.02-0.05 P, NS >0.05

Effects of zeocin on epidermal cell length (Fig 3.24, Table 3.19) was also similar to the effects of HU (Fig. 3.14). Note also that whilst zeocin (all concentrations) treatment resulted in a progressive increase in epidermal cell length in the WT, the exact converse holds true for the mutant genotypes. The very similar trend of decrease in cell length with respect to increasing zeocin for all three mutant genotypes tends to suggest that *WEE1* and *GSTF9* are operating in the same genetic pathway that regulates cell size in the meristem in a treatment that induces the DNA damage pathway. However, cell size measurements in the cortex and stele would be required to verify this tentative conclusion.

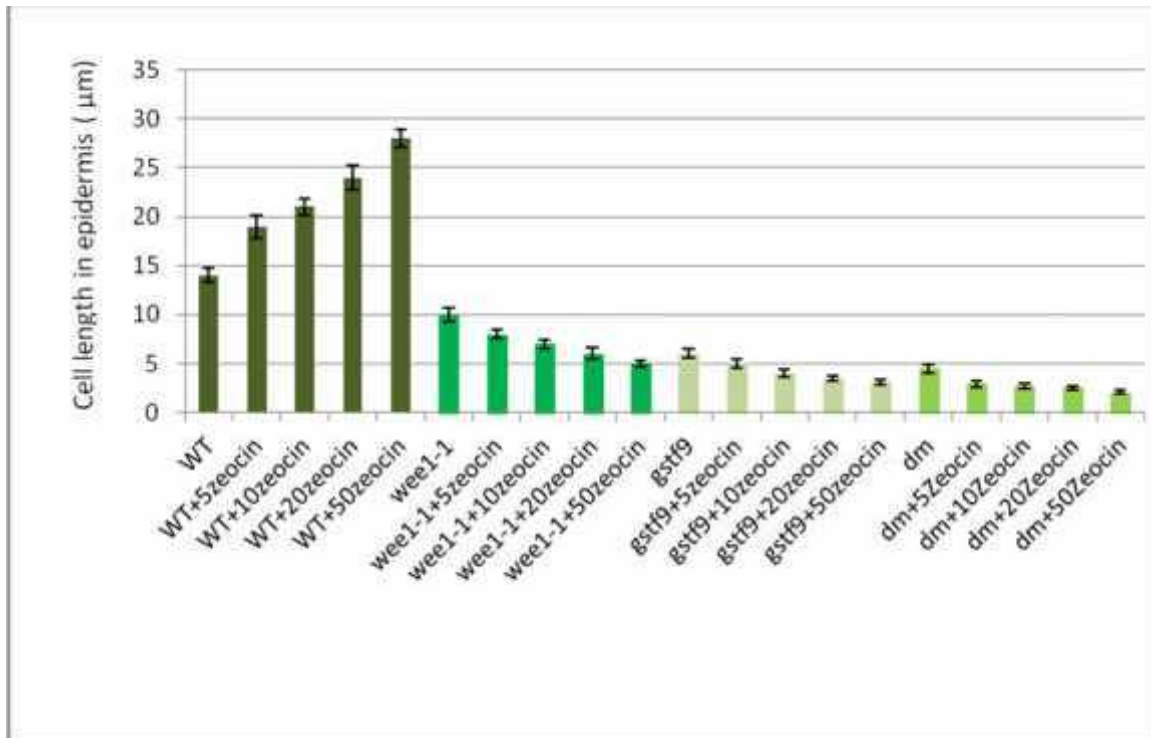


Figure 3.24 The relationship between mean (\pm S.E.) cell length in epidermis of the RAM in different genotypes of Arabidopsis: wild type (WT) , *wee1-1*, *gstf9* and the *dm* \pm four different concentrations of zeocin (5, 10, 20 and 50 μ M) in 10 day old Arabidopsis plants grown in 16 h light and 8 h dark at 21°C (n =20).

Table 3.19 Levels of significant differences between the number of epidermal cells in the RAM in 5, 10 or 20, 50 μ M zeocin compared with the 0 zeocin treatment within a genotype.

	Level of significant difference \pm 5 μ M zeocin	Level of significant difference \pm 10 μ M zeocin	Level of significant difference \pm 20 μ M zeocin	Level of significant difference \pm 50 μ M zeocin
	Cell length RAM	Cell length RAM	Cell length RAM	Cell length RAM
WT	***	***	***	***
<i>wee1-1</i>	*	*	**	**
<i>gstf9</i>	***	NS	NS	NS
<i>dm</i>	*	*	*	*

Key. *** < 0.001, ** = 0.02-0.001 P, * = 0.02-0.05 P, NS >0.05

3.4.4.5 Percentage of cells in each component phase of the cell cycle in RAM of WT, *wee1-1* and *gstf9* ± zeocin treatment

WT responded differently to zeocin compared with HU. Whilst more cells were in G1 phase as zeocin concentration increased, there was also a substantial increase in the percentage of cells in G2, whereas in the HU treatments the percentage in G2 declined progressively (Fig 3.25 compared to Fig 3.17). Hence the induction of the DNA damage checkpoint resulted in a progressive accumulation of cells in G2. In other words it seems likely that the induction of chromosomal damage halted cells in G2. Consistent with this, is a progressive decrease in the mitotic index in response to increasing concentrations of zeocin in WT (Table 3.20), while the mitotic index and percentage of cells in G1, S and G2 were relatively stable in *wee1-1* and *gstf9*. This suggests that in all three mutant genotypes, cells were dividing and hence escaping the DNA damage checkpoint. Moreover the mitotic index data are very near equal to an additive response of *WEE1* and *GSTF9* when the mutants are challenged with zeocin. This further suggests that *WEE1* and *GSTF9* are working through different pathways in the DNA damage checkpoint. However, microdensitometric data for the *dm* would be required to verify this conclusion.

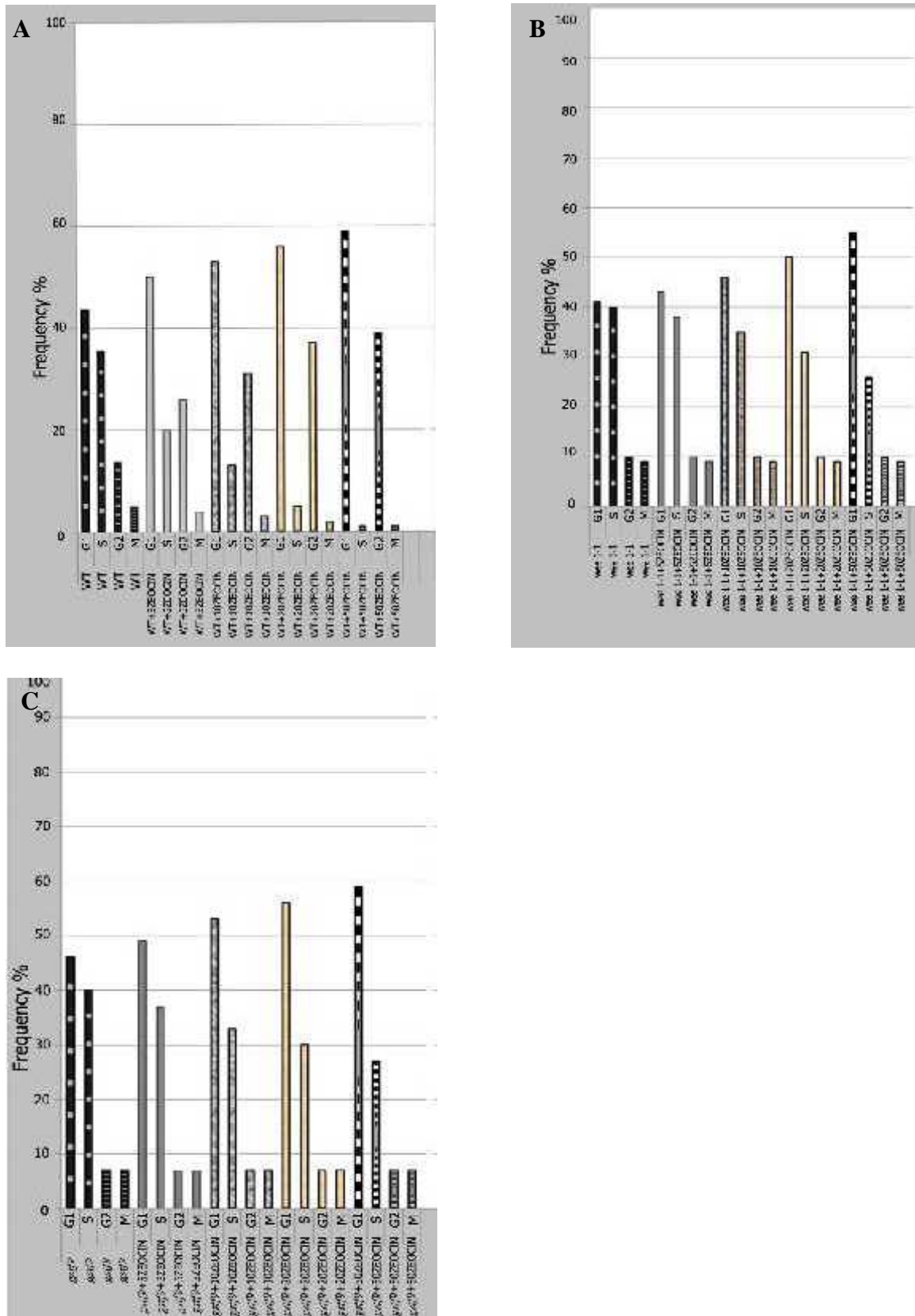


Figure 3.25 The percentage frequency of cells in G1, S-phase, G2 and M-phase in squash preparations from RAMs of 10 day old seedlings of: (A) wild type (WT), (B) *wee1-1*, (C) *gstf9* treated with four different concentrations of zeocin (5, 10, 20 and 50 μM) (n = 20).

Table 3.20 Percentage of cells in M-phase of wild type (WT), *wee1-1*, *gstf9* and the *dm* with zeocin treatment

Mitotic Index	0 μ M zeocin	5 μ M zeocin	10 μ M zeocin	20 μ M zeocin	50 μ M zeocin
WT (%)	5	4	3	2	1
<i>wee1-1</i> (%)	9	9	9	9	9
<i>gstf9</i> (%)	7	7	7	7	7
<i>dm</i> (%)	12	12	12	12	12

3.5 Discussion

Previous studies using BiFC indicated a nuclear site of interaction between *Arath*;WEE1 and GSTF9 (Gemma Cooke, Cardiff Lab., unpublished data), so perhaps GSTF9 is needed for *Arath*;WEE1 function. I tested this hypothesis by examining the phenotype of the two single mutants *wee1-1* and *gstf9* and the double mutant *wee1-1 gstf9* (*dm*). Firstly I checked that the *gstf9* line was indeed homozygous and that transcription of the *GSTF9* gene had been abolished. Although no transcripts were detected using PCR primers that spanned the insertion point of the T-DNA, a product was obtained from the RT-PCR when a primer internal to the T-DNA was used, indicating that there appeared to be some transcription driven by sequences from within the T-DNA which could result in truncated mRNAs and possibly protein. Further work would be required using Northern and Western analysis to confirm this. Meanwhile this mutant can be considered a knock-down of the full *GSTF9* transcript. Next I generated a double mutant deficient in both genes and confirmed its genotype. I then examined how each genotype responded to either HU or zeocin, inducers of the DNA replication and DNA damage checkpoints, respectively.

3.5.1 Primary root elongation of both *wee1-1* and *gstf9* mutant is hypersensitive to HU and zeocin compared to WT

In the work reported in this chapter, HU treatment causes a shorter primary root length in agreement with the data of De Schutter *et al* (2007). Wild type roots grew to a length of

approximately 35 mm over the 10 day period of growth. Increasing concentrations of HU from 1 to 5 mM induced a graduated inhibition of primary root elongation. In the WT, rate of primary root elongation decreased by 1.41-fold in the + compared with the -HU treatment. However, primary root elongation was not completely inhibited. Instead in the + HU treatment, the rate of elongation was reduced. Hence it seems likely that the HU treatment induced the DNA replication checkpoint in WT but the time taken to overcome it had the knock-on effect of a slower rate of elongation compared with WT-HU.

Interestingly in the control (0 HU) treatment, 10-day-old *wee1-1* seedlings had significantly longer primary roots than WT ($P < 0.05$) confirming the earlier observations in the Cardiff lab. Increasing concentrations of HU greater than 1 mM had a greater effect in decreasing primary root length compared with 1 mM.

In the *gst-f9* line, root length was again significantly shorter in the 1, 2 and 5 mM HU compared with the 0 mM HU treatment. Thus these phenotypic analyses support a role for *GSTF9* in the DNA replication checkpoint which would be consistent with the evidence of interaction of *Arath*;WEE1 and *GSTF9*. However the response of *wee1-1* and *gstf9* double mutant suggest a near additive effect of *WEE1* and *GSTF9* in response to the induction of the DNA damage checkpoint in relation to primary root elongation. This indicates that the two genes may be at least in part acting through different pathways to exert their effects.

The zeocin treatment elicited a similar effect on the mutant lines to HU, both showing hypersensitivity to this DNA-damaging agent. Here too the greater effect is exerted by the *WEE1* gene rather than the *GSTF9*, and the effects in the *dm* are partly additive indicating that there are independent effects of the two genes.

3.5.2 Lateral root production in the presence of HU or zeocin was enhanced in *wee1-1* but not *gstf9* mutants compared to WT

In the HU treatments, the mutant phenotypes exhibited similar rates of increase in lateral root formation relative to -HU. The number of laterals in the WT decreased in a graduated fashion with increasing levels of HU or zeocin which was not so for the two mutant genotypes. For the *wee1-1* controls, a significant increase in the number of laterals was evident compared with WT but a highly significant reduction of LR formation was recorded in the 1 mM HU treatment ($P < 0.001$). This behaviour was true for higher concentrations (either 2 or 5 mM) of HU. Treatment with zeocin resulted in a very similar response.

However, note that whereas *wee1-1*, lacking a functional *Arath;WEE1* makes more laterals than WT, *gstf9* lacking GSTF9 but having a functional copy of *Arath;WEE1* is not significantly different from WT in lateral root production. This means that the absence of *GSTF9* alone there is no effect on lateral root production. This is supported by the rate calculated for the double mutant which is not significantly different to the *wee1-1* mutant line in lateral root production. In the 1mM HU treatment, compared with WT the magnitude of increase in the rate of lateral root formation is 1.9 and 2.2 in the *wee1-1* and *dm*, respectively but is no different in *gstf9*. In the 2 mM HU treatment, there is a 2.5 and 2.4 fold increase in the rate for *wee1-1* and *dm* respectively. However, the most substantial increase occurred in *gstf9* (a 3.4 fold increase). In the 5 mM treatment, there is no substantial difference in the rates of lateral root formation between genotypes and most probably indicates that the level of HU has reached toxic levels for all genotypes. Thus the effects of GSTF9 and *Arath;WEE1* on the DNA replication checkpoint, as inferred from the phenotypes of these mutant alleles, seem to be similar but differ in some of their features. The results from the double mutant appear to be

consistent in indicating an effect of the two genes which may at least in part be independent of each other.

Under zeocin treatment as it was observed in the HU treatment, *wee1-1* roots produced more laterals than *gstf9* but the double mutant showed a similar rate to *wee1-1*. Moreover, the response of the double mutant to zeocin treatment was like that of *wee1-1*. However, the effect of 5 μ M zeocin compared to 0 μ M zeocin on the rate of lateral root production in the *dm* matched more closely that of the *gstf9* than *wee1-1* mutant, suggesting that in this feature at least *gstf9* may be exerting the more major effect. These data emphasise that the primary root length, total number of lateral roots, but not the rate of LRP production under zeocin treatment are governed by *WEE1* without any interaction with *GSTF9*.

3.5.3 Root apical meristem length in the presence of HU or zeocin was reduced in *wee1-1* mutants

The length of the root apical meristem (RAM) was estimated as the extent of tightly packed cells at the root tip, resolved by microscopy as a dark area of the root tip in fixed seedlings. It should be noted that these are not definitive measurements of meristem size but are used here on a comparative basis.

In wild type and in the mutant lines, increasing concentrations of both HU and zeocin caused a graduated reduction in meristem length. However, whereas *wee1-1* was hypersensitive to HU and zeocin in its meristem length reduction, *gstf9* was not. The effects on the *dm* were most similar to *wee1-1*. This suggests that whereas *Arath;WEE1* is required for the maintenance of meristem size under HU and zeocin stress, *GSTF9* is not. To my knowledge this is the first time that meristem length has been reported on in relation to abiotic stress.

3.5.4 HU or zeocin affects cell size and number in the epidermal layer of the RAM in both *wee1-1* and *gstf9* mutants compared to WT

In the absence of zeocin or HU, the epidermal cells in the RAM were significantly smaller in *wee1-1*, *gstf9* and the *wee1-1 gstf9* double mutant line. This might be because of premature cell division in the absence of either *WEE1* or *GSTF9*. Gonzalez *et al.* (2007) showed that *S. lycopersicon* *WEE1* has a role in cell size control. In addition studies of model systems in *S. pombe*, *X. laevis* and *H. sapiens* indicated that Wee1 has a critical role in controlling cell size (McGowan and Russell, 1995; Aligue *et al.*, 1997; Michael and Newport, 1998; Goes and Martin, 2001; Watanabe *et al.*, 2004; Watanabe *et al.*, 2005). Also Nurse *et al.* (1977) showed that the Wee1 protein was a negative regulator of cell division in *S. pombe* by delaying entry into mitosis. A similar role of Swe1 was found in controlling the cell size in *S. cerevisiae* (Jorgensen *et al.*, 2002; Harvey and Kellogg, 2003). However a role for *GSTF9* or any other GST in regulating cell size had not, to my knowledge, been previously reported.

There was a clear differential effect of hydroxyurea or zeocin on WT compared with all three mutant genotypes. Whilst increasing levels of HU or zeocin resulted in progressive increases in cell length, the converse occurred in the mutant genotypes. However, note that there were significantly more cells in the epidermis of *wee1-1* compared with WT, and progressively more epidermal cells in *gstf9* ($P < 0.001$), and then the most in *wee1-1 gstf9* ($P < 0.001$) under HU or zeocin stress. Interestingly, the number of epidermal meristematic cells remained remarkably constant in the three mutant genotypes regardless of HU or zeocin concentration. It seems the production of aberrant cells, with suspected incomplete or perturbed DNA replication, is unable to contribute as strongly to elongation growth as unperturbed ones in WT since keep the rate of primary root

elongation fell in WT in the presence of HU or zeocin, in the mutants elongation has stopped.

This indicates that both *Arath;WEE1* and *GSTF9* are important in the DNA replication/DNA damage checkpoint, but the effects to the two genes appear in both cell number and cell length to be additive.

3.5.5 HU or zeocin affects the percentage of cells in each component phase of the cell cycle in the RAM in both *wee1-1* and *gstf9* mutants compared to WT

In *wee1-1*, HU or zeocin treatment did not alter greatly the percentage of cells in each phase although more cells were in G1 at the higher zeocin concentrations. Hence, in the absence of a functional *WEE1*, cells continued to cycle. Again the stability of the mitotic index in the zeocin treatments would be consistent with this view. These data confirm a requirement for *WEE1* in the DNA damage checkpoint. The cell cycle response of *gstf9* to zeocin is remarkably similar to that of *wee1-1*. Hence on the basis of these data, the absence of a functional *GSTF9* also enabled cells to go through the cell cycle even in the presence of a functional *WEE1*. In the *gstf9* mutant these data support the idea of an involvement of *GSTF9* in regulating the DNA repair checkpoint.

In the presence of a functional *WEE1* but the absence of a functional *GSTF9*, it looks as if the DNA replication checkpoint has been induced given the remarkable similarity of nuclear DNA distributions in the two mutant genotypes. Maintenance of the same or very similar percentages of cells in each cell cycle phase in *wee1-1* in response to HU and zeocin confirms a role for *WEE1* in the DNA damage and DNA replication checkpoints. The mitotic index was higher in *wee1-1* than WT in treatments at different concentrations of HU. These data are consistent with the idea that in the absence of a functional *WEE1*,

cells in the RAM were bypassing the DNA replication checkpoint and escaping into mitosis. However, again, there is no evidence to show that HU induced any polyploidy in these RAMs

4. Studying the interaction between Arabidopsis GF14 Š and Arath;WEE1

4.1 Introduction

14-3-3 proteins are highly conserved in plants and animals (Dougherty and Morrison, 2004). There are 15 isoforms of 14-3-3 proteins in Arabidopsis although two of them are pseudo-isoforms. The thirteen functional 14-3-3 proteins in Arabidopsis are divided into two phylogenetic groups, Epsilon and Non-Epsilon, based on their amino acid sequence (DeLille *et al.*, 2001). In a yeast 2-hybrid assay the non-Epsilon group interacts with Arabidopsis WEE1 (Lentz Grønlund *et al.*, 2009). 14-3-3 proteins are distributed widely in all parts of the cell, as a result, they may have different biological roles in the cell (Ferl *et al.*, 2002). The isoforms of 14-3-3 are distributed in the nucleus, plasma membrane, cell wall, and cytoplasm (Bihn *et al.*, 1997). Involvement of Arabidopsis 14-3-3 proteins in activation of the plasma membrane H⁺ATPase has been demonstrated (Jahn *et al.*, 1997; Rosenquist *et al.*, 2000). Some non-Epsilon group 14-3-3 proteins have a physical association with proteins involved in the photoperiodic control pathway; moreover, different groups of 14-3-3 protein mutants exhibit a delay in flowering, and also growth inhibition in hypocotyl (Mayfield *et al.*, 2007). Three 14-3-3 proteins (, and), which belong to the non-Epsilon group (also known as GF14 , and), from Arabidopsis were found to interact with *S. pombe* Cdc25, but only the GF14 isoform could complement an *S. pombe* rad24⁻ mutant (Sorrell *et al.*, 2003). One Arabidopsis 14-3-3 isoform (GF14A) accumulates differentially in the cell's nucleus during the cell cycle. It is excluded from the nucleus throughout most of the cell cycle but accumulates in the nucleus just after

nuclear division, and disappears just before the completion of cytokinesis (Cutler *et al.*, 2000).

In Arabidopsis, Sorrel *et al.*, (2002) showed that the transcription of *GF14* is restricted to proliferative regions of Arabidopsis plants again supporting a role for this protein in cell division. Lentz Grønlund (2007) showed an interaction between GF14 and Arath;WEE1 by 2-hybrid analysis. This interaction was verified *in vitro* by immunoprecipitation and in plant cells, using bimolecular fluorescence complementation (BiFC) (Walter *et al.*, 2004; Lentz Grønlund *et al.*, 2009). Furthermore a putative 14-3-3 binding site was located in the Arath;WEE1 protein at position S485, by homology to other WEE1 proteins. When the WEE1 coding sequence was mutated to encode alanine instead of serine at this position, the 2-hybrid interaction was abolished, although the BiFC signal was affected only in its localisation (Lentz Grønlund *et al.*, 2009). Thus there was strong evidence from this work that there was a specific interaction between GF14 and Arath;WEE1. However the functionality of this interaction had not been tested.

GF14 was over-expressed in Arabidopsis under an oestradiol-inducible promoter (Zuo *et al.*, 2000, Fig. 4.1).

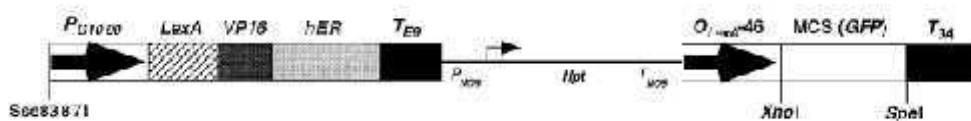


Fig 4.1 A schematic diagram of the XVE vector (Zuo *et al.*, 2000) showing the multiple cloning site MCS. This vector was used for oestrogen receptor-based transactivation which mediates gene expression in transgenic Arabidopsis plants and in this case over-expression of *GF14*. The chimeric transcription factor XVE is composed of LexA (DNA binding domain), VP16 (transcription activation domain), hER (oestrogen receptor regulatory domain) and T_{E9} (terminator) driven by P_{G10-90} (a synthetic promoter). O_{LexA}⁻⁴⁶ contains eight copies of the LexA operator sequence that activate transcription of the *GF14* when the oestrogen binds to the hER region.

In preliminary experiments, over-expressing *GF14* induced a decrease in the rate of primary root elongation compared with WT (Lentz Grønlund *et al.*, Cardiff Lab, unpublished results). This phenotype is similar to that of over-expressing *Arath;WEE1*. This would fit with a hypothesis that *GF14* stabilises *Arath;WEE1* at the protein level, increasing its activity *in vivo*. Hence an over-expression of *GF14* might result in increased WEE1 activity resulting in a phenotype similar to *Arath;WEE1* over-expression. If the effect of *GF14* over-expression is mediated by *Arath;WEE1*, then over-expression of *GF14* in the *wee1-1* mutant background would have a null effect. However, if in the cross, *GF14* expression elicits the same phenotype as in the WT genetic background then we can conclude that the effects are independent of *Arath;WEE1*.

However, later experiments in the Cardiff lab failed to confirm the *GF14* over-expression phenotype probably due to a confounding effect from the oestradiol inducer on root growth; hence it was necessary to start by verifying the *GF14* over-expression phenotype.

In this chapter I present my results aimed at:

- (1) A further investigation of the phenotype of Arabidopsis plants over-expressing *GF14* to identify conditions that induced the *GF14* transgene but did not affect WT root growth
- (2) Establishing whether the *GF14* interaction with *Arath;WEE1* is a requirement for its function by crossing a *GF14* over-expressing line with the *wee1-1* line.

4.2 Materials and methods

4.2.1 Plant material

Over-expressing *GF14* line (line # 42, named here GF14 OEX), WT and a line over-expressing *Arath;WEE1* (line 61) called hereafter *WEE1*OEX were used for this work. Further details are in Chapter 2, Section 2.1.

4.2.2 Phenotypic analysis of an *GF14* overexpressing line

Seeds were sown onto MS (see Sections 2.2 and 2.14) with varying amounts of sucrose and oestradiol and root phenotype was analysed, (see Chapter 2, Section 2.17).

4.2.3 Cross between an *GF14* overexpressing line and *wee1-1*

Seeds of GF14 OEX (line # 42) and the homozygous T-DNA insertion line *wee1-1* were surface sterilised and grown as described in Chapter 2, Section 2.14 and 2.18 and then crossed as described in Chapter 2, Section 2.20.

To confirm the presence of the transgene in GF14 OEX and to confirm that the *wee1-1* line was carrying the T-DNA insertion, PCR was performed using primers: 35STRS, 14-3-3 RV for checking GF14 OEX genotypes and P4b, P6 for checking the *wee1-1* genotype. P60/P61 primers were used to check for the presence of the wild type *Arath;WEE1* gene (For primer sequences see Chapter 2, Section 2.3). The GF14 OEX line was a segregating population so it was a mixture of heterozygotes and hemizygotes (WT were eliminated by the hygromycin selection). Hence the genotypes of the F1 generation were expected to be as shown in Figure 4.2.

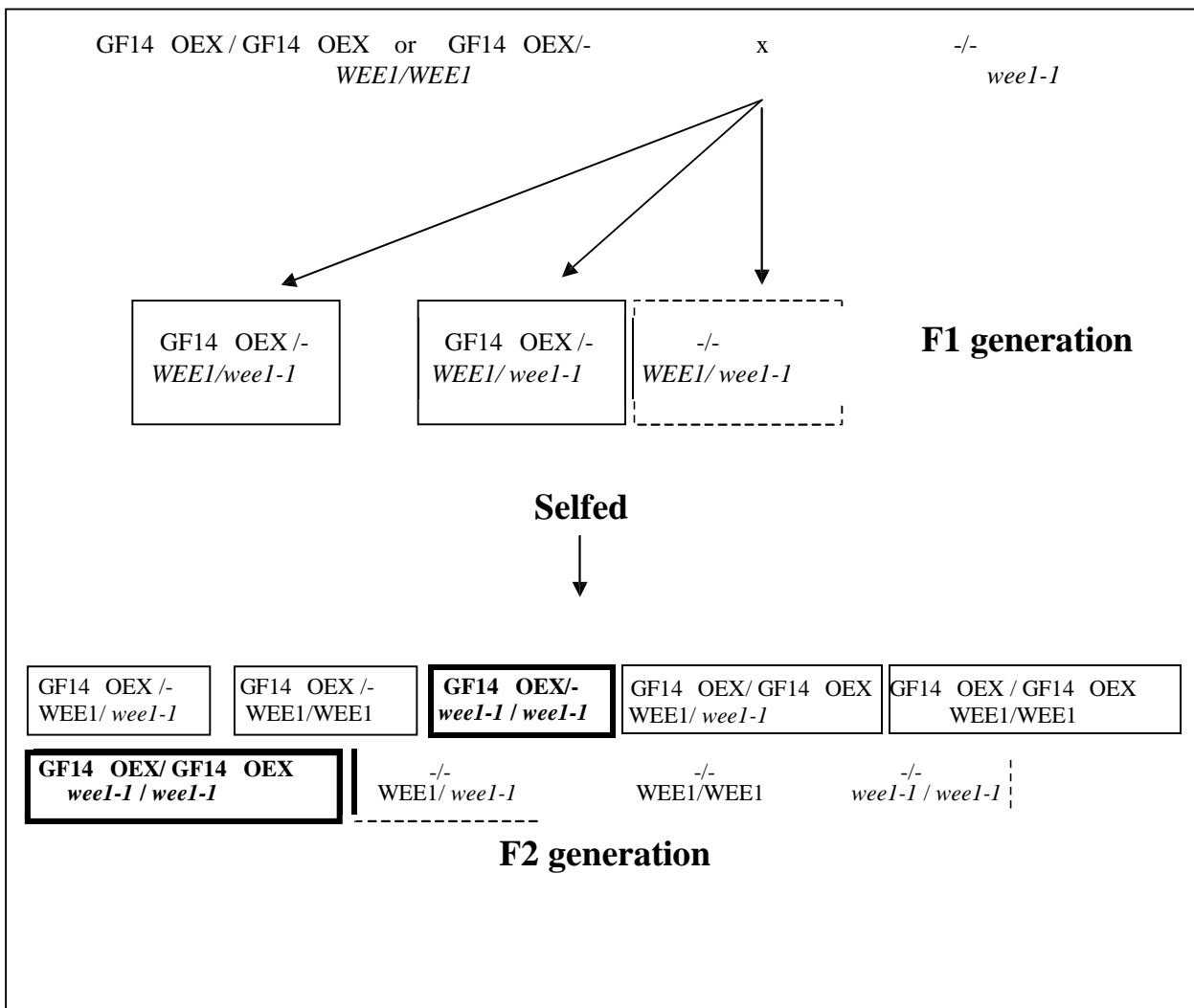


Figure 4.2 The progeny of cross between over-expressing *GF14* (GF14 OEX) and the T-DNA insertion line *wee1-1* showing F1 and F2 generations. WEE1 represents the WT copy of Arath;WEE1. Boxed in thicker lines are the genotypes of interest for phenotypic analysis and in broken lines, genotypes that were eliminated by hygromycin selection.

To recover seeds which were homozygous for the *wee1-1* mutant allele and carried at least one copy of the GF14 OEX transgene, it was necessary to take plants to the next generation (F2). Seeds of the cross were sown and PCR was carried on DNA extracted from leaves of these plants as above to check their genotype before proceeding. Possible genotypes from this generation of the cross are shown in Fig 4.2. One line from these

plants which was positive for both GF14 OEX primers and *wee1-1* primers (but not *Arath;WEE1* primers) was selected. This plant was selfed, 30 seeds of this line were sown and PCR was done on DNA extracted from each leaf. The ones which were positive for GF14 OEX primers and *wee1-1* primers, but negative for wild type primers were selected and the phenotyping on the roots of these seedlings was carried out as described in Chapter 2, Section 2.17.

4.3 Results

4.3.1 Optimising the oestradiol treatment for induction of the *GF14* in the GF14 OEX line

In transgenic Arabidopsis plants, induction of oestradiol activates the expression of the *GF14* under the control of a 35S promoter, whereas the uninduced controls had no detectable transcript (Cardiff lab, unpublished results). However previous work in the Cardiff lab. had suggested that oestradiol might affect root growth in WT, confounding the potential effects of *GF14* over-expression. I tested the oestradiol effect on wild type plants in medium with/without 3% (w/v) sucrose. At 1 or 2 μM of oestradiol with and without sucrose, no significant difference in primary root length was observed compared with the zero control (Table 4.1, Fig. 4.3). However, at a higher concentration of oestradiol (5 μM) with 3% sucrose was a statistically significant reduction in primary root length ($P < 0.05$). In further analysis I therefore sowed the GF14 OEX line on MS with 2 μM oestradiol and with 30 gl^{-1} sucrose to examine primary root length.

Table 4.1 Mean (\pm S.E.) primary root length of 10 day old Arabidopsis WT plants grown on medium \pm oestradiol \pm 30 $g\ l^{-1}$ sucrose. A student unpaired t-test was used to test for differences between in 0 and 1, 2 or 5 μM oestradiol and between 0 and 3% sucrose ($n=14$)

	0 μM oestradiol	1 μM oestradiol	Standard t-test
Medium with sucrose WT	37.1	37.5	NS
Medium without sucrose WT	37.3	37	NS
	0 μM oestradiol	2 μM oestradiol	
Medium with sucrose WT	37.1	37.4	NS
Medium without sucrose WT	37.3	37.8	NS
	0 μM oestradiol	5 μM oestradiol	
Medium with sucrose WT	37.1	25.6	***
Medium without sucrose WT	37.3	36.6	NS

Key. *** < 0.001, ** = 0.02-0.001 P, * = 0.02-0.05 P, NS >0.05

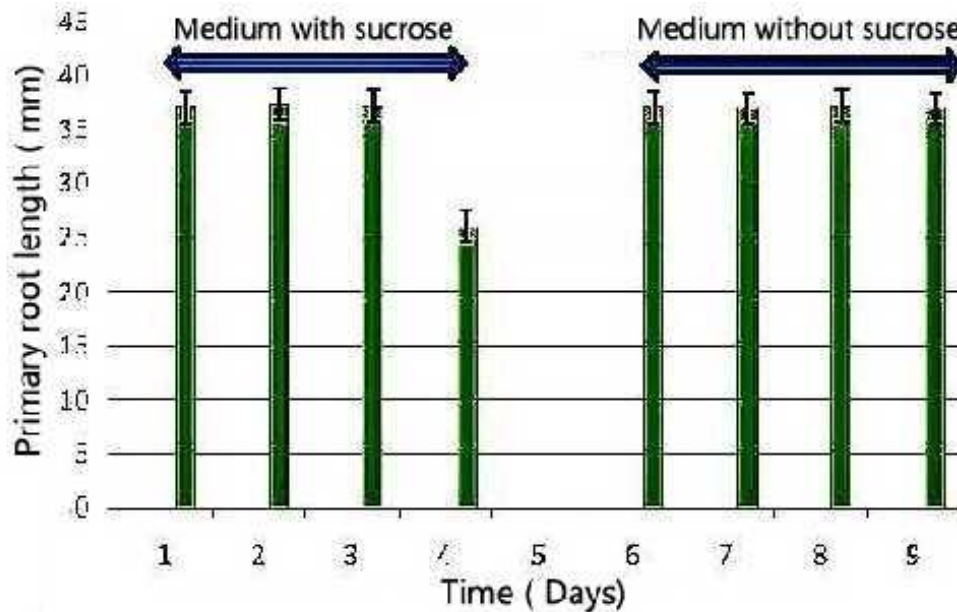


Figure 4.3 Mean (\pm S.E.) primary root length in wild type (WT) Arabidopsis plants grown in medium with 30 g/l and without sucrose and 0, 1, 2 or 5 μM oestradiol in 16 h light and 8 h dark at 21°C. $n=14$

4.3.2 Genotyping progeny from the cross between an GF14 OEX and *wee1-1*.

The seeds of F2 generation of the cross between GF14 OEX and *wee1-1* were sown directly onto soil. After plants became sufficiently large I checked by PCR for the presence of the GF14 OEX transgene and the *wee1-1* allele but absence of the *WEE1* allele. (Fig. 4.4).

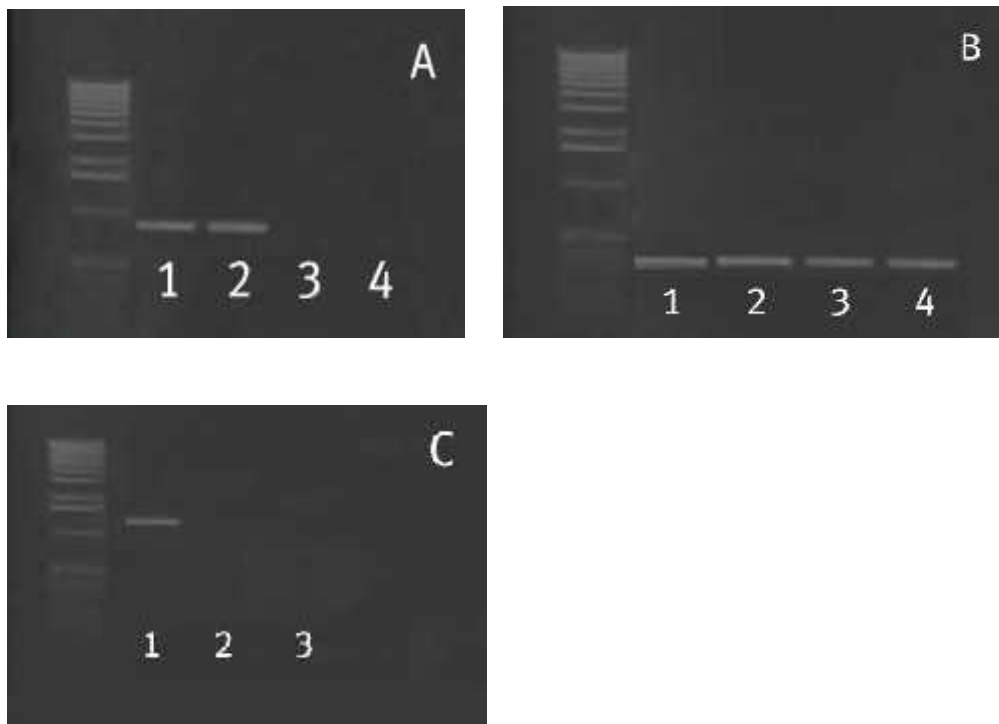


Figure 4.4 PCR carried out for checking plants of the cross between GF14 OEX and *wee1-1* with (A) GF14 OEX primers (35STRS and 14-3-3 RV) lanes: **1**) plant 1 **2**) plant2 **3**) plant 3 **4**) plant 4 (B) *wee1-1* primers (P4b/P6) lanes : **1**) plant 4 **2**) plant3 **3**) plant 2 **4**) plant 1 (C) P60/P61 primers, lanes: **1**) WT plant **2**) plant 3 **3**) plant 4

Plants 3 and plants 4 were positive for both GF14 OEX and *wee1-1* primers (Fig 4.4 (A) and (B) also the absence of the WT *Arath;WEE1* gene was confirmed by testing with P60/P61 primers (Fig4.4(C)).

Seeds from plant 3 were used for further analysis, testing for the presence of the GF14 OEX transgene before use in phenotyping.

4.3.3 Phenotype of progeny from the cross between an GF14 OEX and *wee1-1*

Analysis of primary root length within genotype, and total number of lateral roots and primordia within genotype confirmed that the sucrose/oestradiol (+OE) combination did not affect root growth in WT or in the transgenic line over-expressing *Arath;WEE1* (*WEE1*OEX) compared to the no oestradiol treatment (-OE) (Fig. 4.5). In the GF14 OEX line +oestradiol (+OE) primary root length and number of laterals+primordia were significantly reduced. *WEE1*OEX showed a similar root phenotype to the induced GF14 OEX line, a reduction in both primary root growth and production of lateral roots (Fig. 4.5 and 4.6).

The root phenotype of the progeny from the cross of GF14 OEX * *wee1-1* was also affected by the 2 μ M oestradiol treatment. Seedlings had a significantly shorter primary root length and a significantly reduced total number of lateral roots and primordia compared to WT. Furthermore the total number of laterals + primordia was significantly lower in the GF14 OEX *wee1-1* line compared with GF14 OEX + 2 μ M oestradiol and *Arath;WEE1* OEX + 2 oestradiol although primary root length in the GF14 OEX *wee1-1* line + 2 μ M oestradiol was not significantly different to the GF14 OEX + 2 μ M oestradiol.

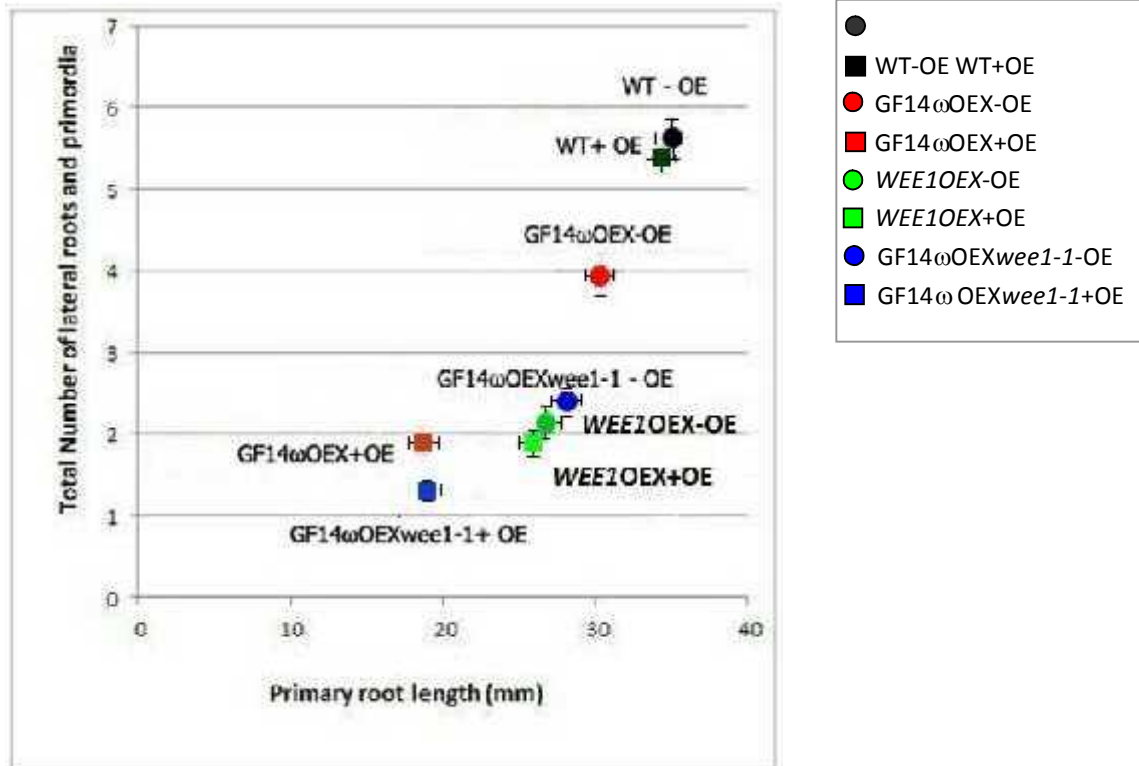


Figure 4.5 Relationship between primary root length and total number of lateral roots and primordia in wild type (WT), GF14 OEX, and GF14 OEX *wee1-1* 10 day old Arabidopsis plants grown in medium with or without 2 μ M oestradiol in 16 h light and 8 h dark at 21°C. n =15

Table 4.2 Within genotype (\pm S.E.) differences in primary root length and total number of lateral roots and primordia of wild type (WT) GF14 OEX, and GF14 OEX *wee1-1* Arabidopsis plants \pm 2 μ M oestradiol treatment n =14.

	Level of significant difference \pm 2 μ M oestradiol treatment primary root length	Level of significant difference \pm 2 μ M oestradiol treatment Total lateral roots and primordia
WT	NS	NS
WEE1OEX	NS	NS
GF14 OEX	***	**
GF14 OEX <i>wee1-1</i>	***	***



Figure 4.6 Root phenotype analysis of 10 day old Arabidopsis WT, *WEE1*OEX, GF14 OEX, and GF14 OEX *weel-1* grown on MS agar plates + 2 μ M oestradiol (OE).

Table 4.3 Rate of lateral root production mm primary root⁻¹ in the different genotypes of 10 day old Arabidopsis seedlings obtained by dividing the x by the y coordinates for each point plotted in Fig. 4.5.

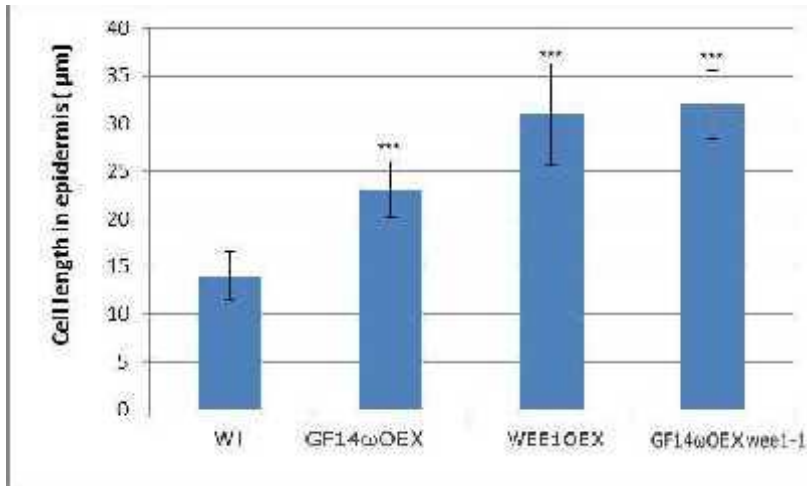
	Rate of lateral root production mm primary root ⁻¹	
	-OE	+OE
WT	0.15	0.14
GF14 OEX	0.13	0.1
<i>WEE1</i> OEX	0.07	0.06
<i>GF14 OEX weel-1</i>	0.08	0.06

In the genotypes–OE, the rate of lateral root formation was highest in WT and did not change significantly with the addition of oestradiol (+OE) (Table 4.3). GF14 OEX –OE would be predicted to have a rate similar to WT which was the case. Moreover, on addition of oestradiol (+OE) GF14 OEX and GF14 OEX *weel-1* rates of lateral root formation were both slower compared with WT: The rates were 1.4 and 2.33-fold slower respectively. *Arath;WEE1* over-expression should result in a slower rate than WT; the data in Table 4.3 confirmed the predictions and agree with other data obtained in the Cardiff lab. showing a similar negative effect of *Arath;WEE1* over-expression on the rate of lateral root production. However, in the cross, *GF14 OEX weel-1* +OE, it was predicted that in the absence of

functional *Arath*;WEE1, the rate would be similar to WT. Instead GF14 ω OEX *wee1-1* + OE cross exhibited a rate remarkably close to that for the GF14 ω OEX. This result is consistent with *GF14* having a negative effect on the rate of lateral production that is independent of its suggested role in stabilising WEE1.

To determine whether the effects on root growth were reflected in changes at a cellular level, cell length in a file of cells in the RAM epidermis was compared between the different lines (grown on medium supplemented with 2 μ M oestradiol). Cell length was significantly greater in the GF14 OEX, *WEE1*OEX and the GF14 OEX *wee1-1* lines compared with wild type (Fig. 4.7, Table 4.4).

(A)



(B)

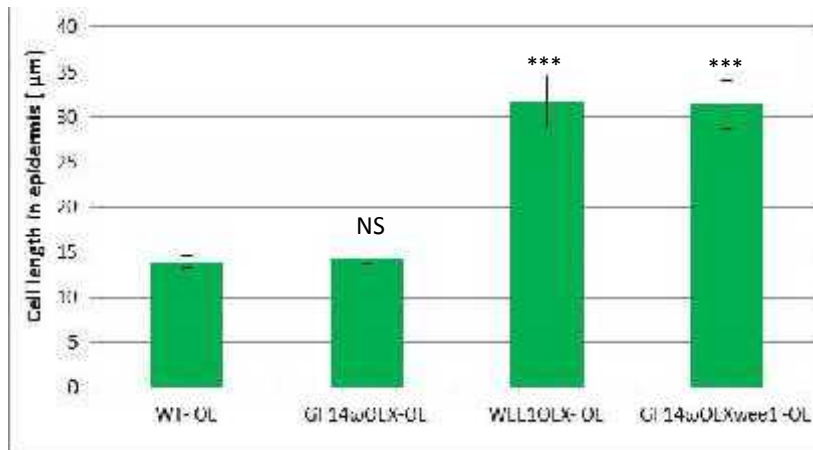


Figure 4.7 Mean cell length (\pm S.E.) in a file of cells in the RAM epidermis of wild type (WT), GF14 OEX, and GF14 OEX *wee1-1* in 10 day old Arabidopsis plants grown in medium + 30 g l⁻¹ sucrose) in 16 h light and 8 h dark at 21°C. n =14 (A) + 2µM oestradiol (B) Minus Oestradiol, P level(s): ***<0.001, NS, not significant from WT.

Table 4.4 Differences in epidermal cell length compared to WT for the different genotypes (GF14 OEX, WEE1OEX and GF14 OEX *wee1-1* ± oestradiol in 10 day old Arabidopsis plants (n =14).

	Level of significant difference ± 2 µM oestradiol treatment	Level of significant difference ± 2 µM oestradiol treatment
	Cell length in RAM's epidermis	Cell length in RAM's epidermis
wee1 OEX	***	***
GF14 OEX	***	NS
GF14 OEXwee1-1	***	***

Key. *** < 0.001, ** = 0.02-0.001 P, * = 0.02-0.05 P, NS > 0.05

4.4 Discussion

My starting hypothesis was that GF14 OEX would display a similar phenotype to over-expression of *Arath;WEE1* but that this phenotype would be suppressed when GF14 was expressed in the *wee1-1* mutant background. The rationale for this is that if the *Arath;WEE1* /GF14 interaction has functional significance then the expected function based on work in other species (see Section 4.1 and chapter 1, section 1.1.5.3) would be to stabilise WEE1. Hence the prediction of a similar effect in GF14OEX to over-expressing *Arath;WEE1*. However if the only effect of GF14 OEX is via the WEE1 interaction, then I would predict that mutation of the *Arath;WEE1* gene would abolish the GF14 OEX phenotype.

The first step was to optimise the oestradiol induction system. Previous work (Zuo *et al.*, 2000) used a range of oestradiol concentrations, but there was no clear indication of an interaction between sucrose and oestradiol. My discovery of an interaction with 30 g l⁻¹ sucrose in the medium explains the interaction seen in WT with some of the Cardiff lab. protocols for growing Arabidopsis. Previous studies by (Lentz Grønlund, 2007) showed over expressing GF14 induced a subtle decrease in the rate of primary root elongation compared with WT in the presence of oestradiol. My results confirm this result and further show a strong effect on production of lateral roots and primordia similar to that seen in the line over-expressing *Arath;WEE1*. So this would seem to confirm my hypothesis that the over-expression of GF14 may be stabilising *Arath;WEE1*.

I then tested whether *Arath;WEE1* is required for the GF14 OEX phenotype or not, and I observed that in the GF14 OEX *wee1-1* line, in which GF14 was induced by oestradiol, the phenotype was very similar to over-expression of GF14 OEX in the WT genetic background, In fact total number of lateral roots and lateral root primordia were even

lower. Thus the phenotype suggests that *Arath;WEE1* is not required for the action of GF14 . This was supported by the analysis of rates of LRP formation, and cell length in epidermal RAM cells where cell size in the GF14 OEX *wee1-1* line was even greater than in the GF14 OEX or the *Arath;WEE1OEX*. This does not exclude the possibility that the interaction between GF14 and Arath;WEE1 may be meaningful but indicates that GF14 also act on root growth and cell size independently of WEE1.

Lentz Grønlund *et al.*, (2009) showed that the interaction between Arath;WEE1 and GF14 was abolished in the S485A mutant. Further study on whether the Arath;WEE1 (S485A) mutant can complement the *wee1-1* mutant may throw further light on the function of GF14 and its relationship to Arath;WEE1.

5. Investigating the effects of expressing *Nicta;WEE1* in *Arabidopsis thaliana* and *Arath;WEE1* in *Nicotiana tabacum*

5.1 Introduction

In fission yeasts, *wee1* is the main genetic element involved in cell size control (Nurse, 1975). While loss of *wee1* function leads to a premature entry of cells into mitosis resulting in a small cell size, over expression of *wee1* has the opposite effect leading to a large cell phenotype due to a delay in mitotic entry (Russell and Nurse, 1987). Induced expression of *Arabidopsis thaliana WEE1* (*Arath;WEE1*) in *Schizosaccharomyces pombe* also delays cell cycle progression resulting in a large mitotic cell phenotype (Sorrell *et al.*, 2002). This indicates that in plants, *Arath;WEE1* may also be involved in regulating cell size. *S. cerevisiae* Swel and *Xenopus laevis* Wee1 proteins are regulated by ubiquitin degradation, while in *Homo sapiens*, WEE1 is regulated by phosphorylation and degradation (Kaiser *et al.*, 1998; Michael and Newport, 1998; Goes and Martin, 2001; Watanabe *et al.*, 2004; Watanabe *et al.*, 2005). A reduced level of endoreduplication was observed by the down-regulation of *Solly;WEE1* in tomato (Gonzalez *et al.*, 2007). It was shown in previous studies that endoreduplication is positively correlated with cell size (Melaragno *et al.*, 1993; Traas *et al.*, 1998). Notably, in the tomato line in which, *Solly;WEE1* was down-regulated, there was a reduced cell size and cell cycles which had a shortened G2 compared with wild type. Also, when *Solly;WEE1* was expressed in synchronised tobacco BY-2 cells, there was a notable delay in the first peak of mitotic index, and an increase in mitotic cell size was reported, (despite the fact that there was an overlap in standard errors in their data on cell size) (Gonzales *et al.*, 2007). Regarding cell size, in BY-2 cells, following synchronisation, over-

expression of *Nicotiana tabacum* (*Nicta;WEE1*) in BY2 cells delayed the mitotic peak but there was a null effect on cell size (Siciliano, 2006).

The over-expression of *Arath;WEE1* in Arabidopsis plants had a negative effect on root growth (Siciliano, 2006; Lentz Grønlund, 2007; Spadafora, 2008): primary root elongation was inhibited, and plants had a lower frequency of lateral root primordia, but they had a longer meristematic root epidermal cell phenotype compared to WT (Lentz Grønlund, 2007). Seemingly in this transgenic line, activation of clusters of cells of the pericycle is less frequent compared with WT cycles arguing for the suppression of many more mitotically competent pericycle cells compared with WT. Since, in Arabidopsis it is from the G2/M transition in the pericycle that lateral root primordia are initiated in Arabidopsis (Dubrovsky *et al.*, 2000) it can be hypothesised that over-expression of *WEE1* suppresses the dephosphorylation of CDKs at many potential sites of lateral root primordium initiation. Interestingly, in Arabidopsis, *WEE1* is spatially expressed at the base of young lateral primordia but not in the apex (G. Cook, unpublished data). Hence over-expression of *WEE1* may cause a delay in mitosis and cells remain in G2 phase, so in this case, when the cells are arrested in G2 they might re-enter the cell cycle with a lower frequency and, consequently, fewer lateral roots will be formed. However analysis of T-DNA insertional mutants in *Arath;WEE1* showed that down-regulation of this gene had no effect on normal plant growth (De Schutter *et al.*, 2007; Lentz Grønlund, 2007) although they did not study these phenotypic effects in as much detail as presented in this chapter. However, a transcriptional response of *Arath;WEE1* in Arabidopsis cell suspensions treated with HU was observed by De Schutter *et al* (2007), and they concluded that this treatment transcriptionally activated the *WEE1* gene. In *Arath;WEE1* loss-of-function plants treated with 1mM HU, the length of primary roots was reduced. Thus although Arabidopsis *WEE1* was shown not to be rate-limiting for cell cycle progression or endoreduplication under normal growth conditions,

upon DNA damage and replication blockage, *Arath;WEE1* was a critical target for ATM/ATR signalling. These results suggest that the WEE1-deficient plants failed to activate a G2 arrest and progressed into mitosis without a fully replicated genome (De Schutter *et al.*, 2007).

As mentioned above, when *Nicta; WEE1* was over-expressed in BY-2 cells it induced a lengthening of G2 phase but did not affect cell size (Spadafora, 2008). Even more surprisingly, Siciliano (2006) found that expression of *Arath;WEE1* in BY-2 cells either under the 35S or a DEX-inducible promoter induced a shortened G2 phase, a premature entry into mitosis and a smaller mitotic cell area. This was confirmed independently by other experiments in the Cardiff Laboratory (Lentz Grønlund, unpublished data).

Prior to my project, *Arath; WEE1* had been transformed into tobacco plants under a constitutive 35S promoter and a reciprocal transformation was carried out generating an *Arabidopsis* line expressing *Nicta;WEE1*. In the latter the tobacco version of *WEE1* (*Nicta;WEE1*) was under the control of an inducible promoter. These transgenic lines allow the possibility to test the effect of ectopic expression of *Arath;WEE1* in tobacco and the ectopic expression of *Nicta;WEE1* in *Arabidopsis*. Hence, the aim of the work reported in this chapter was to analyse cross-species *WEE1* expression through detailed measurement of rates of primary root elongation and lateral root production, and, at the cellular level, apical meristem size, cell number and cell length of epidermal cells within the meristem domain in both tobacco and *Arabidopsis*.

5.2 Materials and methods

5.2.1 Expression of *Nicta;WEE1* in *Arabidopsis*

Two transgenic *Arabidopsis* (Col-0) lines (lines 3 and 11) carrying the *Nicta;WEE1* gene under a DEX inducible promoter (vector pTA7002; Aoyama and Chua 1997), had been

previously characterised to check for presence and expression of the transgene (Cardiff lab., unpublished results). Arabidopsis seeds were sown as described in chapter 2 Section 2.3 onto M&S medium (-DEX) or medium containing 30 μ M dexamethasone for induction of *Nicta;WEE1*. Two bottles were prepared each one containing 1l of M&S medium. After autoclaving, the bottles of medium were left to cool in a sterile laminar flow hood and then 120 μ l of 100 mM dexamethasone (+DEX) were added. Primary root phenotype was assessed as described in chapter 2, Section 2.13.

5.2.2 Expression of *Arath; WEE1* in tobacco plants

Nicotiana tabacum cv Samsung was previously transformed using a leaf disc transformation method with a construct in the pSPYNE 35S vector (Walter *et al.*, 2004), carrying the Arabidopsis *WEE1* gene (*Arath;WEE1*) under the 35s promoter fused to the C terminal portion of YFP and a gene conferring resistance to hygromycin (Anne Lentz Grønland unpublished results). Hygromycin resistant calli were isolated and five independent transformants were recovered from the transformation previous to my project (lines NTArath;Wee1#1, NTArath;Wee1#2, NTArath;Wee1#7, NTArath;Wee1#8, NTArath;Wee1#9). Two of these lines were partially characterised by a student in the Cardiff Lab. (James Davies unpublished results). Seeds from a WT line and an empty vector transgenic line were also sown as controls.

Seeds were sown into compost and grown in a greenhouse with 16 h light, 8 h dark and an average temperature of 4 °C). For seed collection, flowers were bagged before they opened and seed collected when seed pods were mature.

All other methods are as described in the General Materials and Methods (Chapter 2).

5.3 Results

To simplify the nomenclature of the transgenic lines, tobacco lines carrying *Arath;WEE1* are denoted NT-*Arath;Wee1#* 1,2,3 etc and Arabidopsis lines carrying *Nicta;WEE1* are denoted AT-*Nicta;Wee1#* 1,2,3 etc.

5.3.1 Selection of T1 transgenic tobacco lines transformed with *Arath;WEE1*

Five transgenic lines were recovered from the tobacco transformation experiment undertaken before the start of this project. In two lines (lines NT-*Arath;Wee1#2* and NT-*Arath;Wee1#8*) the presence of the transgene and its expression had already been verified in the T1 generation (derived from selfed T0 plants) (James Davies, Cardiff Lab). I tested for the expression of *Arath;WEE1* in T1 lines NT-*Arath;Wee1#1*, NT-*Arath;Wee1#7*, and NT-*Arath;Wee1#9*, and verified expression in a T1 line of NT-*Arath;Wee1#8*, confirming that the transgene was expressed in all five lines. Results from four of these lines are shown in Fig. 5.1.

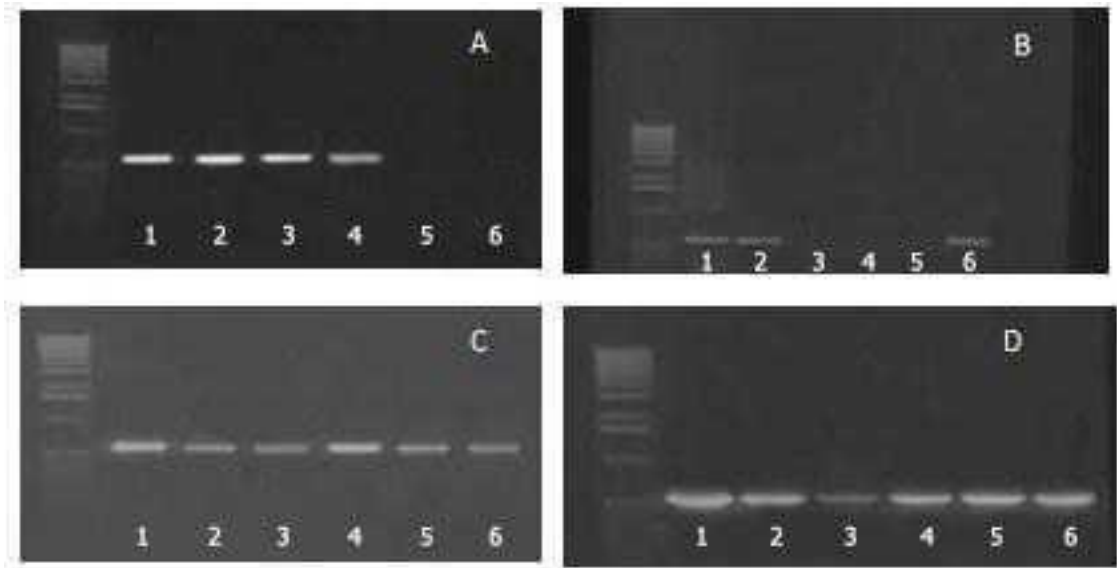


Figure 5.1 RT-PCR with *Arath;Wee1* forward and reverse primers to confirm expression of the transgene in T1 generation plants: (A) NT-Arath;Wee1#1 plants Lane: 1) positive control (cDNA from Arabidopsis), 2) plant 1, 3) plant 2, 4) plant 3, 5) plant 4, 6) plant 5, (B) NT-Arath;Wee1#9 plants: Lanes: 1). plant 1, 2) plant 2, 3) plant 3, 4) plant 4, 5) plant 5, 6) plant 6 (C) NT-Arath;Wee1#7 Lanes: 1) plant 1, 2) plant 2, 3) plant 3, 4) plant 4, 5) plant 5, 6) plant 6 (D) NT-Arath;Wee1#8: Lanes: 1) plant 1, 2) plant 2, 3) plant 3, 4) plant 4, 5) plant 5, 6) plant 6

T1 lines for each of the independent transgenic lines of NT-Arath;Wee1: lines #1, 2, 7, 8 and 9 were selected from individuals expressing the transgene for analysis of WEE1 protein levels and root phenotype.

5.3.2 WEE1 protein levels in the tobacco lines expressing *Arath;WEE1*

Representative plants from each transgenic line were selected, and total proteins were extracted. These were separated by PAGE and used for Western blotting with the WEE1 antibody (Fig. 5.2). Levels of proteins differed between the lines although the WEE1 protein amount in each of the transgenic genotypes was substantially lower than WT.

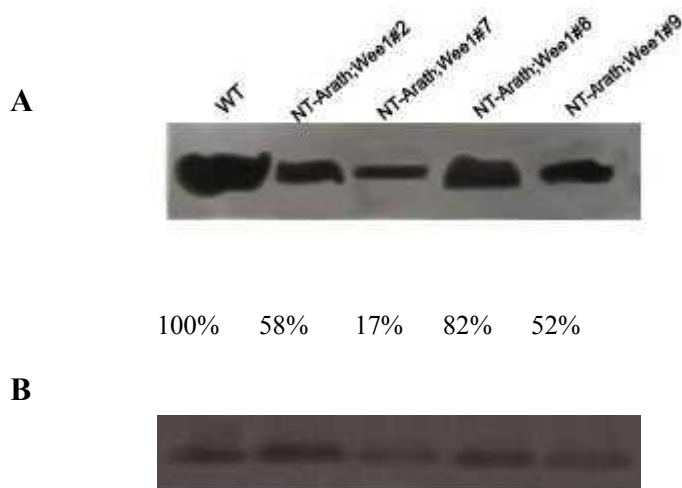


Figure 5.2 (A) Representative Western blot from duplicate experiments showing WEE1 protein levels of wild type, NT-Arath;Wee1#2, NT-Arath;Wee1#7, NT-Arath;Wee1#8 and NT-Arath;Wee1#9. Relative protein levels were determined by quantifying the intensity of the bands and expressing as a ratio to the WT level. (B) corresponding Coomassie stained gel as a loading control.

5.3.3 Root phenotype in tobacco seedlings expressing *Arath; WEE1* grown on Petri dishes

Firstly I analyzed the root phenotype of tobacco seedlings expressing *Arath;WEE1* by measuring primary root length, number of laterals, number of primordia, meristem length, number of epidermal cells in meristem, and cell length in the presence or absence of hydroxyurea.

5.3.3.1 Effect of treatment with HU on primary root growth and production of lateral roots

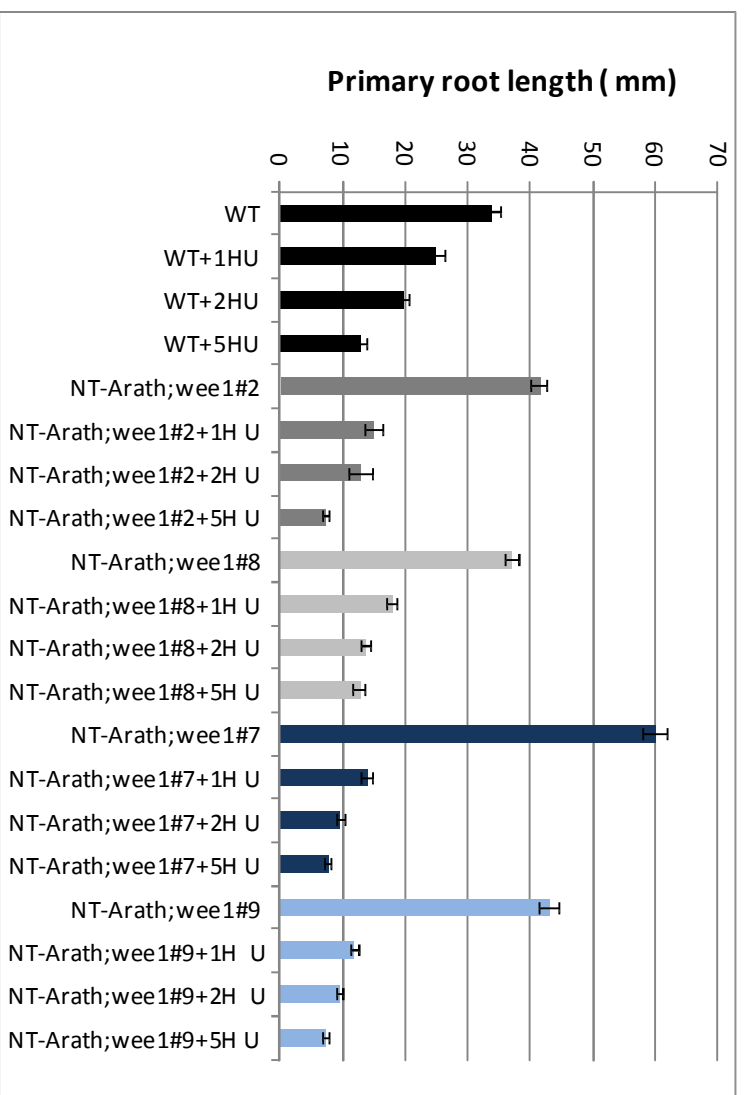
In tobacco transgenic lines NT-Arath;Wee1#2, NT-Arath;Wee1#8 and NT-Arath;Wee1#9 plants, the primary root was significantly longer than WT ($P < 0.01$) (Fig 5.3A, Appendix A). However, in the absence of HU treatment, NT-Arath;Wee1#7 did not show any significant difference in primary root length compared to WT ($P > 0.05$) (Fig 5.3A Appendix A). In all of the transgenic lines tested the primary root length decreased

dramatically with increasing amounts of HU, while this decrease was more gradual for WT (Fig. 5.3A, Table 5.1).

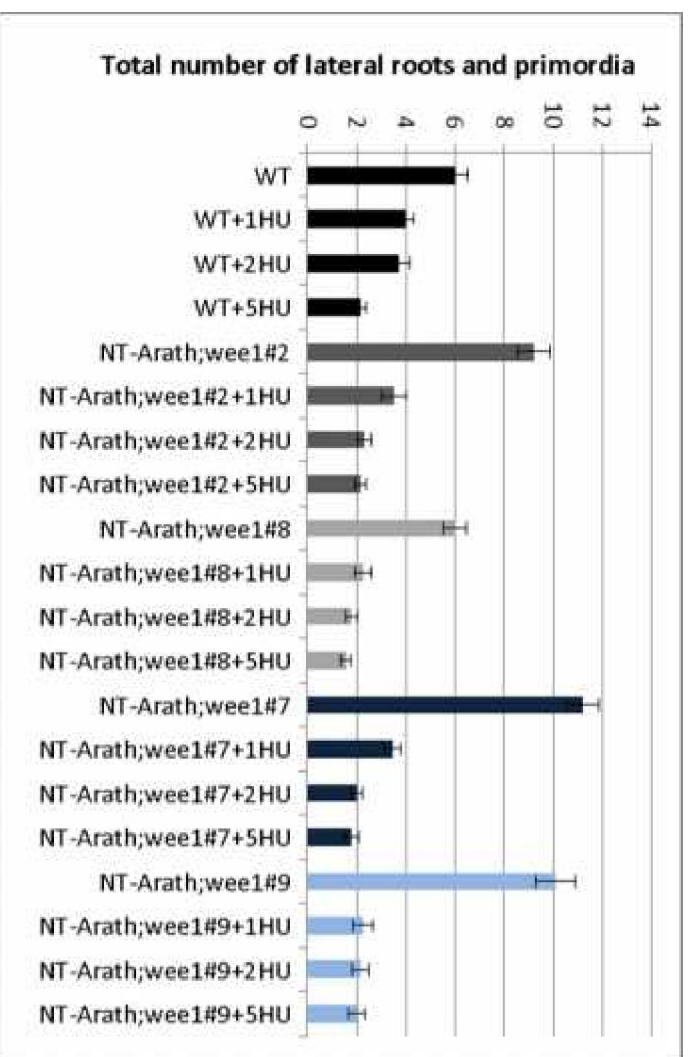
The mean number of lateral roots and primordia in all the transgenic lines tested except tobacco NT-Arath;Wee1#7 plants was significantly greater than WT in the -HU treatment (Fig. 5.3B, Table 5.2). The mean number of lateral roots and primordia decreased with increasing amounts of HU in all lines including WT. However, the decrease in the transgenic line +1mM HU in NT-Arath;Wee1 lines was > 2-fold by only 1.4 fold in wild type. Hence not withstanding the higher levels of WEE1 protein in all NT-Arath;Wee1#8, the transformed lines were hypersensitive to 1 mM HU compared with the untreated control. Thereafter there was a more gradated decrease in root elongation in the 2 and 5 mM HU compared with 1 mM HU treatments (Fig 5.3A).

I then examined whether primary root elongation was coordinated with number of laterals that formed \pm HU (Fig 5.3C). In fact other than lines 2 and 9, + 5mM HU, the rates were not greatly significantly different either between genotypes or within a genotype \pm HU treatment. All datum points in Fig. 5.3C were then assessed by regression analysis and they all conformed to a straight line thereby providing a rate of 0.114 LRP per mm of primary for all genotypes \pm 1 mM HU. Thus in 21 day old seedlings of all genotypes \pm 1mM HU, the number of primordia+laterals and the length of the primary root do indeed alter in a highly coordinated way. For example, 21 day old NT-Arath;WEE1#7-HU formed more primordia and showed a longer primary root compared with NT-Arath;WEE1#7+HU but \pm 1 mM HU they both produced lrp at the same rate per mm of primary.

A



B



C

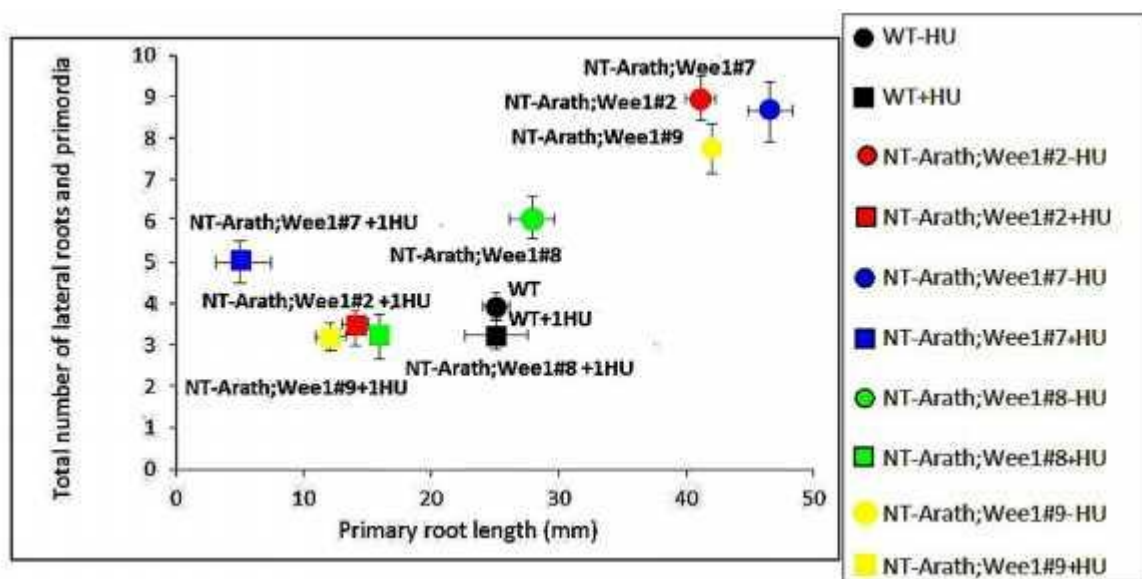


Figure 5.3 (A) Primary root growth in relation to HU concentration (B) Total number of lateral roots and primordia (C) the relationship between mean primary root length and mean no. of lateral roots in the genotypes: wild type (WT), and tobacco line NT-Arath;Wee1#2, NT-Arath;Wee1#7, NT-Arath;Wee1#8 and NT-Arath;Wee1#9 (expressing *Arath;WEE1*), in 21 day old tobacco plants grown in 16 h light and 8 h dark at $21^{\circ}\text{C} \pm 1$ mM HU (1HU). (\pm S.E.) $n = 20$. The regression for all datum points was $y = 0.114x + 2.29$ $P = 0.026$. A regression excluding the outlier, (NT-Arath;wee1 #7+1 HU) was $0.190x - 0.30$ $P < 0.001$

Table 5.1 (a) Levels of significant between primary root length of each transgenic line, and WT, all grown on medium without adding HU (b) Level of significant differences in primary root length within genotype, for WT and each the transgenic lines $\pm 1, 2,$ or 5 mM compared with $\text{WT} \pm 1, 2,$ or 5 .

	WT	NT-Arath;Wee1#2	NT-Arath;Wee1#7	NT-Arath;Wee1#8	NT-Arath;Wee1#9
WT	-	***	NS	***	***

	Level of significant difference + 1mM HU	Level of significant difference + 2mM HU	Level of significant difference + 5mM HU	% change ± 1 mM HU compared to WT
	primary root length	primary root length	primary root length	primary root length
WT	*	*	*	*
NT-Arath;Wee1#2	***	***	***	***
NT-Arath;Wee1#7	***	***	*	***
NT-Arath;Wee1#8	***	***	NS	***
NT-Arath;Wee1#9	***	***	*	***

Key. *** < 0.001 , ** = $0.02-0.001$ P, * = $0.02-0.05$ P, NS > 0.05

Table 5.2 (a) Levels of significant between total number of lateral roots and primordia of each transgenic line, and WT, all grown on medium without adding HU (b) Level of significant differences in total number of lateral roots and primordia within genotype, for WT and each the transgenic lines \pm 1, 2, or 5 mM compared with WT \pm 1, 2, or 5.

	WT	NT-Arath;Wee1#2	NT-Arath;Wee1#7	NT-Arath;Wee1#8	NT-Arath;Wee1#9
WT	-	***	NS	***	***

	Level of significant difference + 1mM HU	Level of significant difference + 2mM HU	Level of significant difference + 5mM HU	% change \pm 1mM HU compared to WT
	Total Number of lateral roots and primordia			
WT	*	*	*	*
NT-Arath;Wee1#2	**	**	NS	*
NT-Arath;Wee1#7	***	**	*	***
NT-Arath;Wee1#8	*	**	*	***
NT-Arath;Wee1#9	**	**	*	***

Key. *** < 0.001, ** = 0.02-0.001 P, * = 0.02-0.05 P, NS > 0.05

Table 5.3 Rate of lateral root production mm primary root⁻¹ in the different genotypes of 21 days old tobacco seedlings obtained by dividing the x by the y coordinates for each point plotted in Fig. 5.3.

	Rate of lateral root production mm primary root ⁻¹			
	-HU	1mM	2mM	5mM
WT	0.18	0.16	0.19	0.17
NT-Arath;Wee1#2	0.22	0.23	0.18	0.29
NT-Arath;Wee1#7	0.19	0.25	0.20	0.23
NT-Arath;Wee1#8	0.16	0.12	0.13	0.12
NT-Arath;Wee1#9	0.23	0.19	0.22	0.27

5.3.3.2 Effect of treatment with HU on meristem length

The meristem length of tobacco NT-Arath;Wee1# 2, NT-Arath;Wee1#7, NT-Arath;Wee1#8, NT-Arath;Wee1#9 were compared (Fig. 5.5).

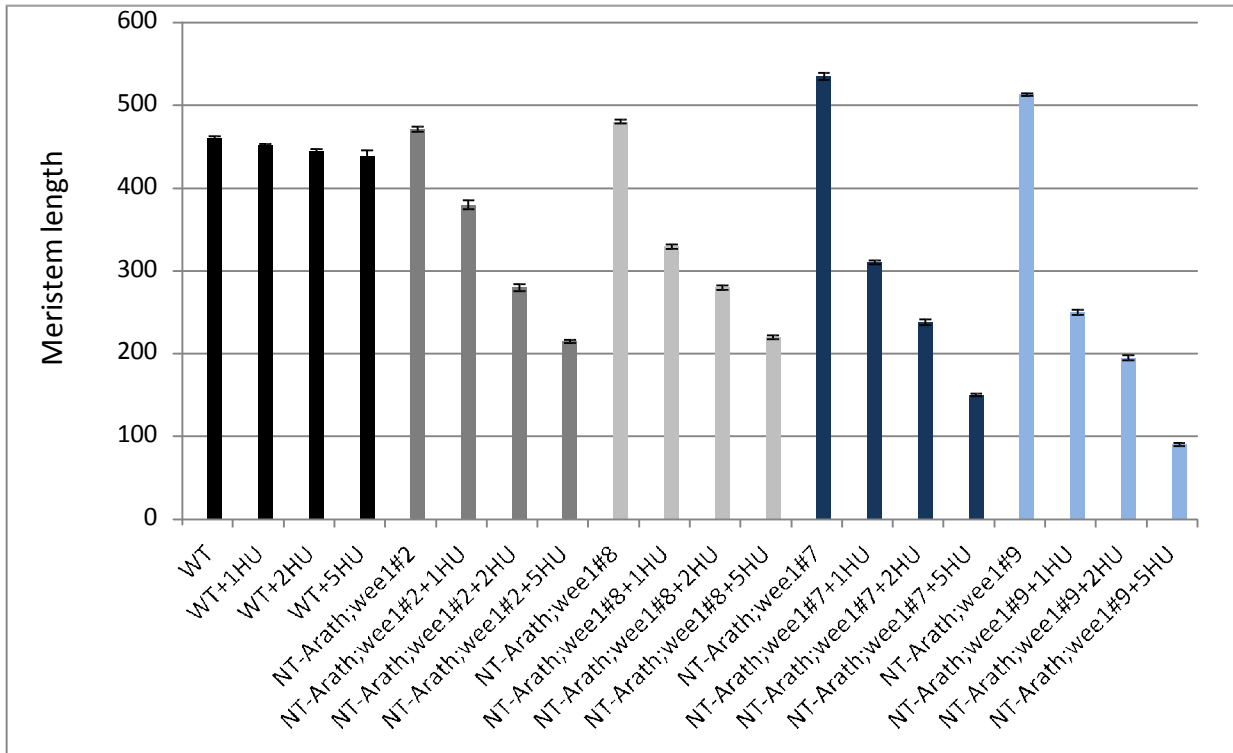


Figure 5.4 Mean (\pm SE.) length of the meristem in 21 day old seedlings of various genotypes of tobacco lines: WT, NT-Arath;Wee1#2, NT-Arath;Wee1#7, NT-Arath;Wee1#8 and NT-Arath;Wee1#9 (expressing *Arath;WEE1*) grown in daily cycles of 16 h light and 8 h dark at 21 °C \pm either 1, 2 or 5 mM hydroxyurea (HU), n =20

Table 5.4 (a) Levels of significant between meristem length of each transgenic line, and WT, all grown on medium without adding HU (b) Level of significant differences in meristem length within genotype, for WT and each the transgenic lines \pm 1, 2, or 5 mM compared with WT \pm 1, 2, or 5.

	WT	NT-Arath;Wee1#2	NT-Arath;Wee1#7	NT-Arath;Wee1#8	NT-Arath;Wee1#9
WT	-	*	**	***	***

	Level of significant difference + 1mM HU	Level of significant difference + 2mM HU	Level of significant difference + 5mM HU	% change \pm 1mM HU compared to WT
	Meristem length	Meristem length	Meristem length	Meristem length
WT	*	*	*	NS
NT-Arath;Wee1#2	*	*	***	**
NT-Arath;Wee1#7	***	***	***	***
NT-Arath;Wee1#8	*	*	***	**
NT-Arath;Wee1#9	**	***	***	***

Key. *** < 0.001, ** = 0.02-0.001 P, * = 0.02-0.05 P, NS >0.05

In the controls, the meristems of NT-Arath;Wee1#7 and NT-Arath;Wee1#9 were significantly longer than WT which did not alter significantly in the 1-5 mM HU treatments (Fig. 5.4, Table 5.4). Treatment with 1mM HU caused only a 1% difference in meristem length in the WT. However, the decrease in the transgenic lines with 1, 2 or 5 mM HU was significantly much greater: Indicating that all the transgenic lines were hypersensitive to HU in their reduction of meristem length.

5.3.3.3 Effect of treatment with HU on number of cells along a file of the epidermal region in the root meristem

In the absence of HU, the mean of number of cells in the epidermal file of the RAM, was significantly higher in all the NT-Arath;Wee1 lines compared with WT. ($P < 0.01$) (Fig. 5.5, Table 5.5). Hence the increased size of the meristem in all the NT-Arath; wee1 lines compared to WT (Fig 5.41, Table 5.4) was positively related to epidermal cell number.

In WT the mean number of cells in the epidermal lineage decreased with increasing amounts of HU and was significantly different ± 1 mM HU, which again fits with the WT meristem length data while in the mutants cell number did not alter significantly $\pm 1, 2$ or 5 mM HU.

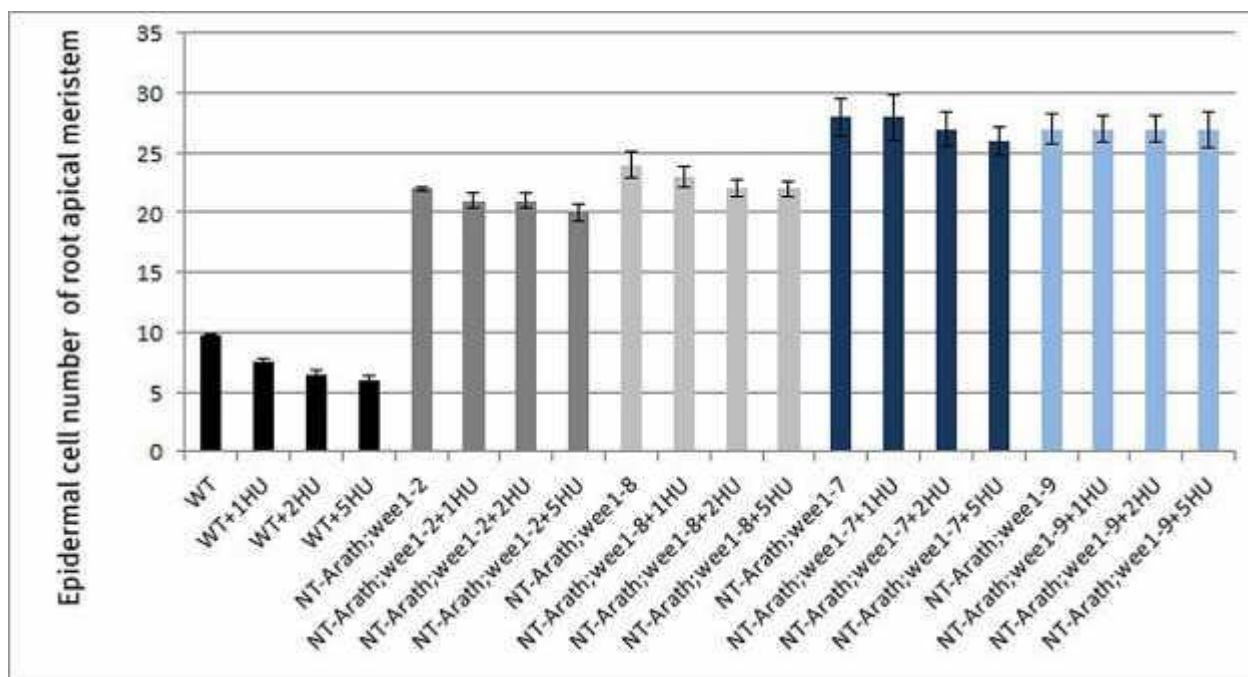


Figure 5.5 The relationship between mean (\pm S.E.) cell number along a file of epidermal region in the root apical meristem in different genotypes of tobacco: wild type (WT) , and transgenic tobacco lines NT-Arath;Wee1#2, NT-Arath;Wee1#7, NT-Arath;Wee1#8 and NT-Arath;Wee1#9 (expressing *Arath;WEE1*) in 21 day old tobacco plants grown in 16 h light and 8 h dark at 21°C. n =20

Table 5.5 (a) Levels of significant between cell number of each transgenic line, and WT, all grown on medium without adding HU (b) Level of significant differences in cell number within genotype, for WT and each the transgenic lines \pm 1, 2, or 5 mM compared with WT \pm 1, 2, or 5.

	WT	NT-Arath;Wee1#2	NT-Arath;Wee1#7	NT-Arath;Wee1#8	NT-Arath;Wee1#9
WT	-	***	***	***	***

	Level of significant difference + 1mM HU	Level of significant difference + 2mM HU	Level of significant difference + 5mM HU	% change \pm 1mM HU compared to WT
	Cell number	Cell number	Cell number	Cell number
WT	*	*	*	*
NT-Arath;Wee1#2	NS	NS	*	*
NT-Arath;Wee1#7	NS	NS	NS	NS
NT-Arath;Wee1#8	NS	NS	NS	NS
NT-Arath;Wee1#9	NS	NS	NS	NS

Key. *** < 0.001, ** = 0.02-0.001 P, * = 0.02-0.05 P, NS > 0.05

5.3.3.4 Effect of treatment with HU on epidermal cell length along a file of the root apical meristem

The increased meristem cell number and meristem size in 0 mM HU in the transgenic lines compared with WT data would suggest that the cells would be smaller in the RAM of the mutant genotypes compared with WT, at all HU concentrations. This hypothesis was tested by measuring epidermal cell length in each genotype (Fig. 5.7).

In all the transgenic lines tested, the mean cell size was indeed smaller in the transgenic lines compared with WT-HU, and the buffering of cell number at increasing HU molarities was consistent with cell length not altering on 1-5 mM HU. However in WT, the mean epidermal cell length increased with increasing amounts of HU (Fig. 5.6, Table 5.6).

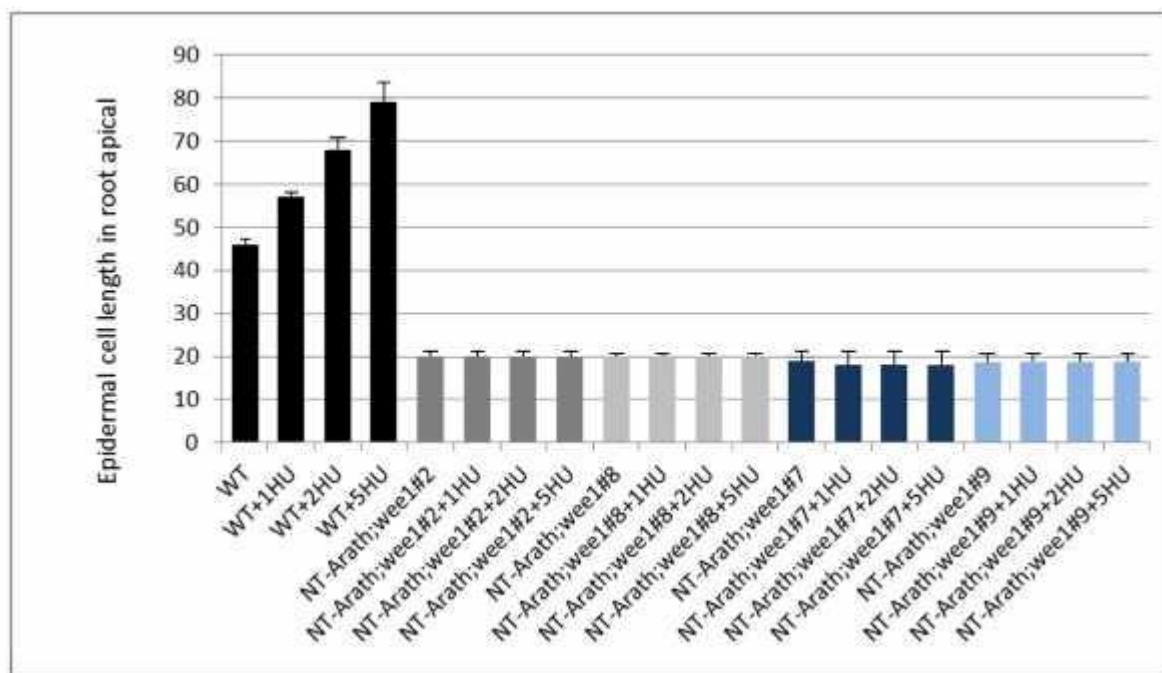


Figure 5.6 The relationship between mean (\pm S.E.) cell length of a file of epidermal cells from the root apical meristem in different genotypes of tobacco: wild type (WT), and transgenic tobacco lines NT-Arath;Wee1#2, NT-Arath;Wee1#7, NT-Arath;Wee1#8 and NT-tArath;Wee1#9 (expressing *Arath;WEE1*) in 21 day old tobacco plants grown in 16 h light and 8 h dark at 21°C. n =20

Table 5.6 (a) Levels of significant between cell length in epidermis of each transgenic line, and WT, all grown on medium without adding HU (b) Level of significant differences in cell length in epidermis within genotype, for WT and each the transgenic lines \pm 1, 2, or 5 mM compared with WT \pm 1, 2, or 5.

	WT	NT-Arath;Wee1#2	NT-Arath;Wee1#7	NT-Arath;Wee1#8	NT-Arath;Wee1#9
WT	-	***	***	***	***

	Level of significant difference + 1mM HU	Level of significant difference + 2mM HU	Level of significant difference + 5mM HU	% change \pm 1mM HU compared to WT
	Cell length	Cell length	Cell length	Cell length
WT	*	*	*	**
NT-Arath;Wee1#2	NS	NS	NS	NS
NT-Arath;Wee1#7	NS	NS	NS	NS
NT-Arath;Wee1#8	NS	NS	NS	NS
NT-Arath;Wee1#9	NS	NS	NS	NS

Key. *** < 0.001, ** = 0.02-0.001 P, * = 0.02-0.05 P, NS > 0.05

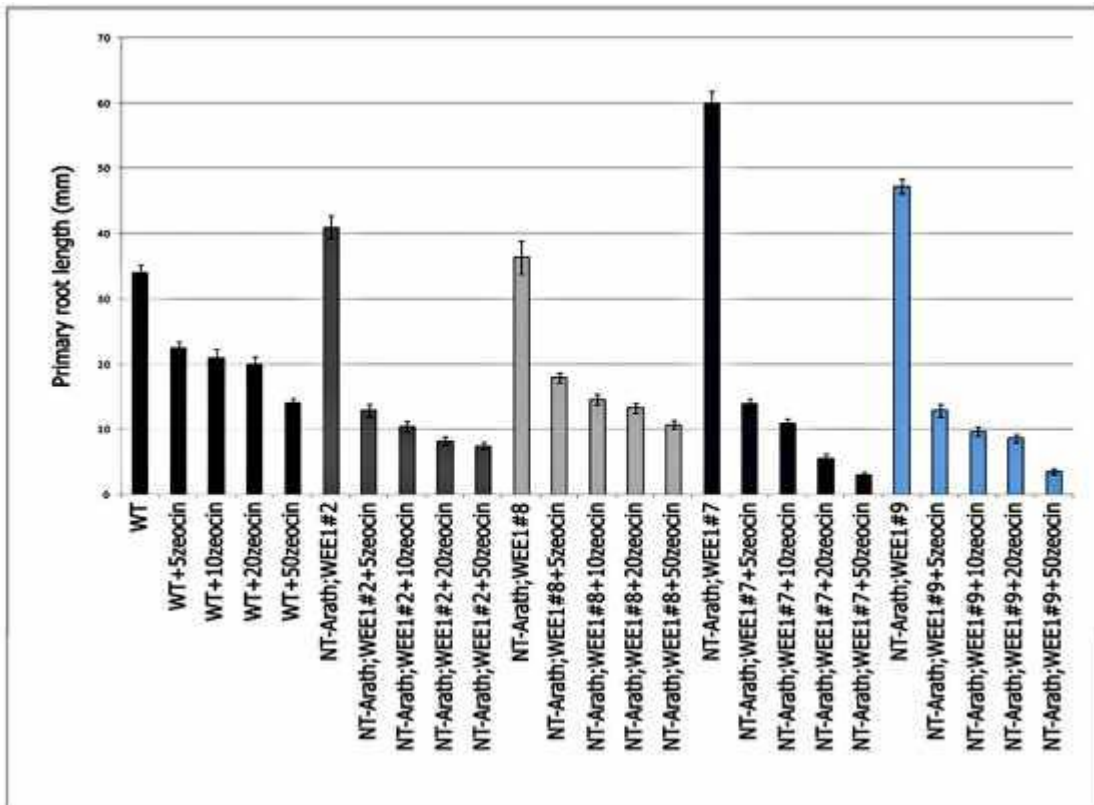
5.3.3.5 Effects of treatment with zeocin on primary root growth and production of lateral roots

The effects of zeocin on primary root length in the mutants (Fig 5.7 A) were remarkably similar to those observed for HU treatment in all of the transgenic lines tested. Notably compared with 0 μ M, there was a hypersensitive response in primary root length at 5 μ M in all transgenic lines (Table 5.7). However thereafter, primary root length decreased in a gradated manner. In the absence of zeocin primary root length was significantly greater than WT in lines NT-Arath;wee1#2, 7, and 9 while there was no difference in line 8.

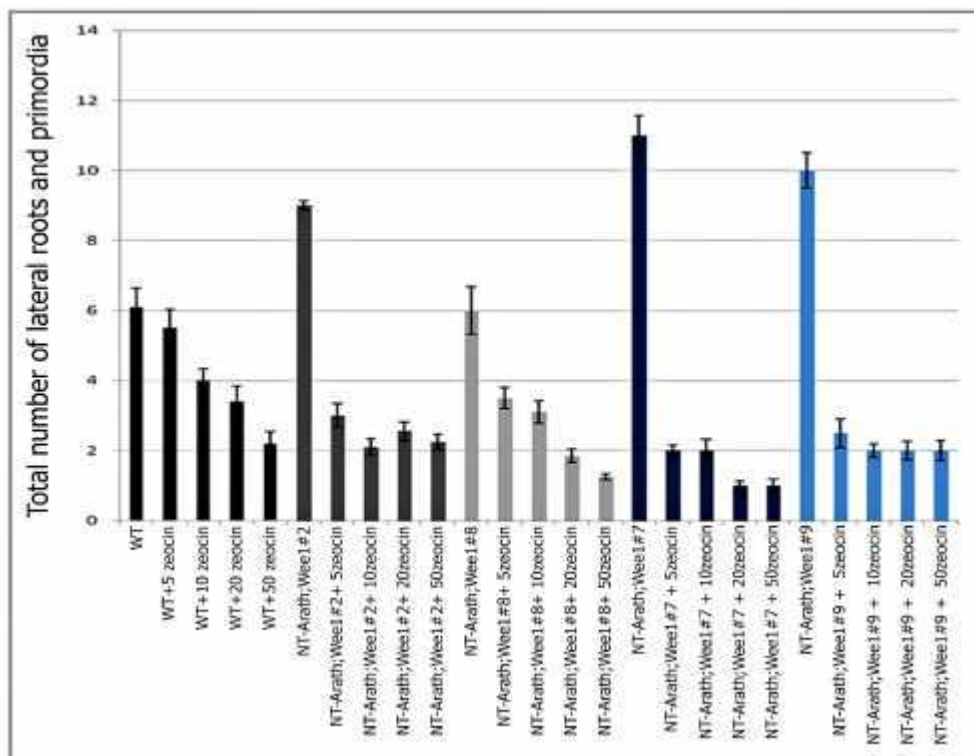
The mean number of lateral roots and primordia in all the NT-Arath;Wee1 lines except #8 were also significantly greater than WT in the absence of zeocin confirming the control data obtained in the HU treatment experiment (Fig 5.8B, Fig. 5.3B). In response to > 10 μ M zeocin, the mean number of lateral roots for each genotype was remarkably similar to those of all genotypes treated with HU. However, and unlike WT, 5 μ M zeocin induced a hypersensitive response in all transgenic lines. At >10 μ M zeocin, number of primordia/lateral roots in each of the transgenic lines were either fluctuating, or, slowly decreasing.

As mentioned above, in WT the data on number of lateral took the form of a graded response from 5 to 50 M zeocin with no indication of a hypersensitive response.

A



B



C

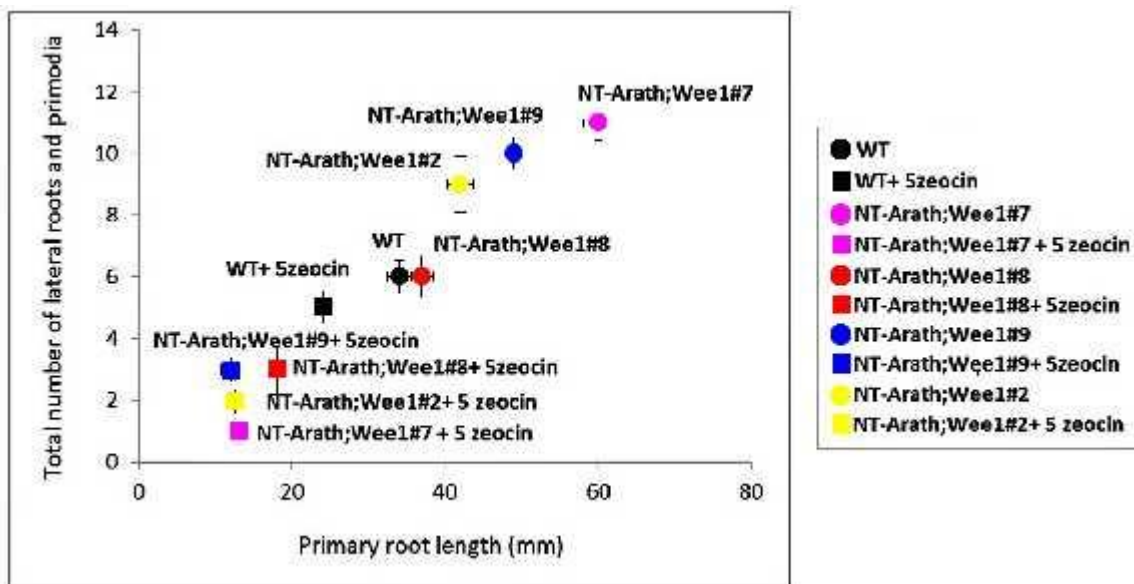


Figure 5.7 (a) Primary root growth in relation to zeocin concentration (b) The mean (\pm S.E.) number of total number of lateral root and primordia (c) The relationship between primary root length and total number of lateral roots and primordia in 14 day old tobacco NT-Arath;Wee1#2 , NT-Arath;Wee1#7, NT-Arath;Wee1#8, NT-Arath;Wee1#9 expressing *Arath*; *WEE1* compared to wild type (WT) \pm 5 μ M zeocin, . \pm SE, n=20

Table 5.7 Level of significant differences in primary root length within genotype, for WT and each the transgenic lines \pm 5, 10, 20, or 50 μ M compared with WT \pm 5, 10, 20, or 50 μ M.

	Level of significant difference + 5 μ M zeocin	Level of significant difference + 10 μ M zeocin	Level of significant difference + 20 μ M zeocin	Level of significant difference + 50 μ M zeocin	% change \pm 5 μ M zeocin compared to WT
	primary root length	primary root length	primary root length	primary root length	primary root length
WT	*	*	**	***	**
NT-Arath;Wee1#2	***	***	***	***	***
NT-Arath;Wee1#7	***	***	***	***	***
NT-Arath;Wee1#8	***	***	***	***	***
NT-Arath;Wee1#9	***	***	***	***	***

Key. *** < 0.001, ** = 0.02-0.001 P, * = 0.02-0.05 P, NS > 0.05

Table 5.8 Level of significant differences in total number of lateral roots and primordia within genotype, for WT and each the transgenic lines \pm 1, 2, or 5 mM compared with WT \pm 1, 2, or 5.

	Level of significant difference + 5 μ M zeocin	Level of significant difference + 10 μ M zeocin	Level of significant difference + 20 μ M zeocin	Level of significant difference + 50 μ M zeocin	% change \pm 5 μ M zeocin compared to WT
	Total number of lateral roots and primordia	Total number of lateral roots and primordia	Total number of lateral roots and primordia	Total number of lateral roots and primordia	Total number of lateral roots and primordia
WT	*	*	**	*	**
NT-Arath;Wee1#2	***	***	***	***	***
NT-Arath;Wee1#7	***	***	***	***	***
NT-Arath;Wee1#8	***	***	***	***	***
NT-Arath;Wee1#9	***	***	***	***	***

Key. *** < 0.001, ** = 0.02-0.001 P, * = 0.02-0.05 P, NS > 0.05

All data for each genotype \pm zeocin were then subjected to a regression analysis to determine the extent with which the data were linked with growth as opposed to development. The regression equation for all genotypes x zeocin treatments is

$y=0.18x+0.23$, $n=24$ $P < 0.001$. Hence all data fall on a straight line resulting in a mean rate of lrp formation per mm of primary of 0.18. As with the HU data, these data are consistent with zeocin affecting growth of the root system. Outliers above the linear regression would have indicated a development effect (e.g. more lrp at the same root length); there were none in the current data set. Thus in the \pm zeocin treatments, the longer the primary root length, the more laterals that form in a proportionate manner.

Table 5.9 Rate of lateral root production mm primary root⁻¹ in the different genotypes of 21 days old tobacco seedlings obtained by dividing the x by the y coordinates for each point plotted in Fig. 5.8.

	Rate of lateral root production mm primary root ⁻¹				
	-zeocin	5 μ M zeocin	10 μ M zeocin	20 μ M zeocin	50 μ M zeocin
WT	0.18	0.21	0.2	0.17	0.13
NT-Arath;Wee1#2	0.21	0.17	0.18	0.22	0.28
NT-Arath;Wee1#7	0.18	0.14	0.2	0.16	0.33
NT-Arath;Wee1#8	0.16	0.16	0.12	0.08	0.09
NT-Arath;Wee1#9	0.20	0.25	0.20	0.25	0.50

Rate of lateral root production per mm of primary root without zeocin was remarkably constant for all genotypes and changed very little with increasing zeocin concentrations (Table 5.9).

5.3.3.6 Effects of treatment with zeocin on root meristem length

Effects of zeocin on root meristem length (Fig 5.8, Table 5.10) were very similar to those observed in the HU treatments (Fig. 5.4): in all of the transgenic lines tested \pm 5 μ M zeocin there was a significant and increasing reduction of meristem length with increasing zeocin treatment. In contrast WT meristem length remained almost unaffected (Fig. 5.8, Table 5.10).

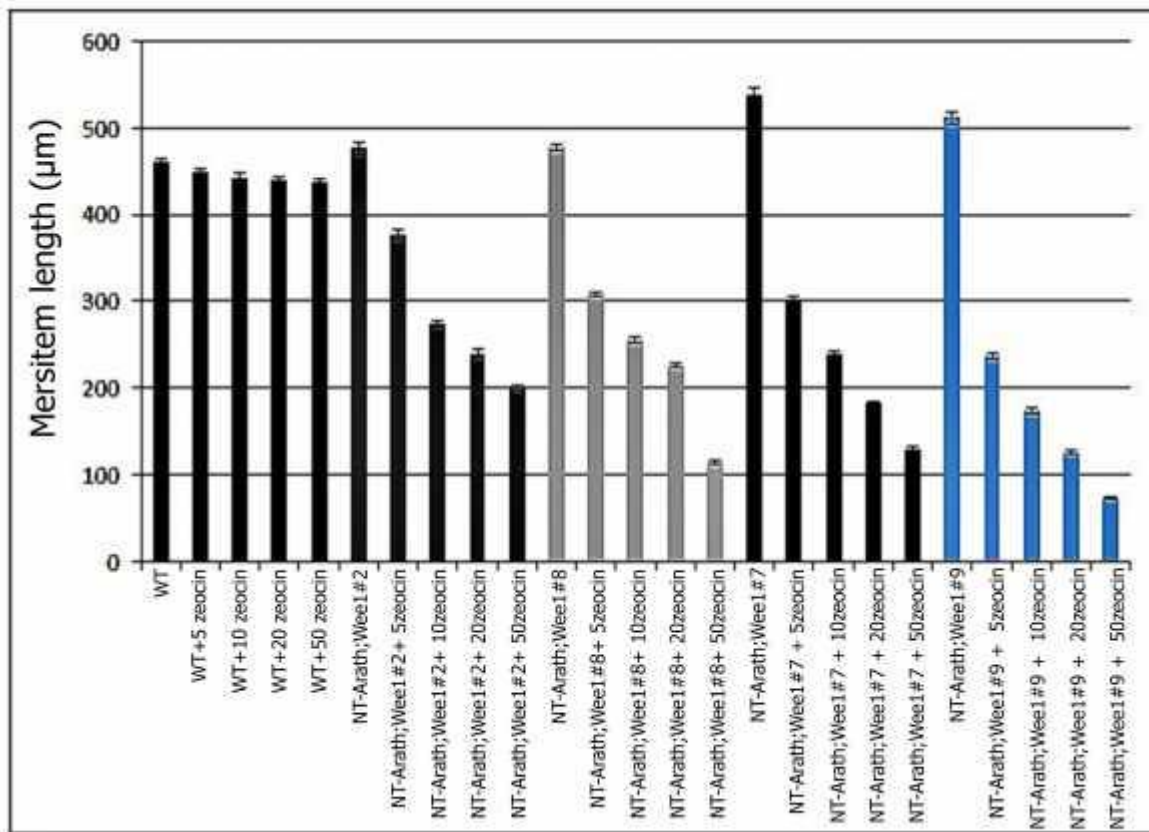


Figure 5.8 Mean (\pm SE.) length of the primary root apical meristem in 14 days old seedlings of various genotypes of tobacco lines: NT-Arath;Wee1#2, NT-Arath;Wee1#7, NT-Arath;Wee1#8 and NT-Arath;Wee1#9 (expressing *Arath;WEE1*) grown in daily cycles of 16 h light and 8 h dark at 21 °C \pm 5, 10, 20 or 50 μ M zeocin. n=20

Table 5.10 Level of significant differences for root apical meristem in different genotype, of tobacco plants expressing *Arath;WEE1* WT \pm 5, 10, 20, or 50 μ M.

	Level of significant difference + 5 μ M zeocin	Level of significant difference + 10 μ M zeocin	Level of significant difference + 20 μ M zeocin	Level of significant difference + 50 μ M zeocin	% change \pm 5 μ M zeocin compared to WT
	Meristem length	Meristem length	Meristem length	Meristem length	Meristem length
WT	NS	NS	NS	NS	NS
NT-Arath;Wee1#2	*	***	***	***	***
NT-Arath;Wee1#7	***	***	***	***	***
NT-Arath;Wee1#8	***	***	***	***	***
NT-Arath;Wee1#9	***	***	***	***	***

Key. *** < 0.001, ** = 0.02-0.001 P, * = 0.02-0.05 P, NS > 0.05

5.3.3.7 Effects of treatment with zeocin on number of cells along a file of the epidermal region in the root meristem

The effects of zeocin on the number of cells along a file of the epidermal region in the root meristem were very similar to those of the HU treatments (see Fig. 5.5): there was a significant decrease in the number of cells in WT, whereas there were no significant changes in the transgenic lines (Fig. 5.9, Table 5.11). As also seen in the HU experiment, the number of cells was much greater in all four transgenic lines compared to WT in the absence of zeocin (Fig. 5.9).

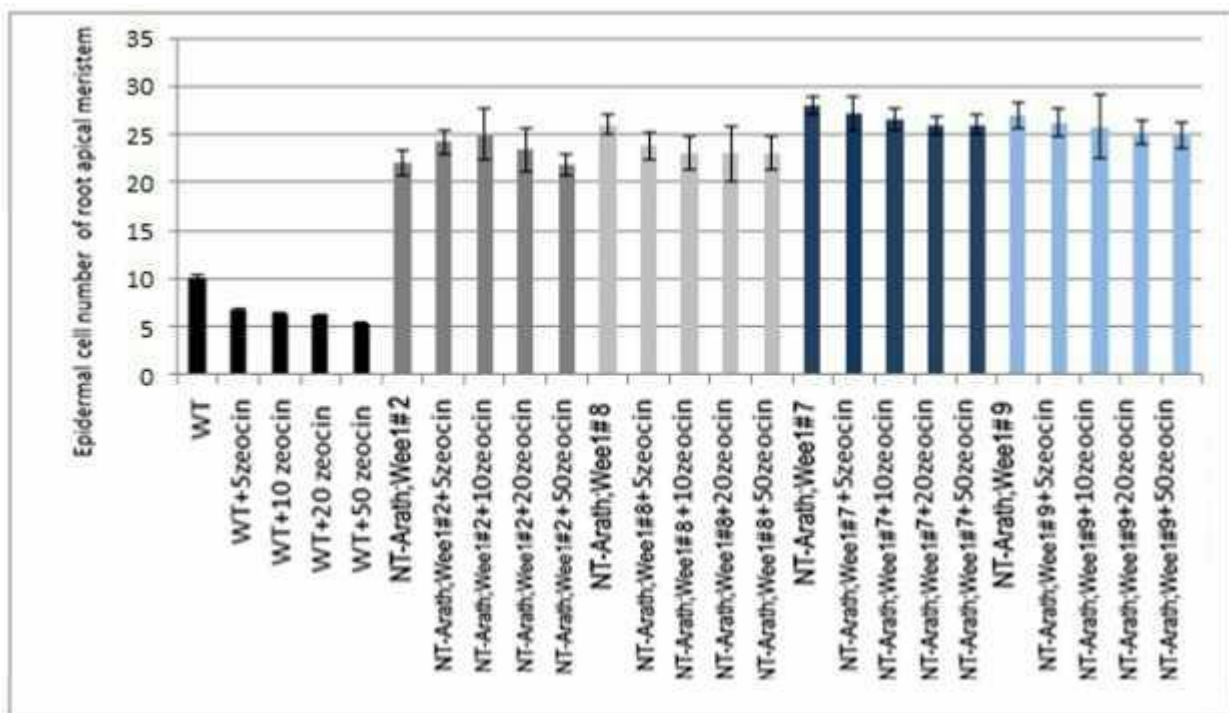


Figure 5.9 Mean (\pm SE.) cell number of root apical meristem in 14 days old seedlings of various genotypes of Tobacco lines NtArath;Wee1#2, NtArath;Wee1#7, NtArath;Wee1#8 and NtArath;Wee1#9 (expressing *Arath;WEE1*) grown in daily cycles of 16 h light and 8 h dark at 21 °C \pm either 0, 5, 10, 20 or 50 μ M zeocin

Table 5.11 Level of significant differences for epidermal cell length in different genotype, of tobacco plants expressing Arath;WEE1 WT± 5, 10, 20, or 50 µM.

	Level of significant difference + 5 µM zeocin	Level of significant difference + 10 µM zeocin	Level of significant difference + 20 µM zeocin	Level of significant difference + 50 µM zeocin	% change ± 5 µM zeocin compared to WT
	Cell number	Cell number	Cell number	Cell number	Cell number
WT	*	*	*	*	*
NT-Arath;Wee1#2	NS	NS	NS	NS	NS
NT-Arath;Wee1#7	NS	NS	NS	NS	NS
NT-Arath;Wee1#8	NS	NS	NS	NS	NS
NT-Arath;Wee1#9	NS	NS	NS	NS	NS

Key. *** < 0.001, ** = 0.02-0.001 P, * = 0.02-0.05 P, NS > 0.05

5.3.3.8 Effects of treatment with zeocin on the length of cells along a file of the epidermal region in the root meristem

Cell length in the transgenic lines was dramatically reduced compared to WT as also found in the HU experiment. Treatment with increasing levels of zeocin resulted in a progressive reduction in cell size in all four transgenic lines, whereas the opposite effect was seen in WT (Fig. 5.10).

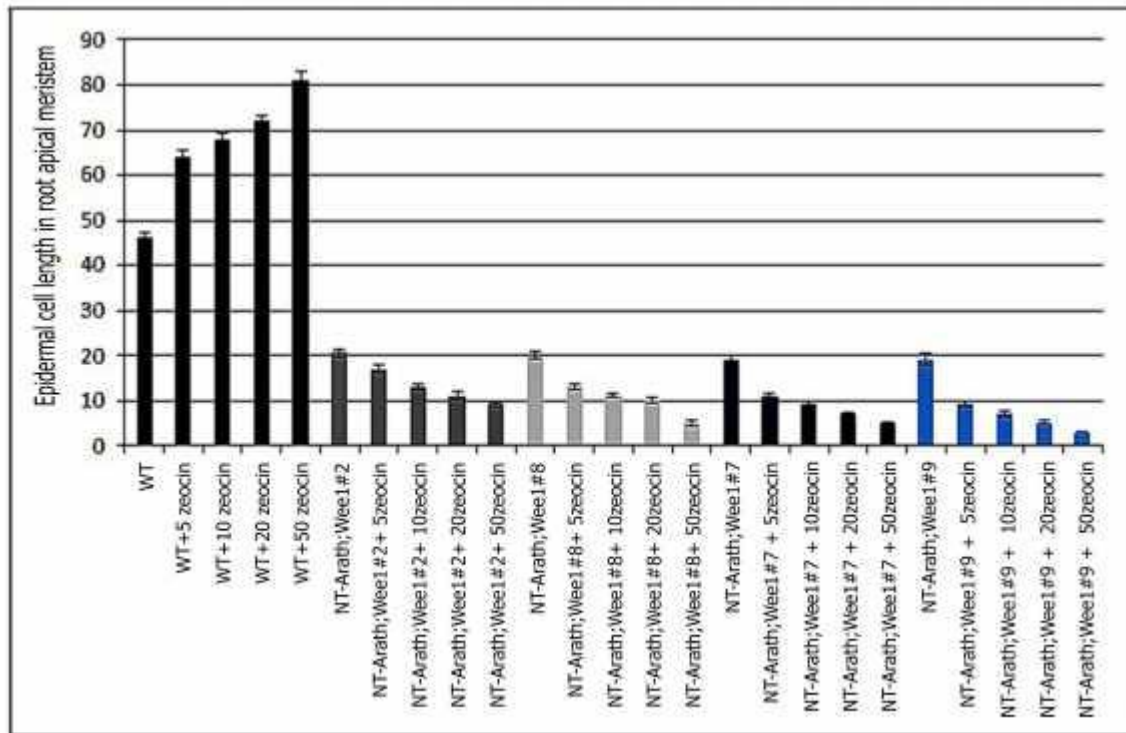


Figure 5.10 The relationship between mean (\pm S.E.) cell length of root apical meristem in 14 days old seedlings in different genotypes of tobacco: WT, line NT-Arath;Wee1#2, NT-Arath;Wee1#7, NT-Arath;Wee1#8 and NT-Arath;Wee1#9 (expressing *Arath;WEE1*) grown in daily cycles of 16 h light and 8 h dark at 21 °C \pm either 0, 5, 10, 20 or 50 μ M zeocin \pm 5, 10, 20, and 50 μ M zeocin

Table 5.12 Level of significant differences for root apical meristem in different genotype, of tobacco plants expressing *Arath;Wee1* WT \pm 5, 10, 20, or 50 μ M zeocin.

	Level of significant difference + 5 μ M zeocin	Level of significant difference + 10 μ M zeocin	Level of significant difference + 20 μ M zeocin	Level of significant difference + 50 μ M zeocin	% change \pm 5 μ M zeocin compared to WT
	Cell length	Cell length	Cell length	Cell length	Cell length
WT	**	**	**	**	**
NT-Arath;Wee1#2	*	*	*	*	*
NT-Arath;Wee1#7	*	*	*	*	*
NT-Arath;Wee1#8	*	*	*	*	*
NT-Arath;Wee1#9	*	*	*	*	*

Key. *** < 0.001, ** = 0.02-0.001 P, * = 0.02-0.05 P, NS > 0.05

5.3.4 Arabidopsis seedlings expressing *Nicta; WEE1*

Two lines expressing *Nicta;WEE1* were selected for further analysis. These are denoted AT-*Nicta;Wee1#3* and AT-*Nicta;Wee1#11*. In both lines the *Nicta;WEE1* was under control of a DEX inducible promoter, hence +DEX were compared to -DEX treatments and to WT. WEE1 protein levels (-DEX) were determined through western blotting and probing with a WEE1 antibody (Fig. 5.11). Both transgenic lines showed significant increases in the level of WEE1 protein compared with WT. Hence these data are completely opposite to those of genotypes in which the Arabidopsis WEE1 was expressed in tobacco.

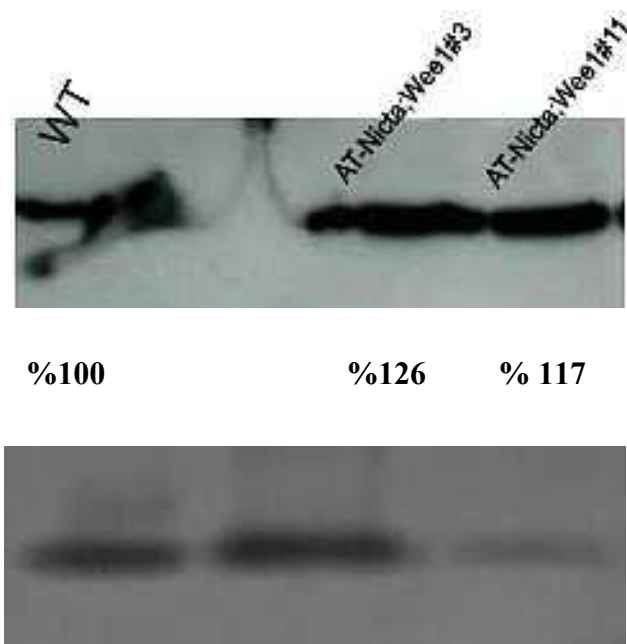


Figure 5.11 WEE1 protein levels of wild type, AT-*Nicta;Wee1#3* and AT-*Nicta;Wee1#11* WEE1. Protein levels were determined by western blotting of samples; the intensity of the bands were quantified and expressed as a ratio of the control. Below the Western blot is the corresponding Coomassie stain loading control.

5.3.4.1 Effect of *Nicta*; *WEE1* expression on primary root length and on the production of lateral roots and primordia

Expression of *Nicta*; *WEE1* in *Arabidopsis* induced by DEX resulted in significantly longer primary roots ($P < 0.01$) compared to both -DEX and the wild type in both transgenic lines. The DEX treatment did not affect wild type primary root length (Fig. 5.12, Table 5.13).

Both primary root length and total number of lateral roots and primordia in AT-*Nicta*; *Wee1*#3 and AT-*Nicta*; *Wee1*#11 under DEX induction were significantly greater ($P < 0.01$) compared with WT or +DEX. However, primary root length and total number of lateral roots and primordia in WT was not significantly different \pm DEX (Figure 5.11, Table 5.14), nor was there a significant difference between WT and transgenic lines - DEX in either character.

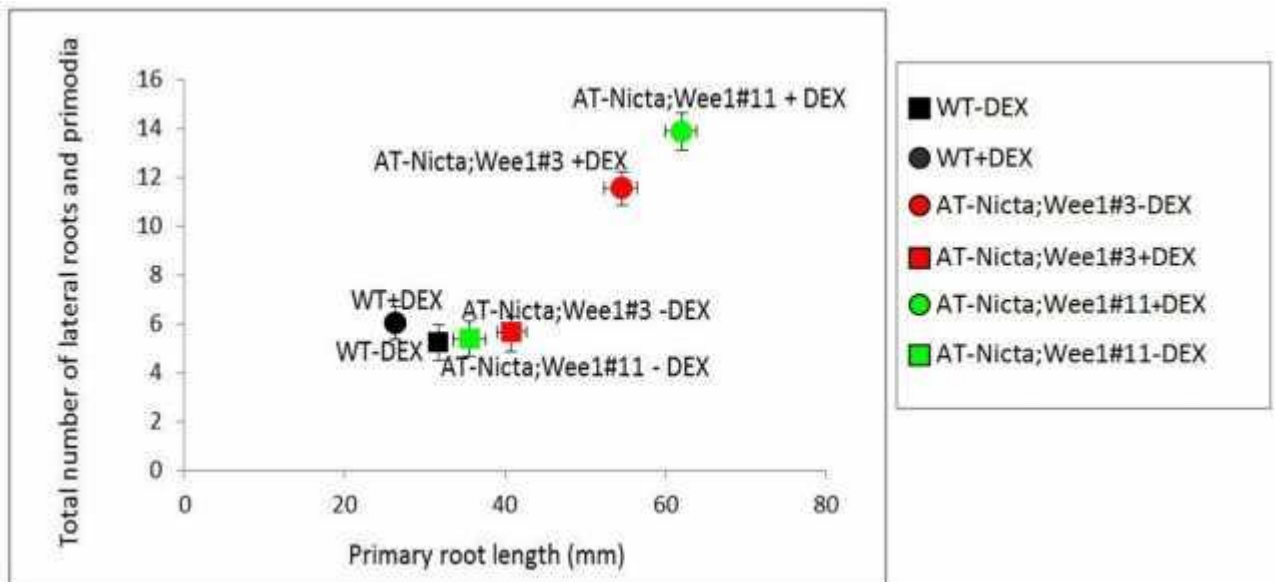


Figure 5.12 The mean (\pm SE) number of lateral roots and lateral root primordia as a function of the mean (\pm SE) primary root length for AT-*Nicta*; *Wee1*#3, and AT-*Nicta*; *Wee1*#11 (expressing *Nicta*; *WEE1*) with DEX and without DEX compared to wild type ($n = 20$), in 10 days old *Arabidopsis* seedlings

Table 5.13 (a) Level of significance between primary root length of each transgenic line, and WT, all grown on medium without adding DEX (b) Level of significant differences in primary root length within genotype \pm DEX

	WT	AT-Nicta;Wee1#3	AT-Nicta;Wee1#11
WT	-	**	***

	-DEX	+DEX	Level of significant difference
	primary root length	primary root length	primary root length
WT	31.4	32.98	NS
AT-Nicta;Wee1#3	28.35	54.43	***
AT-Nicta;Wee1#11	29.58	61.98	***

Key. *** < 0.001, ** = 0.02-0.001 P, * = 0.02-0.05 P, NS > 0.05

Table 5.14 (a) Level of significance between total number of lateral roots and primordia of each transgenic line, and WT, all grown on medium without adding DEX (b) Level of significant differences in total number of lateral roots and primordia within genotype \pm DEX

	WT	AT-Nicta;Wee1#3	AT-Nicta;Wee1#11
WT	-	***	***

	-DEX	+DEX	Level of significant difference
	Total number of lateral roots and primordia	Total number of lateral roots and primordia	Total number of lateral roots and primordia
WT	5.7	5.5	NS
AT-Nicta;Wee1#3	5.6	11.73	***
AT-Nicta;Wee1#11	5.5	13.89	***

Key. *** < 0.001, ** = 0.02-0.001 P, * = 0.02-0.05 P, NS > 0.05

Table 5.15 Rate of lateral root production mm primary root⁻¹ in the different genotypes of 21 days old tobacco seedlings obtained by dividing the x by the y coordinates for each point plotted in Fig. 5.13.

	Rate of lateral root production mm primary root ⁻¹	
	-DEX	+DEX
WT	0.17	0.18
AT-Nicta;Wee1#3	0.16	0.21
AT-Nicta;Wee1#11	0.17	0.22

The induction of tobacco WEE1 in AT resulted in very little change in the rate of lateral root production per mm of primary root (Table 5.15). Hence it can be concluded that the induction

of tobacco WEE1 in AT results in an increase in the growth of the entire root system where the number of laterals that formed were coordinated with respect to primary root length. Once again, hypothesis that the data are linked to changes in morphogenesis can be rejected.

5.3.4.2 Effect of *Nicta*; *WEE1* expression on cell number in a file of epidermal cells of the RAM

Cell number was not affected by DEX treatment in WT, while in the transgenic lines was significantly greater than wild type under DEX induction ($P < 0.01$) (Table 5.16, Fig 5.13).

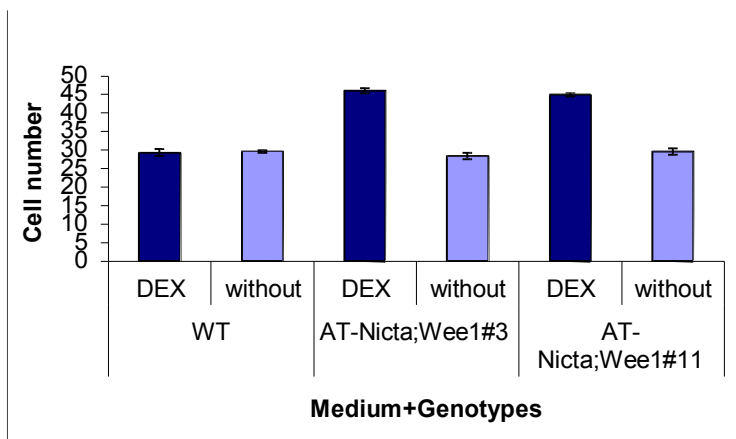


Figure 5. 13 The relationship between mean (\pm S.E.) cell number in epidermis of RAM in wild type (WT), AT-Nicta;Wee1#3, and AT-Nicta;Wee1#11 with or without DEX in 10 day old Arabidopsis plants transformed with *Nicta*; *WEE1* grown in 16 h light and 8 h dark at 21°C. n =20.

Table 5.16 (a) Level of significance between total cell number in file of RAM epidermis of each transgenic line, and WT, all grown on medium without adding DEX (b) Level of significant differences in total cell number in file of RAM epidermis within genotype \pm DEX

	WT	AT-Nicta;Wee1#3	AT-Nicta;Wee1#11
WT	-	***	***

	-DEX	+DEX	Level of significant difference
	Total cell number in file of RAM epidermis	Total cell number in file of RAM epidermis	Total cell number in file of RAM epidermis
WT	29.65	29.27	NS
AT-Nicta;Wee1#3	28.35	45.96	***
AT-Nicta;Wee1#11	29.58	44.85	***

Key. *** < 0.001, ** = 0.02-0.001 P, * = 0.02-0.05 P, NS > 0.05

5.3.4.3 Effect of *Nicta;WEE1* expression on cell length in a file of epidermal cells of the RAM

In the absence of DEX Cell length of RAM epidermal cells in the transgenic lines WT was not significantly different to WT cell length reduced was less than wild type ($P < 0.01$) after treating with DEX . In WT, however cell size was unaffected by DEX treatment (Fig 5.14, Table 5.17).

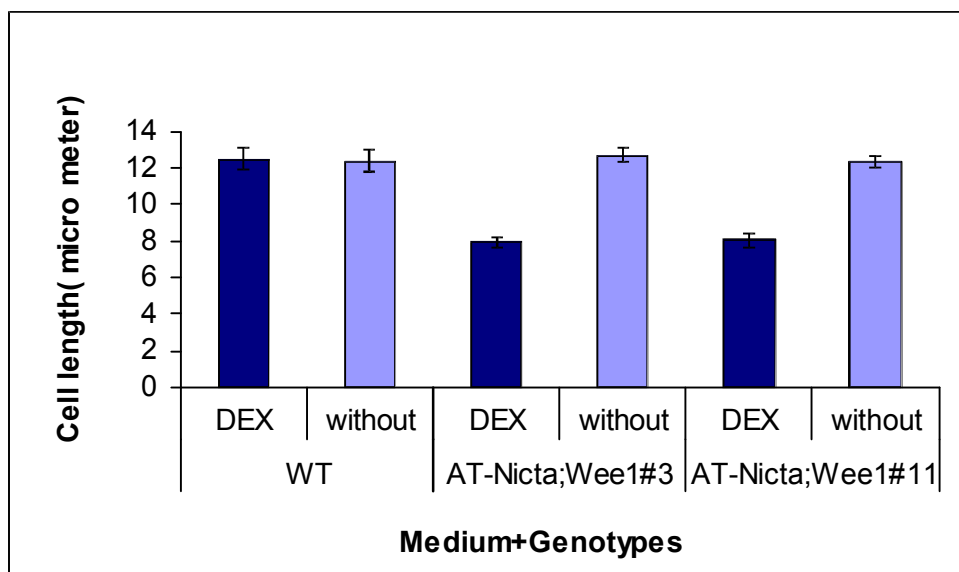


Figure 5.14 .The relationship between mean (\pm S.E.) cell length in epidermis in different genotypes of: wild type (WT) , AT-Nicta;Wee1#3 and AT-Nicta;Wee1#11 with and without DEX treatment in 10 day old Arabidopsis plants transformed with *Nicta;WEE1* grown in 16 h light and 8 h dark at 21°C. n =20.

Table 5.17 (a) Level of significance for RAM epidermal cell length between each transgenic line, and WT, all grown on medium without adding DEX (b) Level of significant differences for RAM epidermal cell length within genotype \pm DEX

	WT	AT-Nicta;Wee1#3	AT-Nicta;Wee1#11
WT	-	***	***

	-DEX	+DEX	Level of significant difference
	RAM epidermal cell length	RAM epidermal cell length	RAM epidermal cell length
WT	12.4	12.5	NS
AT-Nicta;Wee1#3	12.7	7.25	***
AT-Nicta;Wee1#11	12.35	6.05	***

Key. *** < 0.001, ** = 0.02-0.001 P, * = 0.02-0.05 P, NS > 0.05

5.3.4.4 Effect of *Nicta;WEE1* expression on root meristem length

In the absence of DEX meristem length was not significantly different between genotypes (Fig 5.15, Table 5.18). Meristem length was also unaffected in WT +DEX compared to – DEX, also in both transgenic lines treatment with DEX didn't resulted in a significant change in meristem length (Fig. 5.15).

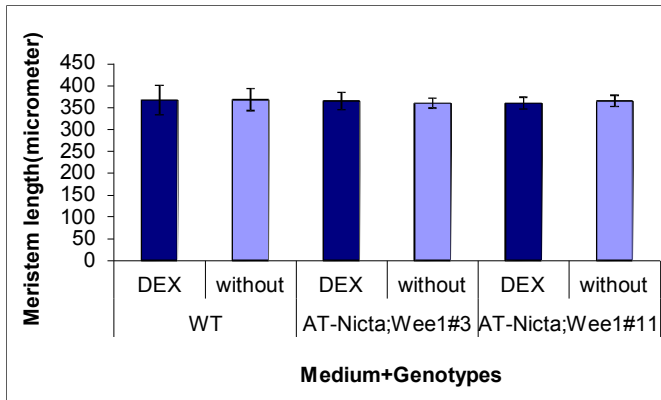


Figure 5.15 The relationship between mean (\pm S.E.) meristem length in epidermis of RAM in wild type (WT), AT-Nicta;Wee1#3, and AT-Nicta;Wee1#11 with or without DEX in 10 day old Arabidopsis plants transformed with *Nicta;WEE1* grown in 16 h light and 8 h dark at 21°C. n =20.

Table 5.18 (a) Level of significance between **root meristem length** of each transgenic line, and WT, all grown on medium without adding DEX (b) Level of significant differences root meristem length within genotype \pm DEX

	WT	AT-Nicta;Wee1#3	AT-Nicta;Wee1#11
WT	-	***	***

	-DEX	+DEX	Level of significant difference
	Root meristem length	Root meristem length	Root meristem length
WT	368	367	NS
AT-Nicta;Wee1#3	360	365	NS
AT-Nicta;Wee1#11	365	360	NS

Key. *** < 0.001, ** = 0.02-0.001 P, * = 0.02-0.05 P, NS >0.05

5.3.4.5 Effect of *Nicta;WEE1* expression on the proportion of cells at different stages in the cell cycle

Microdensitometry was used to assess the proportion of cells in different stages of the cell cycle in the different Arabidopsis genotypes (Fig. 5.16). In the absence of DEX induction,

there was no difference in the relative proportions of cells in M, G1, S, G2 between AT-Nicta;Wee1#3 and AT-Nicta;Wee1#11 compared to WT . However in both transgenic lines +DEX, a doubling of the % cells in M-phase (from 8 to 16) was obtained when compared with WT+DEX. If the hypothesis is that the tobacco WEE1 perturbed the host WEE1 (at RNA, protein or activity levels) then doubling of the % cells in M phase might be because a functional WEE1 is absent at the G2/M transition. However this hypothesis can only be fully tested by data on the duration of each component phase of the cell cycle \pm DEX.

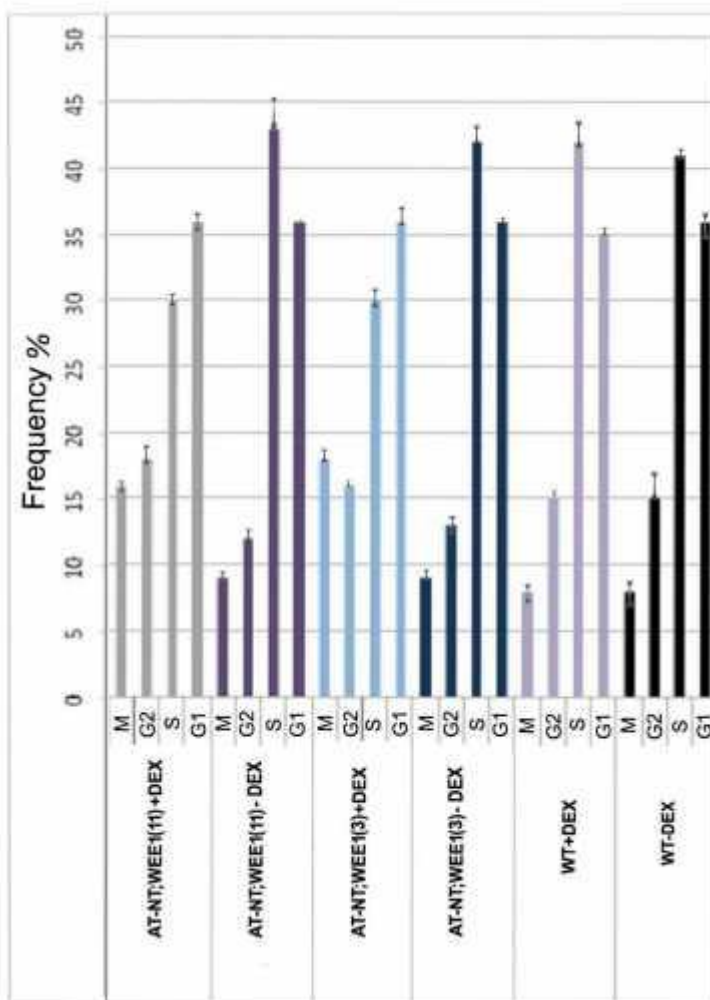


Figure 5.16 Percentage frequency of cells in G1, S, G2 and mitosis in WT \pm DEX, AT-Nicta;Wee1#3 \pm DEX, and AT-Nicta;Wee1#11 \pm DEX, n=14

5.4 Discussion

In the data reported in this chapter, effects of expression of *Arath;WEE1* in tobacco were compared to the effects of expression of *Nicta;WEE1* in Arabidopsis.

Expression of *Arath;WEE1* in tobacco was analysed first to establish whether it affected levels of WEE1 protein. Unexpectedly it seemed that, at least in all the transgenic lines tested, there was a reduction in levels of total WEE1 protein. The antibody used recognises both the tobacco and Arabidopsis WEE1 protein (Lentz Grønlund *et al.*, 2009) hence the results here are taken to represent the total pool of WEE1 protein. Next effects on root phenotype and cellular effects on the RAM were investigated. Since Arabidopsis *wee1-1* mutants are known to be hypersensitive to DNA replication disrupters such as HU (De Schutter *et al.*, 2007), the effect of this chemical and also the DNA damaging agent, zeocin was tested on the tobacco transgenic lines. My hypothesis was that since WEE1 protein appears to be reduced by expression of *Arath; WEE1* in tobacco, the effects on phenotype and response to the DNA replication/ DNA damage checkpoints might be similar to that seen in Arabidopsis mutants that lack a functional WEE1. This would also fit with previous work in the Cardiff lab. (Siciliano, 2006) showing an anomalous effect of *Arath; WEE1* in tobacco BY2 cell cultures. As predicted by my hypothesis, both primary root length and production of lateral roots and primordia were increased in the transgenic tobacco lines. Although De Schutter *et al.* (2007) did not report this effect in the *wee1-1* mutant, subsequent experiments in the Cardiff lab. (Lentz Grønlund, 2007) have shown that *wee1-1* mutants do share this root phenotype. This would be consistent with a role for WEE1 as a negative regulator of entry into mitosis in the normal cell cycle: a reduction in WEE1 might be expected to enable cells to enter mitosis prematurely and hence accelerate root growth and production of lateral roots.

The number of laterals per mm of primary root for each genotype \pm HU are presented in Table 5.3. Both within and between treatments, the magnitude of increase/decrease in the rate of

lateral root production, was remarkably similar for all genotypes. Indeed the largest difference in rate of root production for these genotypes (1.7 fold increase) occurred in the \pm 5mM treatment, (lines #2 and #9). Real differences in rates would be expected to be at least 2-fold. Hence, the differences found between genotypes and within genotype, presented in Fig. 5.3, can be attributed to growth and not to development. For example in NT-Arath;Wee1 #7, #9 #8, the root system was growing significantly faster compared with WT. However, in all transgenic lines, growth of the root system was substantially faster -HU compared with + HU, within genotype. This was particularly so for NT-Arath;Wee1#7 and # 9, which were particularly hypersensitive to HU. Other results in the Cardiff lab, are consistent with over-expression of *WEE1* leading to a reduced number of lateral roots and a decrease in root length. Hence it possible to conclude that in NT-Arath;Wee1 # 7 and 9, the ectopic expression of the *Arath;WEE1* in a tobacco genetic background -HU allowed faster growth of the root system than WT rather than a developmental effect. The latter would have been detected by a significant increase in the rate of lateral root formation in the transgenic lines. In other words it seems highly likely that these lines are, in effect WEE1 knock downs. Note that the lowest amounts of total WEE1 protein were also recorded in lines 7 and 9. So it seems highly likely that endogenous *WEE1* transcription was perturbed by the expression of the alien WEE1. Thus so both of these genotypes, a lack in functional WEE1 (either from the endogenous or exogenous source of *WEE1*), is consistent with the idea that native *WEE1* is a suppressor of growth, but its removal enabled substantial increases in growth compared with WT. Because protein levels were substantially reduced (see Fig. 5.2) it suggests an inhibitory effect of the alien Arabidopsis WEE1 at the transcriptional level such that neither Arabidopsis nor tobacco WEE1 expression led to wild type levels of WEE1 protein. However it is also possible that the expression of Arabidopsis WEE1 interfered with tobacco WEE1 at the translational level.

If so, the effect of *Arath;WEE1* in tobacco would not be dissimilar to the action of an RNAi or an antisense version of WEE1.

The effects of both HU and zeocin on primary root growth and production of lateral roots was consistent with a hypersensitivity of the transgenic lines to these chemicals. This therefore confirms my hypothesis that the effect of expression of *Arath;WEE1* in tobacco is eliciting a down-regulation of WEE1 function, in a similar way to the insertional mutant in Arabidopsis. The cell size phenotype is also in agreement with the results of previous studies of over-expression of *Arath;WEE1* in BY-2 cells (Siciliano, 2006). As previously mentioned, the Wee1 protein is a negative regulator of cell division in *S. pombe* by delaying entry of cells into mitosis (Fantes and Nurse, 1977). In general, knock out or deletion of Wee1 function leads to a premature entry of cells into mitosis resulting in a small cell size, whereas over-expression of *Wee1* has the opposite effect leading to a large cell phenotype in fission yeast, tobacco and tomato (Russell and Nurse, 1987; Sun *et al.*, 1999; Walter *et al.*, 2000; Sorrell *et al.*, 2002; Harvey and Kellogg, 2003). However, the over-expression of *Arath;WEE1* in *N. tabacum* BY-2 cells resulted in a shortened G2 phase and small cell phenotypes (Siciliano, 2006). This phenotype resembles Wee1 loss-of-function mutants in both yeast and animals (Walter *et al.*, 2000; Harvey and Kellogg, 2003).

The induction of the DNA replication checkpoint in WT, would be consistent with a progressive increase in cell size if cells were blocked at a checkpoint but they continued to grow. Indeed in Fig. 5.6, in WT, epidermal cell length was positively related to HU concentration. Clearly, this was not so in the putative knock down mutants. In the presence of HU, cell cycle progression was not blocked presumably because functional WEE1 is missing. Hence such cells would be escaping the DNA replication checkpoint. In the absence of functional WEE1, cell size was highly significantly smaller than WT in 0 mM

HU. This also suggests that even in normal conditions, *WEE1* is part of a system that regulates cell size. These results further suggest a role of WEE1 kinase in determining cell size at division.

Induction of *Nicta;WEE1* in Arabidopsis under DEX treatment resulted in an increased level of WEE1 protein indicating that in contrast to the expression of *Arath;WEE1* in tobacco, the effects here may more closely resemble an over-expression of WEE1. However DEX induction of these lines resulted in increasing primary root elongation, more lateral root primordia, increased number of epidermal cells in the RAM but smaller cell length. Thus all the phenotypic characters were very similar to the expression of *Arath;WEE1* in tobacco plants and in both cases, the phenotype is similar to that seen in Arabidopsis WEE1 mutants such as *wee1-1*. The cell size phenotype is also in agreement with the results of previous studies of over-expression of *Arath;WEE1* in BY-2 cells (Siciliano, 2006).

When *Nicta;WEE1* was over-expressed in *N. tabacum* BY-2 cells its transcription was increased during S phase and decreased during M phase (Gonzalez *et al.*, 2004). However when *Arath;WEE1* was expressed in BY2 cells there was a perturbation of the transcriptional pattern of the endogenous *Nicta;WEE1* during the cell cycle (Siciliano, 2006). Thus it seems that in this case the effects of *Arath;WEE1* are through a perturbation in the transcription pattern. When levels of WEE1 protein were analysed in BY2 cells expressing *Arath;WEE1* they were found to be increased (Lentz Grønlund, 2007) however in my work WEE1 protein levels appeared to be reduced in the tobacco plants when *Arath;WEE1* was expressed. Thus it is possible that in whole plants the mechanism for the interference of the *Arath;WEE1* with the endogenous WEE1 is different. In this case, the effects may be due to an overall reduction in WEE1 protein and hence activity. However when *Nicta;WEE1* was expressed in Arabidopsis, WEE1 protein levels were higher than WT, a more similar situation to the

expression of *Arath;WEE1* in the BY2 cells. The explanation for the apparent WEE1 knock-down phenotype may be because despite the higher levels of WEE1 protein, the expression of *Nicta;WEE1* in some way interferes with endogenous WEE1 function.

The cell size phenotype would result from a reduction in WEE1 action which results in faster transition at the G2 phase to mitosis. Lentz Grønlund (2007) showed that in synchronized wild type *N. tabacum* BY-2 cell culture WEE1 protein level increases during S phase and peaks in late S phase; this protein level decreases as the cells progress into mitosis. In agreement with decreasing protein levels, WEE1 activity decreased when cells entered mitosis (Lentz Grønlund, 2007). However, from the increase in the pool of total WEE1 protein and WEE1 kinase activity (Lentz Grønlund, 2007) it was concluded that the WEE1 kinase activity originated from both *Arath;WEE1* and *Nicta;WEE1*. Nevertheless, expression of *Arath;WEE1* in BY-2 cells does not seem to change the total transcript level of *WEE1*, as shown by Spadafora (2007).

Results which were obtained from microdensitometry experiments in AT-*Nicta;Wee1#3* and AT-*Nicta;Wee1#11* lines showed a decrease in the number of cells during S phase and an increase during M phase; moreover, the proportion of cells in M-phase are approximately double in the both transgenic lines +DEX compared with -DEX. The expression of *Arath;WEE1* in tobacco cells caused a delay in expression of *Nicta;WEE1* transcripts (Siciliano *et al.*, 2006) and levels of WEE1 kinase were found to mirror entry into mitosis, being anticipated when *Arath;WEE1* expression was induced by DEX (Lentz Grønlund, 2007) as a result, cell size is reduced according to the same results I observed in the cell size of RAM epidermis cells. Early work in fission yeast showed that loss of function of WEE1 induces a small cell phenotype (Nurse, 1975); in contrast, over expression of WEE1 delayed mitosis and caused larger cells (Russell and Nurse, 1987). These results suggested that WEE1 is a part of cell size checkpoint by preventing cells to enter into mitosis, and my result is in

agreement with this conclusion. As it was confirmed by Sorrell *et al.* (2002) over expression of *Arath; WEE1* in *S. pombe* resulted in long cells.

As a result, the phenotypic study of roots as well as microdensitometry data showed that the induction of the foreign WEE1 has had a notable impact on the cell cycle. In both DEX induced *Nicta;WEE1* in Arabidopsis lines and in lines where *Arath;WEE1* was expressed in tobacco, a dramatic increase was observed in total number of lateral roots and primordia. As discussed above, the hypothesis would be that rate of lateral root and primordia production results from reducing the WEE1 activity which affects the activity of CDK/Cyclin complexes, this result could be because of a delay in the transcription of tobacco WEE1 and a premature peak of CDKB activity. The explanation could be that expression of *Arath;WEE1* in tobacco, perturbed the expression of the endogenous tobacco *Nicta;WEE1* or the expression of *Nicta;WEE1* in Arabidopsis, perturbed the expression of the endogenous Arabidopsis *Arath;WEE1*, which may cause a lower level of WEE1 protein kinase during G2 phase. This would then result in the dramatic increase in total number of lateral roots and primordia.

All in all the phenotypic results of root growth, cellular meristem characters, and response to zeocin and HU, This indicate a remarkable similarity with the Arabidopsis knockout of insertion mutant *wee1-1* indicating presumably that differences in the sequences of the tobacco and Arabidopsis WEE1 open reading frames are sufficient to elicit a negative response in the transgenic environment effectively shutting down WEE1 activity. Further work will be needed to unravel the key differences in protein sequence that elicit this response and the cellular factors that interact with them. Moreover, albeit not trivial, measurements of WEE1 kinase activity should be undertaken.

6. General Discussion

Arabidopsis WEE1 was identified in the Cardiff lab. ten years ago (Sorrell *et al.*, 2002) and the effects of mutation in the *Arath;WEE1* gene have also been known for some time (De Schutter *et al.*, 2007). However a number of issues remain to be resolved relating to the role of this protein in its interaction with other cellular proteins and this has been the focus of my thesis.

Previous work in the Cardiff lab. had indicated an interaction of Arabidopsis WEE1 with various proteins. Notably WEE1 interacted with a sub-set of stress-related proteins, and of these GSTF9 was one of the strongest interactions (Lentz-Grønlund, 2007). One aim of my work was to gain a better understanding of *Arath;WEE1*'s interaction with *Arath;GSTF9* by using a genetic approach. Further previous work also showed an interaction between *Arath;WEE1* and the putative checkpoint protein, 14-3-3 ω (GF14 ω)(Lentz Grønlund et al., 2009) which I also aimed to investigate further at a functional level using a genetic approach.

I investigated these different WEE1 interactions by performing crosses between lines in which the expression of the candidate interactors was perturbed, and the *Arath;WEE1* insertion mutant *wee1-1*. The effects of these genes in the absence of a functional WEE1 could then be studied in Arabidopsis plants stressed by either hydroxyurea (HU) or zeocin that induce the DNA replication and DNA damage checkpoints, respectively.

Previous work had also established an unexpected effect of *Arath;WEE1* in tobacco BY-2 cells: a reduction of cell size and premature mitosis as opposed to the expected effect of large cell size and extension of G2 phase (Siciliano, 2006). It was therefore timely for me

to investigate expression of *Arath;WEE1* in whole plants of tobacco and conversely, the effect of *Nicta;WEE1* in Arabidopsis.

6.1 Interaction of *Arath;WEE1* with GSTF9

Arath;WEE1 was used as a probe in a 2-hybrid screen to identify a number of interacting proteins including GSTF9. The interaction was confirmed by BiFC and found to occur in the nucleus (Lentz Grønlund, 2007, Cardiff Laboratory unpublished data). To investigate the extent to which these genes might be interacting, a cross was made between *gstf9* and *wee1-1* knockouts, and subsequently their phenotypes were studied. My starting hypothesis was that if the genes were operating in the same pathway as suggested by the protein-protein interaction, then the effect of mutating both genes should be similar to mutating just one of them.

Both mutant genotypes were hypersensitive to HU and zeocin in that dramatic reductions in primary root length and total lateral root production, cell length and meristem length were observed in both the *wee1-1* and *gstf9* mutants. The phenotype of the *Arath;WEE1* mutant in respect of primary root length in the presence of HU had already been described by De Schutter *et al.* (2007), and my results were in agreement with the published data. However my results also indicated an increase in primary root growth in the absence of HU which was not reported by De Schutter *et al.* (2007) and also contrasted with the data of Lentz Grønlund (2007). It is possible that the growth of this mutant in culture is affected by the seed stock and medium composition, and further work will be needed to resolve this aspect of its phenotype. However an increase in primary root growth in the absence of a functional WEE1 would be consistent for a role of WEE1 in negatively regulating G2/M as is well established in animal

and yeast systems (Walter *et al.*, 2000; Harvey and Kellogg, 2003; Asano *et al.*, 2005) and hence potentially delaying primary root growth.

I also showed that the *wee1-1* mutant was hypersensitive to zeocin, which had not previously been shown, although De Schutter *et al.* (2007) showed that zeocin was able to activate *Arath;WEE1* expression. Surprisingly, primary root elongation in the *gst9* mutant was also hypersensitive to HU and zeocin. While the increased sensitivity to abiotic stress treatments such as salt and *N*-acetylcysteine of the *gst9* mutant had already been reported (Dixon and Edwards, 2010), a hypersensitivity to DNA damaging agents and agents that disrupt DNA replication had not previously been reported. These data suggest that this GST may play an important role in this checkpoint. However in the presence of a WT copy of *Arath;WEE1*, but in the absence of chemical agents that activate the DNA damage/ replication checkpoint, primary root elongation was not affected by the *gst9* mutation. This suggests that *GSTF9* is not required for normal root elongation. This is consistent with a stress-responsive role for many GSTs, but little evidence for their involvement in overall normal plant growth (Kitamura *et al.*, 2004; Moons, 2005; Dixon *et al.*, 2009).

In the *wee1-1* mutant, more lateral roots were produced in the absence of HU or zeocin, relative to WT, whereas lateral root production was unaffected by the *GSTF9* mutation. This suggests that while *Arath;WEE1* is required for the normal rate of lateral root production, *GSTF9* is not. This is in agreement with other data for *Arath;WEE1*, since over-expression of this gene results in reduced lateral root production (Lentz Grønlund, 2007). Again the null effect of *GSTF9* mutation confirms a role for this gene in stress response but not in normal growth and development.

In both mutant lines cell number was significantly higher and cell length significantly shorter in the RAM epidermis in the untreated seedlings. In this respect the effects of *GSTF9* mutation appeared greater than those of *Arath;WEE1* mutation. So both genes appear to affect meristem cell number and cell size even in the absence of HU or zeocin. The effects on cell size of *Arath;WEE1* fit with a role for this gene in regulating cell size in other organisms. For example the loss of function *swee1* mutant exhibited a small cell size phenotype (Parker *et al.*, 1993; Tang *et al.*, 1993; Wu and Russell, 1993; Kanoh and Russell, 1998, Harvey *et al.*, 2003). Also loss of WEE1 function in the fission, yeast *wee1*, generated a small size phenotype (Nurse *et al.*, 1980). However a role for *GSTF9* in cell size regulation was unexpected given its null effect on primary and lateral root growth. This may be related to the redox control of the cell cycle (Alfenito *et al.*, 1998; Muller *et al.*, 2000; Dixon *et al.*, 2002; Kili *et al.*, 2004, Rea, 2007, Dixon *et al.*, 2010), but further work is required to understand the specific role of this GST at a biochemical level.

The progressive reduction in cell size with increasing HU and zeocin in both mutants indicates perhaps an increasing escape of the cells into mitosis in the absence of these regulators presumably resulting in cells with damaged or incompletely replicated DNA that leads to the dramatic reduction in root growth under HU or zeocin stress.

Regarding the root length data, I conclude that *WEE1* and possibly also *GSTF9* have roles in the DNA replication and damage checkpoints. However the question of whether the two genes are acting in the same pathway or in different pathways proved to be a complex one. In some aspects the gene effects were additive indicating independent effects whereas in others the phenotype of the double mutant resembled most closely that of the *wee1-1* single mutant (Table 6.1).

Table 6.1 summary of effects of the two genes (*Arath;WEE1* and *GSTF9*) on phenotypic characteristics, and interactions between the two genes

Phenotypic characteristic	Interaction between <i>Arath;WEE1</i> and <i>GSTF9</i>
Primary root elongation (-HU/ zeocin)	slightly additive
Primary root elongation (+HU/ zeocin)	slightly additive?
Rate of lateral root production (-HU/ zeocin)	<i>Arath;WEE1</i> epistatic
Rate of lateral root production (+HU/ zeocin)	additive
RAM epidermal cell length (-HU/ zeocin)	additive
RAM epidermal cell length (+HU/ zeocin)	additive
Number of RAM epidermal cells in file (-HU/ zeocin)	additive
Number of RAM epidermal cells in file (+HU/ zeocin)	additive
Meristem size (-HU/ zeocin)	<i>Arath;WEE1</i> epistatic
Meristem size (+HU/ zeocin)	<i>Arath;WEE1</i> epistatic

From the result of primary root length, total number of lateral roots and primordia, and meristem length, the double mutant suggests that the two genes are also acting at least in part, independently. The interaction between these two genes is only slightly additive in some aspects like primary root length and total number of lateral roots and primordia, which does not indicate a double effect of the combined mutation of both genes in the double mutant. However an additive effect was observed on cell length and cell number of the RAM which shows the double mutant has a stronger response to HU and zeocin than either of the two single mutants. The similar behaviour of the two mutant lines in different studies under stress conditions (DNA replication or DNA damage checkpoints), and the evidence of nuclear interaction of these genes confirms that they are both required for these checkpoints, however a full genetic interaction cannot be confirmed.

To obtain a better knowledge of the role of *Arath;WEE1* and its interaction with *GSTF9* what is required is a better understanding of the role of *GSTF9* at a molecular level. Is it

acting to detoxify the damage caused by the activation of the checkpoint or is it binding to some essential metabolite required for the checkpoint function? Further biochemical analyses of GST function will be required to resolve this point.

6.2 Interaction of *Arath;WEE1* with and *GF14*

To explore this interaction further *GF14* was over-expressed in *Arabidopsis* under an oestradiol-inducible promoter (Cardiff lab unpublished results). The hypothesis was that if the role of *GF14* was to stabilise *WEE1*, as seen in other systems, then an over-expression of *GF14* would result in a similar phenotype to over-expressing *Arath;WEE1*. However problems were encountered previously in obtaining a consistent phenotype from these transgenic lines (Lentz Grønlund, unpublished results). I was able to overcome this problem by establishing an interaction between sucrose and oestradiol, and showed for the first time that over-expression of *GF14* resulted in decrease in the rate of primary root elongation, and total number of lateral roots and primordia compared with WT in the presence of oestradiol, which was similar to that seen in the line over-expressing *Arath;WEE1*. Also cell length in epidermal RAM cells of *GF14 OE wee1-1* line was even greater than in the *GF14 OE* or the *Arath;WEE1* over-expressing line. 14-3-3 proteins are known to regulate the cell cycle in animal and yeast cells through their interactions with *WEE1* and *CDC25* (Forbes *et al.*, 1998; Kumagai and Dunphy, 1999; Lee *et al.*, 2001). Furthermore *GF14* was the only 14-3-3 protein out of three tested that was able to rescue the defects in DNA damage and replication in the *rad24⁻* yeast mutant (Sorrell *et al.*, 2003). Thus an effect on cell length and root growth of over-expressing this gene would be consistent with a role in participating in the transition from G2 to M.

Because of the similar effect to over expressing *Arath;WEE1*, to explore the relationship between GF14 and *Arath;WEE1*, I set up the cross between the GF14 over-expressing line and the *wee1-1* insertion mutant. My hypothesis was that if the phenotype seen in the GF14 over-expressor was due to its interaction with *Arath;WEE1* then in the absence of a functional *WEE1*, this phenotype would be abolished. However this was not the case. The *wee1-1* mutant over-expressing *Arath;GF14* showed a similar reduction primary root length and in the rate of lateral root production, and increase in RAM epidermal cell length as shown by the over-expression of *Arath;GF14* in the WT genetic background. This suggests that *Arath;WEE1* is not required for the action of GF14, and GF14 acts on root growth and cell size independently of *WEE1*. How *Arath;GF14* exerts its regulatory effects on cell size and root growth thus remains to be determined.

Another way in which the interaction between GF14 and *Arath;WEE1* was explored was through mutation of a serine residue (S485) in the *Arath;WEE1* protein which is putatively phosphorylated to allow binding of the GF14 Lentz Grønlund *et al.*, (2009). I began to set up an experiment and transformed Arabidopsis seedlings with a construct of *Arath;WEE1* that incorporates the S485A mutation. I planned to transform this construct both into WT and the *wee1-1* line to establish whether the mutated *Arath;WEE1* could complement the *wee1-1* mutation. My hypothesis was that is the S485 mutation abolishes interaction with over-*Arath; GF14* as indicated by the 2-hybrid analysis Lentz Grønlund *et al.*, (2009), Moreover, if the interaction with this 14-3-3 protein is important for *Arath;WEE1* function then the mutated *Arath;WEE1* would not complement the *wee1-1* mutant, and the expression of this mutated *Arath;WEE1* in WT would not induce the over-expression phenotype seen with the native *Arath;WEE1* over-expression. However due to time constraints I was not able to

complete this work. Further work should be carried out to study the phenotype of the S485A transgenic plants.

6.3 Regulation of *Arath;WEE1* and *Nicta;WEE1*

Arath; WEE1 expression in *Schizosaccharomyces pombe* results a longer cell phenotype compared with WT (Sorrell *et al.*, 2002) as was previously obtained by over expressing the native *cdc2* (Tang *et al.*, 1993; Lundgren *et al.*, 1991; Millar *et al.*, 1991). Expression of *Solly;WEE1* in TBY-2 cells caused a lengthening of the G2 phase (Gonzalez *et al.*, 2007), a similar result was reported by Spadafora *et al.* (2009) by over-expression of *Nicta;WEE1* in TBY-2 cells. Synchronization of BY2 cells by Spadafora (2008) demonstrated that when *Nicta;WEE1* expression was induced, G2 was delayed (Table 6.2). However, surprisingly, Siciliano (2006) showed that the over-expression of *Arath;WEE1* in *N. tabacum* BY-2 cells resulted in a small cell phenotype which is the opposite of the previous findings in *S. pombe* and *A. thaliana*. This suggested an unexpected interaction between *Arath;WEE1* and the tobacco genomic background which I have further pursued in this part of my PhD (Table 6.2).

In my work, inducible expression of *Nicta;WEE1* in *Arabidopsis thaliana* resulted in increased primary root growth, more lateral root primordia, increased number of epidermal cells in the RAM but smaller cell length. In other words, *Nicta;WEE1* expressed in an *Arabidopsis* genetic background exhibited the converse of a predicted negative effect of *WEE1* over expression in *Arabidopsis* e.g. reduced root growth, fewer laterals and a large

Table 6.2 Comparison of phenotypic characters of the effects of WEE1 expression in Arabidopsis and tobacco

		-HU/zeocin	-HU/zeocin	-HU/zeocin	-HU/zeocin	-HU/zeocin	+HU/zeocin	+HU/zeocin	+HU/zeocin	+HU/zeocin	+HU/zeocin	Source of data
line	Protein levels	Primary root	Lateral roots	Meristem length	Cell no. in meristem cell file	Mersitem cell length/cell size	Primary root	Lateral roots	Meristem length	Cell no. in meristem cell file	Mersitem cell length/cell size	
<i>Arath;WEE1</i> in tobacco plants	↓	↑	↑	↑	↑	↓	↓ H	↓ H	↓ H	Reduced effect	Reduced effect	My resaerch
<i>Arath;WEE1</i> in tobacco BY2 cells	↑	N/A	N/A	N/A	N/A	↓	N/A	N/A	N/A	ND	ND	Siciliano, <i>et al.</i> , 2006 Lentz et al., 2007
<i>Arath;WEE1</i> in Arabidopsis plants	ND	↓	↓	ND	ND	↑	-	-	ND	ND	ND	Siciliano, <i>et al.</i> , 2006 Lentz et al., 2007
<i>Nicta;WEE1</i> in BY2 cells	ND	N/A	N/A	N/A	N/A	No change	N/A	N/A	N/A	N/A	ND	Lentz et al., 2007
<i>Nicta;WEE1</i> in Arabidopsis plants	↑	↑	↑	↑	↑	↓	ND	ND	ND	ND	ND	Siciliano, <i>et al.</i> , 2006 ,My resaerch
Arabidopsis <i>wee1-1</i> mutant	↓	↑	↑	↑	↑	↓	↓ H	↓ H	↓ H	Reduced effect	↓	My research- Lentz <i>et al.</i> , 2007, De Schutter et al., 2007

N/A = not applicable, ND = not determined, RD= Reduction, H+ Hypersensitive

cell size phenotype (Gonzalez *et al.*, 2004). Research by Siciliano (2006) confirmed that as expected, the effect of over-expression of *Arath;WEE1* on Arabidopsis root development was to induce a shorter primary root length and fewer number of lateral roots and primordia. Thus it was not an effect of over-expression of WEE1 *per se* that results in the unexpected phenotype but rather a similar effect to that seen in tobacco BY2 cells when *Arath;WEE1* was expressed, suggesting again an unusual interaction between WEE1 and the cellular machinery in the alien genetic background. The total levels of protein Arabidopsis expressing *Nicta;WEE1* were higher than WT, which was similar to the result seen when *Arath;WEE1* was expressed in tobacco BY2 cells (Lentz Grønlund, 2007) (Table 6.2). This suggests that the mechanism may be related to post-translational events that result in an inactive kinase activity although further work is needed to verify this.

To test whether the effects seen in BY2 cells could be confirmed in whole plants, the phenotype of tobacco seedlings which were transformed with the *Arath;WEE1* gene was investigated. Tobacco seedlings that expressed *Arath;WEE1* showed a significantly longer primary root length, greater number of lateral roots and primordia, and smaller epidermal cell size compared to wild type seedlings. Hence, expression of *Arath;WEE1* in a tobacco genetic background, resulted in phenotype more easily associated with loss-of-function *wee1* mutants as opposed to plants with an over-abundance of *WEE1*. In conclusion the effect of expression of *Arath;WEE1* in tobacco seems to be eliciting a down-regulation of WEE1 function. Note also, however, that the expression of *Arath;WEE1* in tobacco BY-2 cells resulted in a delay in the transcriptional peak of native WEE1, from mid S-phase (Gonzalez *et al.*, 2007) to G2 phase (Siciliano, 2006), and this was subsequently confirmed by Lentz Grønlund (2007). In fact Lentz Grønlund (2007) went further in analysing both WEE1 protein levels and kinase activity in BY2 cell lines expressing *Arath;WEE1* under

an inducible promoter. She found that there was an increase in total WEE1 protein on induction of *Arath;WEE1* expression (Table 6.2). From these data she postulated that the mechanism in these cells that results in a premature mitosis is perhaps a triggering of premature WEE1 protein destruction by the excessively high levels of protein. This contrasts with my data where I show that in all the independent transgenic lines analysed, WEE1 protein levels were reduced compared to WT. This discrepancy could be due to the different tissues and vectors used but should be verified further. Hence it is possible that more than one mechanism is operating and that different mechanisms may operate in cell cultures and whole plants to produce similar effects on cell size.

Root phenotype and cellular effects on the RAM under DNA damaging agents such as zeocin and DNA replication agent as HU in both *Nicta;WEE1* expressed in Arabidopsis and *Arath;WEE1* expressed in tobacco plants were consistent with a down-regulation of WEE1 resulting in a phenotype which was similar to that seen in the *wee1-1* mutants (De Schutter *et al.*, 2007). This clearly requires further work to confirm that WEE1 activity is indeed down-regulated but supports the findings of De Schutter *et al.* (2007) that plant WEE1 is part of the pathway that blocks the cell cycle under DNA stress.

6.4 Further work

6.4.1 Interaction of *AtWEE1* with other cellular proteins: GSTF9 and GF14^o

Because of the mixture of epistatic and additive effects of *Arath;WEE1* and *GSTF9* as revealed by the double mutant in further studies an assay of protein kinase activity would be

worthwhile. If the function of two genes are additive i.e. acting independently I would expect in the *gstf9* mutant to have WT levels of WEE1 kinase activity. However if the absence of a functional *GSTF9* affects WEE1 function then the protein kinase activity might be reduced in the *gstf9* mutant. The protein kinase activity is more precise determinant for checkpoint control than WEE1 protein level, as protein level gives the information about the expression pattern, while kinase activity is about the enzyme's activity.

Further study on how GF14 affects the sub-cellular localization of the *Arath; WEE1* (S485A) mutant would be useful, to investigate if S485A mutation of *Arath;WEE1* abolishes GF14 binding in vivo. Lentz *et al.* (2009) showed that this was the case by BiFC however here both proteins are expressed at high levels hence if it were possible it would be useful to repeat these experiments expressing the two proteins at more physiological levels or using immunofluorescence to localise the proteins.

In the work presented here the number of cells in each stage of the cell cycle stages and their mitotic index was measured, but further study on nuclear DNA content in mutant plants using flow cytometry analysis, and also study the duration of the cell cycle using colchicine, cell flow and rate of cell production would be useful.

Also it would be interesting to do different crosses between *wee1-1* and mutants or over-expressors of other candidate G2/M regulator genes such as those from the KRP protein family which have an interaction with CDKBs and which are controlling cell cycle. This would provide further information using genetic tools on the extent to which WEE1 interacts with other cell cycle regulators.

6.4.2 Regulation of *Arath;WEE1* and *Nicta;WEE1*

An obvious missing experiment is the effect of HU or zeocin on root growth and cellular parameters of the transgenic *Arabidopsis* lines expressing *Nicta; WEE1*. This would verify my findings that these lines are behaving like *WEE1* knockdown lines by testing whether they show a hypersensitive response to these checkpoint inducing agents.

Two missing transgenic lines that I identified during this work were the over-expression of *Nicta;WEE1* in tobacco plants and an RNAi or antisense based down-regulation of *Nicta;WEE1* in plants and cell cultures. These would be very useful to complete the picture of the interaction between these two *WEE1* genes and their alien transgenic host plant. I tried to make the gene silenced line to reduce expression of *Nicta;WEE1* in wild type tobacco for better understanding the role of *WEE1* based on an RNAi construct developed in the Cardiff lab, but due to time constraints and infection in some calluses during the transformation procedure at the end of my PhD I could not carry on this experiment. This method which is based on RNA interference (RNAi) was successfully used as a system of study on the role of genes in different organisms before (Tang *et al.*, 2003). Furthermore CDKA and CDKB kinase activity could also be studied in these transgenic lines to investigate the effect of *Nicta;WEE1* silencing.

Another tool that would be very useful would be specific antibodies for *Arath;WEE1* and *Nicat;WEE1*. This would enable us to determine the levels of the transgenic and endogenous proteins in the transgenic lines we already have and would help in the comparison of the protein levels and their transcription in the transgenic plants compared with the wild type plants.

References

1. **Abraham RT. 2000.** Cell cycle checkpoint signaling through the ATM and ATR kinases. *Genes Dev.*, **15**: 2177–2196.
2. **Adragna NC, Fonseca P and Lauf PK. 1994.** Hydroxyurea affects cell morphology, cation transport, and red blood cell adhesion in cultured vascular endothelial cells. *Blood J.***83**: 553-560.
3. **Aitken A. 2002.** Functional specificity in 14-3-3 isoform interactions through dimer formation and phosphorylation. Chromosome location of mammalian isoforms and variants. *Plant Mol Biol* **50**: 993-1010.
4. **Al-Dewachi HS, Wright NA, Appleton DR and Watson AJ. 2008.** The effect of a single injection on hydroxyurea on cell population kinetics in the small bowel mucosa of the rat. *Cell Proliferation.***10**: 203-213.
5. **Alfenito MR, Souer E, Godman CD, Buell R, Mol J, Koes R and Walbot V .1998.** Functional complementation of anthocyanins sequestration in the vacuole by widely divergent glutathione S-transferases. *Plant Cell* **10**: 1135–1149
6. **Aligue R, Wu L and Russell P. 1997.** Regulation of *Schizosaccharomyces pombe* Wee1 tyrosine kinase. *J Biol Chem* **272**: 13320-5.
7. **Alonso JM. 2003.** Genome-wide insertional mutagenesis of *Arabidopsis thaliana*. *Science* **301**: 653–657.
8. **Alonso, J.M., Stepanova, A.N., Solano, R., Wisman, E., Ferrari, S., Ausubel, F.M., and Ecker, J.R. 2003.** Five components of the ethylene-response pathway identified in a screen for weak ethylene-insensitive mutants in *Arabidopsis*. *Proc. Natl. Acad. Sci. USA* **100**: 2992–2997.

9. **Alsterfjord M, Sehnke PC, Arkell A, Larsson H, Svennelid F, Rosenquist M, Ferl RJ, Sommarin M and Larsson C. 2004.** Plasma membrane H(+)-ATPase and 14-3-3 isoforms of *Arabidopsis* leaves: evidence for isoform specificity in the 14-3-3/H(+)-ATPase interaction. *Plant Cell Physiol* **45**, 1202-10.
10. **Altman R and Kellogg DR. 1997.** Control of mitotic events by Nap1 and the Gin4 kinase. *J Cell Biol* **138**:119–130
11. **Aoyama T and Chua NH. 1997.** A glucocorticoid-mediated transcriptional induction system in transgenic plants. *Plant J. Mar* **11**(3):605-612.
12. **Asano S, Park JE, Sakchaisri K, Yu LR, Song S, Supavila P, Veenstra TD and Lee KS. 2005.** Concerted mechanism of Swe1/Wee1 regulation by multiple kinases in budding yeast. *The EMBO Journal* **24**: 2194 - 2204
13. **Atzori L, Dypbukt, JM, Sundqvist K, Cotgreave I, Edman CC, Moldéus P and Grafström RC. 1990.** Growth-associated modifications of low-molecular-weight thiols and protein sulfhydryls in human bronchial fibroblasts. *Journal of Cellular Physiology*, **143**, 1, (April 1990), pp. 165-171, ISSN 0021-9541.
14. **Baber-Furnari BA., Rhind N, Boddy MN, Shanahan P, LopezGirona A and Russell P. 2000.** Regulation of mitotic inhibitor Mik1 helps to enforce the DNA damage checkpoint. *Mol. Biol. Cell* **11**: 1-11
15. **Baldin V and Ducommun B. 1995.** Subcellular localization of human wee1 is regulated during the cell cycle. *J. Cell Science* **108**: 2425-2432.
16. **Barral Y, Mermall V., Mooseker MS and Snyder M. 2000.** Compartmentalization of the cell cortex by septins is required for maintenance of cell polarity in yeast. *Mol. Cell* **5**: 841-851.

17. Barroco RM, Peres A and Droual AM. 2006. The cyclin-dependent kinase inhibitor Orysa;KRP1 plays an important role in seed development of rice. *Plant Physiology* **142**:1053–1064.
18. Becker WM, Kleinsmith LJ and Hardin J. 2003. *The World of the Cell*, Fifth Edition, Benjamin, San Francisco.
19. Beato M. 1989. Gene regulation by steroid hormones. *Cell* **56**: 335-344.
20. Berdy J. 1980. Recent advances and prospects of antibiotic research. *Proc. Biochem.*, **15**: 28-28.
21. Bihn, EA, Paul AL, Wang SW, Erdos G and Ferl RJ. 1997. Localization of 14-3-3 proteins in the nuclei of Arabidopsis and maize. *Plant J* **12**: 1439-1445.
22. Bisbis B, Delmas F, Joubès J, Sicard A, Hernould M, Inzé D, Mouras A and Chevalier C. 2006. Cyclin-dependent kinase (CDK) inhibitors regulate the CDK-cyclin complex activities in endoreduplicating cells of developing tomato fruit. *J Biol Chem* **281**: 7374–7383
23. Bleeker PM, Hakvoort HW, Blik M, Souer E and Schat H. 2006. Enhanced arsenate reduction by a CDC25-like tyrosine phosphatase explains increased phytochelatin accumulation in arsenate-tolerant *Holcus lanatus*. *Plant J* **45**:917-929.
24. Blilou I, Frugier F, Folmer S, Serralbo O, Willemsen V, Wolkenfelt H, Eloy NB, Ferreira PC, Weisbeek P and Scheres B. 2002. The Arabidopsis HOBBIT gene encodes a CDC27 homolog that links the plant cell cycle to progression of cell differentiation. *Genes and Development* **16**: 2566-2575.
25. Bordo, D and Bork P. 2002. The rhodanses /Cdc25 phosphatase superfamily. Sequence-structure-function relations. *EMBO Rep* **3**: 741-746.
26. Boudolf V, Inze D and De Veylder L. 2006. What if higher plants lack a CDC25 phosphatase? *Trends Plant Sci* **11**: 474-9.

- 27. Boudolf V, Vlieghe K, Beemster GT, Magyar Z, Torres-Acosta JA, Maes S, Van Der-Schueren E, Inze D and De-Veylder L. 2004.** The plant-specific cyclin-dependent kinase CDKB1;1 and transcription factor E2Fa-DPa control the balance of mitotically dividing and endoreduplicating cells in Arabidopsis. *Plant Cell* **16**: 2683-92.
- 28. Boutros R., Dozier C and Ducommun B. 2006.** The when and wheres of CDC25 phosphatases. *Curr Opin Cell Biol* **18**, 185-91.
- 29. Brivba K, Fraser G and Sies H. 1993.** Distribution of the monochlorobimane-glutathione conjugate between nucleus and cytosol in isolated hepatocytes. *Biochem J.*, **294**: 631 -633.
- 30. Burssens S, Montagu VM and Inzé D. 1998.** The cell cycle in Arabidopsis. *Plant Physiol. Biochem.* **36**: 9–19.
- 31. Calmels T, Parriche M, Durand G. 1991.** High efficiency transformation of *Tolypocladium geodes* conidiospores to phleomycine resistance. *Curr. Genet.* **20**: 309–31
- 32. Carroll M, Ohno-Jones S, Tamura S, Buchdunger E, Zimmermann J, Lydon NB, Gilliland DG and Druker BJ .1997.** A tyrosine kinase inhibitor, inhibits the growth of cells expressing BCR–ABL, TEL–ABL and TEL–PDGFR fusion proteins. *Blood*, **90**: 4947–4952.
- 33. Casimiro I, Marchant A, Bhalerao RP, Beeckman T, Dhooge S, Swarup R, Graham N, Inzé D, Sandberg G and Casero Pand Bennett M. 2001.** Auxin Transport Promotes Arabidopsis Lateral Root Initiation. *Plant Cell* **13**: 843-852
- 34. Chaubet-Gigot N. 2000.** Plant A-type cyclins. *Plant Mol Biol.***43**: 659-75.

- 35. Cheng M, Olivier P, Diehl AJ, Fero M, Roussel MF, Roberts JM and Sherr CJ. 1999.** The p21(Cip1) and p27(Kip1) CDK 'inhibitors' are essential activators of cyclin D-dependent kinases in murine fibroblasts. *EMBO J* **18**: 1571-1583.
- 36. Cleary AL, Fowke LC, Wang H and John PCL . 2002.** The effect of ICK1, a plant cyclin-dependent kinase inhibitor, on mitosis in living plant cells. *Plant Cell* **20**: 814–82
- 37. Coelho CM, Dante RA, Sabelli PA, Sun Y, Dilkes BP, Gordon-Kamm WJ and Larkins BA. 2005.** Cyclin-dependent kinase inhibitors in maize endosperm and their potential role in endoreduplication. *Plant Physiol.***23**:23-36.
- 38. Coleman TR, Tang Z and Dunphy WG .1993.** Negative regulation of the wee1 protein kinase by direct action of the nim1/cdr1 mitotic inducer. *Cell*, **72**, 919–929.
- 39. Cools T, Iantcheva A, Weimer AK, Boens Sh, Takahashi N, Maes S, Van den Daele H, Isterdael G, Schnittgerc A and De Veyldera L. 2011.** The *Arabidopsis thaliana* Checkpoint Kinase WEE1 Protects against Premature Vascular Differentiation during Replication Stress. *Plant Cell* **63**: 1081-1094.
- 40. Culligan K and Tissier A. 2004.** ATR regulates a G2-phase cell cycle checkpoint in *Arabidopsis thaliana*. *Plant Cell* **16**: 1091-1104.
- 41. Cutler AJ, Rose PA, Squires TM, Loewen MK, Shaw AC, Quail JW, Krochko JE and Abrams SR .2000.** Inhibitors of abscisic acid 8'-hydroxylase. *Biochemistry* **39**: 13614-13624
- 42. D'Arpa P, and Liu LF. 1989.** Topoisomerase-targeting antitumor drugs. *Biochim. Biophys. Acta* **989**: 163–177
- 43. Davies B, Egea-Cortines M, De Andrade Silva E, Saedler H and Sommer H. 1996.** Multiple interactions among floral homeotic MAD box proteins. *EMBO J* **15**: 4330-4343.

- 44. De Lille JM, Sehne PC and Ferl RJ. 2001.** The Arabidopsis 14-3-3 family of signalling regulators. *Plant Physiol.***126**: 35-38.
- 45. De Schutter H, Spaepen M, Mc-Bride WH and Nuyts S . 2007.** The clinical relevance of microsatellite alterations in head and neck squamous cell carcinoma: a critical review. *Eur J Hum Genet.* **15(7)**:734–741.
- 46. De Veylder L, Beeckman T, Beemster GT, Krols L and Terras F. 2001.** Functional analysis of cyclin-dependent kinase inhibitors of *Arabidopsis*. *Plant Cell* **13**: 1653-68.
- 47. Dewitte W, Riou-Khamlichi C, Scofield S, Healy JMS and Jacquard A. 2003.** Altered cell cycle distribution, hyperplasia and inhibited differentiation in *Arabidopsis* caused by the D-type cyclin CYCD3. *Plant Cell.***15**: 79-92.
- 48. Dissmeyer N, Nowack MK, Pusch S, Stals H, Inze D, Grini PE and Schnittger A. 2007.** T-loop phosphorylation of *Arabidopsis* CDKA;1 is required for its function and can be partially substituted by an aspartate residue. *Plant Cell* **19**: 972–985.
- 49. Dixon DP, Skipsey M, Grundy NM and Edwards R. 2005.** Stress-Induced Protein S-Glutathionylation in *Arabidopsis*. *Plant Physiology* **138**:2233-2244
- 50. Dixon DP and Edwards R. 2009.** Selective Binding of Glutathione Conjugates of Fatty Acid Derivatives by Plant Glutathione Transferases. *J Biol Chem* **284**: 21249- 21256.
- 51. Dougherty MK and Morrison DK.2004.** Unlocking the code of 14-3-3. *J Cell Science* **117**: 1875-1884.
- 52. Drocourt D, Calmels T, Reynes JP, Baron M and Tiraby G. 1990.** Cassettes of the *Streptoalloteichus hindustanus* ble gene for transformation of lower and higher eukaryotes to phleomycin resistance. *Nucleic Acids Res.* **18**: 4009

- 53. Droog F, Hooykaas P and Van der Zaal B .1995.** 2,4-dichlorophenoxyacetic acid and related chlorinated compounds inhibit two auxin-regulated type-III tobacco glutathione S-transferases. *Plant Physiol* **107**: 1139–1146.
- 54. Dubrovsky JG, Doerner PW, Colón-Carmona A and Rost TL. 2000.** Pericycle Cell Proliferation and Lateral Root Initiation in Arabidopsis. *Plant Physiol.***124**: 1648-1657.
- 55. Dunphy WG. 1994.** The decision to enter mitosis. *Trend Cell Biology* **4**: pp 202-207.
- 56. Eckardt NA. 2001.**A brief tour of the cell cycle. *Plant Cell* **13**:449-451.
- 57. Edgington NP, Blacketer MJ, Bierwagen TA and Myers AM. 1999.** Control of *Saccharomyces cerevisiae* filamentous growth by cyclindependent kinase Cdc28. *Mol. Cell Biol.* **19**: 1369-1380.
- 58. Edwards K, Johnstone C and Thompson C. 1991.** A simple and rapid method for the preparation of plant genomic DNA for PCR analysis. *Nucleic Acids Research* **19**: 1349.
- 59. Ellege SJ. 1996.** Cell cycle chekpoint: preventing an identity crisis. *J Cell Science* **247**:1664-1672.
- 60. Eklund H, Uhlin U, Farnegardh M, Logan DT and Nordlund P. 2001.** Structure and function of the radical enzyme ribonucleotide reductase. *Prog Biophys Mol Biol* **77**: 177-268.
- 61. Ezhevsky S.A, Nagahara H, Vocero-Akbani AM, Guis DR., Wei MC and Dowdy SF. 1997.** Hypo- phosphorylation of the retinoblstoma protein(pRb) by cyclin D: cdk4/6 coplexes results in active pRb.*Proc Natl Acad Sci U S A* **94**: 10699-10704.

- 62. Fauman EB, Cogswell JP, Lovejoy B, Rocque WJ, Holmes W, Montana VG, Piwnica-Worms H, Rink MJ and Saper, MA. 1998.** Crystal structure of the catalytic domain of the human cell cycle control phosphatase, Cdc25A. *Plant Cell* **93**: 617-625.
- 63. Ferjani A, Horiguchi G, Yano S and Tsukaya H. 2007.** Analysis of leaf development in *fugu* mutants of *Arabidopsis thaliana* reveals three compensation modes that modulate cell expansion in determinate organs. *Plant Physiology* **144**: 988-999.
- 64. Ferl R.J, Manak, MS and Reyes M F. 2002.** The 14-3-3s. *Genome Biology* **27**: 3(7).
- 65. Fiorani F, Bogemann GM, Visser EJW, Lambers H and Voeselek LACJ. 2002.** Ethylene emission and responsiveness to applied ethylene vary among *Poa* species that inherently differ in leaf elongation rates. *Plant Physiology* **129**: 1382–1390
- 66. Fletcher G, Flin R, McGeorge P, Glavin R, Maran N and Patey R. 2003.** Anaesthetists' non-technical skills (ANTS): evaluation of a behavioural marker system. *Br J Anaesth* **90**:580–588
- 67. Fobert PR, Gaudin V, Lunness P, Coen ES, and Doonan JH. 1996.** Distinct classes of cdc2-related genes are differentially expressed during the cell division cycle in plants. *Plant Cell* **8**: 1465-1476.
- 68. Forbes KC, Humphrey T and Enoch T. 1998.** Suppressors of cdc25p overexpression identify two pathways that influence the G2/M checkpoint in fission yeast. *Genetics* **150**: 1361-75.
- 69. Foyer CH, Bloom AJ, Queval G, and Noctor G. 2009.** Photorespiratory metabolism: genes, mutants, energetics, and redox signaling. *Annu. Rev. Plant Biol.* **60**: 455–484.

- 70. Francis D. 2006.** The Plant Cell Cycle. *New Phytot.* **174:** 261-278.
- 71. Francis D. 2003.** *The Plant Cell Cycle and its interferences.* Sheffield Academic Press, pp42-56.
- 72. Fuerst R, Soni R, Murray J and Lindesy K. 1996.** Modulation of cyclin transcript levels in cultured cells of *Arabidopsis thaliana*. *Plant Physiol* **12:** 1023-33.
- 73. Fulcher N and Sablowski R.** Hypersensitivity to DNA damage in plant stem cell niches. 2009. *Proc. Natl Acad. Sci. USA* **106,** 20984–20988.
- 74. Garcia V, Bruchet H, Camescasse D, Granier F, Bouchez D and Tissier A. 2003.** At ATM is essential for meiosis and the somatic response to DNA damage in plants. *Plant Cell* **15,** 119-32.
- 75. Ga A. 1987.** Expression des Genes Plasmidiques de Resistance a la Phleomycine Che; les Eucaryotes. Thesis. University Paul Sabatier. Toulouse, France.
- 76. Gatz C, Frohberg C and Wedenberg R. 1992.** Stringent repression and homogenous depression by tetracycline of a modified CaMV 35S promoter in intact transgenic tobacco plants. *Plant J* **2:**397-404.
- 77. Genschik P, Criqui MC, Parmentier Y, Derevier A, Fleck J. 1998.** Cell cycle dependent proteolysis in plants. Identification of the destruction box pathway and metaphase arrest produced by the proteasome inhibitor mg132. *Plant Cell* **10:**2063-2076.
- 78. Glotzer M, Murray AW and Kirschner MW. 1991.** *Nature* **349:** 132-138.
- 80. Gong HB, Jiao YX, Hu WW, and Pua EC. 2005.** Expression of glutathione S-transferase and its role in plant growth and development in vivo and shoot morphogenesis in vitro. *Plant Mol. Biol* **57:** 53-66.

- 80. Grafi G and Larkins BA .1995.** Endoreduplication in maize endosperm: involvement of M phase-promoting factor inhibition and induction of S phase-related kinases. *Science* **269**: 1262–1264
- 81. Griffiths AJF, Gelbart WM, Lewontin RC, David JH and Suzuki T. 1999.** *An Introduction to Genetic Analysis*. San Francisco: W.H. Freeman. pp250-300.
- 82. Hall JK and Cumming A. 2004.** Role of microzooplankton grazers in the subtropical and subantarctic waters to the east of New Zealand, N. Z. *J. Mar. Freshwater Res.*, **38**: 91 – 101.
- 83. Hamant O, Ma H and Cande WZ. 2006.** Genetics of meiotic prophase in plants. *Annu Rev Plant Biol.* **57**:267-302
- 84. Harper JW .2002.** A phosphorylation-driven ubiquitination switch for cell-cycle control. *Cell Biol* **12**: 104–107.
- 85. Harries A. 1973.** Cell surface movements related to cell locomotion. In *Locomotion of Tissue Cells*. pp3-26. Elsevier, North-Holland.
- 86. Harper JW and Elledge SJ. 1998.** The role of CDk7 in CAK function, a retrospective. *Genes Development*.**12**: 285-289.
- 87. Harvey SL and Kellogg DR. 2003.** Conservation of mechanisms controlling entry into mitosis: budding yeast wee1 delays entry into mitosis and is required for cell size control. *Curr Biol* **13**: 264-275.
- 88. He SS, Liu J, Xie Z, Neill D, and Dotson S. 2004.** *Arabidopsis* E2Fa plays a bimodal role in regulating cell division and cell growth. *Plant Mol Biol* **56**:171-184.
- 89. Himanen K, Boucheron E, Vanneste S, De Almeida Engler J, Inze D and Beeckman T. 2002.** Auxin-mediated cell cycle activation during early lateral root initiation. *Plant Cell* **14**, 2339-51.

- 90. Hirt H.2000.** Connecting oxidative stress, auxin, and cell cycle regulation through a plant mitogen-activated protein kinase pathway. *Proc Natl Acad Sci USA* **97**:2405–2407.
- 91. Huntley RP, and Murray JAHM. 1999.** The plant cell cycle. *Curr. Opin. Plant Biology* **2**:440-446.
- 92. Inzé D .2005.** Green light for the cell cycle. *EMBO J* **24**: 657–662
- 93. Ishikawa M, Soyano T, Nishihama R, and Machida Y. 2002.** The NPK1 mitogen-activated protein kinase kinase kinase contains a functional nuclear localization signal at the binding site for the NACK1 kinesin-like protein. *Plant J* **32**:789–798.
- 94. Ito M. 2000.** Factors controlling cyclin B expression. *Plant Mol Biol* **43**: 677-690
- 95. Jasinski S, Riou-Khamlichi C, Roche O, Perennes C and Bergounioux C, Glab N .2002.** The CDK inhibitor NtKIS1a is involved in plant development, endoreduplication and restores normal development of cyclin D3;1-overexpressing plants. *J Cell Sci* **115**: 973–982
- 96. Jeffrey PD, Russo AA, Polyak K, Gibbs E, Hurwitz J, Massague J and Pavletich NP.1995.** Mechanism of CDK activation revealed by the structure of a cyclinA-CDK2 complex. *Nature* **376**: 313-320.
- 97. Jenuwin T, Allis CD .2001.** Translating the histone code. *Science* **293**:1074–1080.
- 98. John PCL, and Zhang K. 2001.** Cytokinin control of cell proliferation in plants development. *The Plant Cell Cycle and its Interfaces*. CRC Press, Boca Raton, FL,pp 190-211.
- 99. Jiang HU, Liu MJ, Chen IC, Huang CH, Chao LY, and Hsieh HL. 2010.** A Glutathione S-Transferase Regulated by Light and Hormones Participates in the Modulation of Arabidopsis Seedling Development. *Plant Physiol.* **9**: 93–101.

- 100. Jørgensen, PR, Hoffmann M, Kistrup JP, Bryde C, Bossi R and Villholth K. 2002.** Field, laboratory and modeling analysis of preferential flow and pesticide transport in a clay-rich till. *Water Resources Research* **11**:28
- 101. Joubes J, Chevalier C, Dudits D, Herberle-Bors E, Inz D, Umeda M and Renaudin JP. 2000.** CDK-related protein kinases in plants. *Plant Mol Biol.* **43**: 607-620.
- 102. Kellogg DR and Murray AW. 1995.** NAP1 acts with Clb1 to perform mitotic functions and to suppress polar bud growth in budding yeast. *J Cell Biol* **130**: 675–685.
- 103. Kharbanda S, Saleem A, Datta R, Yuan ZM, Weichselbaum R and Kufe D. 1994.** Ionizing radiation induces rapid tyrosine phosphorylation of p34cdc2. *Cancer Res.* **54**: 1412-1414.
- 104. Kilili KG, Atanassova N, Vardanyan A, Clatot N, Al-Sabarna K, Kanellopoulos PN, Makris AM and Kampranis SC. 2004.** Differential roles of tau class glutathione S-transferases in oxidative stress. *J Biol Chem* **279**: 24540–51.
- 105. Kitamura S, Shikazono N, Tanaka A. 2004.** TRANSPARENT TESTA 19 is involved in the accumulation of both anthocyanins and proanthocyanidins in *Arabidopsis*. *Plant J* **37**: 104–114.
- 106. Klein M, Reichelt M, Gershenzon J and Papenbrock J. 2006.** The three desulfoglucosinolate sulfotransferase proteins in *Arabidopsis* have different substrate specificities and are differentially expressed. *FEBS J.* **273**: 122–136.
- 107. Kohli J and Hartusiker E. 1994.** Dynamic of chromosome organization and pairing during meiotic prophase in fission yeast. *J Cell Biol,* **127**: 273-285.

- 108. Kuijit S. 2006.** Analysis of the subcellular localization, function and proteolytic control of the Arabidopsis CDK inhibitor ICK1/KRP1. *Plant Physiol.* **141**: 1293-1305.
- 109. Kumagai A, Dunphy WG. 1991.** The cdc25 protein controls tyrosine dephosphorylation of the cdc2 protein in a cell-free system. *Cell* **64**: 903-914.
- 110. Kumagai A, Dunphy WG. 1999.** Binding of 14-3-3 proteins and nuclear export control the intracellular localization of the mitotic inducer Cdc25. *Genes Dev* **13**:1067-72.
- 111. LaBaer J, Garrett MD, Stevenson LF, Slingerland JM, Sandhu C, Chou HS, Fattaey A and Harlow E. 1997.** New functional activities for the p21 family of CDK inhibitors. *Genes Dev.* **11**:847-862.
- 112. Lan T, Yang Z, Yang X, Liu Y, Wang X and Zeng Q. 2009.** Extensive Functional Diversification of the Populus Glutathione S-Transferase Supergene Family. *The Plant Cell* **21**:3749-3766
- 113. Landrieu I, da Costa M, De Veylder L, Dewitte F, Vandepoele K, Hassan S, Wieruszeski J-M, Corellou F, Faure J-D, Van Montagu M, Inzé D and Lippens G .2004.** A small CDC25 dual-specificity tyrosine-phosphatase isoform in Arabidopsis thaliana. *Proc Natl Acad Sci USA* **101**: 13380–13385.
- 114. Landrieu I, Da Costa M, De Veylder L, Dewitte, F, Vandepoele K, Hassan S, Wieruszeski J-M, Faure J-D, Van montgue M, Inze D and Lippens G. 2004.** A small CDC25 dual specificity tyrosine-phosphate isoform in *Arabidopsis thaliana*. *Proc Nat Acadf Sci USA* **101**: 13380-13385.
- 115. Lee J, Kumagai A and Dunphy WG. 2001.** Positive regulation of Wee1 by Chk1 and 14-3-3 proteins. *Mol Biol Cell* **12**: 551-563.

- 116. Lees EM and Harlow E. 1993.** Sequences within the conserved cyclin box of human cyclin A are sufficient for binding to and activation of cdc2kinase. *Mol Biol Cell* **13**: 1194-1201.
- 117. Lentz A. 2007.** Regulatory mechanism of the plant G2/M transition. *A thesis submitted for the degree of Doctorate of Philosophy of Cardiff University.* 176 pages.
- 118. Lentz Grønlund A , Dickinson JR, Kille P, Harwood JL , Herbert RJ, Francis D and Rogers H, Ulker B and Somssich IE. 2009.** Plant WEE1 Kinase Interacts with a 14-3-3 Protein, GF14 but a mutation of WEE1 at S485 Alters Their Spatial Interaction. *Plant Sci J*, 3: 40-48.
- 119. Lew DJ, Dulic V and Reed SI. 1991.** Isolation of three novel human cyclins by rescue of G1 cyclin(Cln) function in yeast. *Cell* **66**:1197-1206.
- 120. Lewin B. 1997.** *GENES VI.* Oxford: Oxford University Press. pp 471-503.
- 121. Logemann E, Birkenbihl R.P, Ulker B and Somssich IE. 2006.** An improved method for preparing Agrobacterium cells that simplifies the Arabidopsis transformation protocol. *Plant Methods* **2**:16.
- 122. Longtine MS, McKenzie AR, Demarini DJ, Shah NG, Wach A, Brachat A, Philippsen P and Pringle JR . 1998.** Additional modules for versatile and economical PCR-based gene deletion and modification in *Saccharomyces cerevisiae*. *Yeast* **14**: 953–961.
- 123. Lopez-Girona A, Furnari B, Mondesert O and Russell P. 1999.** Nuclear localization of Cdc25 is regulated by DNA damage and a 14-3-3 protein. *Nature* **397**: 172–175.
- 124. Liu J, Ishitani M, Halfter U, Kim CS and Zhu JK. 2000.** The Arabidopsis thaliana SOS2 gene encodes a protein kinase that is required for salt tolerance. *Proc Natl*

Acad Sci U S A. **97**:3730-3734.

- 125. Lu G, Sehnke PC and Ferl RJ. 1994.** Phosphorylation and calcium binding properties of an *Arabidopsis* GF14 brain protein homolog. *Plant Cell.* **6**: 501-10.
- 126. Lundgren K, Walworth N, Boshier R, Dembski M, Kirschner M and Beach D. 1991.** Mik1 and wee1 co-operate in the inhibitory tyrosine phosphorylation of cdc2. *Cell* **64**: 1111-1122.
- 127. Luxová, M. 1981.** Growth region of the primary root of maize (*Zea mays* L.) In Structure and Function of Plant Roots. Martinus Nijhof/Dr W Junk: The Hague/Boston/London. Pp 9-72
- 128. Ma XJ, Lu Q and Grunstein M . 1996.** A search for proteins that interact genetically with histone H3 and H4 amino termini uncovers novel regulators of the Swe1 kinase in *Saccharomyces cerevisiae*. *Genes Dev* **10**: 1327–1340.
- 129. Mariconti L, Pellegrini B, Cantoni R, Stevens R, Bergounioux C, Cella R and Albani D .2002.** The E2F family of transcription factors from *Arabidopsis thaliana*. Novel and conserved components of the retinoblastoma/E2F pathway in plants. *J Biol Chem* **277**: 9911–9919
- 130. Magyar Z, Meszaros T, Mikolezi P, Deak M and Feher A. 1997.** Cell cycle phase specificity of putative cyclin-dependent kinase variants in synchronized alfalfa cells. *Plant Cell* **9**: 223-35.
- 131. Manak MS and Ferl RJ. 2007.** Divalent cation effects on interactions between multiple *Arabidopsis* 14-3-3 isoforms and phosphopeptide targets. *Biochemistry* **46**: 1055-63.
- 132. Martinho RG, Lindsay HD, Fleggs G, De Maggio AJ, Hoekstra MF, Carr**

- AM and Bentley NS. 1998.** Analysis of Rad3 and Chk1 protein kinases defines different checkpoint response. *EMBO J* 17,pp7239-7249.
- 133. McGowan CH and Russell P. 1995.** Cell cycle regulation of human Wee1. *EMBO J.* 14: 2166–2175
- 134. Meister A. 1995.** Glutathione metabolism. *Methods Enzymol.* 251:3-7.
- 135. Menges M, De Jager SM, Gruissem W and Murray JA. 2005.** Global analysis of the core cell cycle regulators of Arabidopsis identifies novel genes, reveals multiple and highly specific profiles of expression and provides a coherent model for plant cell cycle control. *Plant J* 41: 546-566.
- 136. Menon SG, Sarsour EH, Kalen AL, Venkataraman S, Hitchler M and Domann FE. 2007.** Superoxide signaling mediates N-acetyl-L-cysteine-induced G1 arrest: regulatory role of cyclin D1 and manganese superoxide dismutase. *Cancer Res* 67:6392–639
- 137. Michael, W.M., and J. Newport. 1998.** Coupling of mitosis to the completion of S-phase through Cdc34-mediated degradation of Wee1. *Science.* 282:1886–1889
- 138. Mironov V, De Veylder L, Van Montaeue M and Inze D. 1999.** Cyclin-dependent kinases and cell division in plants-the Nexus. *Plant Cell* 11:509-521.
- 139. Moons A. 2005.** Regulatory and functional interactions of plant growth regulators and plant glutathione S-transferases (GSTs). *Plant Hormones* 72:155-202.
- 140. Moore BW and Perez VJ. 1967.** Physiological and Biochemical Aspects of Nervous Integration. Prentice-Hall, Inc, The Marine Biological Laboratory, Woods Hole, 343–359.
- 141. Morris DK and Lundblad V . 1997.** Programmed translational frameshifting in a gene required for yeast telomere replication. *Eur Biol* 7: 969–976

- 142. Mulsant PA, Gatignol M, Tiraby D and G. 1988** .Phleomycin resistance as a dominant selectable marker in CHO cells. *Somatic Genet* **14**: 243-252.
- 143. Kerk N Mand Feldman LJ .1995.** A biochemical model for the initiation and maintenance of the quiescent center: implications for organization of root meristems. *Development* **121**:2825–2833.
- 144. McGowan CH and Russell P. 1995.** Cell cycle regulation of human WEE1. *EMBO J* **14**: 2166–2175.
- 145. Melaragno JE, Mehrotra B and Coleman AW. 1993.** Relationship between Endopolyploidy and Cell Size in Epidermal Tissue of Arabidopsis. *The Plant Cell*, Vol 5, **11**: 1661-1668
- 146. Morgan DO. 1997.** Cyclin-dependent kinases: engines, clock, and microprocessors. *Annual Review Cell Dev Biol* **13**:261-291.
- 147. Muller PR, Coleman TR, Kumagai A and Dunphy WG. 1995.** Mytl: a membrane-associated inhibitory kinase that phosphorelates Cdc2 on both threonine-14 and tyrosine-15 of special interest. *J Cell Sci* **270**:86-90
- 148. Nakayama KI and Nakayama K . 2005.** Regulation of the cell cycle by SCF-type ubiquitin ligases. *Semin Cell Dev Biol* **16**: 323–333
- 149. Nasmyth K. 1993.** Control of the yeast cell cycle by the Cdc28 protein kinase. *Curr Opin Cell Biol* **5**:166-179.
- 150. Nigg EA. 2001.** Mitotic kinases as regulators of cell division and its checkpoints, *Nature Rev Mol Cell Biol* **2** : 21–32
- 151. Nishihama R, Soyano T, Ishikawa M, Araki S, Tanaka H, Asada T, Irie K, Ito M, Terada M and Banno H. 2002.** Expansion of the cell plate in plant cytokinesis requires akinesin-like protein/MAPKKK complex. *Cell* **109**: 87–99.

- 152. Norbury C and Nurse P. 1992.** Animal cell cycles and their control.
Biochem **61**: 441–470
- 153. Nurse P, Thuriaux Pand Nasmyth K. 1976.** Genetic control of the cell division cycle in the fission yeast *Schizosaccharomyces pombe*. *Mol Gen* **146**: 167-178.
- 154. O' Connell MJ, Raleigh JM, Verkade HM and Nurse P. 1997.** Chk1 is a wee1 kinase in the G2 DNA damage checkpoint inhibiting cdc2 by Y15 phosphorylation.
EMBO J **16**: 545-554.
- 155. Ormenese S, De Almeida Engler J, De Groodt R, De Veylder L, Inzé D and Jacqumard A . 2004.** Analysis of the spatial expression pattern of seven Kip related proteins (KRPs) in the shoot apex of *Arabidopsis thaliana*. *Ann Bot* **93**: 575–580
- 156. Park JA, Ahn JW, Kim YK, Kim SJ, Kim JK, Kim WT and Pai HS. 2005.** retinoblastoma protein regulates cell proliferation, differentiation, and endoreduplication in plants. *Plant J.* **42**: 153-163.
- 157. Parker LL, Walter SA, Young PG and Piwnica-Worms H .1993.** Phosphorylation and inactivation of the mitotic inhibitor wee1 by the nim1/cdr1 kinase. *Nature* **363**: 736–738.
- 158. Passmore LA, McCormack EA, Au SW, Paul A, Willison, KR, Harper JW and Barford D. 2003.** Doc1 mediates the activity of the anaphase-promoting complex by contributing to substrate recognition. *EMBO J* **22**: 786–796
- 159. Peng CY, Graves PR, Thoma RS, Wu A, Shaw AS and Piwnica Worms H. 1997.** Mitotic and G2 checkpoint control: regulation of 14-3-3 protein binding by phosphorylation of Cdc25C on serine-216. *Science* **277**: 1501-1505

- 160. Perez L, Czekala NM, Weisenseel A and Lasley BL. 1988.** Excretion of radiolabeled estradiol metabolites in the slow loris (*Nycticebus coucang*) *American J Primatology* **16**: 321-330
- 161. Pettko A, Meszaros T, Horvath GV, Bako L, Csordas Toth E, Blastyak A, Zhiponova M, Miskolczi Pand Dudits D. 2006.** Activation of an alfalfa cyclin-dependent kinase inhibitor by calmodulin-like domain protein kinase. *Plant J* **46**: 111-123.
- 162. Picard D. 1993.** Steroid-binding domains for regulating the functions of heterologous proteins in *cis*. *Trends Cell Biol* **3**: 278-280.
- 163. Porceddu A, Stals H, Reichheld JP, Segers G, De Veylder L, De Pinho Barroco R, Casteels P, Van Montagu M, Inze D and Mironov V. 2001.** A plant-specific cyclin dependent kinase is involved in the control of G2/M progression in plants. *Biol Chem* **276**: 36354-36360
- 164. Pringle JR, Adams AE, Drubin DG and Haarer BK. 1991.** Immunofluorescence methods for yeast. *Meth. Enzymol* **194**: 562-602.
- 165. Rea PA. 2007.** Plant ATP-binding cassette transporters. *Annu. Rev. Plant Biol* **58**: 347-375.
- 166. Reichheld JP, Chaubet N, Shen WH, Renaudin JP and Gigot C. 1996.** Multiple A-Type cyclins express sequentially during the cell cycle in *Nicotiana tabacum* BY2 cells. *Proc Natl Acad Sci. USA* **93**:13819-24
- 167. Renaudin JP, Doonan JH, Freeman D, Hashimoto J and Hirt H. 1996.** Plant cyclins: a unified nomenclature for plant A-, B- and D-type cyclins based on sequence organization. *Plant Mol Biol* **32**: 1003-1018.
- 168. Rhind N, Furnari B and Russell P. 1997.** Cdc2 tyrosine phosphorylation is

- required for the DNA damage checkpoint in fission yeast. *Genes Dev* **11**:504-511
- 169. Rienties IM, Vink J, Borst JW, Russinova E and De Vries SC. 2005.** The *Arabidopsis* SERK1 protein interacts with the AAA-ATPase AtCDC48, the 14-3-3 protein GF14lambda and the PP2C phosphatase KAPP. *Planta* **221**, 394-405.
- 170. Riou- Khamlichi C, Menges M, Healy J and Murray J.2000.** Sugar control of the plant cell cycle: differential regulation of *Arabidopsis* D-type cyclin gene expression. *Mol Cell Biol* **20**: 4513-4521.
- 171. Rosso MG, Li Y, Strizhov N, Reiss B, Dekker K and Weisshaar B. 2003.** An *Arabidopsis thaliana* T-DNA mutagenized population (GABI-Kat) for flanking sequence tag-based reverses genetics. *Plant Mol Biol* **53**: 247-59.
- 172. Rothblum-Oviatt CJ, Ryan CE and Piwnica-Worms H. 2001.** 14-3-3 binding regulates catalytic activity of human Wee1 kinase. *Cell Growth Differ* **12**: 581-589.
- 173. Russell P, Nurse P. 1987.** Negative regulation of mitosis by *wee1+*, a gene encoding a proteinkinase homolog. *Cell* **49**: 559-67.
- 174. Sanchez Y, Wong C, Thoma RS, Richman R., Wu Z, Piwnica-Worms, H and Elledge SJ. 1997.** Conservation of the *chk1* checkpoint pathway in mammals: linkage of DNA damage to CDK regulation through *cdc25*. *Science* **277**: 1497-1501.
- 175. Sappl PG, Carroll AJ, Clifton R, Lister R, Whelan J, Millar A and Singh K .2009.**The *Arabidopsis* glutathione transferase gene family displays complex stress regulation and co-silencing multiple genes results in altered metabolic sensitivity to oxidative stress.*The Plant Journal* **58**:53-68
- 176. Schott EJ and Hoyt MA. 1998.** Dominant alleles of *Saccharomyces cerevisiae* CDC20 reveal its role in promoting anaphase. *Genetics* **148**:599–610.

- 177. Setiady YY, Sekine M, Hariguchi N, Yamamoto T, Kouchi H, Shinmyo A. 1995.** Tobacco mitotic cyclins: cloning, characterization, gene expression and functional assay. *Plant J* **8**:949-57.
- 178. Sherr CJ and Roberts JM. 1994.** CDK inhibitors: positive and negative regulators of G1-phase progression: cycling on cue. *Cell* **79**:551-5.
- 179. Shiloh Y. ATM and ATR: networking cellular responses to DNA damage. Curr. Opin. Genet. Dev** **11**: 71-77 (2001).
- 180. Shulewitz MJ, Inouye CJ, Thorner J. 1999.** Hsl7 localizes to a septin ring and serves as an adapter in a regulatory pathway that relieves tyrosine phosphorylation of Cdc28 protein kinase in *Saccharomyces cerevisiae*. *Mol Cell Biol* **19**: 7123-7137.
- 181. Siciliano I. 2006.** Effect of plant Wee1 on the cell cycle and development in *Arabidopsis thaliana* and *Nicotiana tabacum*. A thesis submitted for the degree of Doctorate of Philosophy of Cardiff University. 229pp.
- 182. Soni R, Carmichael JP, Shah ZH and Murray JA. 1995.** A family of cyclin D homologs from plants differentially controlled by growth regulators and containing the conserved retinoblastoma protein interaction motif. *Plant Cell* **7**: 85-103.
- 183. Sorrell SA, Comettes B, Chaubet-Gigot N, Gigot C and Murray JA. 1999.** Distinct cyclin D genes show mitotic accumulation or constant levels of transcripts in tobacco bright yellow-2 cells. *Plant Physiol* **119**: 343-352.
- 184. Sorrell DA, Marchbank A, McMahon K, Dickinson JR, Rogers HJ and Francis D. 2002.** A WEE1 homologue from *Arabidopsis thaliana*. *Planta* **215**: 518-522.
- 185. Spadafora N, Doonan JH, Herbert RJ, Bitonti BM, Emily Wallace, Rogers**

- HJ and Francis D . 2011.** Arabidopsis T-DNA insertional lines for CDC25 are hypersensitive to hydroxyurea but not to zeocin or salt stress. *Ann Bot* **107**: 1183-1192
- 186. Strompen G, Kasmi F, Richter S, Lukowitz W, Assaad FF, Jurgens G and Mayer U. 2002.** The Arabidopsis HINKEL gene encodes a kinesin-related protein involved in cytokinesis and is expressed in a cell cycle –dependent manner. *Cur Biol* **12**:153-158.
- 187. Sun Y, Dilkes BP and Zhang C. 1999.** Characterisation of maize (*Zea mays* L.) WEE1 and its activity in developing endosperm. *Proc Natl Acad Sci USA* **96**: 4180-4185
- 188. Takahashi H, Chen Z, Du H, Liu Y, and Klessig DF .1997.** Development of necrosis and activation of disease resistance in transgenic tobacco plants with severely reduced catalase levels. *Plant J* **11**: 993–1005
- 189. Tang, Z, Coleman TR, and Dunphy WG. 1993.** Two distinct mechanisms for negative regulation of the Wee1 protein kinase. *EMBO J.***12**: 3427-3436.
- 190. Thornton BR, Toczyski DP. 2003.** Securin and B-cyclin/CDK are the only essential targets of the APC. *Nat. Cell Biol* **5**:1090–1094.
- 191. Tjandra N, Omichinski JG, Gronenborn AM, Clore GM and Bax A. 1997.** *Nat Struct Biol* **4**: 732–738.
- 192. Patrick Laufs, Olivier Grandjean, Claudia Jonak^{1,a}, Kiên Kiêuc, and Jan Traasa. 1998.** Cellular Parameters of the Shoot Apical Meristem in Arabidopsis *Plant Cell* **10**: 1375-1390.
- 193. Trastoy MO, Defais M and Larminat F. 2005.** Resistance to the antibiotic Zeocin

by stable expression of the Sh ble gene does not fully suppress Zeocin-induced DNA cleavage in human cells. *Mutagenesis* **20**: 111-114.

194. Umeda M, Shimotohno A and Yamaguchi M. 2000. Control of cell division and transcription by cyclin-dependent kinase-activating kinases in plants. *Plant Cell Physiol* **46**: 1437-42.

195. Umen JG and Goodenough UW. 2001. Control of cell division by a retinoblastoma protein homolog in *Chlamydomonas*. *Genes Dev* **15**: 1652–1661

196. Vandepoele K, Raes J, De Veylder L, Rouze P, Rombauts S and Inz D. 2002. Genome wide analysis of core cell cycle genes in *Arabidopsis*. *Plant Cell* **14**: 903-16.

197. Verkest A, Weint C, Inzé D, De Veylder L and Schnittger A. 2005
.Switching the cell cycle. Kip-related proteins in plant cell cycle control. *Plant Physiol* **139** (3):1099-106.

198. Verkest A, Manes CL, Vercruyssen S, Maes S, Van Der Schueren E, Beckman T, Genschik P, Kuiper M, Inze D and De Veylder L. 2005. The cyclin-dependent kinase inhibitor KRP2 controls the onset of the endoreduplication cycle during *Arabidopsis* leaf development through inhibition of mitotic CDKA;1 kinase complexes. *Plant Cell* **17**: 1723-1736.

199. Vivancos P, Wolff T, Markovic J, Pallardo FV and Foyer CH. 2010. A nuclear glutathione cycle within the cell cycle. *Biochem J* **431**: 169–178

200. Walter SA, Guadagno SN and Ferrell JE. 2000. Activation of Wee1 by p42 MAPK in vitro and in cycling xenopus egg extracts. *Mol Biol Cell* **11**: 887-96.

- 201. Walter M, Chaban C, Schütze K, Batistic O, Weckermann K, Näke C, Blazevic D, Grefen C, Schumacher K, Oecking C, Harter K and Kudla J . 2004.** Visualization of protein interactions in living plant cells using bimolecular fluorescence complementation. *Plant J* **40**: 428-438.
- 202. Wang G, Midkimins R and Miskimins WK. 1999.** The cyclin-dependent kinase inhibitor p27 is located to the cytosol in Swiss/3T3 cells. *Oncogene* **18**: 5204-5210.
- 203. Wang Y, Jacobs C, Hook KE, Duan H, Booher RN and Sun Y. 2000.** Binding of 14-3-3 beta to the carboxyl terminus of Wee1 increases Wee1 stability, Kinase activity, and G2-M cell population. *Cell Growth Diff* **11**: 211-219.
- 204. Wang W and Chen X. 2004.** HUA ENHANCER3 reveals a role for a cyclin-dependent protein kinase in the specification of floral organ identity in *Arabidopsis*. *Development* **131**: 3147-3156.
- 205. Walter M, Chaban C, Schütze K, Batistic O, Weckermann K, Näke C, Blazevic D, Grefen C, Schumacher K, Oecking C, Harter K and Kudla J . 2004.** Visualization of protein interactions in living plant cells using bimolecular fluorescence complementation. *Plant J* **40**: 428-438.
- 206. Watanabe N, Broome M and Hunter T. 1995.** Regulation of the human WEE1Hu CDK tyrosine 15-kinase during the cell cycle. *EMBO J* **14**: 1878–1891
- 207. Watanabe, N., Arai, H., Nishihara, Y., Taniguchi, M., Hunter, T. and Osada, H. 2004.** M-phase kinases induce phospho-dependent ubiquitination of somatic Wee1 by SCFbeta-TrCP. *Proc. Natl Acad Sci. USA* **101**, 4419-4424.

- 208. Watanabe, N., Arai, H., Iwasaki, J., Shiina, M., Ogata, K., Hunter, T. and Osada, H. 2005.** Cyclin-dependent kinase (CDK) phosphorylation destabilizes somatic Wee1 via multiple pathways. *Proc. Natl Acad Sci. USA* 102, 11663-11668
- 209. Wachter A, Wolf S, Steininger H, Bogs J and Rausch T. 2005.** Differential targeting of GSH1 and GSH2 is achieved by multiple transcription initiation: implications for the compartmentation of glutathione biosynthesis in the Brassicaceae. *Plant J.* **41**:15–30.
- 210. Weingartner M, Criqui MC, Meszaros T, Binarova P, Schmit AC, Helfer A, Derevier A, Erhardt M, Bogre L and Genschik P. 2004.** Expression of a nondegradable cyclin B1 affects plant development and leads to endomitosis by inhibiting the formation of a phragmoplast. *Plant Cell* **1**: 643-657.
- 211. Weinel C, Marquardt S, Kuijt SJH, Nowack MK, Jakoby MJ, Hülskamp M and Schnittger A. 2005.** Novel functions of plant cyclin-dependent kinase inhibitors, ICK1/KRP1, can act non-cell-autonomously and inhibit entry into mitosis. *Plant Cell* **17**: 1704–1722
- 212. Weinert T. 1998.** DNA damage and checkpoint pathways: molecular anatomy and interactions with repair. *Cell* **94**: 555–558.
- 213. Wu HY and Russell MW. 1993.** Induction of mucosal immunity by intranasal application of a surface protein with the cholera toxin B subunit. *Infect Immun* **61**: 314–322.
- 214. Yaffe MB, Rittinger K, Volinia S, Caron PR, Aitken A, Leffers H, Gamblin SJ, Smerdon SJ and Cantley LC. 1997.** The structural basis for 14-3-

3:phosphopeptide binding specificity. *Cell* **91** :961-71.

- 215. Yamaguchi K, Tokuchi H, Fukuzaki Y, Koyama K, Takakuda H, Monma J, Tanaka. 2000.** Preparation and microstructure analysis of chitosan/hydroxyapatite nanocomposites. *J Biomed Mat Res.* **55**:(1) 20–27.
- 216. YOUNG PG, FANIES P. 1987.** Schizosaccharomyces pombe mutants affected in their division response to starvation. *J Cell Sci* **88**: 295-304.
- 217. Zeng Y, Piwnica-Worms H. 1999.** DNA damage and replication checkpoints in fission yeast require nuclear exclusion of the Cdc25 phosphatase via 14-3-3 binding. *Mol Cell Biol* **19**: 7410-9.
- 218. Zhang SH, Liu J, Kobayashi R, Tonks NK. 1999.** Identification of the cell cycle regulator VCP (p97/CDC48) as a substrate of the band 4.1-related protein-tyrosine phosphatase PTPH1. *J Biol Chem* **274**: 17806-17812
- 219. Zuo, J, Qi-Wen N, Chua NH. 2000.** An estrogen receptor-based transactivator XVE mediates highly inducible gene expression in transgenic plants. *Plant J.* **24**: 265-273.

at2g30860 CAAAGATAGGAAACACGTGAGCGCGTGGTGGGATGATATTAGCAGCCGTCTCGCGTGAAGGAGACTGTTGCCAAGTATT
1120

T-DNA insertion -----

174
at2g30860 CATTCCCAGCTTAAGATGTGTTTCATCTTCTTGGTGATGTGCTTCTGTTTTATGAGAGCTTTAATAAAAGTGGAACATAA
1200

T-DNA insertion -----

174
at2g30860 TGTACCTCTTAATGTAAATGTTGCCACCTCTGTGTTCTCTTTCCTTTTGTAGTTTAATAAGTATCTTTATGGCTTTGTGAG
1280

T-DNA insertion -----

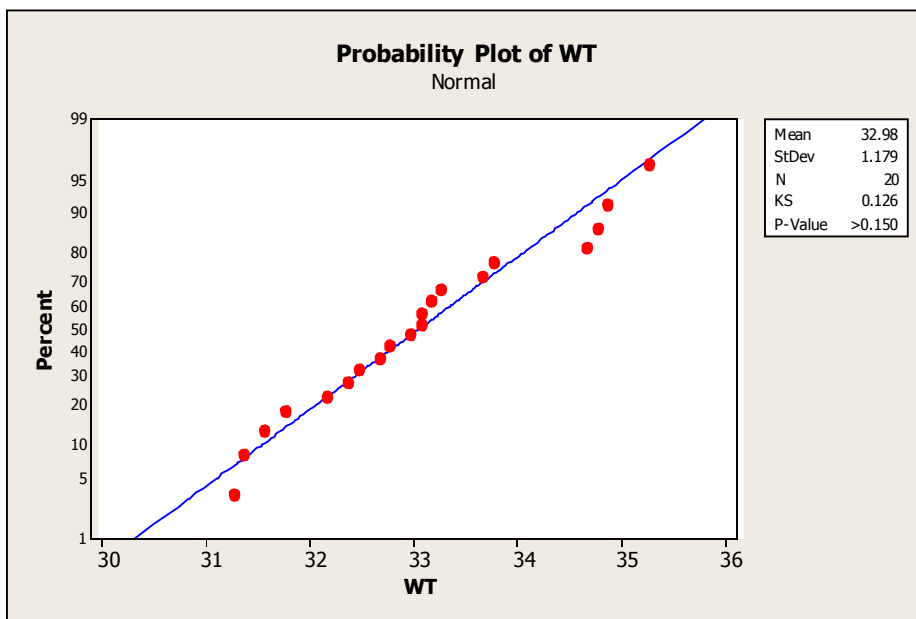
174
at2g30860 GCTTTC AATTTTAAGGAAATGATCTTTTCCCTAGTTCTACTACTTGAATGATTTAACTAGCTTAAGAAAATTAATTATG
1360

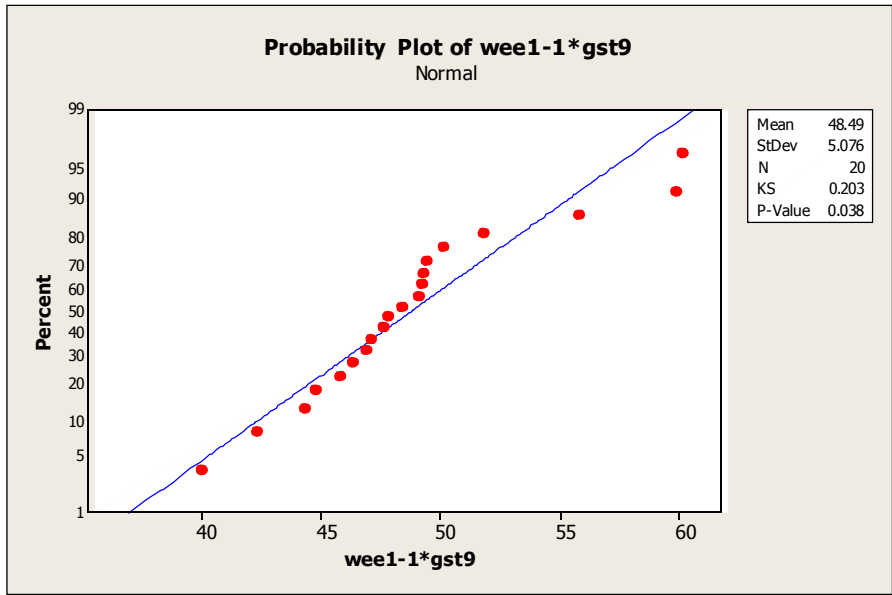
T-DNA insertion ----- 174
at2g30860 AATGAAAGGTCGGATTAGCGCGCAGACGGGAGACCTAGT 1400

T-test for Primary root length in WT and *dm*

Primary Root Length WT

Cross of *wee1-1*
* *gst9*





Two-Sample T-Test and CI: WT, weel-1*gst9

Two-sample T for WT vs weel-1*gst9

	N	Mean	StDev	SE Mean
WT	20	32.98	1.18	0.26
weel-1*gst9	20	48.49	5.08	1.1

Difference = mu (WT) - mu (weel-1*gst9)

Estimate for difference: -15.51

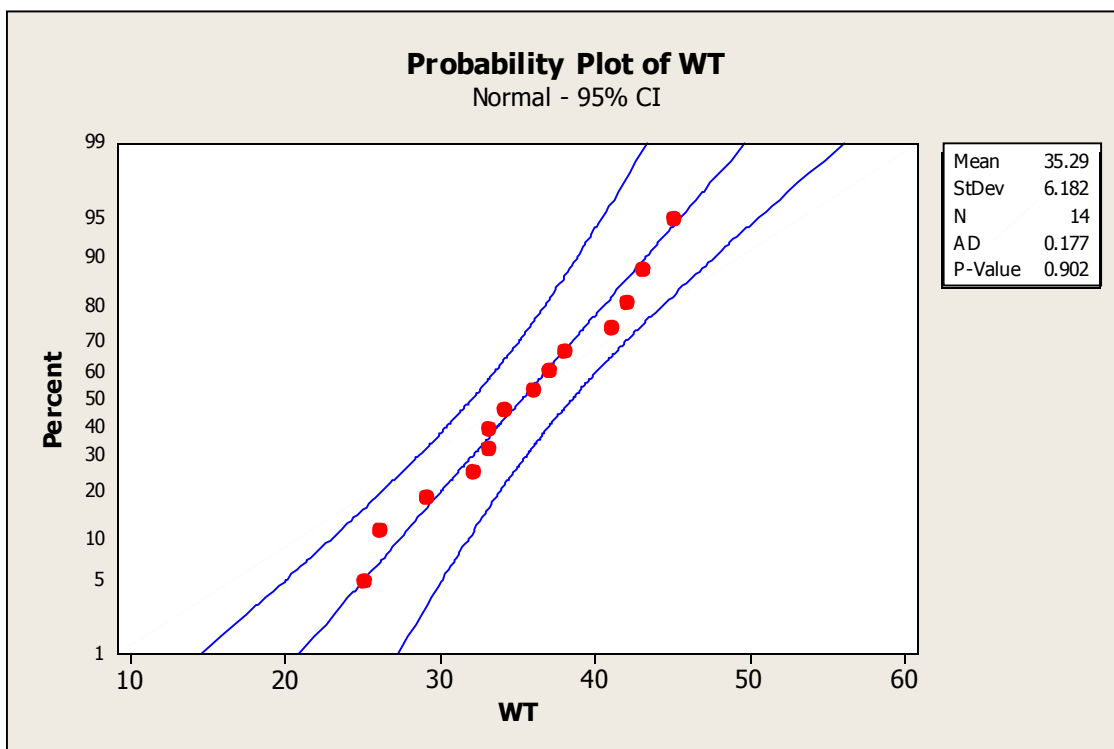
95% CI for difference: (-17.94, -13.09)

T-Test of difference = 0 (vs not =): T-Value = -13.32 P-Value = 0.000 DF = 21

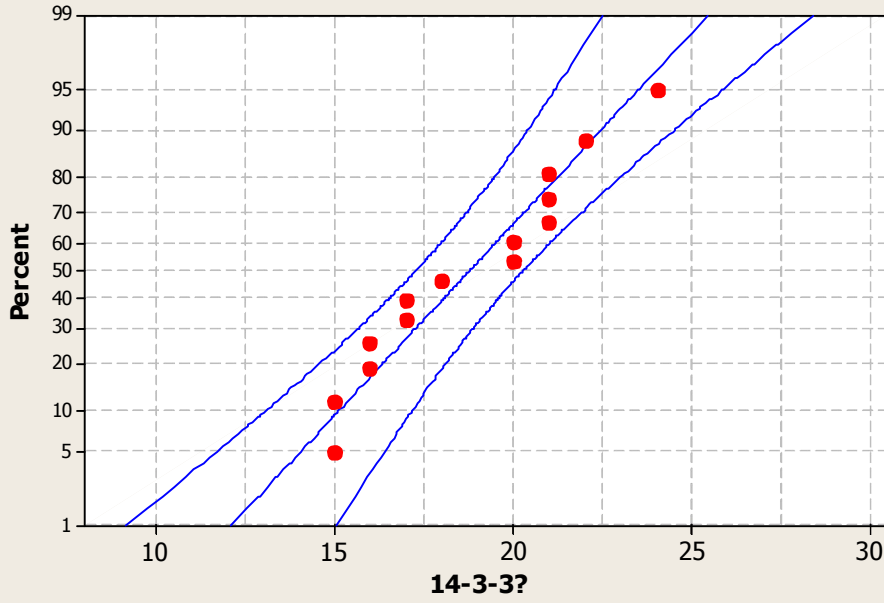
Significant at 0.01 level

Appendix B

T-test for Primary root length in WT and 14-3-3u



Probability Plot of 14-3-3?
Normal - 95% CI



Mean	18.79
StDev	2.860
N	14
AD	0.432
P-Value	0.261

Two-Sample T-Test and CI: WT, 14-3-3u

Two-sample T for WT vs 14-3-3u

	N	Mean	StDev	SE Mean
WT	14	35.29	6.18	1.7
14-3-3u	14	18.79	2.86	0.76

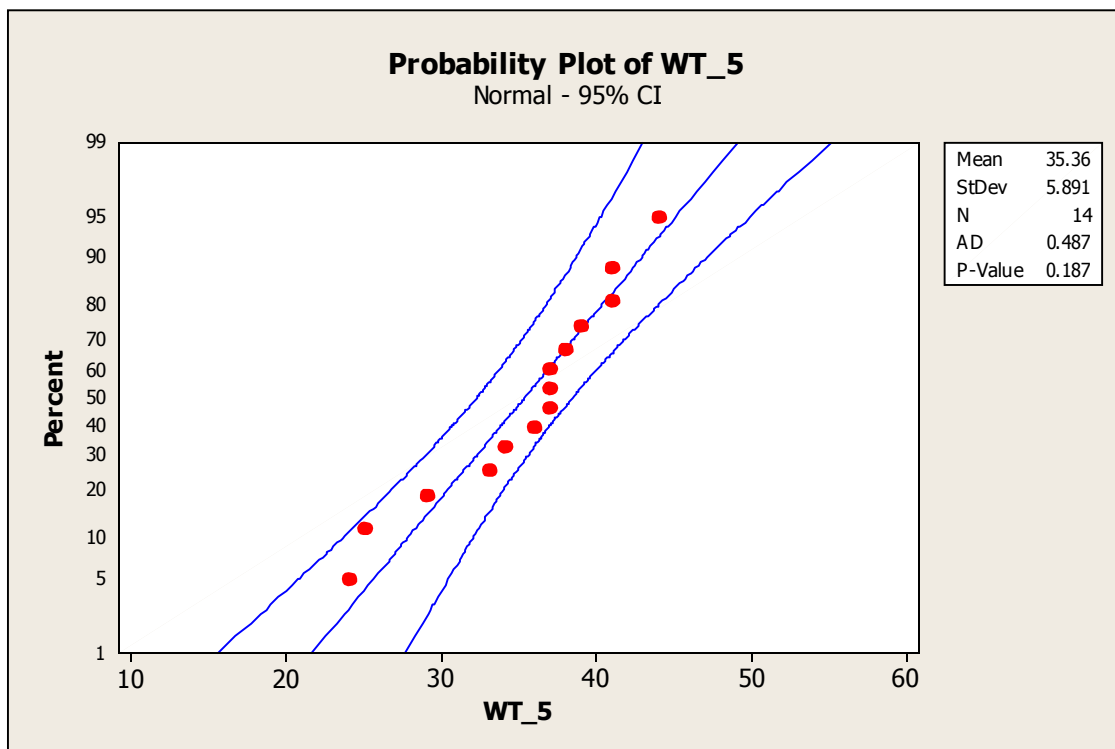
Difference = μ (WT) - μ (14-3-3u)

Estimate for difference: 16.50

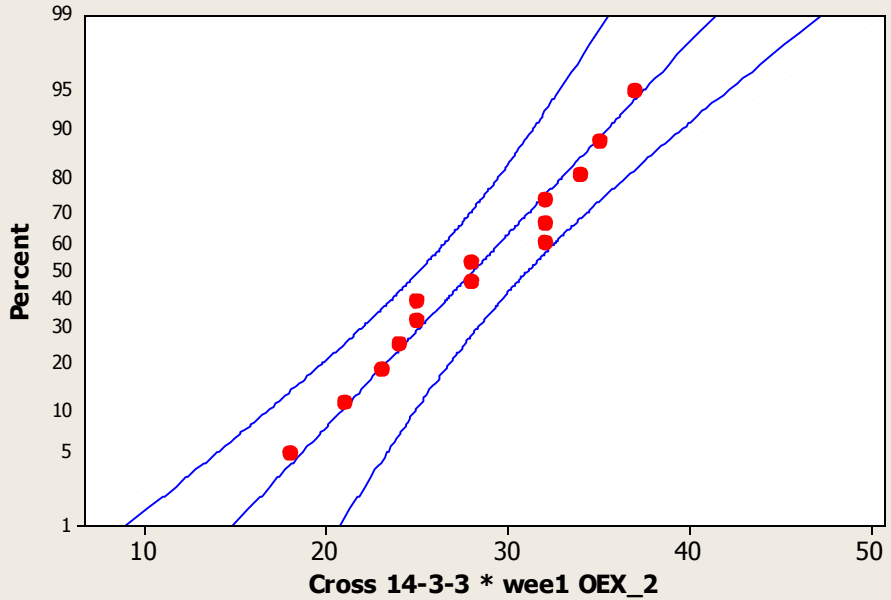
95% CI for difference: (12.68, 20.32)

T-Test of difference = 0 (vs not =): T-Value = 9.06 P-Value = 0.000 DF = 18

T-test for Primary root length in WT and the cross of wee1*14-3-3u



Probability Plot of Cross 14-3-3 * wee1 OEX_2
Normal - 95% CI



Mean	28.14
StDev	5.696
N	14
AD	0.268
P-Value	0.626

Two-Sample T-Test and CI: WT_5, Cross 14-3-3 * weel OEX_2

Two-sample T for WT_5 vs Cross 14-3-3 * weel OEX_2

	N	Mean	StDev	SE Mean
WT_5	14	35.36	5.89	1.6
Cross 14-3-3 * weel OEX_	14	28.14	5.70	1.5

Difference = μ (WT_5) - μ (Cross 14-3-3 * weel OEX_2)

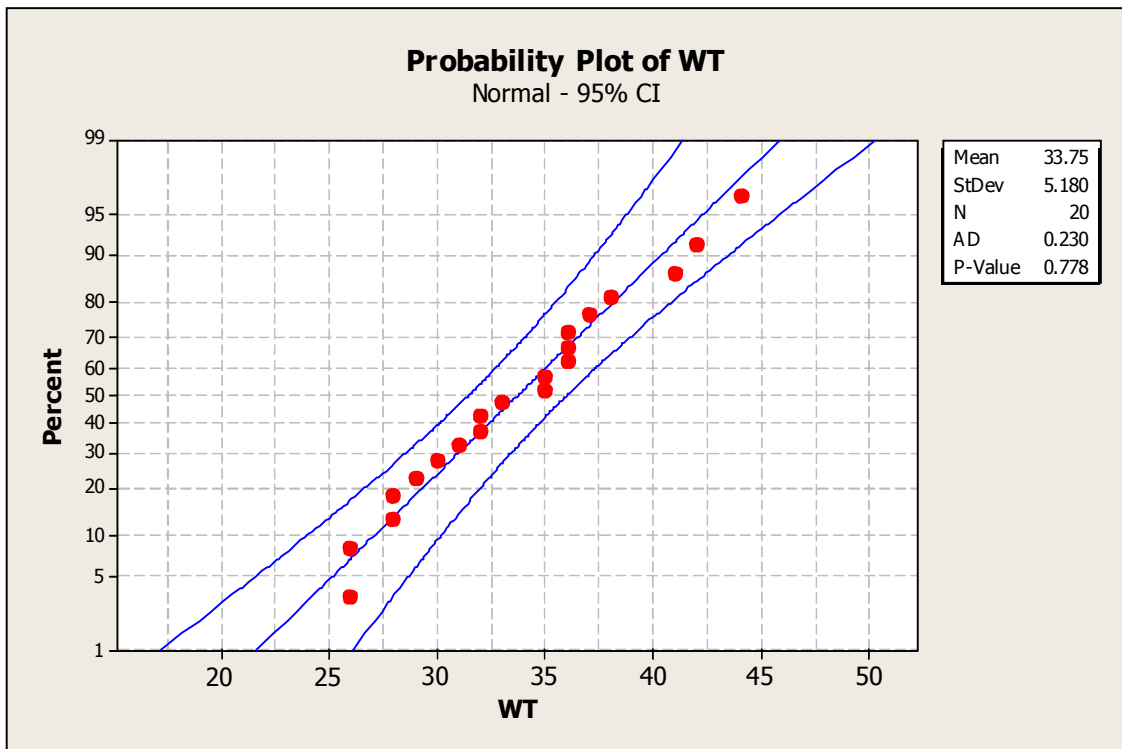
Estimate for difference: 7.21

95% CI for difference: (2.70, 11.72)

T-Test of difference = 0 (vs not =): T-Value = 3.29 P-Value = 0.003 DF = 25

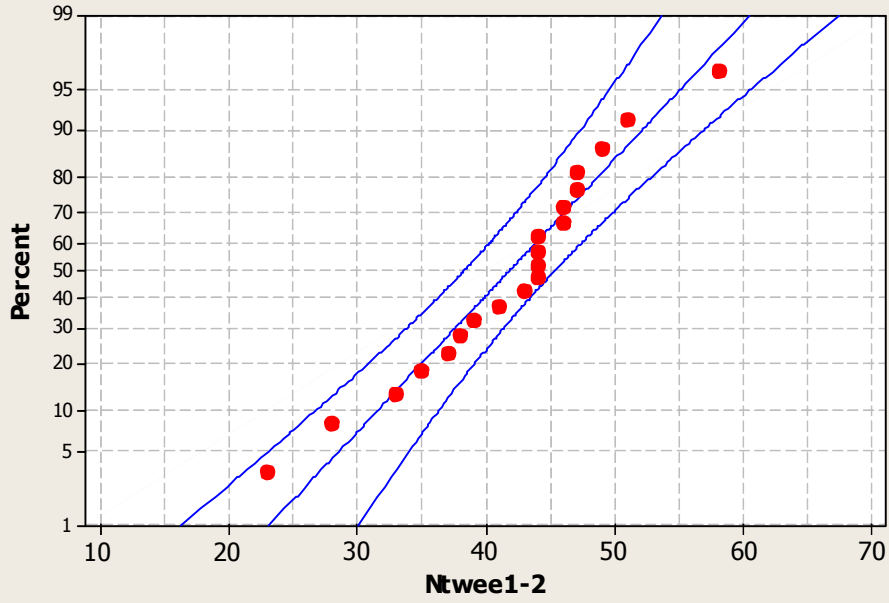
Appendix C

T-test for Primary root length in WT and interaction of over expression of ARATH;WEE1 in NICOTIANA TABACUM



Probability Plot of Ntwee1-2

Normal - 95% CI



Mean	41.85
StDev	8.022
N	20
AD	0.423
P-Value	0.289

Two-Sample T-Test and CI: WT, Ntwee1-2

Two-sample T for WT vs Ntwee1-2

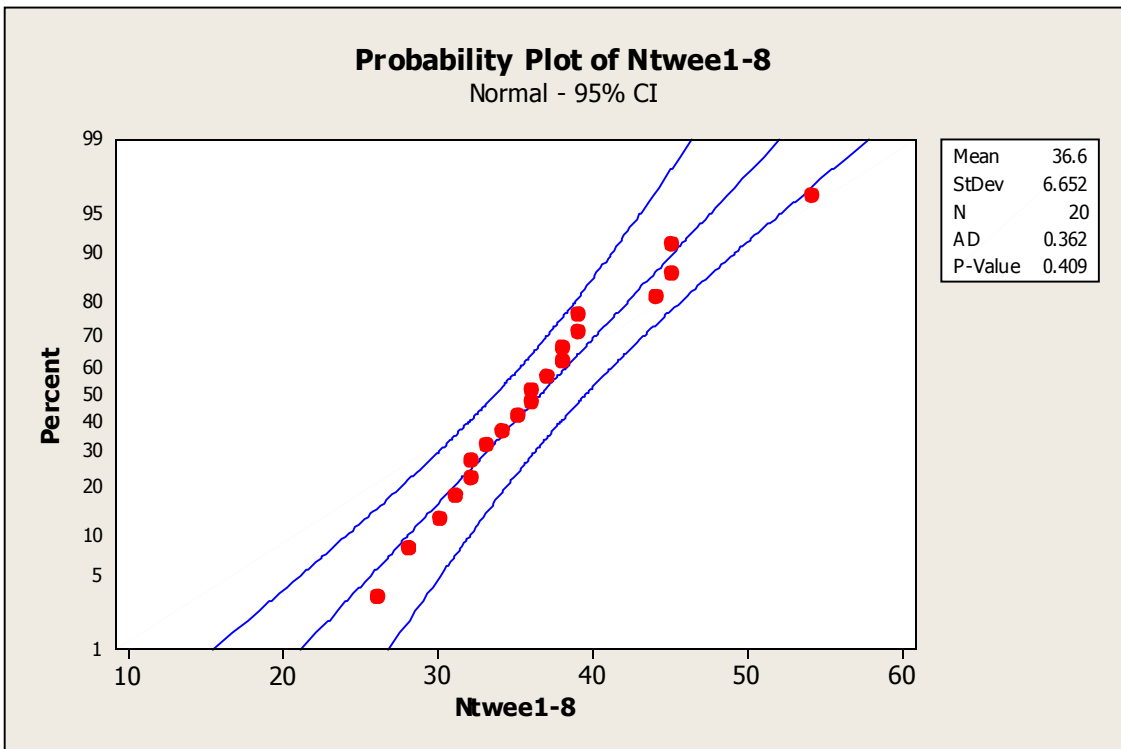
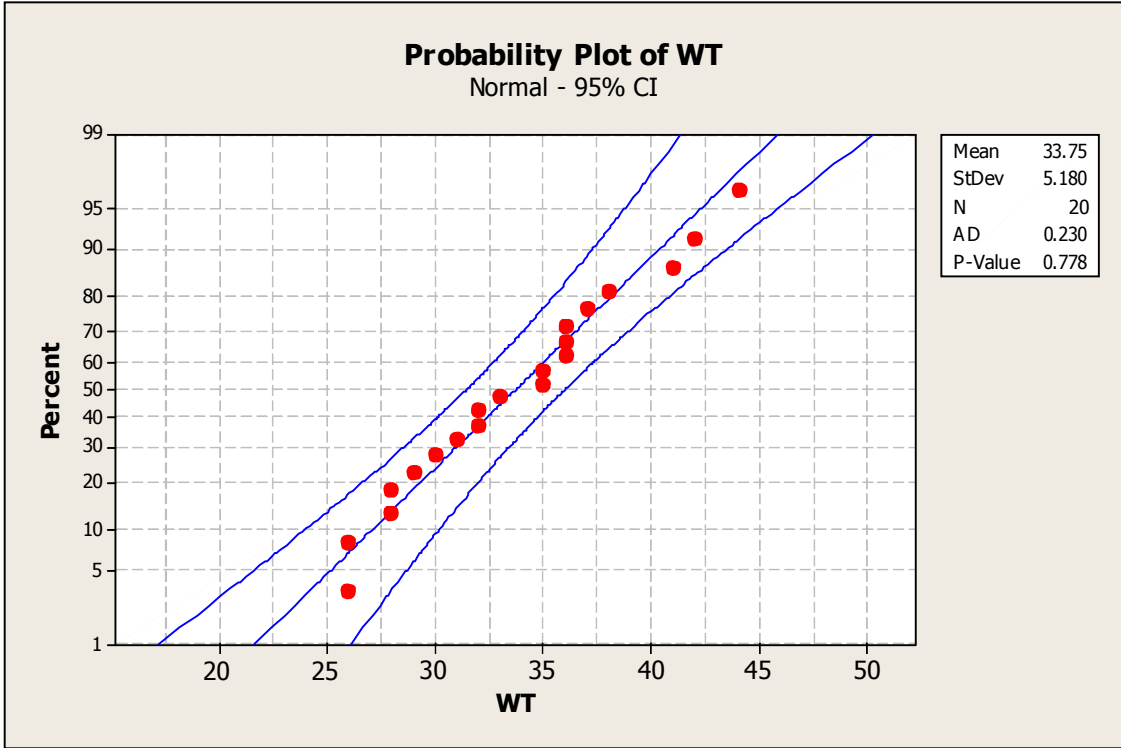
	N	Mean	StDev	SE Mean
WT	20	33.75	5.18	1.2
Ntwee1-2	20	41.85	8.02	1.8

Difference = mu (WT) - mu (Ntwee1-2)

Estimate for difference: -8.10

95% CI for difference: (-12.45, -3.75)

T-Test of difference = 0 (vs not =): T-Value = -3.79 P-Value = 0.001 DF = 32



Two-Sample T-Test and CI: WT, Ntwee1-8

Two-sample T for WT vs Ntwee1-8

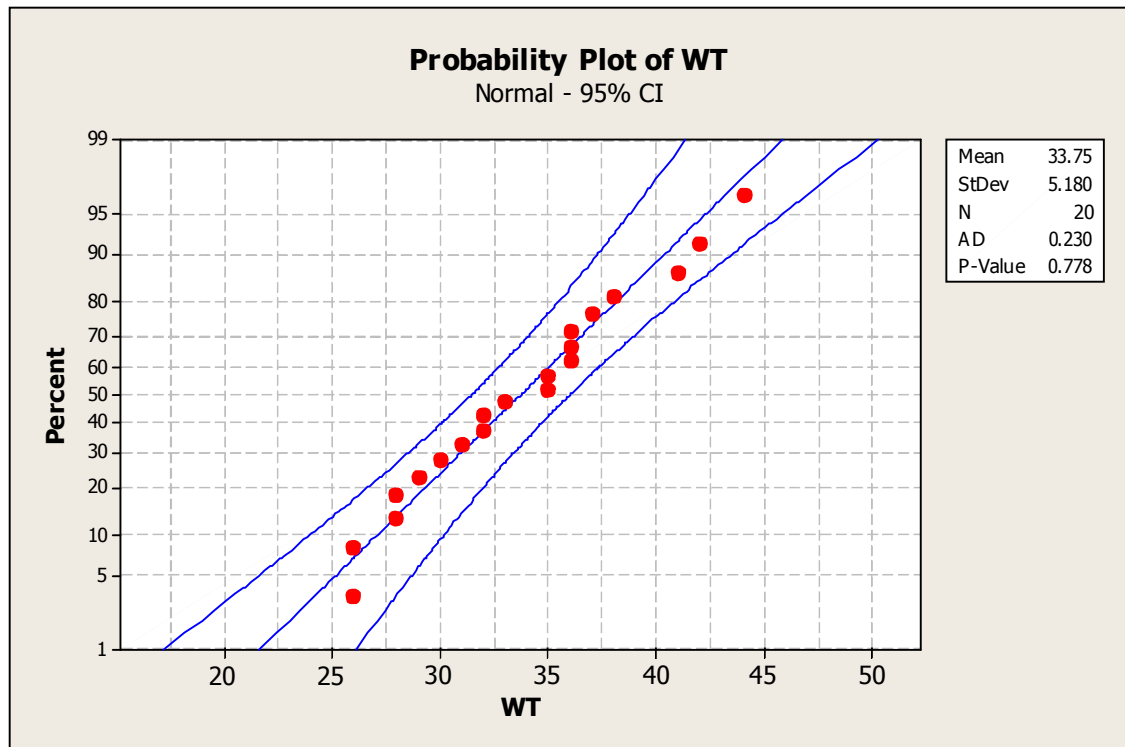
	N	Mean	StDev	SE Mean
WT	20	33.75	5.18	1.2
Ntwee1-8	20	36.60	6.65	1.5

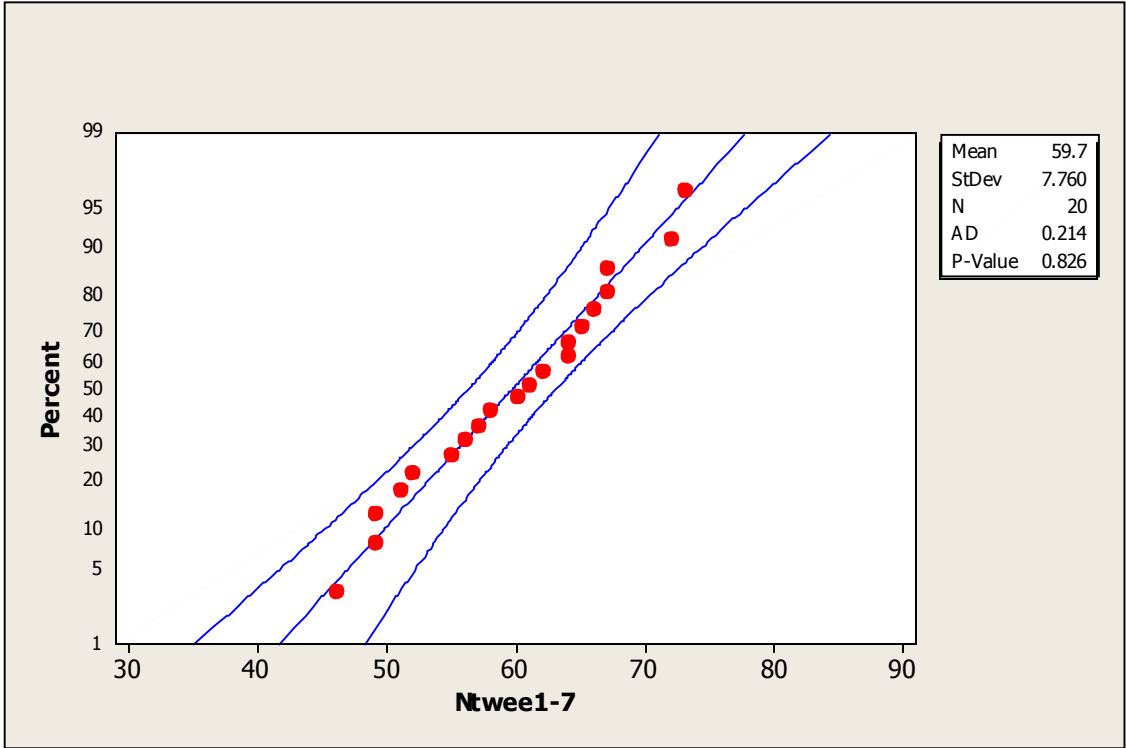
Difference = μ (WT) - μ (Ntwee1-8)

Estimate for difference: -2.85

95% CI for difference: (-6.68, 0.98)

T-Test of difference = 0 (vs not =): T-Value = -1.51 P-Value = 0.140 DF = 35





Two-Sample T-Test and CI: WT, Ntweel-7

Two-sample T for WT vs Ntweel-7

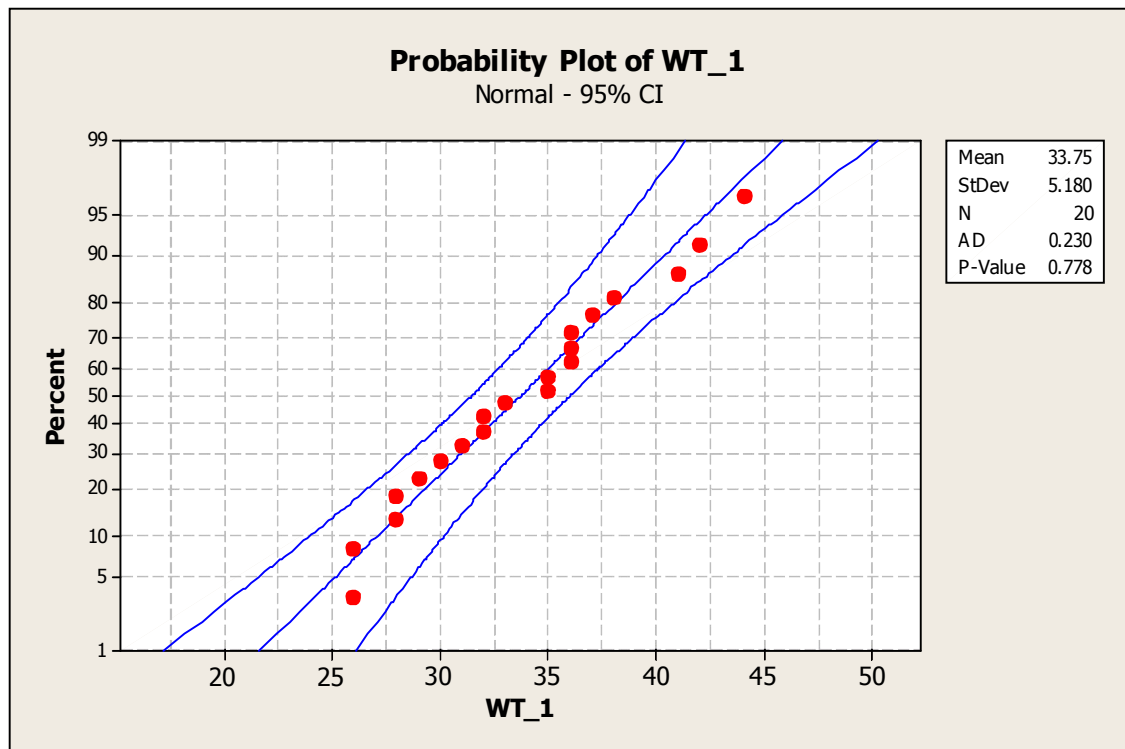
	N	Mean	StDev	SE Mean
WT	20	33.75	5.18	1.2
Ntweel-7	20	59.70	7.76	1.7

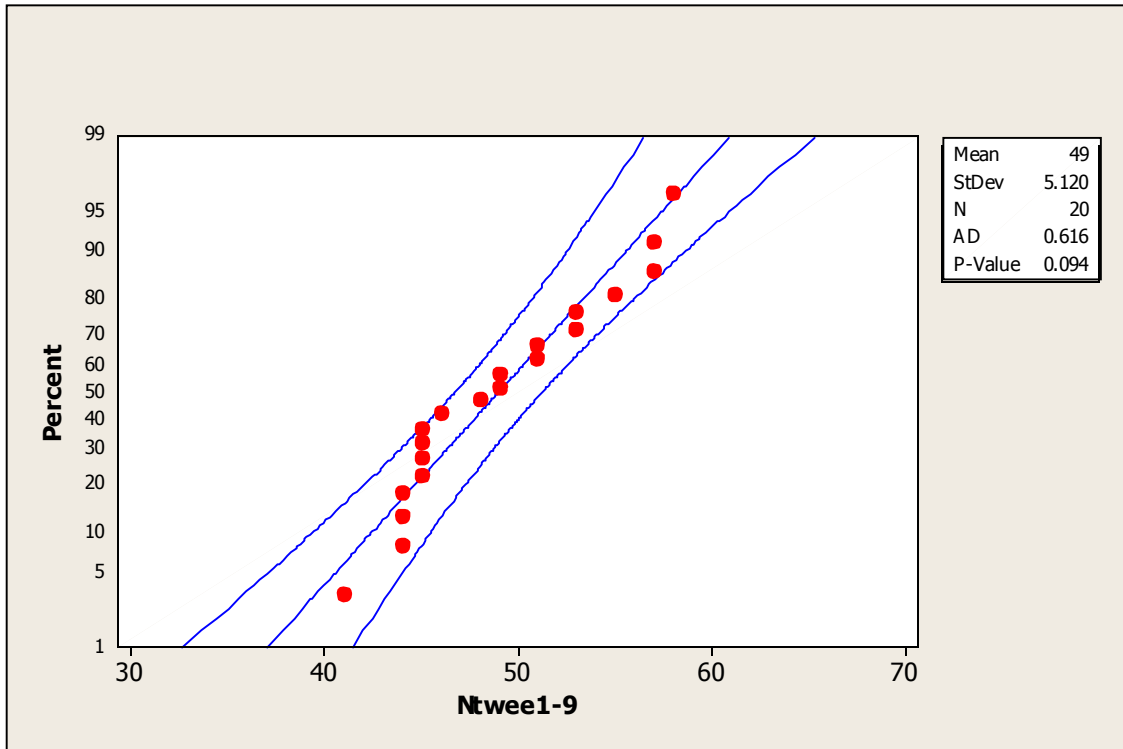
Difference = μ (WT) - μ (Ntweel-7)

Estimate for difference: -25.95

95% CI for difference: (-30.19, -21.71)

T-Test of difference = 0 (vs not =): T-Value = -12.44 P-Value = 0.000 DF = 33





Two-Sample T-Test and CI: WT_1, Ntweel-9

Two-sample T for WT_1 vs Ntweel-9

	N	Mean	StDev	SE Mean
WT_1	20	33.75	5.18	1.2
Ntweel-9	20	49.00	5.12	1.1

Difference = μ (WT_1) - μ (Ntweel-9)

Estimate for difference: -15.25

95% CI for difference: (-18.55, -11.95)

T-Test of difference = 0 (vs not =): T-Value = -9.36 P-Value = 0.000 DF = 37

